RESEARCH REPORT

IDENTIFICATION OF CAUSES AND DEVELOPMENT OF STRATEGIES FOR RELIEVING STRUCTURAL DISTRESS IN BRIDGE ABUTMENTS

by

Rigoberto Burgueño

Zhe Li

Report No. CEE-RR – 2008/02

February 2008

Department of Civil and Environmental Engineering
Michigan State University
East Lansing, Michigan

1. Research Report RC-1508	2. Government Accession No.	3. MDOT Project Manager: Roger Till, P.E.
4. Title and Subtitle Identification Of Causes And Development Of Strategies For Relieving Structural Distress In Bridge Abutments		5. Report Date February 13, 2008
7. Author(s) Rigoberto Burgueño and Zhe Li		6. Performing Organization Code
9. Performing Organization Name and Address Michigan State University Department of Civil and Environmental Engineering 3546 Engineering Building East Lansing, MI 48824-1226		8. Performing Org Report No. CEE-RR – 2008/02
12. Sponsoring Agency Name and Address Michigan Department of Transportation Construction and Technology Division P.O. Box 30049 Lansing, MI 48909		10. Work Unit No. (TRAIS)
		11. Contract Number: 2002-0532
		11(a). Authorization Number: 12
15. Supplementary Notes		13. Type of Report & Period Covered 12-27-04 to 12-31-07
		14. Sponsoring Agency Code

16. Abstract

Structural distress in the abutments walls of bridges in the form vertical cracks along the visible wall height and u-shape cracks under girder supports is problem that the Michigan Department of Transportation has been trying to understand and address. While possible causes of damage have been hypothesized, the specific mechanisms and their relative importance as a cause of the damage are not well understood. The objective of this research was thus to identify the causes behind abutment damage, propose solution strategies and develop prediction models to improve maintenance and future design.

Given the time-dependent nature of the problem, the research was based on the use of field inspection data from the National Bridge Inventory record for Michigan's bridges. However, data from manual inspections is qualitative, unbalanced, subjective, with errors and incomplete. The research approach was thus to use statistical methods, data mining techniques, and artificial intelligence models to interpret the information captured in this database. Statistical analyses were used to extract an information database from the general inspection record and thus identify parameters that could serve as explanatory variables in prediction models. A family of bridges sharing statistically significant parameters related to abutment damage was carefully inspected and four bridges were monitored for 1-year. Strains and displacements on the abutment walls of the monitored bridges were used as a dynamic database for the identification of damage sources. A large case-matrix of finite element simulations was used to develop a virtual database of abutment performance to support the evidential database in prediction models and help establish the relative importance of damage-causing mechanisms. Four different artificial neural networks (ANN) models were developed and validated to predict the structural condition of existing and new bridge abutments. The individual ANN models provided satisfactory performance but suffered from the unbiased and subjectivity of the inspection databases. ANN ensembles with novel data handling techniques and diverse voting in virtual committees were developed and proven to alleviate these problems and led to improved accuracy in the prediction models. An ANN ensemble model was implemented into a computer program (SbNet) that can predict bridge abutment condition and life-time degradation given design parameters or a bridge identification number.

The findings indicate that the main causes behind abutment distress are the pressures from pavement approaches and temperature gradients. Strategies to relieve these effects are well known and they include: the use of flexible pavements, pavement pressure relief joints, improved expansion joint seals, smaller skew angles, use of expansion bearings at abutments, and the elimination of pin-and-hanger assemblies.

17. Key Words Abutments, ANN, bridges, damage, damage models, distress, field inspections, neural networks, prediction models.	18. Distribution Statement No restrictions. This document is available to the public through the Michigan Department of Transportation.

19. Security Classification (report) Unclassified	20. Security Classification (Page) Unclassified	21. No of Pages 183 + Appendices	22. Price

IDENTIFICATION OF CAUSES AND DEVELOPMENT OF STRATEGIES FOR RELIEVING STRUCTURAL DISTRESS IN BRIDGE ABUTMENTS

by

Rigoberto Burgueño, Ph.D.
Associate Professor of Structural Engineering

Zhe Li
Graduate Research Assistant

Department of Civil and Environmental Engineering
Michigan State University
East Lansing, MI 48824-1226

February 2008

DISCLAIMER

The opinions, findings, conclusions and recommendations presented in this report are those of the authors alone and do not necessarily represent the views and opinions of Michigan State University or the Michigan Department of Transportation.

ABSTRACT

Structural distress in the abutments walls of bridges in the form vertical cracks along the visible wall height and u-shape cracks under girder supports is problem that the Michigan Department of Transportation has been trying to understand and address. While possible causes of damage have been hypothesized, the specific mechanisms and their relative importance as a cause of the damage are not well understood. The objective of this research was thus to identify the causes behind abutment damage, propose solution strategies and develop prediction models to improve maintenance and future design.

Given the time-dependent nature of the problem, the research was based on the use of field inspection data from the National Bridge Inventory record for Michigan's bridges. However, data from manual inspections is qualitative, unbalanced, subjective, with errors and incomplete. The research approach was thus to use statistical methods, data mining techniques, and artificial intelligence models to interpret the information captured in this database. Statistical analyses were used to extract an information database from the general inspection record and thus identify parameters that could serve as explanatory variables in prediction models. A family of bridges sharing statistically significant parameters related to abutment damage was carefully inspected and four bridges were monitored for 1-year. Strains and displacements on the abutment walls of the monitored bridges were used as a dynamic database for the identification of damage sources. A large case-matrix of finite element simulations was used to develop a virtual database of abutment performance to support the evidential database in prediction models and help establish the relative importance of damage-causing mechanisms. Four different artificial neural networks (ANN) models were developed and validated to predict the structural condition of existing and new bridge abutments. The individual ANN models provided satisfactory performance but suffered from the unbiased and subjectivity of the inspection databases. ANN ensembles with novel data handling techniques and diverse voting in virtual committees were developed and proven to alleviate these problems and led to improved accuracy in the prediction models. An ANN ensemble model was implemented into a computer program (SbNet) that can predict bridge abutment condition and life-time degradation curve given design parameters or a bridge identification number.

The findings indicate that the main causes behind abutment distress are the pressures from pavement approaches and temperature gradients. Strategies to relieve these effects are well known and they include: the use of flexible pavements, pavement pressure relief joints, improved expansion joint seals, smaller skew angles, use of expansion bearings at abutments, and the elimination of pin-and-hanger assemblies.

AKNOWLEDGEMENTS

TABLE OF CONTENTS

LIST OF FIGURES

LIST OF TABLES

1   Introduction

1.1   Problem Statement

Highway bridges in the state of Michigan are suffering from distress in the form of cracks and concrete spalling in their abutment walls (Figure 1-1). The forms of abutment distress are on the front side of the abutment wall and are of the following types: U-shape concrete spalling under girder supports (Figure 1-2), vertical cracks between girders (Figure 1-3 a), and vertical cracks underneath girders (Figure 1-3 b). The distress seems to be incremental, with cracks and concrete spalling growing with time as a consequence of factors not yet fully known. Additional effects from corrosion due to leaky joints worsen or increase the damage. Thus, while initially the cracks are cosmetic, with little effect on serviceability or safety of the bridge, with time they can severely degrade the integrity of the abutment wall. In some cases, the degradation due to damage under girder supports can be extensive and thus compromise structural integrity. The Michigan Department of Transportation (MDOT) has traditionally been addressing this problem by continuously monitoring the condition of this distress and then acting on repairs to restore the integrity of the abutment wall. It is of interest, however, to improve the understanding the causes behind this damage and develop strategies to alleviate it.

Figure 1-1 Concrete spalling in the abutment wall of bridge B 2.1

Figure 1-2 Pull-out of concrete block in the abutment wall of Bridge A 1.7
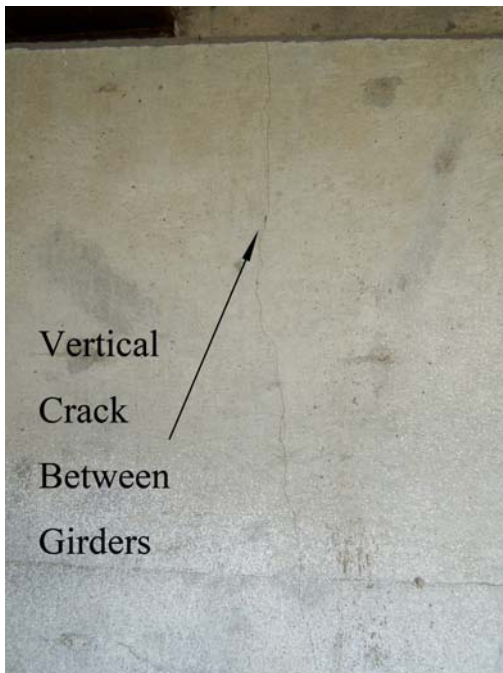
a) Bridge A 1.4 b) Bridge B 1.1
Figure 1-3 Vertical cracks in abutment walls

The causes of the mentioned abutment wall damage are not clearly known. Possible sources include corroded, or "frozen," bearings and expansion details (e.g., pin and hanger assemblies),

underperforming expansion joints, and the pressure generated by the thermal movement of pavement approaches (or "pavement growth"). While these individual problems are fairly well known, the relative importance of these causes on the distress observed in substructure elements for different types of bridges in Michigan is not. Focused and effective strategies for relieving the structural distress in substructures can only be developed after a better understanding of the different causes and their relative importance is established. Further, the ability to forecast potential problems in abutments and knowing how to avoid such problems will improve the management of maintenance and future design of bridges.

1.2   Project Background

Dealing with the above-mentioned abutment distresses problems is not new to MDOT and the repair of such distress is common. While the specific mechanisms causing the damage are not known, there is common agreement on the possible causes. These include: the "growth" of approach pavements, temperature effects, underperforming expansion details due to corrosion, age, etc. A review on these potential sources of damage follows.

The interface between the bridge superstructure and embankments is a well-known source of large maintenance problems (Briaud et al. 1997, Long et al. 1998). A relevant problem at this interface is the so-called "pavement growth" phenomena, which refers to the movement and expansion of pavements against the bridge deck. The causes for pavement growth are complex, encompassing, among them, pavement motions due to temperature effects, incorrect design of approach slabs, improper design of sleeper slabs, expansive soils, soil consolidation, soil embankment movement, drainage, etc. Burke (1998, 2004) found that pavement growth was generated through years of temperature variation cycles and failure of expansion joint sealing. The process is illustrated in Figure 1-4. Concrete slabs were connected with expansion joints with sealing at the finish of the pavement construction. During the winter season, temperature decreases and concrete slabs contract, thus increasing the gap at joints. Debris falls into the expansion joint gaps if the joint sealing didn't work well. During the temperature increase in the summer period concrete slabs expand closing the expansion joint gaps and compact the deposited debris inside of it. The compacted debris thus take part of the space in the expansion joint gap. With the next winter cycle the pavement joints will again open allowing more debris to deposit in the joint gaps, which will later be once again compacted when the gap closes during

the summer season. The repetition of this process over the years will fill and compact the space in the expansion joints. The reduction of free space in the expansion joint gaps generates compressive pressure between adjacent pavement slabs. The pressure can be large enough to mobilize the slabs or can result in upwards buckling of the pavement, or pavement blowup.

Sealing
Expansion joint

Concrete pavement (New)

Sealing opened
Debris fell into opened spac

Contracted

In winter

Debris compacted
in the sealing
Pressure generated

Expanded

In summer

Years of cycles

Huge pressure accumulated
in concrete slabs

15 to 30 years later
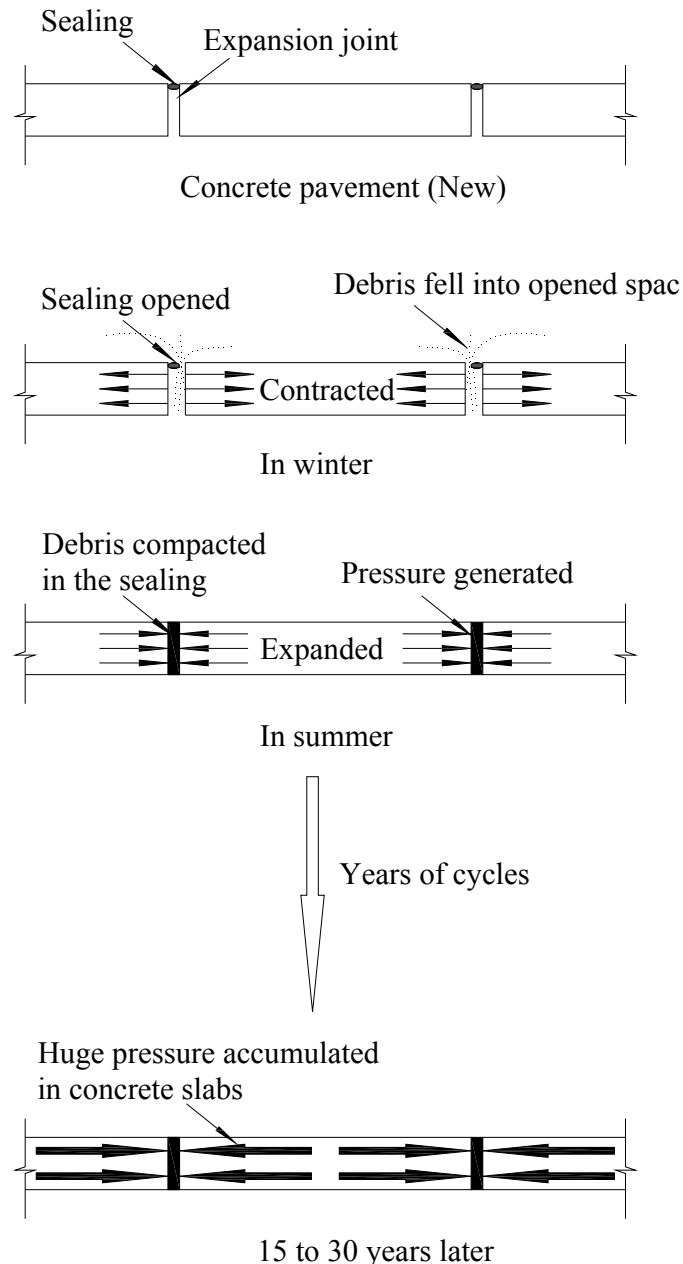
Figure 1-4 Generation of pavement pressure

If the pavement slabs move towards the approaches of a bridge and the expansion joints at the pavement/superstructure interface cannot accommodate the pavement movement, the

generated pavement pressures against the bridge deck transfer forces to the girders and these subsequently transfer the loads to their bearing or anchorage detail on top of the abutment wall thus leading to damage below the girder supports as illustrated in Figure 1-5.

Figure 1-5 Concrete pullout caused by pavement pressure

Temperature loads can possibly influence bridge abutment through in the longitudinal and transverse direction. Temperature induced longitudinal movements are typically addressed by providing movement joints on the superstructure. The type of joint depends on the superstructure

type. Reinforced and prestressed concrete bridges typically consist of simple spans and joints are placed at the continuation of spans on top of piers. Movement is accommodated by the girder bearing supports. For steel girder bridges, longitudinal thermal movements can also be addressed using simply supported side spans with moveable bearing supports on top of piers or abutment walls.

In addition, pin and hanger assemblies, which introduce a shear-link mechanism in the steel girder are common connection details featured in many older, and even some modern, multi-span steel bridges. The concept of pin and hanger assemblies is advantageous when large thermal movements or potential differential settlements are anticipated. Design provisions assume free rotational and axial movement at the pin-hanger girder connection. This assumption, however, is found to be invalid in a very large number of cases in which a certain degree of fixity results from corrosion or friction.

Expansion of corrosion products, termed pack rust, may cause the pin-hanger details to "lock" or have considerable friction (El-khoury et al. 1996). An extreme case is shown in Figure 1-6 a. This "locking" causes a complex stress distribution on both the pin and the hanger and in some cases had led to failures of the pin-hanger assembly (Askeland et al. 1987, Bellnoit et al. 1990). In addition, the altered behavior of the pin-hanger detail can also have a significant influence on the overall bridge system behavior (Elewa 2004). Both the superstructure and substructure systems will experience larger stresses than those considered during design. For example, the steel girders will experience larger axial stresses and in return larger horizontal reaction forces will be developed at the abutments when pin-hanger details lock-up. Also, for skew bridges, large transverse forces on abutments and piers can lead to tensile cracks on the abutment stem and the cantilever part of the pier caps due to temperature cycle loading alone (Elewa 2004).

a) Corroded Expansion Joint Details   b) Aged or Restrained Bearing Supports

Figure 1-6 Potential Causes for Substructure Distress

Temperature effects due to transverse movements are usually less of a concern since the superstructure tend to have less material and stiffness associated with this direction. Nonetheless, the vertical cracks observed in abutment walls between girder supports seem to be the consequence of restrained temperature movements between girders supports and the abutment wall. This possible source of damage is schematically shown in Figure 1-7.

Bridge bearings (Figure 1-6 b) are designed to transmit the weight of the superstructure and the traffic load it supports to the substructure. They are also designed to allow changes in geometry of the superstructure resulting from live load, temperature variations, and possible foundation settlements. It is common practice that the expansion bearings are provided to guide the movements and rotations in the longitudinal direction. However, this measure can restrain movements in other directions, particularly transverse movements due to temperature or due to bridge geometry (skew) effects (Tindal and Yoo 2003). Moreover, the longitudinal expansion devices can "freeze", or harden leading to increase friction resistance or movement restraint (Roeder 1989). The resulting restraining forces will induce forces that may not have been considered during design and which can consequently lead to damage in both the superstructure and the substructure (Elewa and Burgueño 2004, Kuliki et al. 1986, Roeder 2003) as seen in Figure 1-1.
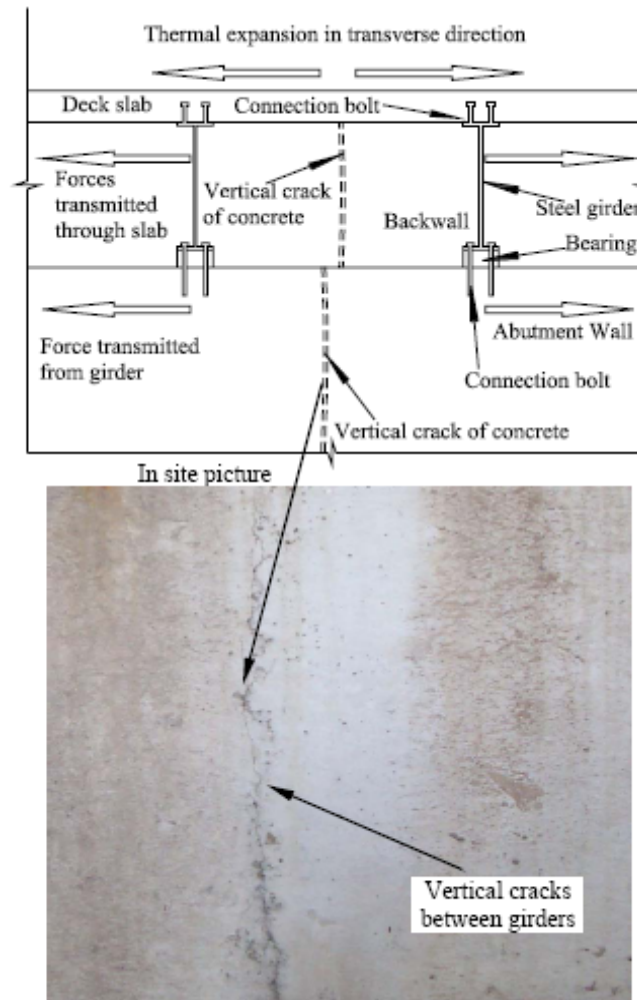
Figure 1-7 Bridge abutment damage with their possible causes

While the above-mentioned causes are potential contributors to abutment distress, their relative importance is not well understood and there also could be other unidentified causes. The consequences of the suspected causes are, however, real, i.e., structural distress in abutments and piers. In order to keep bridges in good condition, MDOT maintains a bridge inspection database according to the National Bridge Inventory (NBI) system (Hartle et al., 1991), which is based on the manual inspection of bridge structural members at an interval of no more than two years. More than 100 variables are included in this record, from design and service parameters to elements inspection results for each highway bridge. Element inspection results include the rating of the different structural elements of the bridge system; that is abutment, pier, deck, etc. The element rating consists of a variable describing physical condition of bridge and is coded to

10 qualitative values from its worst case at "0" (failed condition) to its best condition at a "9" (new condition). A larger number implies better structural condition, and vice-versa. The rating of "4" can be considered as a threshold since it corresponds to a poor condition. It can thus be said that bridges with an abutment rating equal or less than "4" have a significant level of abutment distress. An in-depth exploration and effective application of this MDOT manual inspection database was thus considered a key source of information on the identification of the causes of abutment distress as well as for the development of prediction models and distress alleviation strategies.

The NBI structural appraisal database provides historical and evidential data on the degradation of bridge abutments together with the associated design and service parameters of the bridges in question. However, use of the data has inherent difficulties since the database is quantitative, it relies on subjective decisions, and the problem is most likely highly coupled and highly nonlinear. Statistical analyses and advanced data handling techniques realize the nonlinear mapping of the available data to the damage and its sources.

Regression and correlation analyses permits investigating the associations, and, if present, the characteristics of the associations, among various observable quantities. For example, it would be of interest to know there is any association between corroded pin-and-hanger assemblies and abutment vertical cracks and, if so, what kind of association exists. These associations can further be expressed in the prediction of one or more of the associated variables. Regression analysis can offer a sensible and sound approach for examining associations among variables and for obtaining good rules for prediction and have been applied to projects similar to this (Myers et al. 2001). However, traditional statistical models do not have accurate predictive capabilities outside the experimental domain used for their development. This is particularly relevant for the type of problem at hand since structural appraisal database may be incorrect or incomplete. Predictive simulation tools that are based on known outcomes, either evidential or analytical, and that are less sensitive to errors or gaps in the database can be more powerful in this situation. Artificial neural networks feature these advantages and are thus one of the most powerful tools for developing predictive models based input-output association.

Artificial neural networks (ANNs) are essentially models for computation and knowledge representation inspired by the understanding and abstraction of the biological structure of

neurons and the operation of the human brain (Kartam et al. 1997). A neural network is a highly interconnected network of simple linear or nonlinear processors, or operations, in parallel fashion (Figure 1-8). Each processing unit receives multiple inputs through weighted connections from neurons in the previous layer to which it is connected, performs appropriate computation (adding inputs, computing a new activation level, or comparing input to a threshold value), and transmits output to other processing units or as a network output using an assigned transfer function. Thus, a neural network performs operations by propagating changes in activation, or stimulation, through weighted connections between the processors, and it stores what has been "learned" as strengths of the connections between the processors. The system adjusts the weights of internal connections to minimize errors between the network output and target output. This learning occurs even when the input data contains errors or is incomplete, which is one of the problems that must be addressed for structural distress in bridge substructures. The propagation of the activation and thus the "computation" performed by the network depends on the layout and the strengths of the connections between the processors. A neural network thus has the ability to synthesize through training an associative memory that may generate appropriate output when presented with an un-familiar set of inputs. For this reason ANN models belong to a class of algorithms known as artificial intelligence methods.
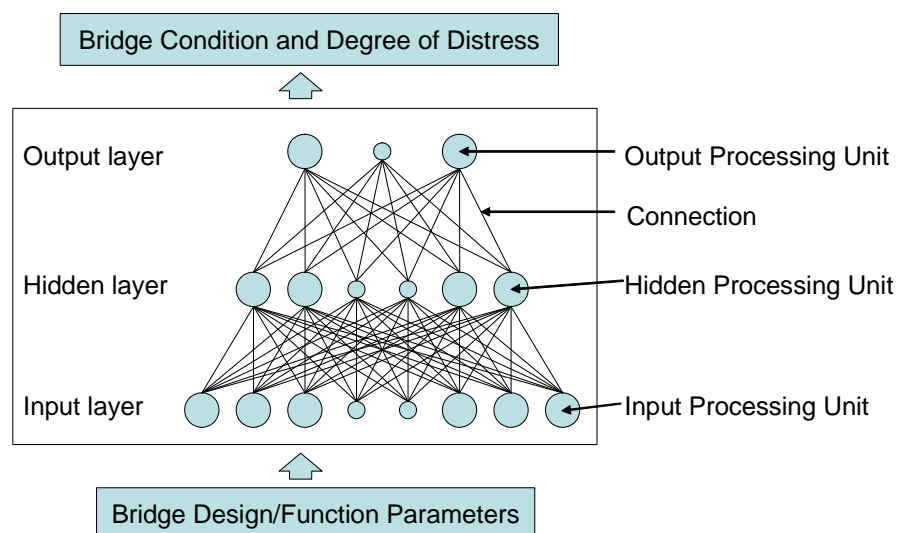
Figure 1-8 Schematic of a Feed-Forward Neural Network

The non-linear nature of ANNs makes them suitable for performing functional approximation, classification, and pattern recognition. Neural networks thus have many qualities that make them particularly attractive in pattern-recognition applications that are not easily achieved by other means. Some of the important qualities of neural networks are (Graybill and Iyer 1994):

- They "learn" by example and can be conditioned to respond correctly to a stimulus;

- They can automatically perform knowledge abstraction and statistical analyses on data that is presented to them and this information becomes encoded into the network internal structure;

- They can generally respond correctly even in the presence of noise or uncertainty in the in-formation network making them suitable for use in poor signal/data environments.

- They can satisfactorily predict the outcome of complex problems or those with high degree of nonlinear behavior.

ANNs are then highly useful to problems where patterns of information represented in one form need to be mapped into patterns of information in another form. Applications of ANNs to civil engineering is increasingly common including: classification/interpretation tasks (inverse mapping from observations to known causes), diagnosis (inverse mapping from observed effect to cause), modeling (mapping from cause to effect), and control (inverse mapping from observed state to control applied forcing functions).

This goal of this research was thus to employ and develop a combination of evidential data (inspection reports), dynamic data (field monitoring) and analytical data (finite element analyses) to understand the causes of structural distress in bridge abutments and their relative importance, and for the development of diagnosis, or prediction, tools through artificial intelligence algorithms. The definitions of overall and specific objectives are outlined in the next section.

1.3　Research Objective

The objectives of this research are to identify the causes behind structural distress in bridge abutments, establish their relative importance, and identify strategies for relieving such distress. The objectives were met through the five tasks outlined below:

➢ *Task I. Information Database*: Identify the mechanisms that lead to abutment distress and the relevant input parameters (e.g., bridge type, bearing/expansion joint corrosion, pavement growth, etc.) by creating an information database. The database was assembled by literature review, by State DOT surveys, by reviewing MDOT field inspection reports and by field visits to typical bridges.

➢ *Task II. Field Monitoring:* Develop and implement an effective one-year field monitoring plan for 4 typical bridges with and without signs of abutment distress to evaluate damage patterns for different bridge super- and sub-structures; Record behavior of the abutment wall interact with super-structure and environment; and identify possible causes of typical damage.

➢ *Task III. Parameter Analysis and Diagnosis Model*: Develop finite element models to predict effects of different assumed damage scenarios, use parametric analyses to investigate behavior of bridges of different design parameters, and use artificial neural networks to identify the relative importance of the causes for abutment distress and to develop diagnosis tools for predicting, and thus managing and avoiding, such distress.

➢ *Task IV. Distress Relieving Strategies*: Develop and recommend effective strategies for relieving the structural distress in abutments by directly addressing the causes leading to distress with due consideration of their relative importance.

➢ *Task IV. Final Reporting*: Prepare a final report documenting the complete research effort and the identified recommendations in accordance with MDOT requirements.

The proposed approach and the specific work tasks were executed in a systematic manner to ensure project success. CTE Engineers, a local consulting firm, assisted the research team by providing certified bridge evaluation expertise for the field evaluations proposed in Task I. As an outcome, the proposed research permits MDOT design and maintenance engineers to have a quantifiable understanding of the relative importance of the causes leading to abutment distress

and ways to minimize or avoid them. In addition, the project delivered software that can predict bridge abutment condition using bridge design parameters so that the management of maintenance and the development of new designs for bridges can be improved.

1.4   Scope and Organization

This report presents the research work related to the identification of causes behind structural distress in bridge abutments and the development of strategies for relieving this damage. The report is organized in eight chapters following the research general research tasks outlined in Section 1.3. Chapter 2 presents the effort aimed at developing a suitable database of abutment distress records for use in statistical analyses and the development of predictive models. Chapter 3 summarizes the statistical analyses conducted on the evidential abutment distress database with the objective of identifying significant design and service parameters that may be the source of the structural distress. Chapter 4 provides a summary of the field evaluation of bridge structures with different levels of abutment damage done with the objective of verifying the inspection database and identifying critical and non-critical parameters regarding abutment distress. Chapter 5 outlines finite element simulation studies aimed at developing a virtual database of bridge response due to different parameters and to identify the relative importance of abutment damage sources. Chapter 6 outlines the theory, methods and results on the implementation of artificial neural networks for the development of diagnosis models to predict the life-time structural condition of bridge abutments. Chapter 7 deals with a discussion based on the results from the project on what the potential causes behind abutment distress might be and recommends methods to alleviate the problem. Chapter 8 presents a summary of the research findings and the concluding recommendations from this research project. Finally, additional data and results from the different parts of the project are provided in five different appendices with the objective of keeping the length of the main report as short as possible.

2 Information Database (Task I)

2.1 Introduction

In order to identify the potential causes of bridge abutments directly and develop an information and data bank for the other analyses and simulations in this research, an information database was created. Four approaches were taken to development of the database: literature review, exploration of MDOT field inspection database, field visits to typical bridges, and State DOT surveys. A major part of the information database was data from the National Bridge Inventory bridge inspection records, which document design and operation parameters as well as abutment inspection ratings of highway bridges. The information database provided important information for the subsequent simulations, analyses, as well as field instrumentations in this research.

2.2 Literature Review (Subtask I.1)

The uncertainties on the causes behind the observed abutment damage motivated the need for a more extensive literature review with the attempt to learn more about this type of distress. Continuous literature review throughout the length of this project failed to identify any published document that described a problem similar to the one being addressed by this project. Attention then focused on trying to identify literature related to the causes hypothesized as the sources of damage. Even then, some information was found on the suspected sources of damage but without information or direct correlation to the distress in abutment walls. A brief overview follows.

Several projects have evaluated the negative effects of rusted or "locked" pin-hanger assemblies on steel girder bridges. Little documentation exists on the distress induced by this effect and most work has focuses on the potential danger of hanger fracture or pin slip (due to pushing forces from the rust buildup). Nonetheless, some analytical work has provided evidence that the reaction forces at the abutments due to locked pin-hangers can be significant and as analyses suggest values as high as 2.5 times the stress level to initiate yield when full fixity is assumed (Elewa 2004).

Recent publications (Burke 1998, 2004) indicate that pavement growth is one of the possible causes of abutment damage, which is consistent with the expectations of MDOT bridge

engineers. As discussed in Chapter 1, the phenomenon consists on the gradual movement of pavement slabs as joint gaps between them are reduced due to debris thus generating substantial pressures, and consequently movement, upon thermal expansion of the slabs. From the information provided by Burke (1998, 2004), Richards (1979) and Shober (1997), the magnitude of the induced compressive stress on bride deck slabs by the movement of pavement slabs towards bridge abutments is estimated to be approximately 1,000 psi

While the literature review process failed in identifying any direct published work on abutment distress, the related information on the possible sources of damage provided ideas for the systematic organization of the information database. It also helped clarify the mechanisms that could lead to abutment distress. The identification of important parameters in the damage of bridge abutments was necessary in order to extract relevant data and predictive parameters from the National Bridge Inventory (NBI) database, which was to be used as an evidential, or historical, database of damage for statistical analyses and diagnosis model development. While the NBI rating has provided a good mechanism to constantly evaluate the state of highway infrastructure, its use for statistical and predictive model development posed considerable problems since the data was highly scattered and clear patterns were not easily identifiable. The subjectivity and large deviation of the visual inspection for highway bridges used in the NBI database are discussed in a research report by the Federal Highway Administration (FHWA 2001) and a paper of Phares et al. (2001). The inspection process was found to be subjective and with large deviation, which supported initial struggles in interpreting the data and later provided justification to assess its variability.

In addition to the information mentioned in this section, considerable published information made part of this study. Rather than providing a complete summary of this effort here, the relevant literature information for different topics is presented in the appropriate sections throughout the report.

2.3   Exploration of MDOT NBI Database (Subtask I.1)

In order to keep bridges in good condition, MDOT maintains a bridge inventory database according to the National Bridge Inventory (NBI) system (Hartle et al., 1991), which was based on the manual inspection of bridge structural members at an interval of no more than two years.

The raw inventory database is organized by inspection cases; a unique ID was given for each inspection case, the bridge design, operation parameters and structural condition during that inspection are recorded with that inspection ID for further reference. The raw bridge inventory database includes values of more than 100 variables for each inspection case, and bridge abutment inspection rating is one of these variables. A 0-9 scale rating is used to record the conditions of highway bridge abutments, where a larger number means better condition and 0-4 means distress in the structural member. The following description of the abutment conditions according to each rating is taken from Michigan Structure Inventory and Appraisal Coding Guide (MDOT 2003).

9 NEW CONDITION. No deficiencies in any of the structural components that will affect the long term performance.

8 GOOD CONDITION. All structural components are sound and functioning as designed. There may be superficial cracking or weathering of protective coatings and/or dirt contamination on structural components.

7 GOOD CONDITION. All members retain full section properties and function as designed. There may be minor cracking in structural components

6 FAIR CONDITION. All members retain full section properties and function as designed. There may be some deterioration affecting structural members such as minor cracking, scaling, small scattered spalls, or shallow scour. Some protective coating failures.

5 FAIR CONDITION. Moderate deterioration affecting structural members such as cracking, scaling scattered spalls, minor settlement or shallow scour. Minor section loss in low or no stress areas. All members continue to function as designed.

4 POOR CONDITION. Considerable deterioration affecting structural members such as cracking, scaling,scattered spalls, partial settlement or, scour. . All members continue to function as designed.

3 SERIOUS CONDITION. Considerable deterioration affecting structural members. Structural, hydraulic,and/or load analysis may be necessary to determine if the structure can continue to function without restricted loading or immediate repairs.

2 CRITICAL CONDITION. Deterioration has progressed to the point where the structure will not support design loads and must be posted for reduced loads.

1 IMMINENT FAILURE CONDITION. Bridge is closed to traffic, but corrective action may put the bridge back in service.

0 FAILED CONDITION. Bridge closed.

Commercial software Infomaker 10.0 (Sybase Inc. 2004) was used to retrieve data from the raw bridge inventory database. The following exploration and analyses of the data was finished using commercial statistical software SPSS 13.0 (SPSS 2004) and SAS 9.0 (SAS 2004).

2.3.1 Initial data screening

Raw inventory data retrieved from the NBI database was initially screened to exclude outliers and erroneous observations. The criteria for this initial screening are shown in Table 2-1. Most of the MDOT highway bridges are in one of the three structural types: simple/cantilevered steel, continuous steel and prestressed concrete. Scatter plot matrix of abutment rating of simple/cantilevered steel bridges and seven parameters is shown in Figure 2-1. Each cell in the matrix was a scatter plot described the distribution of observations concerning two parameters on the abscissa and ordinate. It can be seen from Figure 2-1 that the database was highly complicated and no clear trend can be observed. Some observations had almost identical predictors' values but with abutment rating differentiated from each other by more than 1. Those confusing observations were highly detrimental to the development of prediction models as well as identification of causes of abutment damage. Thus, they were deleted from the database. The deleted observations accounted for less than 3% of all the observations.

Table 2-1 Criteria for data extraction

#	Parameters	Criteria
1	*userbrdg_legal_cd**	1
2	*abutment rating*	0~9
3	*built year*	>0
4	*maximum span*	>0
5	*deck area*	>0
6	*deck width*	>0
7	*skew angle*	>=0
8	*average daily total traffic*	>0
9	*truck percentage*	not equal -1
10	*type of design/construction*	>=0 & not equal 18 & not equal 19
11	*inspection year*	no earlier than built year
12	*year at which daily traffic was measured*	>=0

* userbrdg_legal_cd is MDOT Legal system, 1=MDOT, 2=County Primary, 3=County Local, 4=City Major, 5=City Minor, 6=Other. Userinsp_abut_rtg_cd is abutment rating.
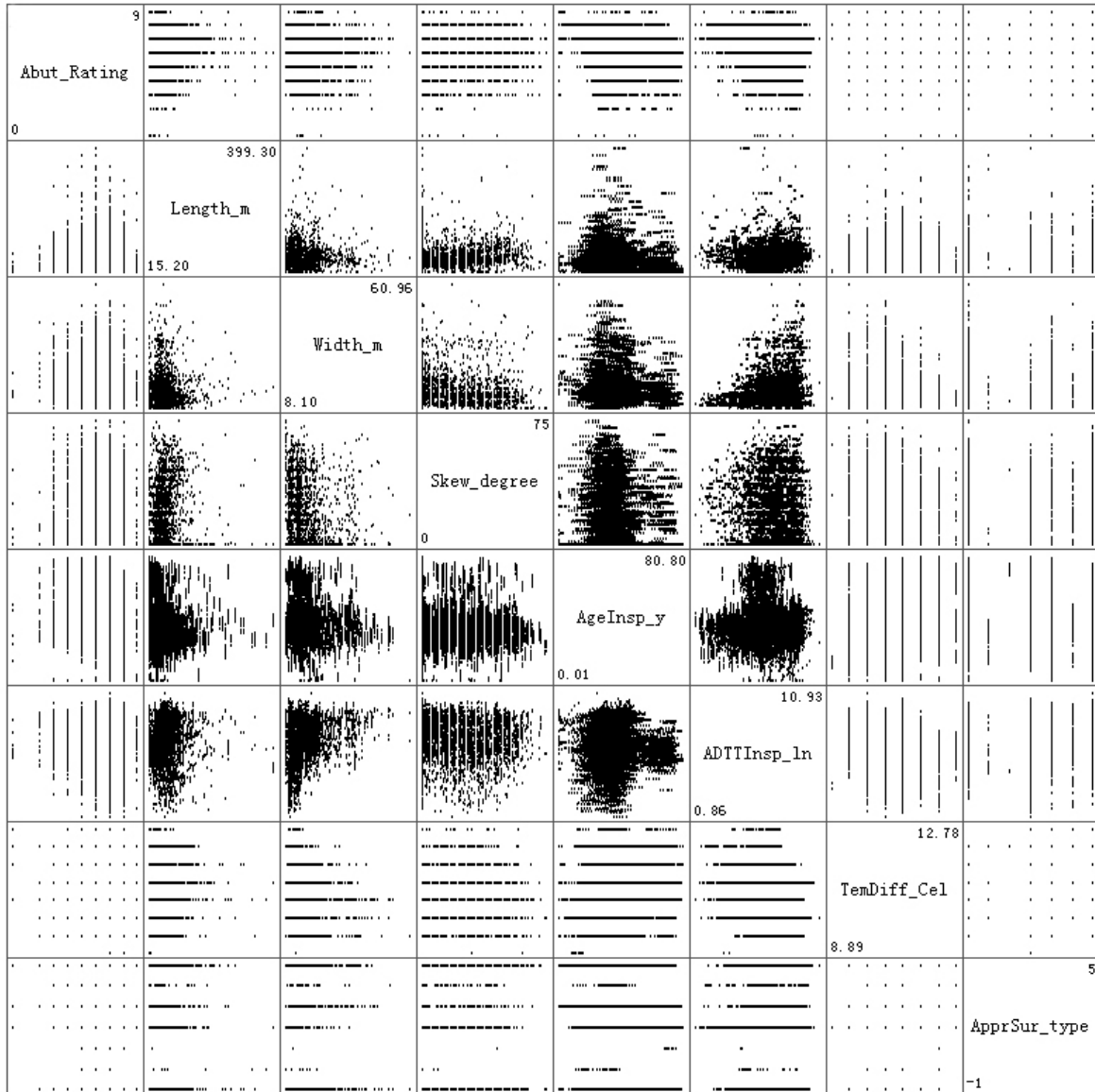
Figure 2-1 Scatter plot matrix of simple/cantilevered steel bridges

2.3.2 Parameter definition

The definitions for the variables used in this study are listed in Table 2-2.

<center>**Table 2-2 Parameter Definition**</center>

Parameter	Definition
design load	live load for which the structure was designed
*Matdiff**[1]*	annual temperature difference
*Ageinsp**[2]*	age of bridges at the time of inspection
*Apprsurstif**[3]*	approach surface stiffness
*ADTT**[4]*	average daily truck traffic at the time of inspection
maxspan	maximum span of the bridges
length:	total length of the bridge (m)
deck width	total deck width (m)
pinnum	number of pins
radskew	skew angle of the bridge (rad)
skew:	Skew angle of the bridge (degree)
*Materialmain**[5]*	main structure type

[1]: The difference between mean annual maximum temperature and mean annual minimum temperature for each county in Michigan, which were estimated from corresponding graphs.

[2]: Obtained by subtracting built year from inspection date (months and days are converted to years after divided by 12 and 365 respectively).

[3]: It was converted to three indicator variables in the statistical and ANN models.

[4]: Average daily truck traffic at the time of inspection. The average daily truck traffic (ADTT) is the product of the average daily traffic and corresponding truck percentage for each bridge. The average daily traffic data given in the database MICH021704.db is not always measured in the same year for each bridge. Since average daily traffic changes with time, the application of the average daily traffic data directly as input of ANN without accounting for the year in which it is measured will introduce additional errors on the model. Thus, all of the ADTT retrieved for the individual bridges were converted to the ADTT measured at the time of inspection by the following procedure.

First, estimate the ADTT increase rate (ADTTinc) by Eqn. (2-1) for each bridge:

$$ADTTinc = \left(\frac{ADTT_{predicted}}{ADTT_{measured}} \right)^{\lambda} - 1 \qquad \text{(2-1)}$$

$$\lambda = \frac{1}{(Year_{predicted} - Year_{measured})} \qquad \text{(2-2)}$$

where: $ADTT_{measured}$ is the ADTT in the year in which it is measured, $Year_{measured}$ is the measured year for $ADTT_{measured}$ (months and days are converted to years after divided by 12 and 365 respectively), $ADTT_{predicted}$ is the predicted ADTT in the future, $Year_{predicted}$ is the year in which ADTT in the future is predicted.

The ADTT at the time of inspection ($ADTT_{insp}$) is then calculated as:

$$ADTT_{insp} = ADTT_{measured} \cdot \left(ADTTinc + 1 \right)^{\kappa} \qquad \text{(2-3)}$$

<center>19</center>

$$\kappa = (Year_{insp} - Year_{measured}) \qquad\qquad\qquad \textbf{(2-4)}$$

[5]: It was transformed to four indicator variables in the artificial neural network application.

2.3.3 Deficiencies of MDOT NBI database

Further exploration and advanced use of MDOT NBI database was constrained by these inherent difficulties:

a) The database is highly complicated and no conspicuous trend or correlation could be extracted. There is no one to one relationship between cause and effect of structural damage, which means many causes can lead to the damage of the abutment. Moreover, the relationship could be highly nonlinear; thus, very hard to be extracted if not impossible by simple statistical means.

b) Subjectivity exists in the manual inspection methods and a large variance happens in the adopted structural evaluation ratings. For the NBI system, it has been found that for the same structure, its ratings assigned by 49 bridge inspectors from 25 state departments were dispersed, with only 68 percent of them within ±1 (in a scale of 0 to 9) around the mean, 95 percent of them fall in ±2 around the mean (Phares et al. 2001). Even if all the bridges with the same design parameters were inspected by the same engineer, the ratings might still be different because the construction qualities can not be identical.

c) The values of some variables in some observations are missing or subjected to error. For instance, the approach pavement type (a parameter of importance to the damage of bridge abutments) for some bridges in NBI database in the State of Michigan is missing.

d) The distribution of the inspection records is unbalanced. Cases of severe damage are relatively rare in comparison with the large number of bridge abutments in relatively good condition.

2.4 Survey of State DOT (Subtask I.1)

The survey of state DOT on their experience with similar problems was submitted. To this date 26 surveys have been completed. Most of the states indicated not having the problem

experienced in Michigan. Only two states (Ohio and Ontario, Canada) indicated similar problems. The survey form is repeated in section 2.4.1 for reference.

2.4.1   SURVEY Form

1. Do the bridges in your state currently/previously suffer from growing distress in abutment walls? If the answer is NO please go to Question 6. If your answer is YES please continue.
   a. ___Yes
   b. ___No

2. What type of abutment distress is/was observed in the bridges in your State?
   a. ___Vertical cracks
   b. ___U-shape cracks under girder supports
   c. ___Both (a) and (b)
   d. ___Other: _____

3. What do you think are the most probable causes for the observed abutment distress in your state bridges?
   a. ___Temperature effects
   b. ___Inappropriate design of expansion joints/bearings
   c. ___Inappropriate operation of expansion joints/bearings due to corrosion
   d. ___Pavement growth
   e. ___Others: _____
   f. ___Don't know

4. Has your state developed strategies to alleviate or eliminate distress in bridge abutments?
   a. ___Yes. Please cite method: _____
   b. ___Not yet but we are currently developing one. Please cite method:
      _____
   c. ___No.

5. Has your state conducted or is currently conducting any research aimed at identifying the causes for abutment distress or to develop strategies to relieve this same damage?
   a. ___Yes. We have conducted prior research.
      i. Please cite reference/report: _____
   b. ___Yes, we are currently conducting some research.
      i. Please cite reference/report:
   c. ___No, we have not engaged in any research related to this problem.

6. Are you aware of any research related to distress in abutment walls conducted by others?
   a. ___Yes. Please cite: _____
   b. ___No

7. Are you aware of damage to abutment walls similar to the one being experienced in Michigan bridges?
   a. ___Yes. Please cite: _____
   b. ___No

Please provide the following respondent's information:
   Name:
   Position:
   Organization:
   Mailing address:
   Phone number:

Email address:

Thank you for your assistance in completing this survey.

2.4.2   Result Summary

The result of the survey is summarized in Table 2-3. Most of the states indicated not having the problem experienced in Michigan.

Table 2-3 Results of survey of state DOT

State	Q1	Q2	Q3	Q4	Q5	Q6	Q7	Name
AL	b					b	b	Buddy Black
AL (2)	b	a				b	b	Fred Conway
AK								
AZ								
AR								
CA								
CO								
CT								
DE	a	a	a, e (Differential settlement), f	c	c	b	a	Jiten K. Soneji
DC								
FL	b					b	b	Richard I. Kerr
FL (2)	b					b	b	Lex Collins
GA	b					b	b	Paul V. Liles, Jr.
HI	a	a	e (shrinkage of concrete with some contribution from temperature effects)	c	c	b	b	Paul Santo
ID								
IL	a	a	a, c, d	a (Use more integral abutments, and convert existing bridges to semi-integral abutments)	c	b	b	Tom Domagalski
IN								
IA	b*					b**	b	Bruce Brakke

*Present Michigan DOT design information requires abutment walls to be a minimum thickness of 2'-0. Iowa's standard integral abutment is 3'-0 thick and relatively heavily reinforced. Iowa's stub abutment details show a 1'-3 backwall and a 3'-8 thickness below the girder seat. Standard Iowa abutment details are available of the Iowa DOT web site, Office of Bridges and Structures pages.

**South Dakota had a problem with abutment movement (which is different from the Michigan problem). The 1990 report is indexed by TRIS.

State	Q1	Q2	Q3	Q4	Q5	Q6	Q7	Name
KS	a	a	a	b (Our Abutment problems are generally minor in nature - hairline vertical cracks for the most part or water damage from leaky expansion joints. We do have some isolated cases where we have pushed the limits on integral abutments and we will continue to do so to eliminate expansion joints. We have had some isolated cases of design (poor geology) or construction problems but these were isolated cases.)	c	b	b	Donald E. Whisler
KY								
LA								
ME								
MD	b					b	b	Earle S. Freedman
MA	b					b	b	Alexander K. Bardow
MI								
MN								
MS	a	a	a, b, c, e (Traffice impact)	c	c	b	b	BRIDGE INSPECTOR
MO	b					b	b	Dennis Heckman
MT	b					b	b	Kent Barnes
NE	b					b	b	Terry Holman
NV	a	a	a, e (Possible settlement issues)	a (Epoxy injection of cracks)	c	b	b	Marc S. Grunert
NH								

State	Q1	Q2	Q3	Q4	Q5	Q6	Q7	Name
NJ	a	C	c, e (Settlement or rotation of substructure units)	c	c	b	a (We have many examples of bridges with u-shaped cracks under bearings and vertical cracks in piers. The vertical cracks are usually the result of vertical differential settlements and the u-shaped cracks are usually caused by frozen bearings or substructure rotation.)	James Lane
NM	a	C	a, c	b (We replace bearing devices as needed. Have been reactive to date. Not proactive with repairs. Generally see this on pier caps more that abutments.)	c	b	a (At NMDOT we usually see this at the piers rather than the abutments, however we have had)	Jimmy D Camp
NY	a	a, d (Alkali-Silica reactions)	d	c	c	b	b	William J. Moreau
NC								
ND	b					b	b	Tim Schwagler
MP								
OH								
OK	a	c	d, e (construction method & practice)	c	c	b	b	Ali Salami
OR								
PA								
RI	b					b	b	David Fish
SC								
SD								

State	Q1	Q2	Q3	Q4	Q5	Q6	Q7	Name
TN	b						b	a (We would need to see pictures or sketches in order to say.)	Edward P. Wasserman
TX	b					b	b		Keith Ramsey
UT									
VT									
VA									
WA	b					b	b		Bijan Khaleghi
WV									
WI	a	a	a, e (Inappropriate operation of expansion joints due to debris; differential settlement for abutments constructed on spread footings.)	a (Limit bridge length for integral, fixed seat abutments with wing piles; clean expansion joints as necessary; most abutments are constructed on piles.)	c	b	b		Bill Dreher
WY	a	d (Movement of the abutments in toward the bridge)	e (earth force)	a (Fabric reinforced backfill)	c	b	b		Jerry Ellerman
Alberta (CAN)	b					b	b		Raymond Yu
Ontario (CAN)		B					b	a (vertical cracks due to shrinkage and temperature effect for wide abutments, usually occur in abutments wider than 20 m without control joint)	David Lai

2.5   Field Visit to Typical Bridges (Subtask I.2)

Considering the difficulties in the analysis of the MDOT NBI database, field visits to typical bridges were conducted to provide supplementary information for this research.

2.5.1   Objective

Field visit of typical bridges has following objectives:

➢ Perform a more detailed evaluation of the identified parameters;

➢ Collecting information for developing an effective field instrumentation plan;

➢ Evaluate damage patterns for different bridge super- and sub-structures;

➢ Identify potential causes of typical abutment damages.

Field visits of 44 bridges were done in two phases with the cooperation of CTE Engineers (Lansing, MI). Nine (9) simple/cantilevered steel bridges, 8 continuous steel bridges and 9 prestressed concrete bridges were visited in Phase 1; and as a supplement to Phase 1, 2 simple/cantilevered steel bridges, 6 continuous steel bridges and 10 prestressed concrete bridges were inspected in Phase 2. Phase 1 was carried out from May 31 to June 7, 2006. The bridges visited in Phase 1 were decided based on the common features of bridges susceptible to abutment distress. Upon the completion of the first inspection phase it was found that additional information was necessary since the collected data was not enough to cover all major bridges and damage scenarios. Phase 2 was then carried out from June 28 and June 29, 2006.

Typical damage patterns for bridge abutments can be summarized as: U-shaped pulled out of concrete, vertical cracks in the abutment wall (between girders), and vertical cracks in the abutment wall (underneath girders). Possible causes of these damage patterns are approach pavement growth, transverse expansion of the superstructure, and unintended or unaccounted fixity of bearings. Detailed inspection records with photographs were created for all bridges as part of the information database and served as basis for the selection of bridges for field monitoring (Task II).

2.5.2 Selection of Bridges

The typical bridges visited in this research were decided based on the common features of those susceptible to abutment distress identified through statistical analyses.

2.5.2.1 *Frequency Analysis*

Frequency analyses about the key parameters were carried in order to determine the bridges with high possibility to show poor abutment rating. The data set for the frequency analysis was organized in two ways. One se of data was defined by extracting only the last inspection for each bridge to account for the current situation of MDOT highway bridges. The second set of data was determined by extracting the last four inspections for each bridge to overcome the subjectivity in inspection process.

The conclusions from the frequency analysis are summarized as the follows:

1. Simple or cantilevered steel bridges with length>=250 ft, deck area>=15000 ft^2, average daily traffic>=30,000, deck width>=60 ft, and product of deck width and skew between 1 and 600 ft^2 had a high possibility of poor abutment rating.

2. Continuous steel with length>=400 ft, deck area>=15,000 ft^2, skew <=20°, operation capacity rating less than 50 ton or between 90 tons to 110 tons, and a product of skew angle and deck width of less than 600 ft^2 had a high possibility of poor abutment rating.

3. Prestressed concrete bridges with length between 150 and 200 ft or between 250 and 300 ft, deck area less than 2,500 ft^2, between 10,000 and 12,500 ft^2, or greater than 20,000 ft^2, and deck width less than 20 ft or between 60 and 80 ft had a high possibility of poor abutment rating.

2.5.2.2 *Common Features of Bridges Prone with Poor Abutment Rating*

The common features of the bridges that were prone to show poor abutment rating were identified. They are listed below for each of the three main types of superstructures under consideration.

A) *Simple or cantilevered steel bridges:* Bridges with length >= 250 ft, deck area >= 15000 ft^2, average daily traffic >= 30,000, deck width >=60 ft, and a product of deck width and skew between 1 and 600 (ft-deg) had a high possibility of poor abutment rating.

B) *Continuous steel bridges:* bridges with length >= 400 ft, deck area >= 15,000 ft^2, skew <= 20°, operation capacity rating less than 50 tons or between 90 and 110 tons, and a product of skew angle and deck width less than 600 (ft-deg) had a high possibility of poor abutment rating.

C) *Prestressed concrete bridges:* bridges with length between 150 and 200 ft or between 250 and 300 ft, deck area less than 2,500 ft, between 10,000 and 12,500 ft^2 or greater than 20,000 ft^2, and deck width less than 20 ft or between 60 and 80 ft had a high possibility of poor abutment rating.

2.5.2.3 Selection criteria

The criterion for the selection of bridges in Phase 1 is listed in Table 2-4, Table 2-5, and Table 2-6 for reference. For Phase 2, the selection criterion for simple/cantilevered steel bridges was not changed, as shown in Table 2-4. The criterion for continuous steel bridges changed slightly as shown in Table 2-7, since not enough unrepaired candidates were available based on the original criteria. For prestressed concrete bridges, Phase 2 focused on bridges with I-girder beams or spread box beams, whose populations were small, thus no additional criterion was applied except for the beam type.

For convenience of field instrumentation and thus enhance the efficiency of the research, the selection of bridges for field instrumentation focused on the counties surrounding Lansing. These counties are Barry (08), Calhoun (13), Clinton (19), Eaton (23), Genesee (25), Gratiot (29), Ingham (33), Ionia (34), Jackson (38), Livingston (47), Montcalm (59), Oakland (63), Saginaw (73), Shiawassee (76), Washtenaw (81), and Wayne (82). The number in the parenthesis was the MDOT county number.

Table 2-4 Criteria for simple/cantilevered steel bridge selection (in both phases)

#	Parameters	Criteria
1	*Length*	>=250ft
2	*deck area*	>=15,000ft2
3	*average daily total traffic*	>30,000
4	*deck width*	>60ft
5	*approach surface type*	"Concrete" or "Unknown"

Table 2-5 Criteria for continuous steel bridge selection (Phase 1)

#	Parameters	Criteria
1	*Length*	>=400ft
2	*deck area*	>=15,000ft2
3	*Skew*	<20
4	*skew multply deck width*	<600ft
5	*approach surface type*	"Concrete" or "Unknown"

Table 2-6 Criteria for simple prestressed concrete bridge selection (Phase 1)

#	Parameters	Criteria
1	*Length*	150ft~300ft
2	*deck area*	10,000ft2~15,000ft2
3	*deck width*	<20ft or 60~80ft

Table 2-7 Criteria for continuous steel bridge selection (Phase 2)

#	Parameters	Criteria
1	*Length*	>=400ft
2	*deck area*	>=15,000ft2
3	*Skew*	<20
4	*approach surface type*	"Concrete" or "Unknown"

Bridges were assigned simple ID labels for easy identification in the inspection planning as well as for the field evaluation. The ID nomenclature in the form "X n.n", where X is a capitalized letter indicating the structural type of the bridge, "A" means simple/cantilevered steel bridges, "B" represents continuous steel bridges and "C" stands for prestressed concrete bridges. The "n" before the dot is a number identifying the inspection phase, with "1" means Phase 1 and "2" means Phase 2. The "n" after the dot means the serial number of the bridge within certain structural type and inspection phase.

2.5.3   Inspection Phase 1

Nine (9) simple/cantilevered steel bridges, 8 continuous steel bridges and 9 prestressed concrete bridges were inspected during Phase 1. Relevant bridge features and results are shown in Table 2-8, Table 2-9 and Table 2-10. All of the prestressed concrete bridges inspected during Phase 1 had adjacent box beams and were relatively new; thus, no conspicuous damage was observed. For the steel bridges (both simple and continuous) visited in Phase 1, the typical damage patterns in their abutments is described in the following.

Table 2-8 Simple/cantilevered Steel Bridges Field Assessment Result (Phase 1)

ID	Bridge Key	Abut_rtg	Approach pavement	Length(ft)	Yearbuilt	ADT total	Skew	Location	Inspection
A1.1	82182123000S120	4 (R)*	HMA+shared with A1.2	280.84	1970	143000	20	IN DETROIT	✓**
A1.2	82182123000S130	4 (R)*	Concrete+shared with A1.1	331.037	1970	15300	45	IN DETROIT	✓**
A1.3	82182102000S060	7(6-7)*	Concrete	251.97	1976	38500	7	1.2 MI W OF PLYMOUTH	✓**
A1.4	(82182292000S050	7(6 &7)*	HMA (strait cracks conc?)	269.03	1974	32000	5	3/4 MI W OF W OF LI WAYNE	✓**
A1.5	82182293000R030	7 (3-4 & 5)*	Asphalt (some degradation, connector w/brige)	206.037	1972	48500	41	IN LIVONIA	✓**
A1.6	82182292000S110	7 (7)*	conc+HMA (strait cracks)	269.029	1974	32000	0	3/4 MI W OF WAYNE C LTS	✓**
A1.7	82182291000S110	4 (3 & 4-5)*	Concrete	359.91	1972	49000	0	IN ROMULUS	✓**
A1.8	25125132000S230	7 (7)*	Unknown in database, no comment in inspection	439.96	1976	63000	4	IN FLINT	✓**
A1.9	82182293000R020	8 (7 & 5-6)*	Concrete & Asphalt over Conc?	284.777	1971	55500	5	IN LIVONIA	✓**

* Information in the parentheses means the rating assigned to the bridge during the field evaluation, "R" means the bridge had been repaired, "-" means different ratings were assigned to two abutments, such as, 6-7 here means rating "6" for abutment A and rating "7" for abutment B;

** Symbols are used to categorize the candidates, where "✓" means good candidate, "*" means the candidate provided limited information, and additional candidate is needed, "×" means the information doesn't match, or the structure type is not common, we need to replace the candidate with a new one;

Table 2-9 Continuous Steel Bridges Field Assessment Result (Phase 1)

ID	Bridge	Abut_rtg	Approach pavement	Length(ft)	Yearbuilt	ADTtotal	Skew	Location	Inspection
B 1.1	63163103000S050	3 (4 & 3)	RC s ~30' w/ cracks ~ 10'	669.947	1971	56300	3	IN ROYAL OAK	✓****
B 1.2	82182194000S170	3 (6-7 & 3)	HMA overlag on Conc. Prob Conc. road for same feature	248.031	19700	16560	4	IN DETROIT	✓****
B 1.3*	34134044000B014	6	Reinforced Concrete	414.042	1959	15000	0	.2 MI W OF PORTLAND	×****
B 1.4	82182252000S330	5 (7)	Concrete	659.12	1969	17730	0	IN DETROIT OVER I-75 RAMP	✓****
B 1.5**	82182195000P020	6	_	917.98	1970	83000	0	IN DETROIT	×****
B 1.6*	34134081000R010	7	Concrete	414.042	1950	11800	0	IN BELDING	×****
B 1.7***	63163172000S190	7 (7 & 2+)	Concrete	546.92	1990	9000	1	I-75 EAST OF PONTIAC	✓****
B 1.8*	34134044000B013	6	Concrete	414.04	1959	15000	0	0.2 MI W OF PORTLAND	×****

* The structure system of B1.3, B 1.6 and B1.8 are not common, it has two main girders to support the structure;

** Bridge B 1.5 is a pedestrian bridge, even though the adt is shown to be 83000;

***There is some confusion about location of bridge B 1.7; it was inspected in the second phase even though the skew angle did not match.

**** Symbols are used to categorize the candidates, where "✓" means good candidate, "*" means the candidate provided limited information, and additional candidate is needed, "×" means the information doesn't match, or the structure type is not common, we need to replace the candidate with a new one;

Table 2-10 Prestressed Concrete Bridges Field Assessment Result (Phase 1)

ID	Bridge	Abut_rtg	Approach pavement	Length(ft)	Yearbuilt	ADTtotal	Skew	Location	Inspection
C 1.1*	82182022000R010	3		284.9	2003	25000	17	4.0MI W OF TAYLOR	✗**
C 1.2*	82182022000R020	2		284.9	2003	25000	17	4.0MI W OF TAYLOR	✗**
C 1.3	63163102000S230	6		154.86	1986	20000	0	IN ROYAL OAK	✗**
C 1.4	63163102000S330	6 (6-7)	Asphalt (transverse to bridge)	174.87	1987	2400	0	SOUTHF'LD,W/CENT PK BLVD.	✓**
C 1.5	59159032000B010	7 (7 & ?)	Asphalt	175.85	1994	15000	0	IN GREENVILLE	✓**
C 1.6	13113012000B010	7 (6)	Asphalt (distress patterns)	173.88	1982	5000	0	0.2 MI N OF I-94 BL	✓**
C 1.7	63163102000S190	7		153.87	1985	1500	0	EAST OF COOLIDGE	✗**
C 1.8	82182123000S290	9 (7 & 8-9)	Conc w/ slee per slab (near abut)	173.88	2001	11970	0	IN DETROIT	✓**
C 1.9	82182022000R100	8	HMA	165.03	1996	0	48	CITY OF ROMULUS	✓**

* C 1.1 and C 1.2 were completely reconstructed;

** Symbols are used to categorize the candidates, where "✓" means good candidate, "*" means the candidate provided limited information, and additional candidate is needed, "✗" means the information doesn't match, or the structure type is not common, we need to replace the candidate with a new one; All the five bridges with ✓ for the inspection all adjacent box beams.

2.5.3.1   U — shape pull out

The abutment of bridge A 1.7 with U-shape pull out damage is shown in Figure 2-2 a. It can be seen from Figure 2-2 b that the pavement and approach slab for this bridge are of concrete; which would generate much larger compression pressures due to "pavement growth" with time. Upon inspection of the bridges, it was strongly believed that this type of damage was induced by the compression forces generated by pavement expansion or pavement growth, which transferred forces from the integral backwall through the girder anchor bolts down to the abutment wall.

(a) U – shape pull out underneath girder   (b) Concrete approach pavement
Figure 2-2 Abutment Distress and Pavement for Bridge A 1.7

2.5.3.2   Vertical cracks between girders

Another typical damage pattern observed were vertical cracks in the abutment wall located between girders, as shown in Figure 2-3. Figure 2-3a shows the general view of the abutment wall and part of the superstructure. The vertical cracks in the abutment wall can be seen in the close-up view in Figure 2-3b. It was strongly believed that this type of damage pattern is mainly caused by the restrained support forces generated due to transverse thermal expansion of superstructure system.

2.5.3.3 *Vertical cracks underneath girder through dowel*

The third important observed damage pattern was that of vertical cracks in the abutment wall located underneath the girder, as shown in Figure 2-4a. It can be seen from Figure 2-4b that the bearing of this bridge has corroded, thus providing unintended fixity at the girder supports. Thus, displacements or rotations of the superstructure will cause additional stress in the abutment due to the increased stiffness of the bearing.

Vertical crack in abutment wall (between girders, amplified in the right figure)
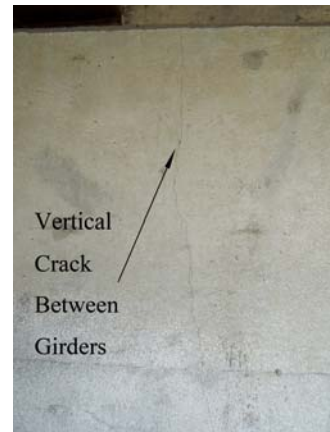
Vertical
Crack
Between
Girders

(a) General view of abutment wall   (b) Detailed view of the vertical

Figure 2-3 Overview and Close-up of Abutment Distress for Bridge A 1.4
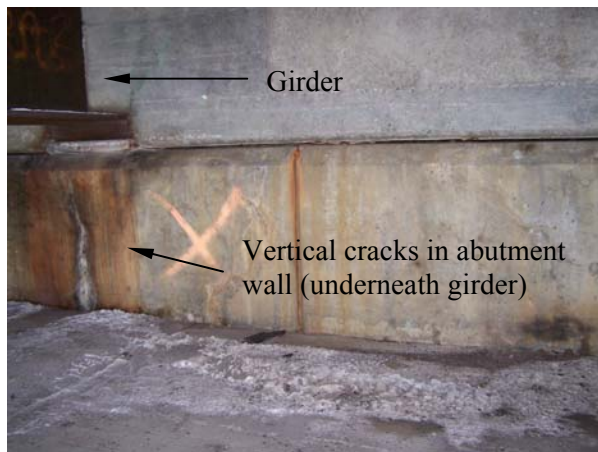
Girder

Vertical cracks in abutment wall (underneath girder)
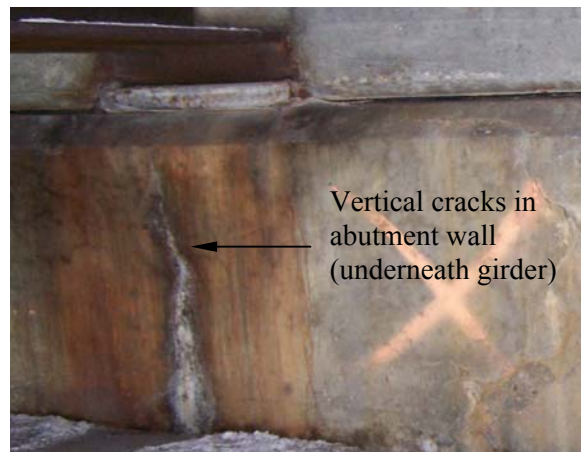
Vertical cracks in abutment wall (underneath girder)

(a) General view of abutment wall   (b) Detailed view of the vertical cracks between

Figure 2-4 Abutment Distress in Bridge B 1.1

2.5.3.4 Discussion

Most of the objectives for field inspection were reached during Phase 1. However, there were still some issues needed to be solved and thus made an additional inspection phase necessary. These issues are listed and described below.

a) A few candidates had been repaired or reconstructed completely. One of these bridges is A 1.1, as shown in Figure 2-5a. Concrete "patches" under each girder seem to have repaired U-shape girder pull out damage in the abutment wall. The superstructure type of a few bridges didn't meet the inspection goals.

b) All the prestressed concrete bridges visited were with adjacent box beams. They were relatively new and almost no sign of distress was present, as shown in Figure 2-6.

c) Two of the bridge candidates were difficult to be located and identified.

(a) Repaired abutment wall with U – shape patch   (b) Concrete approach pavement

Figure 2-5 Bridge A 1.1

(a) General view of abutment and adjacent box   (b) Detailed view of the abutment wall (good

Figure 2-6 Bridge C 1.6

2.5.4 Inspection Phase 2

In order to solve the issues remaining from Phase 1 and thus make the field evaluation representative and effective, Phase 2 was carried out. Two (2) simple/cantilevered steel bridges, 6 continuous steel bridges and 10 prestressed concrete bridges were inspected in Phase 2. The typical damage patterns were similar to those in Phase 1, summarized in Section 2.3. Vertical cracks in the abutment walls of prestressed concrete bridge with I girder are shown in Figure 2-7 and minor cracks in the abutment wall of a prestressed concrete bridge with spread box beams are shown in Figure 2-8.
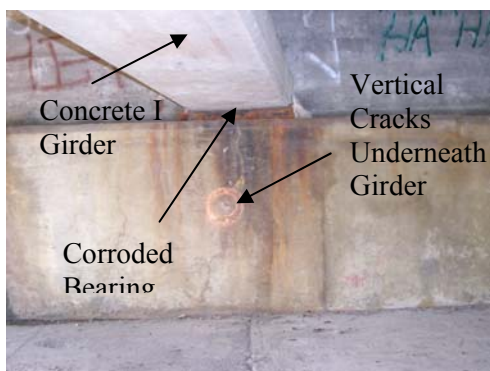
(a) Abutment wall and I Girder   (b) Detailed view of crack in abutment wall
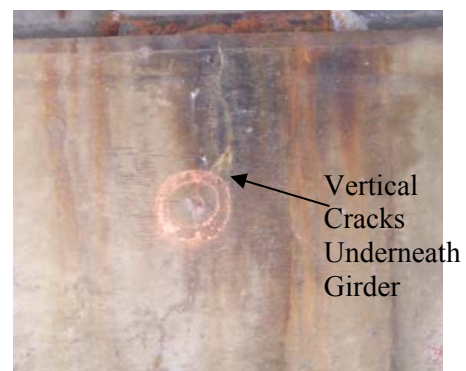
Figure 2-7 Abutment Distress in Prestressed I-girder Bridge – Bridge C 2.3
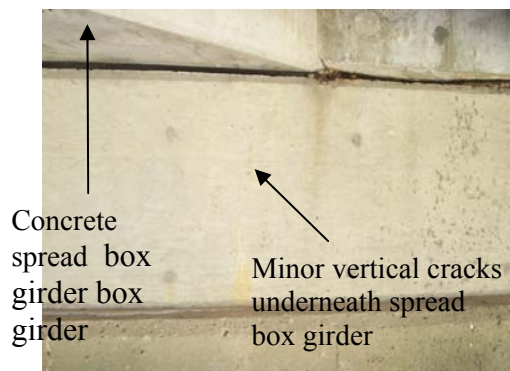
| (a) Abutment and spread box | (b) Detailed view of minor crack in the abutment |
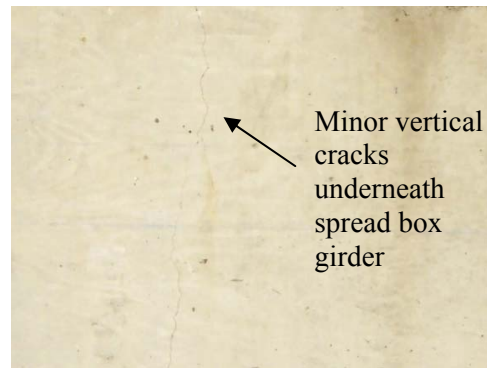
Figure 2-8 Abutment Distress in Prestress Spread-Box Beam Bridge – Bridge C 2.5

The bridges visited during both phases of the field inspection were representative for major types of MDOT highway bridges and were selected with parameters that categorized them to be susceptible to abutment distress. The field inspection and assessment was very helpful in identifying typical damage patterns and their possible causes. Detailed inspection records and photographs for each inspected bridge were documented as part of the information database and served as basis for selection of bridges for field instrumentation.

Table 2-1 Simple/cantilevered steel candidates (Phase 2)

ID	Bridge key	Abut_rtg	Beam	Approach pavement	Max_span(ft)	Skew	Yearbuilt	Adttotal	Location	Inspection
A 2.1	25125031000S110	7 (6)*	I Girder	Asphalt over Con**	63.976	14	1954	30611	W LTS OF FLINT	✓
A 2.2	82182022000S560	8 (7-8 & 7)*	I Girder	Asphalt**	190.945	48	1996	119000	CITY OF ROMULUS	✓

* value in the parenthesis is field inspection rating;

** information updated according to field inspection

Table 1-2 Continuous steel candidates after check (Phase 2)

ID	Bridge key	Abut_rtg	Beam	Approach pavement	Max_span(ft)	Skew	Yearbuilt	Adttotal	Location	Inspection
B 2.1	82182194000S150	4 (3-4 & 7)*	I Girder	Conc & HMA over Conc**	94.8163	16	1970	6800	IN DETROIT	✓
B 2.2	73173101000S150	5 (7&6)*	I Girder	Concrete**	119.751	9	1971	9945	2.6 MI N OF SAGINAW	✓
B 2.3	82182104000S040	6 (4-5)*	I Girder	Concrete over Asphalt?**	74.803	0	1971	7000	IN HIGHLAND PARK	✓
B 2.4	73173101000S190	6 (5-6)*	I Girder	Concrete**	119.751	0	1971	8490	1.6 MI N OF SAGINAW	✓
B 2.5	33133171000S040	7 (7)*	I Girder	Conc**	107.94	0	1970	26000	IN LANSING (M143 MICHIGAN	✓
B 2.6	33133171000S100	7 (7)*	I Girder	Conc**	107.94	0	1970	32500	IN LANSING (M143 MICHIGAN	✓

*value in the parenthesis is field inspection rating;

** information updated according to field inspection

Table 1-3 Prestressed concrete candidates (Phase 2)

ID	Bridge key	Abut_rtg	Beam	Approach pavement	Max_span(ft)	Skew	Yearbuilt	Adttotal	Location	Inspection
C 2.1	63163174000S061	4 (4)*	I Girder	Asphalt over Con**	49.869	5	1964	67500	IN TROY	✓
C 2.2	63163174000S081	4 (7&4)*	I Girder	HUA over Con**	62.992	0	1964	67500	IN TROY	✓
C 2.3	82182292000R010	5 (7&5)**	I Girder	Asphalt over Conc**	52.822	0	1974	32000	2.2 MI.W OF WAYNE	✓
C 2.4	25125132000S060	6 (7)*	I Girder	Conc**	62.992	1	1971	27400	IN FLINT	✓
C 2.5	47147065000R033	7	SpreadBox	Concret	67.913	47	1962	21500	3.5 MI SE OF M-155	✗***
C 2.6	19119033000S090	8 (8)*	I Girder	Asphalt**	105.971	0	1993	900	3.0 MI S OF ST JOHNS	✓
C 2.7	19119033000S070	8 (8)*	I Girder	Asphalt**	105.971	0	1993	8500	5.0 MI S OF ST JOHNS	✓
C 2.8	25125031000S010	8 (8)*	SpreadBox	Concret	72.835	30	1957	12000	OWEN RD (1 MI W / FENTON)	✗***
C 2.9	33133084000S140	8 (7-8 & 8)*	SpreadBox	Asphalt over Conc & Conc*	72.835	18	1963	37000	I-96 WB	✓
C 2.10	33133084000S020	9	SpreadBox	Concret	69.882	6	1963	16000	I-496 NB & US-127	✗***

* value in the parenthesis is field inspection rating;

** information updated according to field inspection

*** might be completely reconstructed.

2.6 Database Creation (Subtask I.3)

The information gathered in Subtasks I.1 and I.2 was organized into a consistent database to be used for field monitoring (Task II), finite element modeling and parametric studies (Subtask III.1), statistical and regression analyses (Subtask III.2), neural network simulations (Subtask III.3), and identification of potential causes of damage in bridge abutments.

After examining the field inspection database, it was found that the longest bridge is up to 1,9248 ft. However, more than 99.8% of them have their length less than 3281 ft. Thus, in this analysis bridges with lengths of more than 3,281 ft had been removed as outliers from the dataset. Due to some unknown error, the inspection data was prior to the built year for a few bridges. Thus, these records were removed from the dataset. Skew angle should be a value between 0 and 90 degrees. Since "99" in the record indicates a major variation in skew of the substructure units and "90" doesn't make sense in reality, the inspections records of bridges with skew values equal 90 or 99 were removed from the data set. Since more than 99.8% of the bridges have average daily truck traffic less than 30,000, the inspections about the bridges with average daily truck traffic greater than 30,000 were removed from the dataset. The criteria to refine the dataset are shown in Table 1-4. After filtering by the mentioned criteria, 905 inspections were deleted and the refined dataset was composed of 19,615 inspections.

Table 1-4 Criteria to refine the data set

#	Parameters	Criteria
1	*Length*	> 0 ft and < = 3281 ft
2	*Deckwidth*	> 0 ft
3	*skew angle*	> 0º and <= 75º
4	*Age at inspection*	>= 0
5	*Approachtype*	>= 0
6	*average daily truck traffic at inspection*	> 0 and <= 30, 000

2.7 Discussion

An information database was created in this research through four procedures: literature review, exploration of MDOT field inspection database, field visit to typical bridges, and State DOT surveys. A major part of the information database consists of bridge inspection records which documented design and operation parameters as well as abutment inspection ratings of MDOT highway bridges. The information database served as a foundation for the subsequent simulations, analyses, as well as field instrumentations in this research.

3 Statistical Analyses (Subtask III.2)

3.1 Introduction

Statistical analyses in this research served three major functions:

➢ Evaluate relative significance of different design parameters in the development of bridge abutment distress;

➢ Check the feasibility of developing regression models to predict bridge abutment condition given design and operation parameters;

➢ Provide information and guidance for other analyses, simulations, and instrumentation of this research;

Statistical analyses were carried out using the information database created in chapter 2. It consisted of frequency analysis, correlation analysis, factorial analysis, hypothesis tests, and regression analysis. The statistical analyses in the first year of this research were finished using commercial software SPSS 13.0 (SPSS 2004), the other part of statistical analyses were finished using commercial software SAS 9.0 (SAS 2004).

3.2 Frequency Analyses

Frequency analyses were aimed at finding out the distribution of highway bridge populations and identify common features of highway bridges that were susceptible to abutment damage. A large number of frequency analyses had been done in the first year of this research, which also included frequency analyses after further grouping the database. Since simple/cantilevered steel bridges account for more than 60 percent of the whole bridge population, frequency analyses were focused on this structural type when the database was sub divided.

3.2.1 Approach pavement type

Pavement pressure was one of the potential causes of bridge abutment damage, thus, approach pavement surface type was an important parameter. The frequency analysis of MDOT highway bridge inspections records concerning approach type was shown in Figure 3-1, in which, each column represents one structural type, where "*simstl*" means inspections of

44

simple/cantilevered steel bridges, "*constl*" denotes inspections of continuous steel bridges, and "*prscrt*" represents inspections of prestressed concrete bridges. Each row represents one type of approach surface type. For example, "*Bimcon*" means freeway designed bituminous concrete on aggregate base. The label "*unknown*" means there is a "_" for the corresponding value in the database. The ratios of poor abutment for each category in Figure 3-1 are shown in Figure 3-2.

After a detailed evaluation of Figure 3-1 and Figure 3-2, it can be concluded that for simple/cantilevered steel bridges and continuous steel bridges, the ratio of bridges with poor abutment rating was quite high for concrete approach types and "unknown" approach types. It was thus determined that the research work should focus on bridges with concrete approach type and "unknown" approach type. For prestressed concrete bridges, the ratio of poor abutment rating do not seem different for any of the approach types: Bitumen, Concrete or "Unknown", and the ratios of these three are much higher then those of "Bitumen Concrete." Thus the research work on prestressed concrete bridges should focus on bridges with these three types of approach pavement.
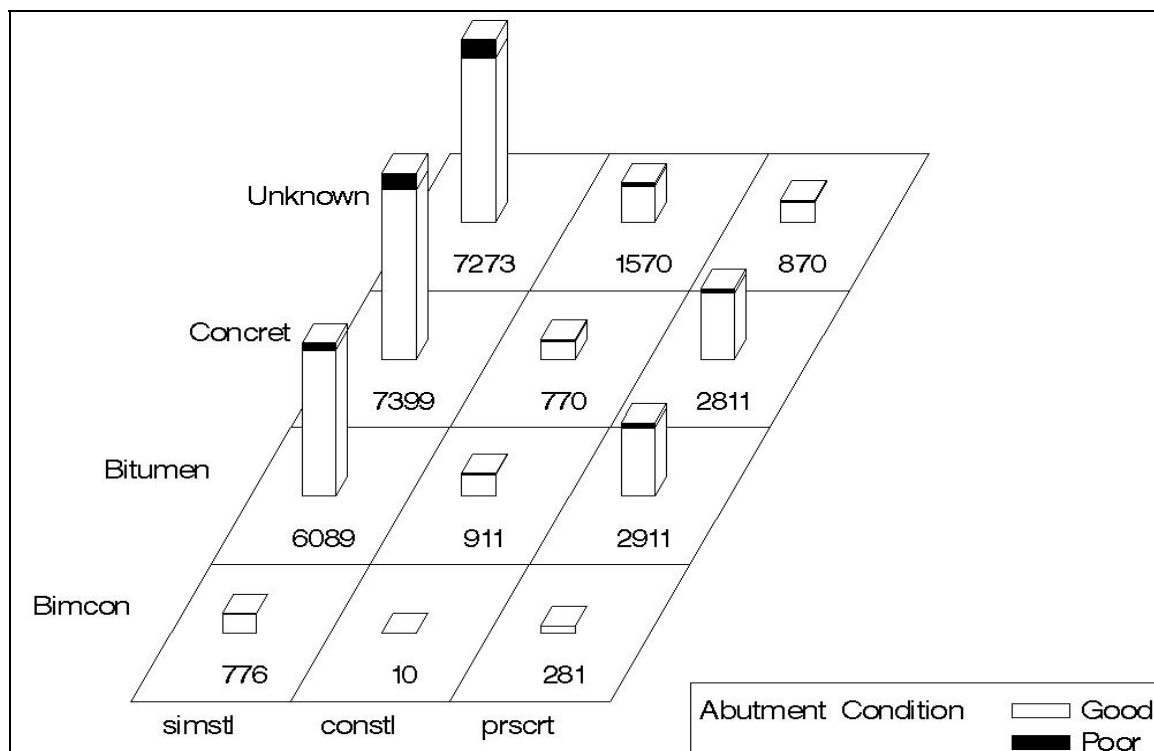
Figure 3-1 Frequency analysis of highway bridge inspections
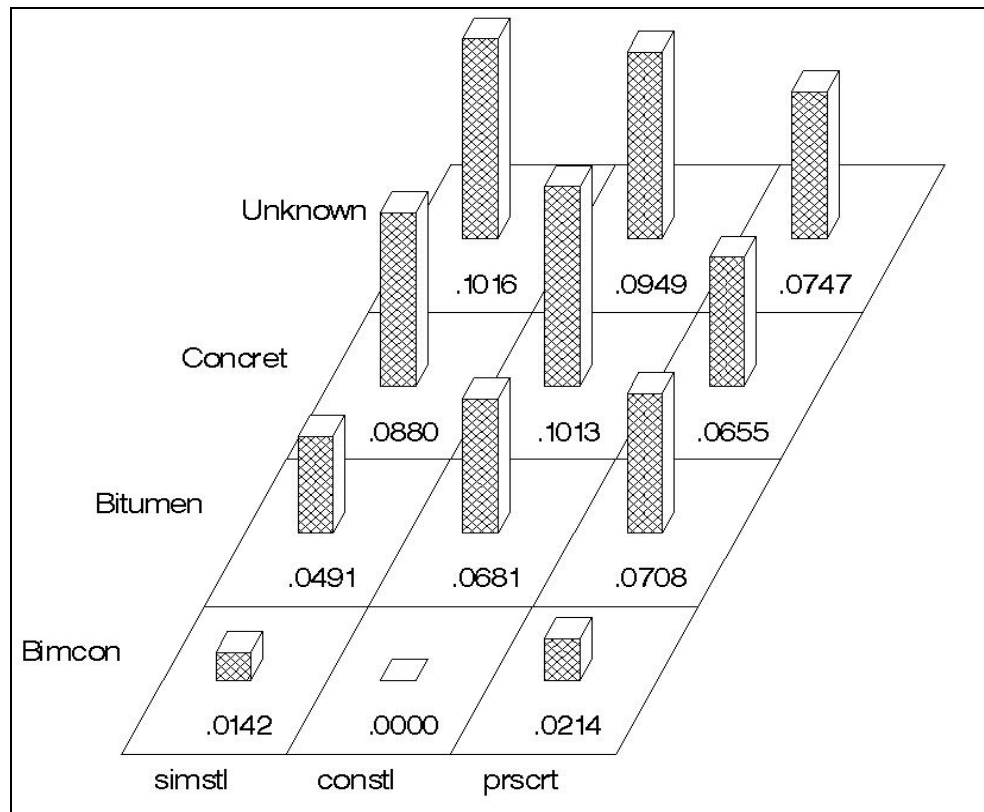
Figure 3-2 Ratio of poor abutment rating

3.2.2 Year Built

The number of simple or cantilevered steel bridges categorized by year built is shown in Table 3-1. The number of all bridge inspections and the number of bridge inspections with reported poor abutment rating were counted. The ratio between the number of bridge inspections which show poor abutment rating (0-4) and number of all the bridge inspections in each category is also shown in the table. A bar chart showing the proportion of the bridge records with poor abutment rating among all bridge inspections is given in Figure 3-3. The data shows that simple/cantilevered bridges built before 1930, between 1941 and 1945, between 1971 and 1975 have a higher records of poor abutment performance.

Table 3-1. Simple or cantilevered steel bridge inspections categorized by year built

abut_rtg \ Year built	<= 1929	1930 - 1949	1950 - 1959	1960 - 1969	1970 - 1979	1980+
0-4	88	134	91	333	395	31
0-9	391	1615	2235	7495	4657	756
0-4/0-9	22.5%	8.3%	4.1%	4.4%	8.5%	4.1%
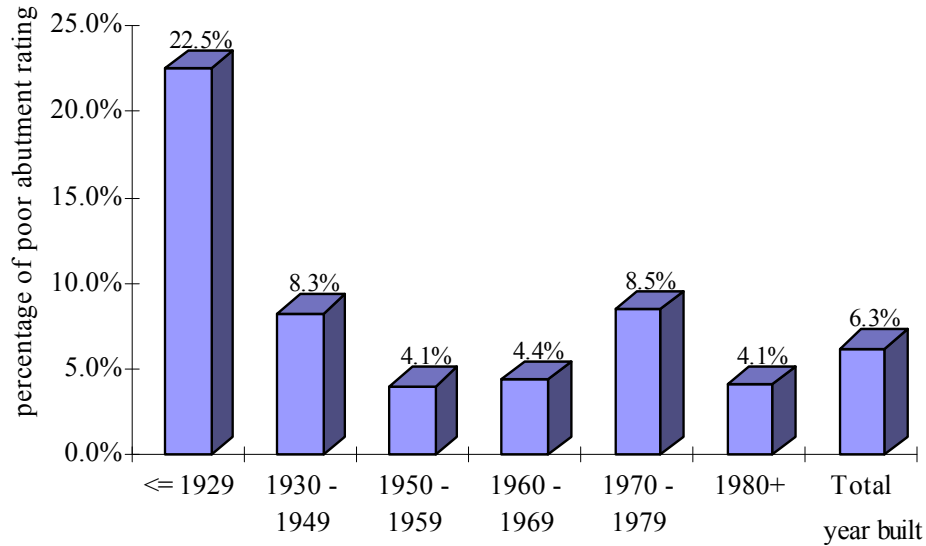
Figure 3-3. Abutment Rating per Year Built for Simple Steel Bridges

3.2.3 Age at Inspection

The count of simple or cantilevered steel bridges categorized by age at inspection are shown in Table 3-2. A bar chart with the record of abutment rating as a function of the age at inspection is shown in Figure 3-4. Similar to the year built records, the data confirms that older bridges, specifically those with an age at inspection greater than 60, show higher abutment distress levels.

Table 3-2. Simple or cantilevered steel bridge Inspections categorized by age at inspection

abut_rtg \ Age_at_insp	<= 26	27 - 36	37 - 46	47 - 56	57 - 76	77+	Total
0-4	162	501	157	54	169	6	1049
0-9	3427	6946	4283	891	1310	35	16892
0-4/0-9	4.7%	7.2%	3.7%	6.1%	12.9%	17.1%	6.2%
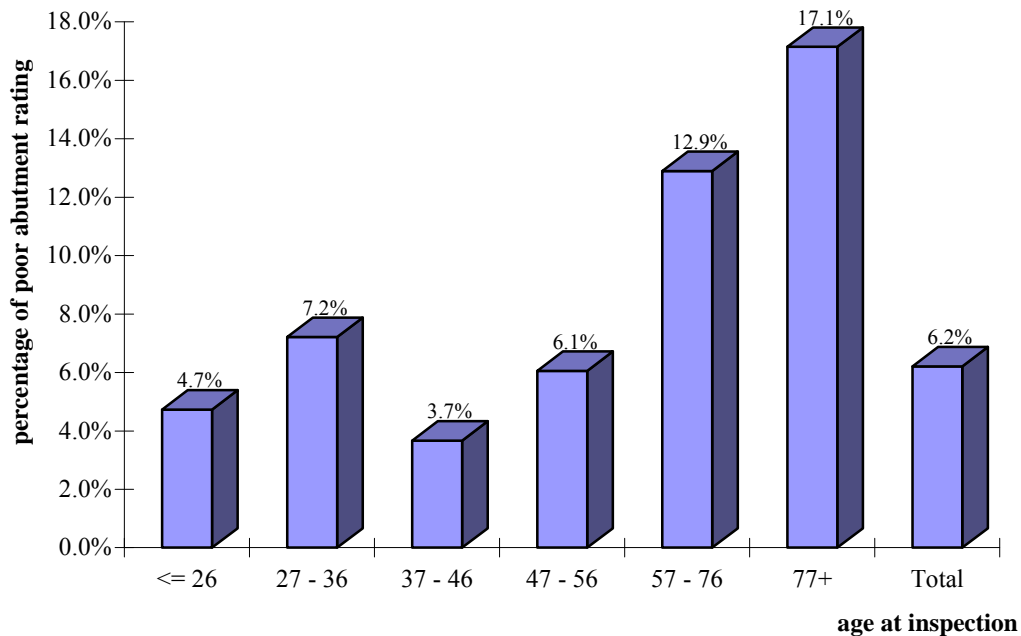
Figure 3-4. Abutment Rating per Age at Inspection for Simple Steel Bridges

3.2.4   Average Daily Total Traffic (ADT Total)

The abutment rating for simple or cantilevered steel bridges categorized by average daily total traffic is shown in Table 3-3. The data is represented graphically in the bar chart of Figure 3-5. The data shows that bridges with higher average daily total traffic have, in general, more incidences of poor abutment rating.

Table 3-3. Abutment Rating for Simple or Cantilevered Steel Bridge Inspections by ADT Total

abut_rtg \ adttotal	<= 1000	1001 - 10000	10001 - 50000	50001 - 100000	100001+	Total
0-4	11	368	509	148	36	1072
0-9	1196	7489	7286	919	257	17147
0-4/0-9	0.9%	4.9%	7.0%	16.1%	14.0%	6.3%
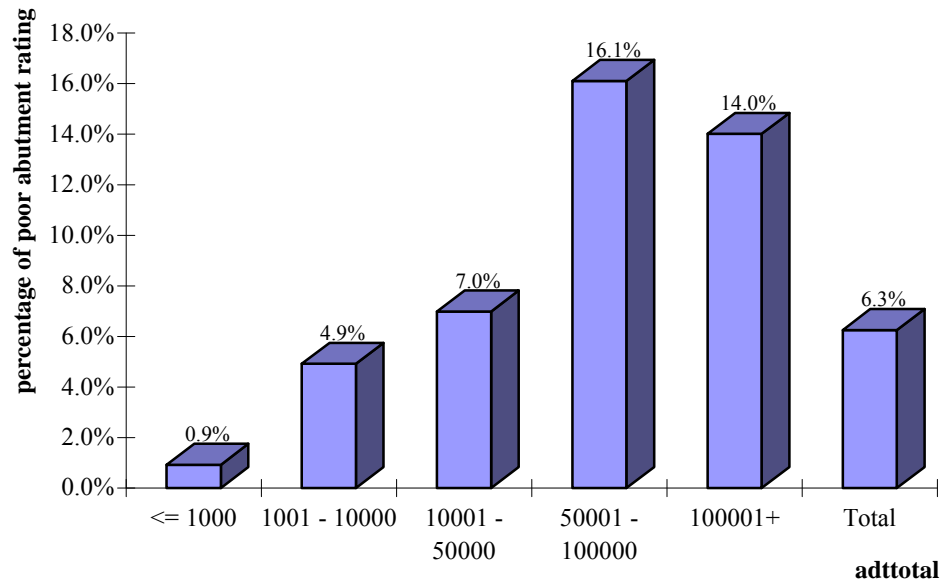
Figure 3-5. Abutment Rating for Simple or cantilevered steel bridges by ADT Total

3.2.5 Average Daily Truck Traffic (ADTT)

The count of simple or cantilevered steel bridges categorized by average daily truck traffic (ADTT) is shown in Table 3-4 and represented graphically in a bar chart in Figure 3-6. As with the ADT total values, the data indicates that poor abutment rating is more often reported in bridges with higher ADTT.

Table 3-4. Simple or Cantilevered Steel Bridge Inspections Categorized by ADTT

ADTT abut_rtg	<= 100	101 - 500	501 - 1000	1001 - 5000	5001+	Total
0-4	60	260	192	327	104	943
0-9	1857	4843	3007	4807	919	15433
0-4/0-9	3.2%	5.4%	6.4%	6.8%	11.3%	6.1%
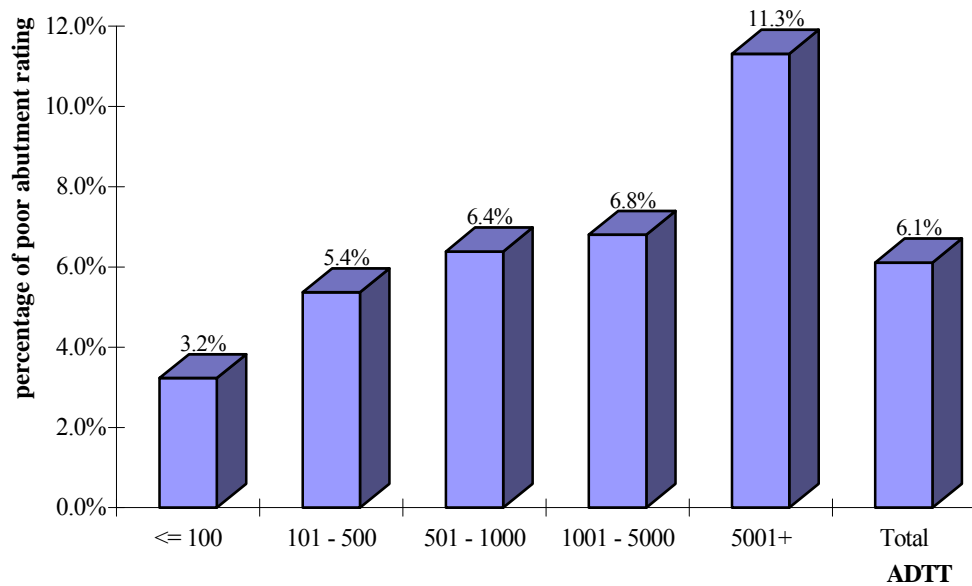
Figure 3-6. Proportion of poor abutment rating in terms of ADTT

3.2.6 Deck Width

The distribution of abutment ratings for simple or cantilevered steel bridges categorized in terms of deck width is given in Table 3-5. The ratio of bridges with poor abutment rating over the total number of records is shown in Figure 3-7. The data indicates that lower abutment rating is most often associated with wide bridges.

Table 3-5 Simple or cantilevered steel bridges categorized by deck width

Deckwidth / Abut_rtg	<= 20.0	20.1 - 30.0	30.1 - 35.0	35.1 - 40.0	40.1 - 45.0	45.1 - 50.0	50.1 - 55.0	55.1 - 60.0
0-4	0	75	29	146	101	151	59	95
0-9	1	1095	1826	2066	2674	2755	950	1325
0-4/0-9	0.0%	6.8%	1.6%	7.1%	3.8%	5.5%	6.2%	7.2%

Deckwidth / Abut_rtg	60.1 - 65.0	65.1 - 70.0	70.1 - 75.0	75.1 - 80.0	80.1 - 90.0	90.1+	Total	
0-4	86	50	69	20	47	144	1072	
0-9	1009	890	581	326	452	1199	17149	
0-4/0-9	8.5%	5.6%	11.9%	6.1%	10.4%	12.0%	6.3%	
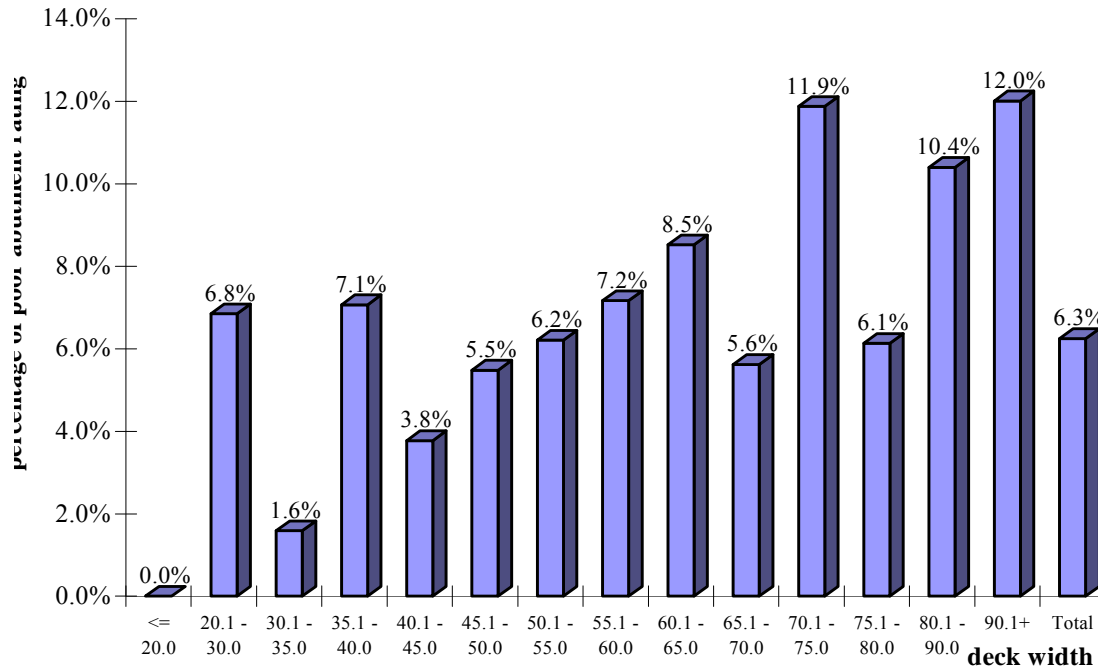
Figure 3-7. Proportion of poor abutment rating for different deck widths

3.2.7 Discussion

Through frequency analyses it was found that abutment damage was more common for bridge systems that have the following characteristics:

  ➢ Year built: pre 1980
  ➢ Age at inspection: more than 30 years.
  ➢ ADT Total: greater than 25,000
  ➢ ADDT: greater than 5,000
  ➢ Deck width: greater than 70 ft.
  ➢ Superstructure types: steel simple/cantilever, steel continuous, prestressed concrete
  ➢ Region: equal damage in all regions.

3.3　Correlation Analysis

Correlation analysis is an important statistical tool that provides means of drawing inferences about the strength of the relationship between two or more variables. That is, it is a measure of the degree to which the values of these variables vary in a systematic manner. Thus it provides a quantitative index of the degree to which one or more variables can be used to predict the values of another variable. Correlation analysis was applied in this research in an attempt to reveal the association between bridge abutment rating and explanatory parameters, such as design and operation variables. The degree of linear association between bridge abutment rating and explanatory parameters was reflected by value of correlation coefficient R. The value of R is in [-1, 1], the larger R value, the higher degree of linear correlation exists between bridge abutment ratings and explanatory variables.

3.3.1　Statistical theorem about covariance and correlation

Many indexes of correlation exist. The method that is used most frequently is the *Pearson product-moment* correlation coefficient. The conception of the Pearson correlation coefficient is to separate the variation of values of random variable *Y* into two parts: linear variation with random variable *X* and nonlinear variation. The correlation coefficient is defined as the ratio of linear variation to the total variation. That is, the fraction of the total variation that is explained by the linear relationship between *Y* and *X*.

Based on the concept mentioned above, Equation (3-1) is used to calculate the correlation coefficient *R*:

$$R = \frac{\sum\limits_{i=1}^{n} x_i y_i - \frac{1}{n}\left(\sum\limits_{i=1}^{n} x_i\right)\left(\sum\limits_{i=1}^{n} y_i\right)}{\sqrt{\sum\limits_{i=1}^{n} x_i^2 - \frac{1}{n}\left(\sum\limits_{i=1}^{n} x_i\right)^2}\sqrt{\sum\limits_{i=1}^{n} y_i^2 - \frac{1}{n}\left(\sum\limits_{i=1}^{n} y_i\right)^2}} \tag{3-1}$$

where x_i is the ith value of random variable *X*, i=1, 2, … , n; and y_i is the ith value of random variable *Y*, i=1, 2, … , n. If the linear variation of values equals the total variation, the correlation coefficient will equal 1. If the relationship between *X* and *Y* is inverse and the linear variation

equals the total variation in magnitude, R will equal -1. These conditions represent the extremes, but both values indicate a perfect association, with the sign only indicating the relationship. A correlation coefficient of zero, which is sometimes called the null correlation, indicates no linear association between the two variables X and Y (Ayyub and McCuen 1997).

The physical characteristics of the correlation coefficient are elaborated in Figure 3-8. The schematic in Figure 3-8a indicates that there is no linear relationship between the two random variables because; i.e., as the value of X is increased it is not certain whether Y will increase or decrease; the correlation coefficient is expected to be close to zero, and the two random variables can be considered to be uncorrelated. Figure 3-8b indicates a positive correlation between X and Y, that is, Y increases as X increases. However, the relationship is not perfectly linear, indicating that R is expected to be between 0 and 1.0. Figure 3-8c shows an example of perfectly positive correlation between the two random variables X and Y, Y increases linearly as X increases, data points (X, Y) form a straight line with a positive slope rate in the X, Y plane, the correlation coefficient is expected to be close to one. Figure 3-8d illustrated a case of perfectly negative correlation between the two random variables; thus, Y decreases linearly as X increases, data points (X, Y) form a straight line with a negative slope rate, indicating that R (expressed as ρ in the figure) is close to negative one. Figure 3-8e and Figure 3-8f indicates that there could be some nonlinear relationship between the two random variables, but since the relationship is not linear, R is expected to be zero.

If the correlation coefficient needs to be calculated from observed sample values, it is rare to obtain values of precisely zero, +1 or -1. Two random variables can be considered to be statistically independent if the absolute value of correlation coefficient is less than 0.3; and they can be considered to be perfectly correlated if the absolute value of correlation coefficient is greater than 0.9 (Haldar and Mahadevan 2000).

(a) ρ = 0

(b) 0<ρ<1

(c) ρ = 1

(d) ρ = -1

(e) ρ = 0
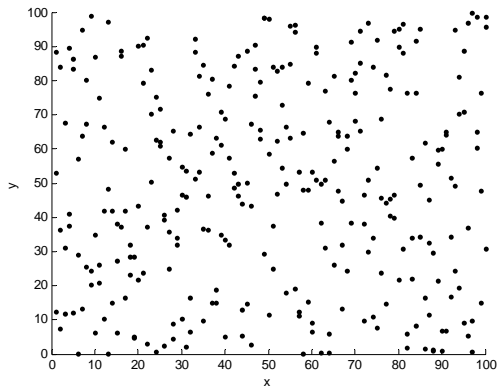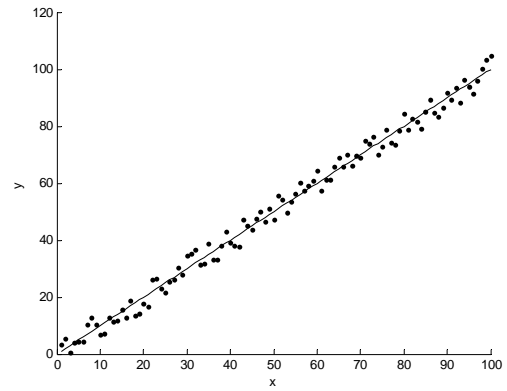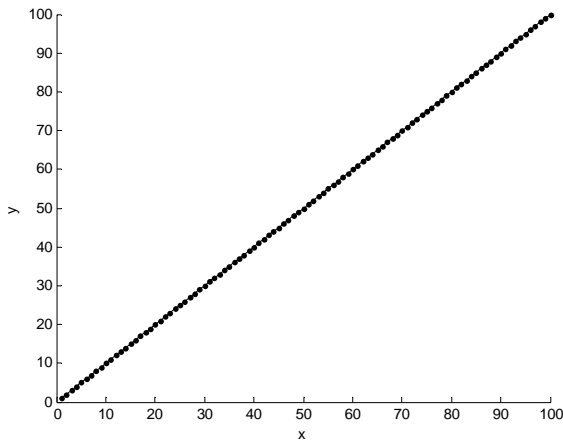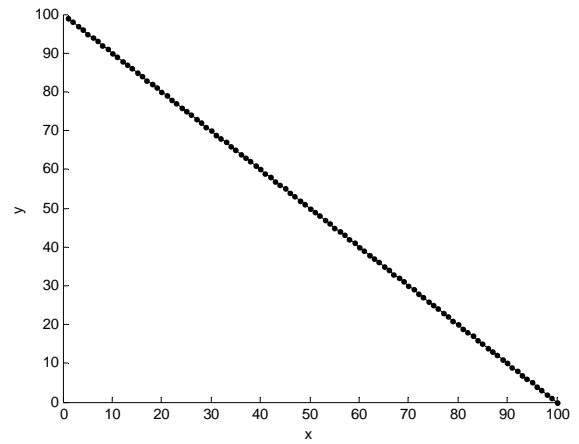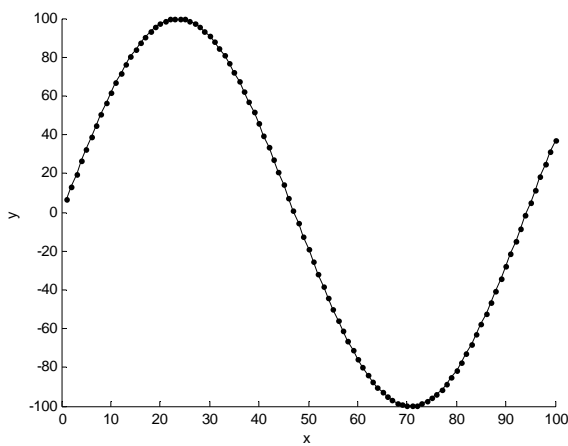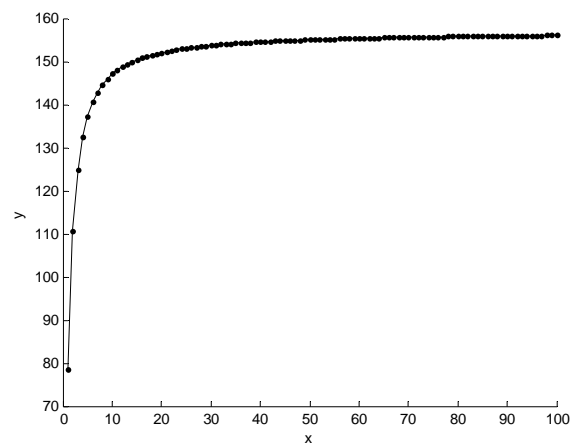
(f) ρ = 0

Figure 3-8. Schematic representations of the correlation of two random variables

3.3.2 Analysis on entire database

Efforts were made to discover correlations between bridge abutment rating and explanatory variables through analyzing the whole database; however, the Pearson correlation coefficients are less than 0.3 except for the one between abutment rating and pier rating, which is consistent with the observations from the parametric studies. Figure 3-9 is one of the scatter plots generated in the course of these analyses. It can be seen that the scatter graph between abutment rating and average daily total traffic (two variables) is similar with Figure 3-8 a, which means the two random variables can be considered as uncorrelated.
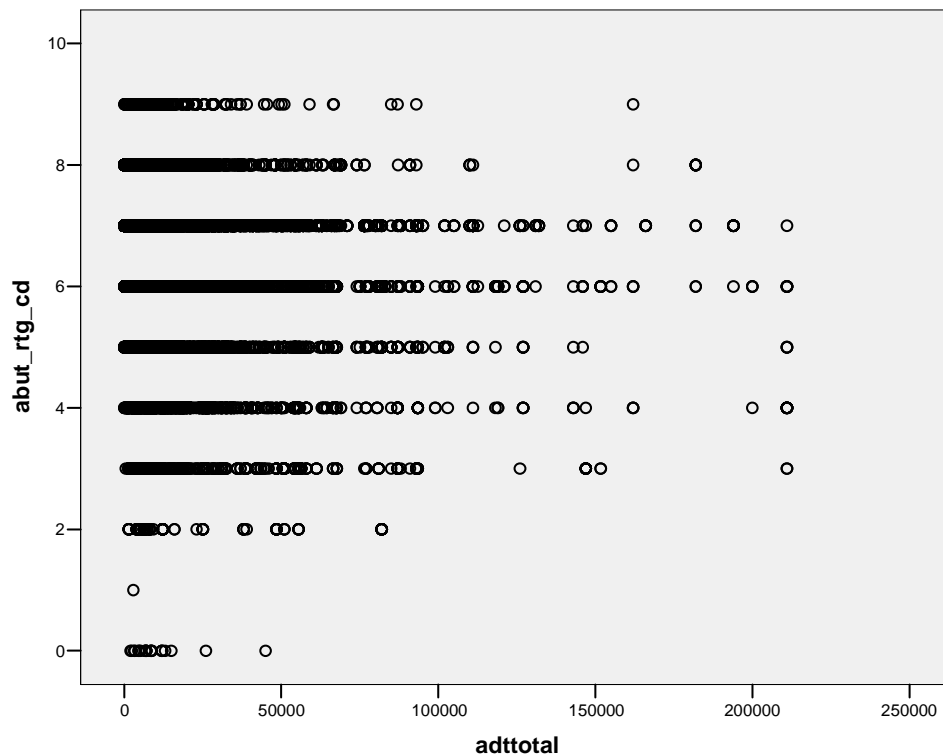
Figure 3-9.Scatter Plot for Abutment Rating and Average Daily Total Traffic

Table 3-6 shows the correlation coefficients between abutment rating and different parameters when using the entire database. It can be seen in Table 3-6**Error! Reference source not found.** that the Pearson correlation coefficients are less than 0.3 except for the one between abutment rating and pier rating, which is consistent with the observations from the parametric studies.

Table 3-6 Pearson Correlations between Abutment Rating and Other Parameters

		abut_rtg_cd	age_at_insp	yearbuilt	adttotal	ADTT	deckwidth	region_num	pier_rtg_cd	pin_type_cd	pin_num
abut_rtg_cd	Correlation	1.000	-0.252	0.162	-0.151	-0.110	-0.119	-0.024	0.356	0.085	-0.125
	Sig. (2-tailed)		0.000	0.000	0.000	0.000	0.000	0.000	0.000	0.000	0.000
	N	22491	21787	22491	22484	20525	22491	22491	13010	22491	6656
age_at_insp	Correlation	-0.252	1.000	-0.984	-0.048	-0.045	-0.044	0.098	-0.346	-0.261	-0.126
	Sig. (2-tailed)	0.000		0.000	0.000	0.000	0.000	0.000	0.000	0.000	0.000
	N	21787	27874	27874	27861	25151	27869	27874	12734	27874	8901
yearbuilt	Correlation	0.162	-0.984	1.000	0.051	0.058	0.065	-0.071	0.242	0.224	0.101
	Sig. (2-tailed)	0.000	0.000		0.000	0.000	0.000	0.000	0.000	0.000	0.000
	N	22491	27874	28889	28862	26162	28882	28889	13027	28889	9083
adttotal	Correlation	-0.151	-0.048	0.051	1.000	0.737	0.514	-0.064	-0.190	-0.016	0.298
	Sig. (2-tailed)	0.000	0.000	0.000		0.000	0.000	0.000	0.000	0.006	0.000
	N	22484	27861	28862	28869	26145	28858	28869	13022	28869	9083
ADTT	Correlation	-0.110	-0.045	0.058	0.737	1.000	0.397	0.073	-0.173	-0.033	0.247
	Sig. (2-tailed)	0.000	0.000	0.000	0.000		0.000	0.000	0.000	0.000	0.000
	N	20525	25151	26162	26145	26191	26156	26191	11608	26191	7971
deckwidth	Correlation	-0.119	-0.044	0.065	0.514	0.397	1.000	-0.086	-0.100	0.025	0.409
	Sig. (2-tailed)	0.000	0.000	0.000	0.000	0.000		0.000	0.000	0.000	0.000
	N	22491	27869	28882	28858	26156	28882	28882	13027	28882	9083
region_num	Correlation	-0.024	0.098	-0.071	-0.064	0.073	-0.086	1.000	-0.059	0.054	0.187
	Sig. (2-tailed)	0.000	0.000	0.000	0.000	0.000	0.000		0.000	0.000	0.000
	N	22491	27874	28889	28869	26191	28882	28923	13027	28923	9083
pier_rtg_cd	Correlation	0.356	-0.346	0.242	-0.190	-0.173	-0.100	-0.059	1.000	0.156	-0.079
	Sig. (2-tailed)	0.000	0.000	0.000	0.000	0.000	0.000	0.000		0.000	0.000
	N	13010	12734	13027	13022	11608	13027	13027	13027	13027	4482
pin_type_cd	Correlation	0.085	-0.261	0.224	-0.016	-0.033	0.025	0.054	0.156	1.000	0.323
	Sig. (2-tailed)	0.000	0.000	0.000	0.006	0.000	0.000	0.000	0.000		0.000
	N	22491	27874	28889	28869	26191	28882	28923	13027	28923	9083
pin_num	Correlation	-0.125	-0.126	0.101	0.298	0.247	0.409	0.187	-0.079	0.323	1.000
	Sig. (2-tailed)	0.000	0.000	0.000	0.000	0.000	0.000	0.000	0.000	0.000	
	N	6656	8901	9083	9083	7971	9083	9083	4482	9083	9083

Based on the analysis in this section, this kind of calculation throughout the whole database can provide very limited information about which parameters correlated with abutment rating. It was thus concluded that further statistical analyses needed to consider data subdivisions to improve variable correlations.

3.3.3 Analysis on categorized databases

3.3.3.1 *Division by main structure type, maximum span, skew and approach type*

Since the correlation obtained from the analysis on the entire database provided limited information, the database was sub-divided into categories to evaluate the correlation coefficients based on each individual data group. Data with common features was categorized in the same division. This rationale for dividing the database followed from the consideration that for bridges with common features, the mechanism which caused degradation of abutment rating would have similar effects on them.

The database was first categorized by the main superstructure type, maximum span, skew angle, and approach surface type. Figure 3-10 shows the diagram of the division of the database. Table 3-7 shows the correlation coefficients between abutment rating and other parameters for simple/cantilevered steel bridges. One of the individual correlation tables from which Table 3-7 is constructed, is shown in Table 3-8. Table 3-8 contributed to the 11th row in Table 3-7. Figure 3-11 shows the scatter plot for abutment rating and age at inspection. It can be seen that there was some degree of negative correlation between the two parameters; the correlation coefficient was expected to be a value between -0.3 and -0.9. The analysis showed that the correlation value was -0.555. Thus, for this category of bridges, with maximum span between 60 and 100 ft, skew angle greater than 45˚ and flexible surface approach, the age at inspection is, to some extent, negatively correlated with abutment rating.
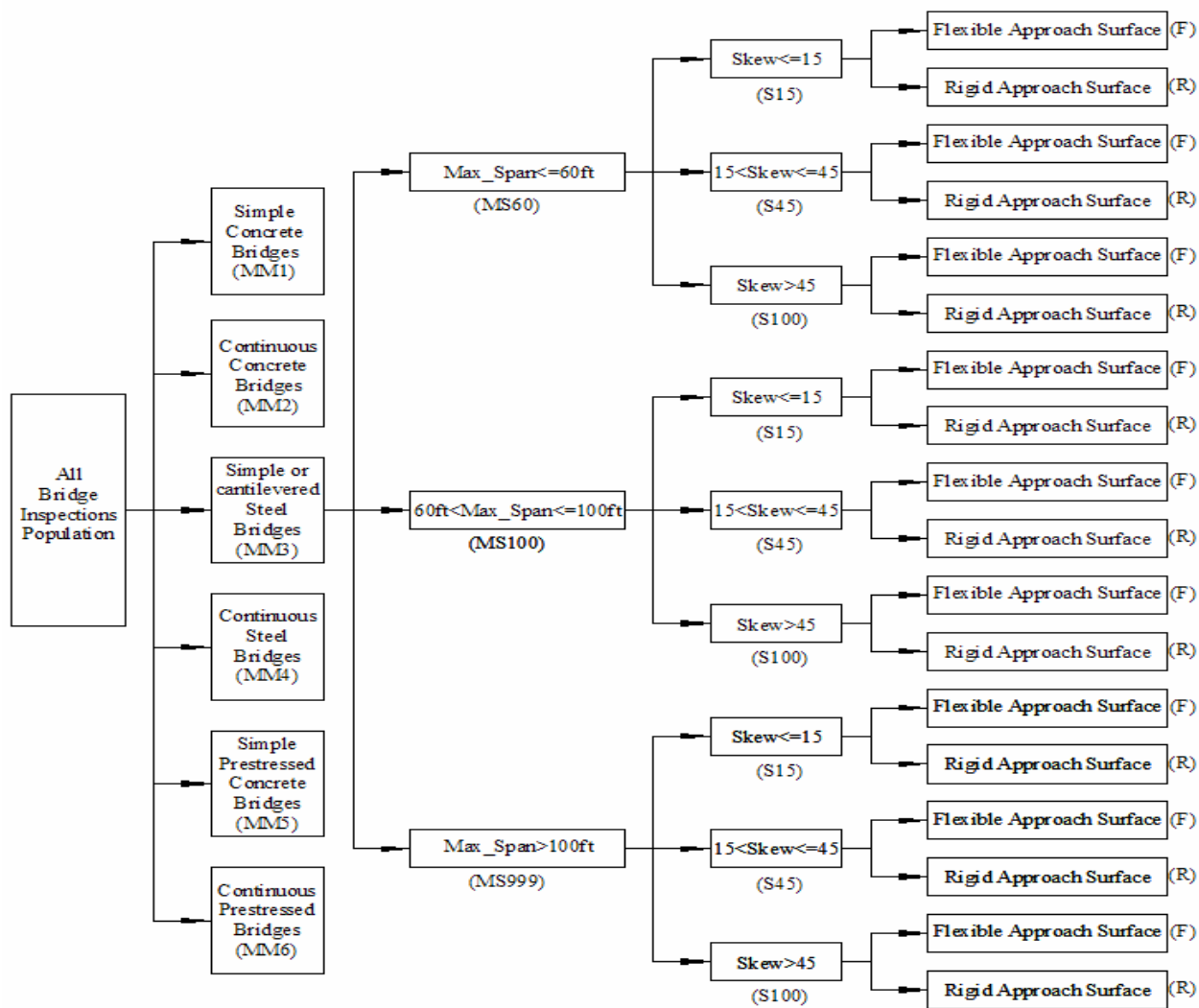
Figure 3-10. Database Sub-Division for Statistical Correlation Analyses

Table 3-7 Correlations between abutment rating and other parameters for simple/cantilevered steel bridges

categories		parameters	age_at_insp	yearbuilt	ADTtotal	ADTT	deck width	region_num	pier_rtg_cd	pin_type_cd	pin_ num
maximum span<= 60 ft	skew<=15	Flexible	**-0.325**	**-0.325**	-0.002	0.026	-0.014	0.030	**0.386**	0.087	0.175
		Rigid	-0.247	0.263	-0.247	-0.125	-0.188	-0.113	0.244	-0.160	-0.099
	15<skew<=45	Flexible	**-0.450**	**0.455**	-0.205	-0.071	-0.187	-0.186	**0.490**	0.231	**0.583**
		Rigid	-0.285	0.118	**-0.361**	-0.191	**-0.309**	-0.041	**0.491**	0.079	-0.024
	skew>45	Flexible	-0.134	0.148	-0.056	-0.060	0.045	0.059	.	0.198	.
		Rigid	**-0.662**	**0.730**	**0.335**	**0.322**	0.177	**0.431**	**-0.364**	-0.012	**0.478**
60ft< maximum span<= 100ft	skew<=15	Flexible	-0.253	0.243	**-0.315**	-0.171	**-0.367**	-0.082	0.242	0.106	-0.071
		Rigid	-0.129	0.149	-0.221	-0.264	-0.290	-0.045	**0.338**	0.056	-0.162
	15<skew<=45	Flexible	-0.188	0.146	**-0.433**	**-0.345**	**-0.357**	0.035	**0.432**	0.057	-0.152
		Rigid	-0.076	-0.004	-0.210	-0.193	-0.115	-0.109	0.266	0.140	**-0.313**
	skew>45	Flexible	**-0.555**	**0.582**	-0.071	-0.036	-0.164	0.014	**0.684**	0.271	**-0.813**
		Rigid	-0.110	0.146	-0.122	0.019	-0.107	-0.029	**0.391**	0.153	**-0.347**
maximum span> 100 ft	skew<=15	Flexible	**-0.474**	**0.472**	-0.237	-0.213	-0.219	0.081	**0.432**	0.157	0.174
		Rigid	-0.051	0.098	-0.181	-0.230	-0.107	-0.055	**0.332**	0.002	-0.151
	15<skew<=45	Flexible	-0.122	0.065	-0.217	-0.203	-0.160	-0.225	**0.314**	0.000	-0.008
		Rigid	-0.217	0.199	-0.013	0.065	**-0.300**	-0.170	0.291	-0.009	**-0.465**
	skew>45	Flexible	-0.182	0.162	**-0.421**	-0.235	**-0.360**	0.256	0.245	-0.085	**-0.518**
		Rigid	-0.047	-0.163	-0.084	-0.206	0.081	-0.227	**0.517**	**0.322**	-0.238
Correlation>0.3/total divisions			0.278	0.278	0.278	0.111	0.278	0.056	0.667	0.056	0.444

Table 3-8. Pearson Correlations between Abutment Rating and Other Parameters for MM3MS100S100F

		abut_rtg_cd	age_at_insp	yearbuilt	ADTtotal	ADTT	deckwidth	region_num	pier_rtg_cd	pin_type_cd	pin_num
abut_rtg_cd	Correlation	1.000	-0.555	0.582	-0.071	-0.036	-0.164	0.014	0.684	0.271	-0.813
	Sig. (2-tailed)		0.000	0.000	0.528	0.761	0.142	0.898	0.000	0.014	0.000
	N	82	82	82	82	75	82	82	47	82	17
age_at_insp	Correlation	-0.555	1.000	-0.994	-0.343	-0.333	-0.201	-0.176	-0.293	-0.489	-0.808
	Sig. (2-tailed)	0.000		0.000	0.000	0.001	0.037	0.068	0.046	0.000	0.000
	N	82	108	108	108	98	108	108	47	108	23
yearbuilt	Correlation	0.582	-0.994	1.000	0.329	0.321	0.186	0.176	0.290	0.488	0.953
	Sig. (2-tailed)	0.000	0.000		0.001	0.001	0.054	0.068	0.048	0.000	0.000
	N	82	108	108	108	98	108	108	47	108	23
adttotal	Correlation	-0.071	-0.343	0.329	1.000	0.988	0.976	-0.307	-0.416	0.522	0.946
	Sig. (2-tailed)	0.528	0.000	0.001		0.000	0.000	0.001	0.004	0.000	0.000
	N	82	108	108	108	98	108	108	47	108	23
ADTT	Correlation	-0.036	-0.333	0.321	0.988	1.000	0.963	-0.455	-0.514	0.554	0.938
	Sig. (2-tailed)	0.761	0.001	0.001	0.000		0.000	0.000	0.001	0.000	0.000
	N	75	98	98	98	98	98	98	41	98	23
deckwidth	Correlation	-0.164	-0.201	0.186	0.976	0.963	1.000	-0.321	-0.415	0.444	0.935
	Sig. (2-tailed)	0.142	0.037	0.054	0.000	0.000		0.001	0.004	0.000	0.000
	N	82	108	108	108	98	108	108	47	108	23
region_num	Correlation	0.014	-0.176	0.176	-0.307	-0.455	-0.321	1.000	0.186	-0.301	-0.117
	Sig. (2-tailed)	0.898	0.068	0.068	0.001	0.000	0.001		0.210	0.002	0.596
	N	82	108	108	108	98	108	108	47	108	23
pier_rtg_cd	Correlation	0.684	-0.293	0.290	-0.416	-0.514	-0.415	0.186	1.000	0.312	-0.870
	Sig. (2-tailed)	0.000	0.046	0.048	0.004	0.001	0.004	0.210		0.033	0.000
	N	47	47	47	47	41	47	47	47	47	12
pin_type_cd	Correlation	0.271	-0.489	0.488	0.522	0.554	0.444	-0.301	0.312	1.000	.(a)
	Sig. (2-tailed)	0.014	0.000	0.000	0.000	0.000	0.000	0.002	0.033		0.000
	N	82	108	108	108	98	108	108	47	108	23
pin_num	Correlation	-0.813	-0.808	0.953	0.946	0.938	0.935	-0.117	-0.870	.(a)	1.000
	Sig. (2-tailed)	0.000	0.000	0.000	0.000	0.000	0.000	0.596	0.000	0.000	
	N	17	23	23	23	23	23	23	12	23	23
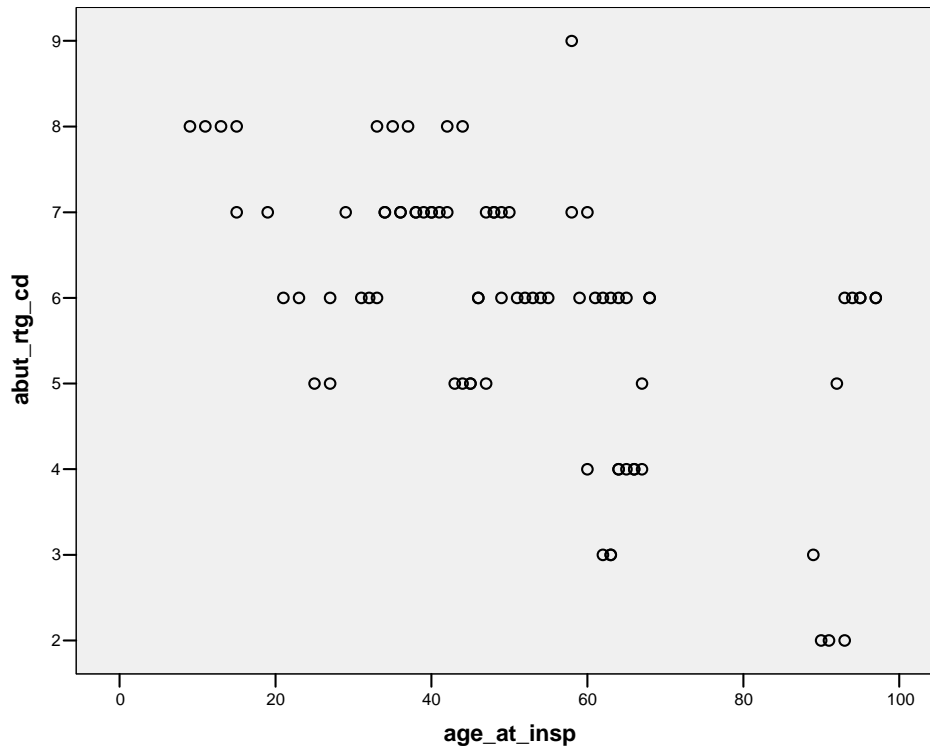
Figure 3-11. Scatter Plot for Abutment Rating and Age at Inspection

All of the correlation coefficients greater than 0.3 were highlighted in Table 3-7 for ease of identification. The last row showed the ratios between the number of divisions with correlation coefficients greater than 0.3 and the total number of divisions. This analysis showed that pier rating is positively correlated with abutment rating. Pin-hanger condition was shown to be positively correlated with abutment rating when the maximum span is less than 60 ft, and it was negatively correlated with abutment rating when maximum span is greater than 60 ft. It was also shown that average daily total traffic (ADTT), age at inspection and deck width have negative correlations with abutment rating, to some extent, and that year built has a positive correlation with abutment rating, also to some extent. The correlations between the above parameters and abutment ratings were less noticeable for bridges with spans less than 100 ft. It should also be mentioned that the subdivision of simple/cantilevered steel bridges with maximum spans no greater than 60 ft, skew angles greater than 45° and flexible approach surfaces should be neglected because they only contain 38 inspections. Upon checking the database, it was found out that these inspection records corresponded to only 6 bridges (bridge keys:

82182252000S280, 35135031000R010, 83183032000B010, 66166013000B040, 82182052000R010, and 82182252000S360). Thus, the sample population is too small to be reliable. Further analysis of the data shows that in approximately more than 70% of the data sub-divisions, the average daily total traffic, age at inspection, deck width and year built have greater absolute correlation coefficients than region number and pin type. Thus, it can be seen that, in addition to pier rating and pin-hanger type, these four parameters are also important indexes of abutment distress.

Other data sub-divisions also showed some extent of correlations between abutment rating and predictive parameters by conducting analyses on reduced data sets obtained by removing inspection records for reconstructed bridges. For example, age at inspection was an important factor that directly correlated with abutment rating for continuous steel bridges.

Analyses on all the data sub-divisions charted out in Figure 3-10 were carried out in a similar manner as described throughout this section. Detailed results on these analyses are not provided here due to avoid increasing the report length. The observations noted in these analyses were similar to the ones previously discussed.

3.3.3.2 *Division by Region, Structure Type, Max Span, Skew and Approach Surface*

The bridge inspection population was further categorized for the analyses presented in this section. Specifically, the sub-divisions now considered the location (county) of the bridges in question. It is reasonable that when more parameters are added into the process of the category, the population in each sample will become smaller. The data, however, is expected to have more common features and thus the effect of other parameters should be more noticeable since the mechanism they act upon will be more similar.

Then the database was categorized by the order of region, main structure type, maximum span, skew angle, and approach surface type. Figure 3-12 shows the diagram of the division of the database. Table 3-9 shows the count of simple or cantilevered steel bridges in the Metro region. Table 3-10 shows the correlation coefficients between abutment rating and other parameters for simple or cantilevered steel bridges in the Metro region. One of the individual correlation tables from which Table 3-10 is constructed is shown in Table 3-11. This table was

exported from the analysis carried out by SPSS. Table 3-11 contributes to the 9th row in Table 3-10.
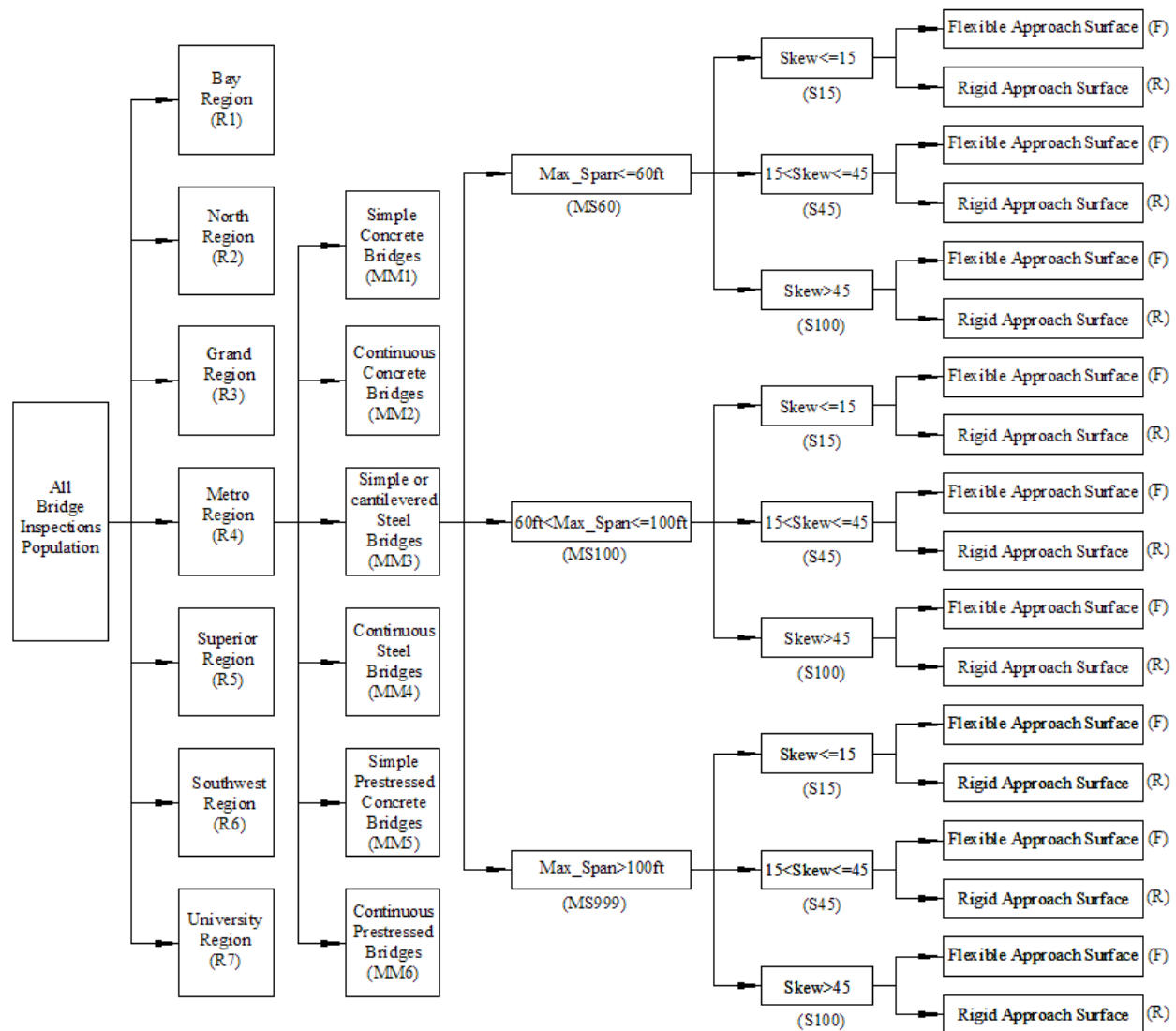
Figure 3-12. Sub-Division of Database with Region into Account

Figure 3-13 shows the scatter plot for abutment rating and deck width for Metro Region bridges with spans between 60 and 100 ft, skew angle between 15° and 45° and flexible surface approach. We can see clearly that this graph is similar to Figure 3-8b, which shows that there is some extent of negative correlation between the two parameters. The correlation value for these two variables was found to be -0.695.

Table 3-9 Population of Simple or Cantilevered Steel Bridges

parameter	Simple or cantilevered steel bridges in Metro region					
maxspan_ft	<= 60.0					
skew	<= 15°		16° - 45°		46° +	
appr_sur	Flexible	Rigid	Flexible	Rigid	Flexible	Rigid
Count	107	271	43	207	23	80
maxspan_ft	60.1 - 100.0					
skew	<= 15°		16° - 45°		46° +	
appr_sur	Flexible	Rigid	Flexible	Rigid	Flexible	Rigid
Count	164	379	152	543	37	391
maxspan_ft	>100.1					
skew	<= 15°		16° - 45°		46° +	
appr_sur	Flexible	Rigid	Flexible	Rigid	Flexible	Rigid
Count	69	166	65	143	53	218
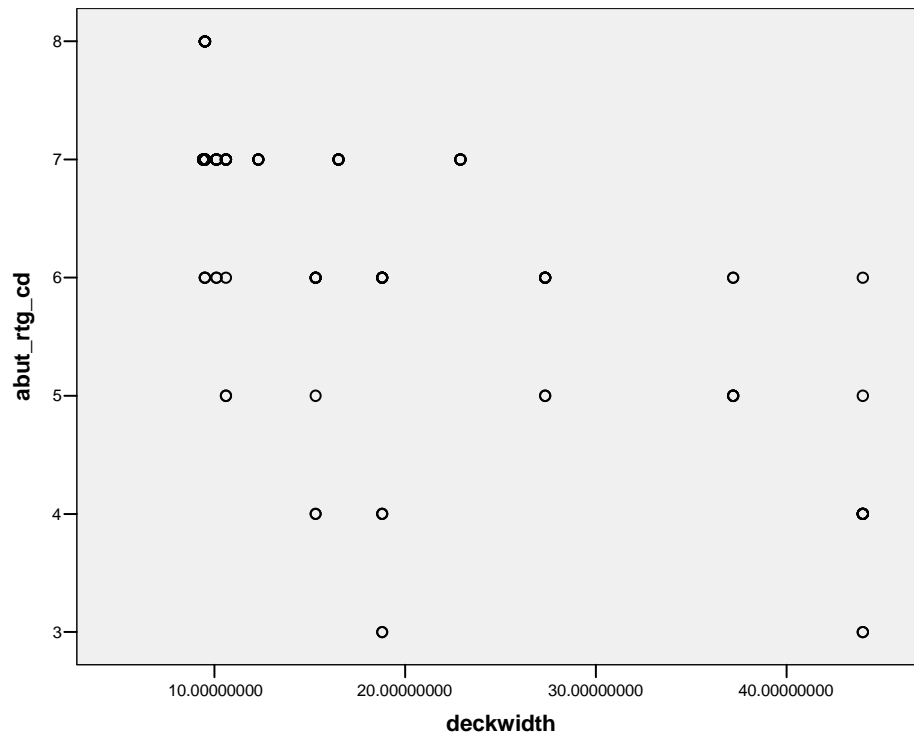
Figure 3-13. Scatter Plot for Abutment Rating and Deck Width

Table 3-10. Correlations between Abutment Rating and Other parameters for R3MM3

categories		parameters	age_at_insp	yearbuilt	adttotal	ADTT	deck width	pier_rtg_cd	pin_type_cd	pin_num
maximum span<= 60 ft	skew<=15	Flexible	-0.170	0.144	**0.312**	**0.365**	**0.356**	0.134	0.141	.
		Rigid	**-0.460**	**0.462**	0.112	-0.029	-0.250	**0.480**	**-0.369**	-0.075
	15<skew<=45	Flexible	**0.330**	**-0.353**	-0.279	-0.282	0.149	**-0.713**	.	.
		Rigid	**-0.500**	0.120	**-0.436**	-0.292	-0.507	**0.635**	0.237	**0.655**
	skew>45	Flexible	**0.510**	**-0.577**	**-0.534**	**-0.420**	**-0.577**	.	.	.
		Rigid	0.128	-0.166	**0.313**	**0.344**	0.162	-0.629	**-0.389**	.
60ft< maximum span<= 100ft	skew<=15	Flexible	**-0.316**	**0.320**	-0.141	-0.057	**-0.359**	**0.361**	-0.177	**-0.569**
		Rigid	-0.133	0.151	-0.249	-0.201	**-0.399**	**0.333**	-0.093	-0.149
	15<skew<=45	Flexible	0.036	0.020	**-0.705**	**-0.687**	**-0.695**	**0.554**	0.152	**-0.686**
		Rigid	-0.022	-0.038	-0.198	**-0.331**	-0.129	0.190	0.206	**-0.372**
	skew>45	Flexible	**-0.391**	**0.445**	0.271	**0.405**	0.198	-0.100	0.257	.
		Rigid	-0.102	0.127	-0.052	0.136	-0.119	0.172	0.164	**-0.607**
maximum span> 100 ft	skew<=15	Flexible	**-0.671**	**0.673**	0.247	0.222	**-0.803**	**0.448**	-0.270	**-0.946**
		Rigid	-0.009	0.016	-0.024	-0.289	-0.134	**0.795**	0.105	-0.107
	15<skew<=45	Flexible	-0.043	0.049	-0.246	**-0.515**	-0.262	0.153	-0.070	**0.443**
		Rigid	-0.177	0.206	0.176	0.239	**-0.471**	0.271	0.078	**-0.747**
	skew>45	Flexible	-0.010	0.081	**-0.394**	**-0.324**	**-0.384**	**0.631**	-0.182	**-0.517**
		Rigid	-0.147	-0.123	-0.031	-0.239	0.180	**0.590**	**0.388**	-0.039
Correlation>0.3/total divisions			0.389	0.333	0.333	0.444	0.444	0.556	0.167	0.500

65

Table 3-11. Pearson Correlations between Abutment Rating and Other Parameters for R3MM3MS100S45F

		abut_rtg_cd	age_at_insp	yearbuilt	adttotal	ADTT	deckwidth	region_num	pier_rtg_cd	pin_type_cd	pin_num
abut_rtg_cd	Correlation	1.000	0.036	0.020	-0.705	-0.687	-0.695	.(a)	0.554	0.152	-0.686
	Sig. (2-tailed)		0.692	0.822	0.000	0.000	0.000	.	0.000	0.093	0.000
	N	123	123	123	123	110	123	123	86	123	71
age_at_insp	Correlation	0.036	1.000	-0.903	-0.427	-0.492	-0.312	.(a)	-0.165	-0.708	-0.400
	Sig. (2-tailed)	0.692		0.000	0.000	0.000	0.000	.	0.129	0.000	0.000
	N	123	152	152	152	136	152	152	86	152	94
yearbuilt	Correlation	0.020	-0.903	1.000	0.415	0.488	0.296	.(a)	0.141	0.802	0.429
	Sig. (2-tailed)	0.822	0.000		0.000	0.000	0.000	.	0.194	0.000	0.000
	N	123	152	152	152	136	152	152	86	152	94
adttotal	Correlation	-0.705	-0.427	0.415	1.000	0.995	0.896	.(a)	-0.466	0.165	0.917
	Sig. (2-tailed)	0.000	0.000	0.000		0.000	0.000	.	0.000	0.043	0.000
	N	123	152	152	152	136	152	152	86	152	94
ADTT	Correlation	-0.687	-0.492	0.488	0.995	1.000	0.899	.(a)	-0.583	0.144	0.918
	Sig. (2-tailed)	0.000	0.000	0.000	0.000		0.000	.	0.000	0.094	0.000
	N	110	136	136	136	136	136	136	76	136	78
deckwidth	Correlation	-0.695	-0.312	0.296	0.896	0.899	1.000	.(a)	-0.581	0.071	0.857
	Sig. (2-tailed)	0.000	0.000	0.000	0.000	0.000		.	0.000	0.386	0.000
	N	123	152	152	152	136	152	152	86	152	94
region_num	Correlation	.(a)	.(a)	.(a)	.(a)	.(a)	.(a)	.(a)	.(a)	.(a)	.(a)
	Sig. (2-tailed)	.	.	.	.	.	.		.	.	.
	N	123	152	152	152	136	152	152	86	152	94
pier_rtg_cd	Correlation	0.554	-0.165	0.141	-0.466	-0.583	-0.581	.(a)	1.000	0.245	-0.596
	Sig. (2-tailed)	0.000	0.129	0.194	0.000	0.000	0.000	.		0.023	0.000
	N	86	86	86	86	76	86	86	86	86	51
pin_type_cd	Correlation	0.152	-0.708	0.802	0.165	0.144	0.071	.(a)	0.245	1.000	.(a)
	Sig. (2-tailed)	0.093	0.000	0.000	0.043	0.094	0.386	.	0.023		0.000
	N	123	152	152	152	136	152	152	86	152	94
pin_num	Correlation	-0.686	-0.400	0.429	0.917	0.918	0.857	.(a)	-0.596	.(a)	1.000
	Sig. (2-tailed)	0.000	0.000	0.000	0.000	0.000	0.000	.	0.000	0.000	
	N	71	94	94	94	78	94	94	51	94	94

Correlation coefficients in Table 3-10 greater than 0.3 and 0.5 are highlighted to identify variables with some degree of correlation. The last row shows the ratios between the number of data sub-divisions with correlation coefficients greater than 0.3 and the total number of data sub-divisions. It is shown in Table 3-10 that pier rating is positively correlated with abutment rating. However, the degree of correlation for pier rating decreased slightly in comparison with Table 3-7. For pin type, some correlation to abutment rating seems to exist, but the sign of the correlation is not consistent. It is also shown that average daily total traffic, average daily truck traffic, age at inspection and deck width have negative correlations with abutment rating, to some extent, and that year built has a positive correlation with abutment rating, there are a few correlation coefficient values which have opposite signs to the general trend for the 5 selected parameters. Further analysis is needed to find out the reason.

Analyses of the inspection record for the other five main superstructure types were similarly made and the outcomes are summarized in the following. Inspections on simple concrete bridges are mostly found in the categories of maximum span no greater than 60 ft and skew angle no greater than 45˚. It was found that pier rating had good correlation with abutment rating and that age at inspection has a good correlation with abutment rating to some extent.

For continuous concrete bridges most of inspection records are for spans less than 100 ft and skew angles less than 45°. It was found that pier rating had a relevant correlation with abutment rating, but not as high as seen for simple concrete bridges. Age at inspection and built year also have a correlation with abutment ratings. The correlation for these two parameters is relatively good. Compare to the mentioned parameters, average daily traffic also was noted have a weaker correlation with abutment rating.

Most of the continuous steel bridges are in the categories of skew angle less than 15˚. It was found that age at inspection has good correlation with abutment rating and that average daily traffic has correlation with abutment rating to some extent. Contrary to other structure types, pier rating did not show good correlation with abutment rating.

Inspections for simple span prestressed concrete bridges showed good correlation between pier rating and abutment rating, which was best among all structure types. Average daily traffic was found to be only slightly correlated with abutment rating.

The number of inspections for continuous prestressed concrete bridges is very small. The largest number of inspection records (31) is for bridges with maximum spans greater than 100 ft skew angles no greater than 15˚, and with a flexible approach surface. Analysis of this data showed that there is good correlation between average daily traffic and average daily truck traffic with abutment rating. To some extent, a correlation between age at inspection and abutment rating was also seen. It should be noted that this observations are only stated for completeness as their statistical significance is questionable due to the small number of inspection records.

3.3.4 Analysis of Bridges with Abutment Ratings no Greater than 4

Further statistical analyses were carried out on a sub-population of records for which their abutment rating is no greater than 4. The total number of inspection records for this case is 1773. Since the number of inspections is not very large, the sample is only divided by main structure type. Table 3-12 shows the number of bridge inspections with abutment rating no greater than 4 in each division. Table 3-13 shows the correlation coefficients between abutment rating and other parameters for bridges with poor abutment rating.

Table 3-12. Population of Bridges with Poor abutment Rating

Main structure type	Simple concrete	Continuous concrete	Simple or cantilevered steel	Continuous steel	Simple prestressed concrete	Continuous prestressed concrete
Count	92	54	1072	182	367	6

It is shown in Table 3-13 that average daily truck traffic is an important parameter that correlates well with poor abutment rating for continuous concrete bridges. For continuous steel bridges, year built was seen to have some influence on the abutment rating and for simple prestressed concrete bridges, and pier rating had a high correlation to abutment rating. It shall be mentioned that the identical values in the bottom row of the table make little sense since this data sub-division only contained 6 inspections on 2 bridges (bridge keys: 11111053000R010 and 78178031000B010).

3.3.5 Analysis of Bridges without Reconstruction Records

Since reconstruction details are unknown and the reconstruction of the abutment will change the abutment rating dramatically, bridges with reconstruction records were filtered out. The analysis in this section is based on the bridges without reconstruction and the number of inspection samples was 22,819. The database was categorized by the order of main structure type, maximum span, skew angle, and approach surface type. Figure 3-14 shows the diagram of the division of the sample. Table 3-14 shows the number of simple or cantilevered steel bridges without reconstruction in each division. Table 3-15 shows the correlation coefficients between abutment rating and other parameters for simple or cantilevered steel bridges without reconstruction.

One of the individual correlation tables from which Table 3-15 was constructed is shown in Table 3-16. This table is exported from the analysis carried out by SPSS. Table 3-16 contributes to the 13th row in Table 3-15. Figure 3-15 shows the scatter plot for abutment rating and year built. We can see that this graph is similar to Figure 3-8b, which shows that there is some extent of positive correlation between the two parameters; the value of the calculated correlation coefficient was 0.422. Thus, for this sub-division of data, bridges with maximum spans greater than 100 ft, skew angle no more than 15˚ and flexible surface approaches, year built is, to some extent, positively correlated with abutment rating.

Table 3-13. Correlations Between Abutment Rating and Other Parameters by Structure Type

parameters / categories	age_at_insp	yearbuilt	ADTtotal	ADTT	deck width	pier_rtg_cd	maxspan_ft	skew	pin_ num
Simple Concrete	-0.068	0.145	0.080	0.078	0.061	.	0.220	-0.064	.
Continuous Concrete	0.175	-0.101	-0.072	**-0.656**	-0.420	-0.579	0.135	0.196	.
Simple or Cantilevered Steel	0.069	-0.071	-0.006	-0.063	-0.032	-0.083	-0.020	-0.027	-0.009
Continuous Steel	0.260	**-0.319**	-0.071	-0.041	-0.210	-0.255	-0.049	0.000	-0.225
Simple Prestressed Concrete	0.003	-0.035	0.078	-0.004	0.025	**0.394**	-0.267	-0.057	-0.021
Continuous Prestressed Concrete	.	**-0.316**	**-0.316**	**0.316**	**-0.316**	.	**-0.316**	**-0.316**	.

Table 3-14. Division of Simple or Cantilevered Steel Bridge Inspections without Reconstruction

parameter	Simple or cantilevered steel bridges without reconstruction					
maxspan_ft	<= 60.0					
skew	<= 15		16 - 45		46+	
appr_sur	Flexible	Rigid	Flexible	Rigid	Flexible	Rigid
Count	1090	693	493	567	23	48
maxspan_ft	60.1 - 100.0					
skew	<= 15		16 - 45		46+	
appr_sur	Flexible	Rigid	Flexible	Rigid	Flexible	Rigid
Count	881	879	1098	1127	43	457
maxspan_ft	>100.1					
skew	<= 15		16 - 45		46+	
appr_sur	Flexible	Rigid	Flexible	Rigid	Flexible	Rigid
Count	318	344	346	329	172	332

Table 3-15. Correlations between Abutment Rating and Other Parameters for NoReconMM3

categories		parameters	age_at_insp	yearbuilt	ADTtotal	ADTT	deck width	region_num	pier_rtg_cd	pin_type_cd	pin_ num
maximum span<= 60 ft	skew<=15	Flexible	**-0.377**	0.274	-0.027	0.060	0.005	-0.013	**0.316**	0.141	0.150
		Rigid	-0.235	0.248	-0.158	-0.187	-0.210	-0.117	0.281	-0.191	-0.003
	15<skew<=45	Flexible	**-0.338**	**0.335**	-0.250	-0.162	-0.166	-0.162	**0.383**	0.249	0.591
		Rigid	-0.227	0.011	**-0.357**	-0.220	**-0.337**	-0.075	0.446	0.120	-0.004
	skew>45	Flexible	**-0.422**	**0.435**	0.036	0.008	0.145	**0.329**	.	**0.393**	.
		Rigid	**0.315**	-0.249	0.121	0.130	0.159	-0.204	**-0.405**	-0.267	-0.183
60ft< maximum span<= 100ft	skew<=15	Flexible	-0.151	0.143	**-0.314**	-0.181	**-0.365**	-0.009	0.235	0.087	-0.102
		Rigid	0.047	-0.009	-0.276	**-0.377**	**-0.378**	-0.013	0.270	0.037	-0.229
	15<skew<=45	Flexible	-0.199	0.142	-0.295	-0.250	-0.261	0.054	**0.330**	0.054	0.067
		Rigid	-0.116	-0.027	-0.174	-0.179	-0.006	-0.116	**0.312**	0.115	-0.188
	skew>45	Flexible	**-0.533**	**0.514**	**-0.675**	**-0.685**	**-0.392**	**0.574**	**0.515**	-0.171	.
		Rigid	-0.148	0.156	-0.138	0.071	-0.139	-0.011	**0.232**	0.074	**-0.348**
maximum span> 100 ft	skew<=15	Flexible	**-0.425**	**0.422**	-0.244	-0.204	**-0.389**	0.042	**0.396**	0.030	0.174
		Rigid	-0.124	0.170	-0.109	-0.194	-0.040	-0.032	**0.344**	0.033	-0.253
	15<skew<=45	Flexible	-0.122	0.065	-0.217	-0.203	-0.160	-0.225	**0.314**	0.000	-0.008
		Rigid	-0.206	0.185	-0.089	-0.018	**-0.373**	-0.204	0.240	-0.046	**-0.493**
	skew>45	Flexible	-0.141	0.094	**-0.485**	-0.317	**-0.357**	0.224	0.172	-0.004	**-0.487**
		Rigid	-0.086	-0.140	-0.073	-0.221	0.092	-0.226	**0.549**	0.348	-0.295
Correlation>0.3/total divisions			0.333	0.222	0.222	0.111	0.389	0.111	0.556	0.056	0.167

Table 3-16. Pearson Correlations between Abutment Rating and Other Parameters for NoReconMM3MS999S15F

		abut_rtg_cd	age_at_insp	yearbuilt	ADTtotal	ADTT	deckwidth	region_num	pier_rtg_cd	pin_type_cd	pin_num
abut_rtg_cd	Correlation	1.000	-0.425	0.422	-0.244	-0.204	-0.389	0.042	0.396	0.030	0.174
	Sig. (2-tailed)		0.000	0.000	0.000	0.003	0.000	0.494	0.000	0.628	0.054
	N	267	267	267	267	213	267	267	142	267	124
age_at_insp	Correlation	-0.425	1.000	-0.977	0.019	-0.126	0.086	0.075	-0.671	-0.279	-0.101
	Sig. (2-tailed)	0.000		0.000	0.738	0.042	0.124	0.179	0.000	0.000	0.222
	N	267	318	318	318	263	318	318	142	318	149
yearbuilt	Correlation	0.422	-0.977	1.000	-0.023	0.125	-0.093	-0.054	0.659	0.285	0.084
	Sig. (2-tailed)	0.000	0.000		0.687	0.043	0.098	0.341	0.000	0.000	0.308
	N	267	318	318	318	263	318	318	142	318	149
adttotal	Correlation	-0.244	0.019	-0.023	1.000	0.924	0.650	-0.289	-0.067	-0.166	0.400
	Sig. (2-tailed)	0.000	0.738	0.687		0.000	0.000	0.000	0.429	0.003	0.000
	N	267	318	318	318	263	318	318	142	318	149
ADTT	Correlation	-0.204	-0.126	0.125	0.924	1.000	0.502	-0.263	-0.005	-0.029	0.199
	Sig. (2-tailed)	0.003	0.042	0.043	0.000		0.000	0.000	0.956	0.637	0.028
	N	213	263	263	263	263	263	263	115	263	122
deckwidth	Correlation	-0.389	0.086	-0.093	0.650	0.502	1.000	-0.307	-0.056	-0.152	0.425
	Sig. (2-tailed)	0.000	0.124	0.098	0.000	0.000		0.000	0.512	0.007	0.000
	N	267	318	318	318	263	318	318	142	318	149
region_num	Correlation	0.042	0.075	-0.054	-0.289	-0.263	-0.307	1.000	-0.208	0.171	-0.190
	Sig. (2-tailed)	0.494	0.179	0.341	0.000	0.000	0.000		0.013	0.002	0.020
	N	267	318	318	318	263	318	318	142	318	149
pier_rtg_cd	Correlation	0.396	-0.671	0.659	-0.067	-0.005	-0.056	-0.208	1.000	0.176	0.214
	Sig. (2-tailed)	0.000	0.000	0.000	0.429	0.956	0.512	0.013		0.036	0.054
	N	142	142	142	142	115	142	142	142	142	82
pin_type_cd	Correlation	0.030	-0.279	0.285	-0.166	-0.029	-0.152	0.171	0.176	1.000	-0.166
	Sig. (2-tailed)	0.628	0.000	0.000	0.003	0.637	0.007	0.002	0.036		0.044
	N	267	318	318	318	263	318	318	142	318	149
pin_num	Correlation	0.174	-0.101	0.084	0.400	0.199	0.425	-0.190	0.214	-0.166	1.000
	Sig. (2-tailed)	0.054	0.222	0.308	0.000	0.028	0.000	0.020	0.054	0.044	
	N	124	149	149	149	122	149	149	82	149	149
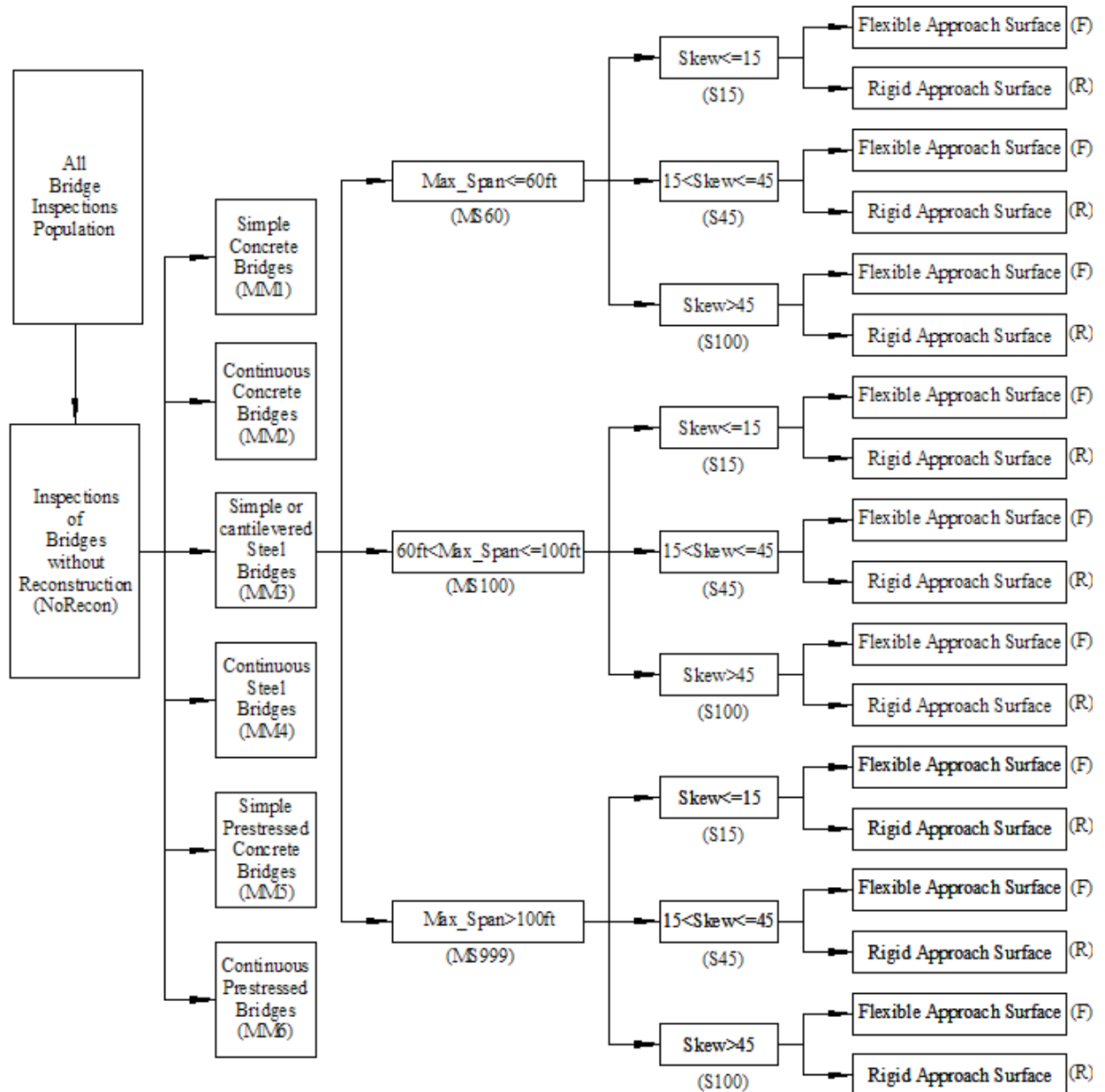
Figure 3-14. Database Sub-Division for Studies without Reconstruction Records
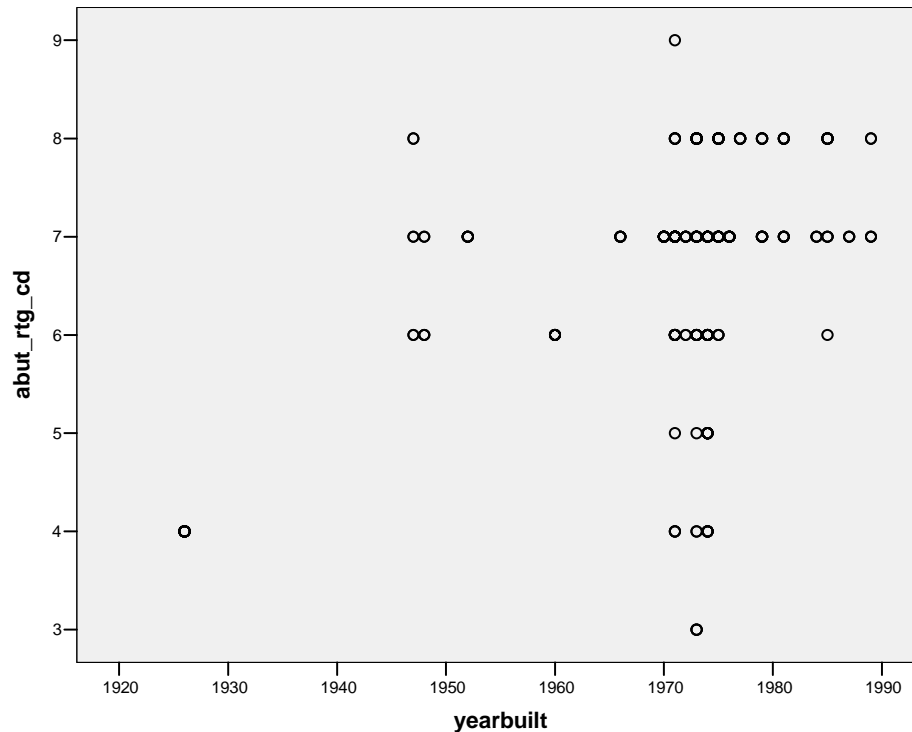
Figure 3-15. Scatter Graph for Abutment Rating and Year Built without Reconstruction Data

Correlation coefficients in Table 3-15 greater than 0.3 are highlighted. The last row shows the ratios between the number of data divisions with correlation coefficients greater than 0.3 and the total number of data divisions. The results in Table 3-15 show that pier rating is positively correlated with the abutment rating. We can see that deck width and age at inspection also have a relatively good negative correlation with abutment rating. Other parameters that show some degree of correlation with abutment rating are year built, which has a positive correlation, and average daily total traffic, which has a negative correlation. Average daily truck traffic does not have good correlation with abutment rating. Perhaps it is due to the fact that bridges with high average daily truck traffic are more likely to undergo reconstruction. Pin-hanger condition did not correlate well to abutment rating in this analysis.

The analyses about all the other subdivisions shown in Figure 3-14 were carried out and the results were interpreted in a similar manner. Detailed results are not given here for brevity.

74

3.3.6 Discussion

Statistical analyses and exploration of correlation coefficients between abutment rating and different parameters were carried out as part of Task III.2. The search for the key parameters by the different paths was represented by sorting the bridge population in the database in sub-divisions or sub-categories. Generally, no clear association between highway bridge abutment rating and explanatory variables can be found through correlation analyses in this research. Deck width, pin condition, age at inspection, built year, average daily total traffic, and average daily truck traffic were all shown to have some degree of correlation to abutment rating. The correlation coefficients differ according to the different data categorization and subdivision and evidence was not strong enough to support more general positive conclusion.

3.4 Factorial Analysis

In order to check if the qualitative variables "pin type" and "approach type" are significant for the response variable "abutment rating" in simple/cantilevered steel bridge, a factorial analysis was carried out by the generalized linear regression model procedure "SAS PROC GLM" (SAS 2004).

In the factorial design, the qualitative variable "*pin type*" had two levels "without pin and hanger assembly" and "with pin and hanger assembly". The qualitative variable "*approach type*" had three levels "rigid", "flexible" and "unknown", six covariates which were used in the generalized linear regression model in the section 3.6.2 were added to this model as covariates. They are: "*length*", "*deck width*", "*age at inspection*", "*average annual temperature difference*", "*ADTT at inspection*", and "*maximum span*".

A type III analysis of variance (ANOVA) model is shown in Table 3-17. It can be seen from Table 3-17 the interaction term between "*pintype*" and "*approachtype*" was significant under a type I error rate of 0.01%. Thus, the effect of the levels of one factor within the levels of another factor needs to be explored. It can also be seen that factor "*approachtype*" was also significant under a type I error rate of 0.01%. Even though the factor "*pintype*" was significant under type I error rate of 5%, the evidence was not very strong. This also justifies the model

selected in section 3.6 in which the dummy variable "*pintype*" was dropped by the Mallow's C_p criterion.

Table 3-17 Type III Model ANOVA

Source	DF	Type III SS	Mean Square	F Value	Pr > F
pintype	1	4.4429765	4.4429765	3.88	0.0487
approachtype	2	213.3615663	106.6807832	93.28	<.0001
pintype*approachtype	2	68.3002383	34.1501192	29.86	<.0001

The tests of difference in factorial effects were carried out based on the results shown in Table 3-17. All the covariate values in the model were set to be constant in each test, three scenarios were considered according to covariate values "0", "-1" and "1". It can be seen from the residual plots in section 3.6 that these three values encompassed the samples that were most frequent. The factorial effects when covariates had a value of "0" are shown in Table 3-18. It can be seen from Table 3-18 that the effect of pin type was not significant for bridges with flexible approach. However, for the bridges with the rigid approach or unknown approach, the effect of pin type was significant. For bridges with unknown approach, the abutment rating of bridges with pins was significantly higher than those without pins; however, for bridges with rigid approach, the abutment rating of the bridges with pins were significantly lower than those without pins under type I error rate 0.01%. The difference of the effect of approach types were always significant under type I error rate 0.01% no matter whether pins were present or not. The abutment ratings of bridges with flexible approach type were significantly higher than those for bridges with the other two approach types, irrespective of whether pins were present or not. For bridges with pins, the abutment ratings of those with unknown approach type were significantly higher than bridges with rigid approach type. While for bridges without pins, the abutment rating of bridges with rigid approach type was significantly higher than those with unknown approach type.

Table 3-18 Test of factorial effects (covariates values are 0s)

Parameter	Estimate	Standard Error	t Value	Pr > |t|
difference of pin within flexible approach	-0.04114956	0.03323335	-1.24	0.2157
difference of pin within unknown approach	0.13349996	0.03284630	4.06	<.0001
difference of pin within rigid approach	-0.20110190	0.02906627	-6.92	<.0001
difference of flexible and unknown approach for bridges with pin	0.14724270	0.03054469	4.82	<.0001
difference of flexible and rigid approach for bridges with pin	0.33472950	0.02906192	11.52	<.0001
difference of unknown and rigid approach for bridges with pin	0.18748679	0.02915546	6.43	<.0001
difference of flexible and unknown approach for bridges without pin	0.32189222	0.03275441	9.83	<.0001
difference of flexible and rigid approach for bridges without pin	0.17477716	0.03089728	5.66	<.0001
difference of unknown and rigid approach for bridges without pin	-0.14711506	0.03057656	-4.81	<.000

In the factorial analyses, qualitative variables were designated as "factor", and values of qualitative variables were signified as "level", for instance, "approach surface type" had three levels: bitumen, concrete and unknown. The pairwise comparison between the levels of one factor within the levels of the other factor when covariates values are taken as "1" is shown in Table 3-19, in which the pin effect was significant for all levels of approach type; however, the effect of approach type between flexible and rigid approach was not significant when the bridges have pins. Also, the difference of effects between flexible and unknown approach type was not significant when the bridge did not have pins. The effects of approach type seem significant under a type I error rate of 0.01% for all other pair-wise comparisons.

The contrast of factorial effects when covariates values are "-1"s are shown in Table 3-20. It can be seen from Table 3-20 that the difference between the two levels of one factor within certain levels of the other factor are statistically significant under type I error rate 5%.

Table 3-19 Test of factorial effects (covariate values are "1")

Parameter	Estimate	Standard Error	t Value	Pr > |t|
Difference of pin within flexible approach	-0.41508906	0.04002556	-10.37	<.0001
Difference of pin within unknown approach	-0.24043955	0.03888585	-6.18	<.0001
Difference of pin within rigid approach	-0.57504140	0.03525264	-16.31	<.0001
difference of flexible and unknown approach for bridges with pin	-0.22669680	0.03726158	-6.08	<.0001
difference of flexible and rigid approach for bridges with pin	-0.03921000	0.03608456	-1.09	0.2772
difference of unknown and rigid approach for bridges with pin	-0.18645271	0.03665075	-5.09	<.0001
difference of flexible and unknown approach for bridges without pin	-0.05204729	0.03826144	-1.36	0.1737
difference of flexible and rigid approach for bridges without pin	-0.19916234	0.03622778	-5.50	<.0001
Difference of unknown and rigid approach for bridges without pin	-0.52105456	0.03732069	-13.96	<.0001

Table 3-20 Test of factorial effects (covariate values are "-1")

Parameter	Estimate	Standard Error	t Value	Pr > |t|
Difference of pin within flexible approach -1	0.33278995	0.03986517	8.35	<.0001
Difference of pin within unknown approach	0.50743946	0.04034869	12.58	<.0001
Difference of pin within rigid approach	0.17283761	0.03780628	4.57	<.0001
Difference of flexible and unknown approach for bridges with pin	0.52118221	0.03820862	13.64	<.0001
Difference of flexible and rigid approach for bridges with pin	0.70866900	0.03700624	19.15	<.0001
difference of unknown and rigid approach for bridges with pin	0.56142630	0.03659468	15.34	<.0001
difference of flexible and unknown approach for bridges without pin	0.69583172	0.04079378	17.06	<.0001
difference of flexible and rigid approach for bridges without pin	0.54871666	0.03973913	13.81	<.0001
difference of unknown and rigid approach for bridges without pin	0.22682444	0.03820191	5.94	<.0001

3.5 Hypothesis Tests

Hypothesis tests performed on the data for prestressed concrete bridges were done to investigate the association between beam type and abutment condition, and between approach surface type and abutment condition. Specifically, chi-square hypothesis tests were applied in the research. Chi-square distribution is the sum of squares of independent standard normal deviates (Snedecor and Cochran 1989). In chi-square test, the test statistic has a chi-square distribution if the null hypothesis is true. The result of the hypothesis is expressed in the probability of obtain a statistic value if the null hypothesis is true. If the probability is low (such as 5%), it is reasonable to reject the null hypothesis. It was found that beam type is associated with abutment distress since the hypothesis of no association between approach surface type and abutment distress can not be rejected.

3.5.1 Association between abutment rating (0-9) and design parameters

The frequency analysis considering beam types and abutment ratings is shown in Table 3-21 for reference. The null hypothesis for the chi-square test is that of "*no association between abutment rating and beam section type*". The result of the chi-square test is shown in Table 3-22. It can be seen from Table 3-22 that we can reject the null hypothesis under the type I error rate (probability of reject true hypothesis) being less than 0.01%. It should be pointed out that 53% of the cells had expected counts less than 5. Thus, the chi-square test was not valid test.

The frequency analysis considering approach surface type and abutment ratings is shown in Table 3-23. The null hypothesis for the chi-square test was "*no association between abutment rating and approach surface type*". The result of the chi-square test is shown in Table 3-24. It can be seen from Table 3-24 that we can reject the null hypothesis under type I error rate less than 0.01%. Again, 47% of the cells had expected counts less than 5 and thus the chi-square test was not valid.

Table 3-21 Frequency analysis by girder type and abutment rating

Abutment Rating / Beam		0	2	3	4	5	6	7	8	9	Total
Adjac Box	Freq	1	2	9	27	39	48	72	25	0	223
	Pct	0.11	0.22	0.98	2.93	4.23	5.2	7.8	2.71	0	24.16
	Row Pct	0.45	0.9	4.04	12.11	17.49	21.52	32.29	11.21	0	
Spread Box	Freq	1	2	8	6	8	21	12	0	0	58
	Pct	0.11	0.22	0.87	0.65	0.87	2.28	1.3	0	0	6.28
	Row Pct	1.72	3.45	13.79	10.34	13.79	36.21	20.69	0	0	
I Girder	Freq	6	1	12	51	62	157	294	53	3	639
	Pct	0.65	0.11	1.3	5.53	6.72	17.01	31.85	5.74	0.33	69.23
	Row Pct	0.94	0.16	1.88	7.98	9.7	24.57	46.01	8.29	0.47	
Others	Freq	0	0	1	0	0	0	2	0	0	3
	Pct	0	0	0.11	0	0	0	0.22	0	0	0.33
	Row Pct	0	0	33.33	0	0	0	66.67	0	0	
Total	Freq	8	5	30	84	109	226	380	78	3	923
	pct	0.87	0.54	3.25	9.1	11.81	24.49	41.17	8.45	0.33	100

Table 3-22 Chi-square Test for H_0: no association between abutment rating and beam type

Statistic	DF	Value	Prob
Chi-Square	24	84.7567	<.0001

Table 3-23 Frequency analysis by approach surface type and abutment rating

Abutment Rating / Approach		0	2	3	4	5	6	7	8	9	Total
BituCon	Freq	0	0	0	3	9	7	13	0	0	32
	Pct	0	0	0	0.33	0.98	0.76	1.42	0	0	3.49
	Row Pct	0	0	0	9.38	28.13	21.88	40.63	0	0	
Bitumen	Freq	4	4	16	33	44	84	174	38	0	397
	Pct	0.44	0.44	1.75	3.6	4.8	9.17	19	4.15	0	43.34
	Row Pct	1.01	1.01	4.03	8.31	11.08	21.16	43.83	9.57	0	
Concrete	Freq	3	1	9	40	48	111	149	14	0	375
	Pct	0.33	0.11	0.98	4.37	5.24	12.12	16.27	1.53	0	40.94
	Row Pct	0.8	0.27	2.4	10.67	12.8	29.6	39.73	3.73	0	
Unknown	Freq	1	0	5	7	8	22	40	26	3	112
	Pct	0.11	0	0.55	0.76	0.87	2.4	4.37	2.84	0.33	12.23
	Row Pct	0.89	0	4.46	6.25	7.14	19.64	35.71	23.21	2.68	
Total	Freq	8	5	30	83	109	224	376	78	3	916
	pct	0.87	0.55	3.28	9.06	11.9	24.45	41.05	8.52	0.33	100

Table 3-24 Chi-square Test for H_0: no association between abutment rating and apprsur_type

Statistic	DF	Value	Prob
Chi-Square	24	90.2601	<.0001

3.5.2 Association using abutment condition (distress or not)

Further analyses were performed by regrouping the prestressed concrete bridges in the following way: categorized bridges with abutment rating less than or equal 4 as "with abutment distress" and assigning the other bridges in the category "no abutment distress". Two reasons accounted for the regrouping of the prestressed concrete bridges.

First, our primary concern was whether the bridge has abutment distress instead of differentiating between a rating of "7" or "8". Thus the frequency analysis and hypothesis test on whether the bridge had abutment distress was more rational. Second, as mentioned in the section 3.5.1, for the frequency analysis, there were many cells that have counts of less than 5; and, thus, the hypothesis tests were not valid. After converting the abutment ratings to abutment conditions, each cell would have enough counts to facilitate the hypothesis tests.

The result of frequency analysis concerning abutment condition and beam type is shown in Table 3-25. Results of the corresponding chi-square hypothesis test are shown in Table 3-26. The null hypothesis H_0 is: no association between abutment condition and beam type. It can be seen from Table 3-26 that the null hypothesis test is rejected under a type I error rate of less than 0.01%. The conclusion is that for prestressed concrete bridges, there is association between abutment condition and beam type.

Similarly, the frequency analysis results concerning abutment condition and approach surface type are shown in Table 3-27. Results of the corresponding chi-square hypothesis test are shown in Table 3-28. The null hypothesis H_0 is: No association between abutment condition and approach surface type. It can be seen from Table 3-28 that the null hypothesis can not be rejected even under type I error rate of 50%. The conclusion here is for prestressed concrete bridges, there is no association between abutment condition and approach surface type.

Table 3-25 Frequency analysis by girder type and abutment condition

Abutment Condition / Beam		Good	Poor	Total
Adjac Box	Freq	184	39	223
	Pct	19.93	4.23	24.16
	Row Pct	82.51	17.49	
Spread Box	Freq	41	17	58
	Pct	4.44	1.84	6.28
	Row Pct	70.69	29.31	
I Girder	Freq	569	70	639
	Pct	61.65	7.58	69.23
	Row Pct	89.05	10.95	
Total	Freq	794	126	920
	pct	86.3	13.7	100

Table 3-26 Chi-square Test for H_0: no association between abutment condition and beam type

Statistic	DF	Value	Prob
Chi-Square	2	18.7403	<.0001

Table 3-27 Frequency analysis by approach surface type and abutment condition

Abutment Condition / Approach		Good	Poor	Total
BituCon	Freq	29	3	32
	Pct	3.17	0.33	3.49
	Row Pct	90.63	9.38	
Bitumen	Freq	340	57	397
	Pct	37.12	6.22	43.34
	Row Pct	85.64	14.36	
Concrete	Freq	322	53	375
	Pct	35.15	5.79	40.94
	Row Pct	85.87	14.13	
Unknown	Freq	99	13	112
	Pct	10.81	1.42	12.23
	Row Pct	88.39	11.61	
Total	Freq	790	126	916
	pct	86.24	13.76	100

Table 3-28 Chi-square Test for H_0: no association between abutment condition and apprsur_type

Statistic	DF	Value	Prob
Chi-Square	3	1.1198	0.7723

3.6 Regression Analysis

Regression analysis is an area of statistics that deals with methods for investigating the associations, and, if present, the characteristics of the associations, among various observable quantities (Graybill and Iyer 1994). These associations can further be expressed in the form of mathematical expressions, which may allow the prediction of the unobservable value of a variable based on the observed value of one or more associated or related variables. These models may also help to determine how one can manipulate a given variable to control the value of an associated or related variable. Thus, regression analysis offers a sensible and sound approach for examining associations among variables and for obtaining good rules for prediction. Regression models are thus widely used in engineering analysis and have been successfully applied in a project to evaluate the causes behind precast I-girder end cracking (Myers et al. 2001).

Regression analysis is a commonly used method for obtaining a prediction function μ_y for predicting the values of a *response variable Y* using *predictor variables X_1, ..., X_k*. While the true regression function of a real problem is seldom known, it is possible to postulate a class of functions such that one of the functions in the class will serve as an approximation of the true regression function and is accurate enough for the problem at hand. The regression functions depend on the predictor variables (X_i) and unknown parameters β_i, which are estimated based on statistical analyses of the sample data.

Deductions about population parameters are based on the information provided by samples. Ideally, the collection of data involves random sampling of well-defined populations. As inferred from the discussion of Task I, not all of the bridges will have the same variables or present the same type of distress (output). Thus, the population database can be considered as simple random sampling, that is, a random sample of n items from the entire population of N items is selected

and the values for the response variable Y and the predictor variables $X_1 ... X_k$ for each item in the sample is recorded.

Linear regression models are linear of coefficients (Montgomery et al. 2006, Myers et al. 2002, Weisberg 2005). The linear regression model can use first order of explanatory variables or high order of explanatory variables. While multiple linear regression with first order of explanatory variables are adequate for modeling a wide variety of relationships between response variables and predictor variables, many situations require terms of higher order of explanatory variables to be considered. The underlying assumption in the process of fitting a regression model is that the residuals are *normally, independently and identically distributed* (NIID) variables. This assumption concerning the distribution of residuals can not be satisfied by the regression model and thus the model is not valid.

3.6.1   Diagnostic of Regression Model

The evaluation of the subsets of the explanatory variables is carried out in this section by fiting linear regression models for bridges in each of the main structure types based on the suitable subsets of explanatory variables identified in the above sections.

The underlying assumption in the process of fitting a regression model is that the residuals are *normally, independently and identically distributed* (NIID) variables. Therefore, the idea of evaluating the explanatory variable subsets by the fitness of the linear models based on the subset. The fitness of model is then accessed by the analysis of residuals. A residual is defined as the difference between value of observation and the predicted value obtained from the regression model. The expression of normal distribution with "0" mean and "1" variance (standard normal distribution) is as defined in Equation (3-2), while the plot of a standard normal distribution is shown in Figure 3-16.

$$y = \frac{1}{\sqrt{2\pi}} \exp(-x^2) \qquad\qquad \textbf{(3-2)}$$
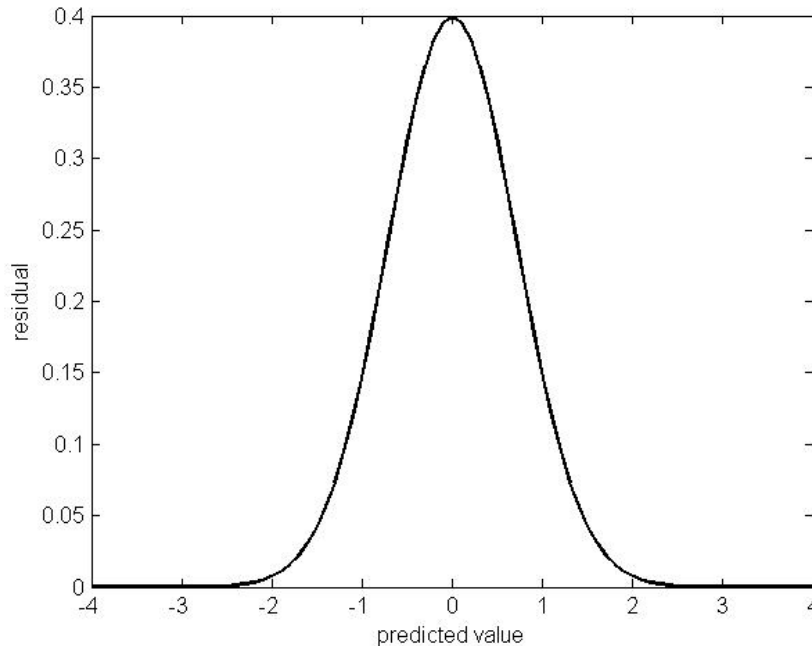
Figure 3-16 Plot of standard normal distribution

One of the basic methods to test the fitness of the model is to test the NIID of the residuals. several popular procedures to perform this test are described in the following paragraphs.

Residual Plot: This is a scatter plot of residuals against predicted values or predictors. The plot of NIID residuals shall have a relative constant variance along the predicted values or predictors. Furthermore, such a residual plot shall not show any structured distribution such as curvature of any form, there shall not be too many outliers in the plot. For linear regression models, the sum of the residuals shall always equal to zero. A sample of a residual plot is shown in Figure 3-17. Figure 3-17 is an example of residual plot for a proper linear regression model and it consequently matches the properties mentioned above.

Residual vs. predicted values
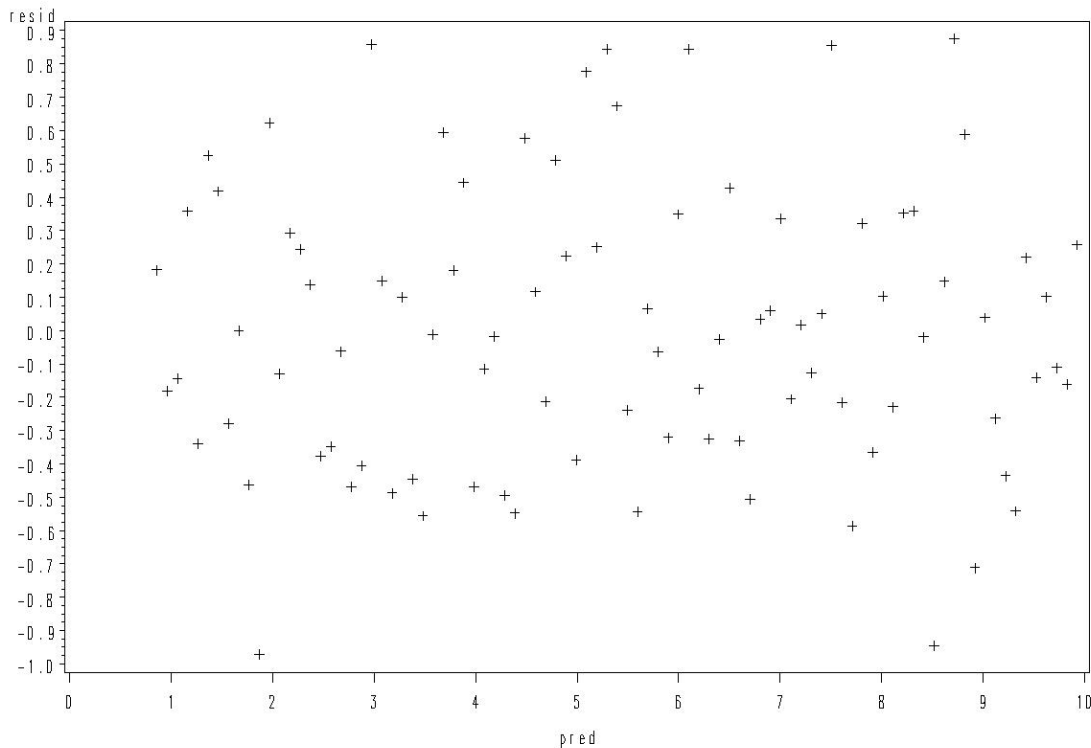
Figure 3-17 Sample of residual plot

Stem and leaf plot: This plot uses the first few digits of a variable as the "stems" and the remaining digits are listed as a "leaf." The length of leaf reflects the number of variables whose first a few digits begin with the stem. As shown in Figure 3-18a, the stem "5" represents the residuals with 0.5, (5×10^{-1} according to the note). Leaf "12899" shows that there are five residuals beginning with 0.5, they are 0.51, 0.52, 0.58, 0.59, and 0.59, respectively. Consequently, a stem and leaf plot is similar to a horizontal bar chart; the difference being that a stem-leaf plot provides more stems than the intervals of a bar chart. The frequency of variables beginning with each stem is listed on the right hand. Stem and leaf plots are a useful tool to detect the nature of variable distribution. It can also reveal the shape of the distribution, expose skewness of the distribution, so and so forth (Freund and Wilson1997). It can be seen from Figure 3-18a that the residuals are normally distributed since the shape of the stem and leaf plot is similar to normal distribution.

86

```
Stem Leaf                      #        Boxplot
   8 44668                     5           |
   7 8                         1           |
   6 27                        2           |
   5 12899                     5           |
   4 234                       3           |
   3 245566                    6           |
   2 224569                    6        +-----+
   1 000245588                 9        |     |
   0 234567                    6        |  +  |
  -0 6632210                   7        *-----*
  -1 876443321                 9        |     |
  -2 8643111                   7        |     |
  -3 98754332                  8        +-----+
  -4 99776440                  8           |
  -5 965441                    6           |
  -6                                       |
  -7 1                         1           |
  -8                                       |
  -9 75                        2           |
     ----+----+----+----+
Multiply Stem.Leaf by 10**-1
        (a)                                 (b)
```

Figure 3-18 A sample of stem and leaf plot and box plot

Box plot: A box plot is used to show distribution shapes and outliers. It is determined in the following way: the two ends of the box are Q_1 (25% quartile) and Q_3 (75% quartile), so the length of the box is *interquartile* range. The vertical lines beyond the end of box have a length of 1.5 times of interquartile range. A sample of box plot is shown in Figure 3-18b. The mild outliers are represented by 0 and extreme outliers are denoted by * in the plot. The horizontal line in the box shows the position of the median; if it is in the middle of the box, the distribution is expected to be symmetrical (Freund and Wilson1997). It can thus be seen that the distribution in Figure 3-18b is symmetrical since the horizontal line is in the middle of box and the two vertical lines are approximately equal. There are no outliers in this box plot. The plotted data is thus an example of an approximately normal distribution.

Normal probability plot: This is a plot of the ordered values of variables against the percentiles of the theoretical normal distribution. If the variables are perfectly normally distributed the plot shall be a straight line. Thus, the normality of the variables can be evaluated by the *closeness* of the plot to the straight line that would be obtained for an ideal normal distribution. An instance of normal probability plot is shown in Figure 3-19. A "+" symbol serves as reference line in the plot, and a "*" symbol is plotted from the residuals of the regression model. It can be seen from Figure 3-19 that the residuals "*" are quite close to the

reference line ("+" symbols), if they are not completely overlapped. This plot is thus an example of residuals which are approximately have a normal distribution.
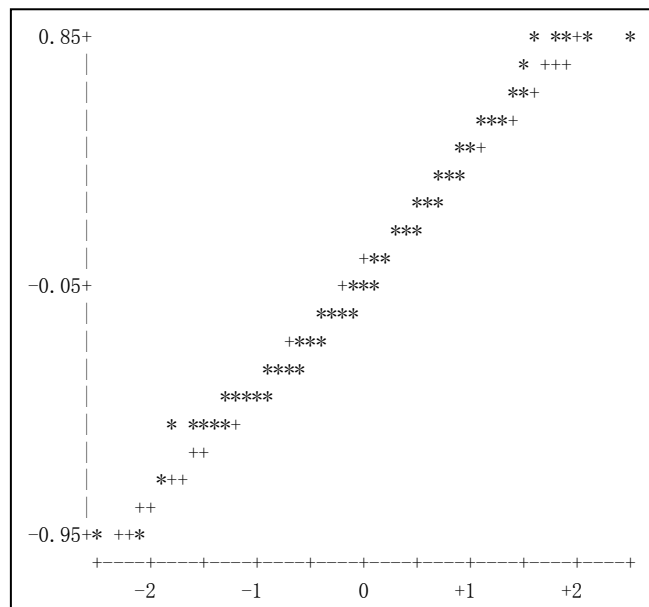
```
0. 85+                                    *  **+*      *
    |                                      *  +++
    |                                    **+
    |                                  ***+
    |                                **+
    |                              ***
    |                            ***
    |                          ***
    |                        +**
-0. 05+                     +***
    |                     ****
    |                   +***
    |                 ****
    |               *****
    |            *  ****+
    |                ++
    |            *++
    |           ++
-0. 95+*  ++*
    +----+----+----+----+----+----+----+----+----+----+
        -2        -1         0        +1        +2
```
Figure 3-19 An example of normal probability plot

3.6.2   Linear regression using first order of explanatory variables

3.6.2.1   *Selection of explanatory variables*

(a)Automatic search Procedures

There are many computer programs available for the automatic search of a single subset: *best subset* regression and *stepwise* regression. The latter procedure was applied in the work of this quarter.

Stepwise regression is based on an iterative procedure. There is a sequence of t-tests on the explanatory variables at each stage. It can be classified as forward stepwise regression, backward stepwise regression, etc, depending on the iteration. It may be initiated with no variables in the model and add variables in it later on, or it could be started with all the variables in the model and variables can be later deleted from it (Kutner et al. 2005). Forward stepwise procedure was used in this research to search for a proper subset of explanatory variables to build the model for the problem. The forward stepwise automatic searching was carried out on three subsets of

database classified by main structure type. The final single subset of explanatory variables and their statistics for all three structure type bridges are shown in Table 3-29, Table 3-30 and Table 3-31, respectively.

The subset of explanatory variables for *simple/cantilevered steel bridges* selected by the forward stepwise procedure is shown in Table 3-29. It can be seen from Table 3-29 that eight variables are included in the subset, each of them with significance value of less than 0.0015. Even though this can not ensure that the subset is optimal, it can still provide valuable reference for the identification of key parameters, especially after the models were verified.

Table 3-29 Subset of explanatory variables for simple/cantilevered steel bridges

Step	Variable Entered	Partial R-Square	Model R-Square	F Value	Pr > F
1	matdiff	0.0343	0.0343	729.06	<.0001
2	ageinsp	0.0282	0.0625	615.94	<.0001
3	deckwidth	0.0301	0.0925	679.06	<.0001
4	apprsurstif	0.0054	0.0979	121.93	<.0001
5	ADTTinsp	0.0015	0.0994	34.22	<.0001
6	maxspan	0.0014	0.1008	31.22	<.0001
7	pin_num	0.0005	0.1013	12.05	0.0005
8	radskew	0.0004	0.1018	10.08	0.0015

The subset of explanatory variables for *continuous steel bridges* selected by the forward stepwise procedure is shown in Table 3-30. Similar to the simple/cantilevered steel bridges, 8 variables were involved in the results. While maximum span is not included in the subset, design load is present instead. The statistical significance based on F-test were all less than 0.0001, except for the last two variables. The last variable, deck width, does not seem to be significant enough from this analysis.

The subset of explanatory variables for *prestressed concrete bridges* selected by the forward stepwise procedure is shown in Table 3-31. It can be noticed that only 4 explanatory variables were involved in the results. The statistical significance based on F-test for all variables was less than 0.0001, except for the last variables. However, the last variable, inspection age, seems to still have enough significance.

Table 3-30 Subset of explanatory variables for continuous steel bridges

Step	Variable Entered	Partial R-Square	Model R-Square	F Value	Pr > F
1	ageinsp	0.1139	0.1139	373.66	<.0001
2	pin_num	0.0286	0.1425	96.97	<.0001
3	radskew	0.0213	0.1638	74.06	<.0001
4	ADTTinsp	0.0163	0.1802	57.89	<.0001
5	apprsurstif	0.006	0.1861	21.25	<.0001
6	designload	0.0058	0.1919	20.85	<.0001
7	matdiff	0.0012	0.1932	4.48	0.0344
8	deckwidth	0.0007	0.1938	2.34	0.1261

Table 3-31 Subset of explanatory variables for continuous steel bridges

Step	Variable Entered	Partial R-Square	Model R-Square	F Value	Pr > F
1	maxspan	0.0179	0.0179	120.48	<.0001
2	matdiff	0.0111	0.029	75.83	<.0001
3	radskew	0.0048	0.0339	33.1	<.0001
4	ageinsp	0.0012	0.0351	8.49	0.0036

(b) Criterion based on all combinations

There are many criteria for the selection of proper models from all combinations, such as R_p^2, $R_{a,p}^2$, C_p, AIC_p, SBC_p and $PRESS_p$. Mallow's C_p criterion was used in the work of this quarter. Mallow's C_p is computed as

$$C_p = \frac{SSE_p}{MSE(X_1, X_2, ..., X_{P-1})} - (n - 2p)$$ (3-3)

where SSE_p is the sums of the square error of the model in consideration, and MSE is the mean squared error of the full model that included all the explanatory variables. SSE_p is the summation of two terms. One is the error due to bias, that is, the model does not reflect the relationship between dependent and independent variables properly. The second component is due to variation, that is the sampling error. Thus, when C_p is plotted against p, and a line $C_p = p$ is drawn on the plot, $C_p s$ of models with little bias will fall in the vicinity of the line, $C_p s$ of models with significant bias will fall high above the line, and $C_p s$ of models without bias will fall below the line. The assumption underlining the calculation of Mallow's C_p factor is that the full model,

including all the explanatory variables, has no bias. That is, *MSE* is an unbiased estimator of variation σ^2.

In the application of Mallow's C_p criterion, we seek a Mallow C_p that is small and close to the *p* value. A small C_p value means a small total square error. A C_p value close to *p* ensures the bias term to be small. A small C_p value itself can not ensure a small bias, so the model with a larger subset of explanatory variables with only a slightly larger C_p value might be preferable in comparison with models with slightly smaller C_p values and smaller *p* values. The C_p value for the full model (including all the explanatory variables) is *p* (Kutner et al. 2005).

Mallow's C_p values for the inspections on the three selected types of structures are shown in Table 3-32, Table 3-33 and Table 3-34 respectively. The subsets of explanatory variables for *simple/cantilevered steel bridges* seem to be good as tested by Mallow's C_p criterion are shown in Table 3-32. It can be seen from Table 3-32 that the most suitable subset is the first one, since its C_p value is small and close to the number of variables *p*. It is reassuring to find out that the first subset exactly matches the subset obtained by the stepwise automatic selection, as seen by comparing with Table 3-29. Thus, the first subset was selected and tested.

Table 3-32 Explanatory variable subsets of simple/cantilevered steel bridges and their Mallow's Cp

Number of variables *p*	C_p	Variables in Model
8	7.8121	deckwidth radskew matdiff apprsurstif maxspan pin_num ageinsp ADTTinsp
9	9.2912	length deckwidth radskew matdiff apprsurstif maxspan pin_num ageinsp ADTTinsp
9	9.5881	deckwidth radskew matdiff apprsurstif maxspan pin_num designload ageinsp ADTTinsp
10	11	length deckwidth radskew matdiff apprsurstif maxspan pin_num designload ageinsp ADTTinsp

The subsets of explanatory variables for *continuous steel bridges* that seem to be good as tested by Mallow's C_p value are shown in Table 3-33. It can be seen from Table 3-33 that no single subset stands out without doubt to be the most suitable one. It could be said, however, that the

first, third and last subsets are better than the remaining two. It is found, however, that the first subset exactly matches the subset obtained by the stepwise automatic selection as compared with Table 3-30. Thus, the first subset was selected and tested.

Table 3-33 Explanatory variable subsets of continuous steel bridges and their Mallow's C_p

Number of variables	C_p	Variables in Model
8	9.7556	deckwidth radskew matdiff apprsurstif pin_num designload ageinsp ADTTinsp
7	10.097	radskew matdiff apprsurstif pin_num designload ageinsp ADTTinsp
9	10.6276	length radskew matdiff apprsurstif maxspan pin_num designload ageinsp ADTTinsp
9	10.9638	length deckwidth radskew matdiff apprsurstif pin_num designload ageinsp ADTTinsp
10	11	length deckwidth radskew matdiff apprsurstif maxspan pin_num designload ageinsp ADTTinsp

Table 3-34 Explanatory variable subsets of prestressed concrete bridges and their Mallow's C_p

Number of variables	C_p	Variables in Model
4	3.0985	radskew matdiff maxspan ageinsp
5	3.5341	length radskew matdiff maxspan ageinsp
5	4.2216	radskew matdiff maxspan ageinsp ADTTinsp
5	4.4377	radskew matdiff apprsurstif maxspan ageinsp
6	4.4413	length radskew matdiff maxspan ageinsp ADTTinsp
6	4.6891	length radskew matdiff apprsurstif maxspan ageinsp
5	4.7343	radskew matdiff maxspan designload ageinsp
5	4.8276	deckwidth radskew matdiff maxspan ageinsp
6	4.9978	length radskew matdiff maxspan designload ageinsp
5	5.0223	radskew matdiff maxspan pin_num ageinsp
6	5.3394	length deckwidth radskew matdiff maxspan ageinsp
6	5.5046	length radskew matdiff maxspan pin_num ageinsp

Subsets of explanatory variables for prestressed concrete bridges that seem to be good as tested by Mallow's C_p value are shown in Table 3-34. It can be seen from Table 3-34 that all the subsets of explanatory variables are good for regression models. In addition, it can be found that the first subset exactly matches the subset obtained from the stepwise automatic selection when compared with Table 3-31. Thus, the first subset was selected and tested.

3.6.2.2   *Simple and cantilevered steel bridges*

The residual plot for the regression model of single or cantilevered steel bridges is shown in Figure 3-20. It can be seen from Figure 3-20 that the variance of the residuals is not constant, and thus the magnitude of the residual is large. The stem and leaf plot and box plot for single or cantilevered steel bridges are shown in Figure 3-21. It can be seen from Figure 3-21 that the distribution of the residuals is not normal, and the distribution is skewed. The Normal Probability Plot for simple/cantilevered steel bridges are shown in Figure 3-22. Again, it can be seen from Figure 3-22 that the plot is close to the reference line but that distribution is skewed. Based on the evaluation of Figure 3-20, Figure 3-21 and Figure 3-22, it can be concluded that the residuals of the regression model for simple and cantilevered steel bridges are not NIID.

Figure 3-20 Residual plot for the model of simple/cantilevered steel bridges

```
              Histogram                    #         Boxplot
  4.75+*                                    1            *
      .
      .
      .*                                    4            0
      .*                                   18            0
      .*                                   57            0
      .******                             565            |
      .****************                   1845           |
      .*****************************************  4845   +-----+
      .*******************************************  5307 *--+--*
      .***************************        3061         +-----+
      .****************                   1679           |
 -1.25+***********                        1168           |
      .******                             569            |
      .*****                              529            0
      .***                                297            0
      .****                               371            0
      .**                                 113            0
      .*                                   53            *
      .*                                   10            *
      .
      .*                                    3            *
      .*                                    4            *
      .*                                    3            *
 -7.25+*                                    7            *
      ----+----+----+----+----+----+----+----+---
      ●   may represent up to 111 counts
```
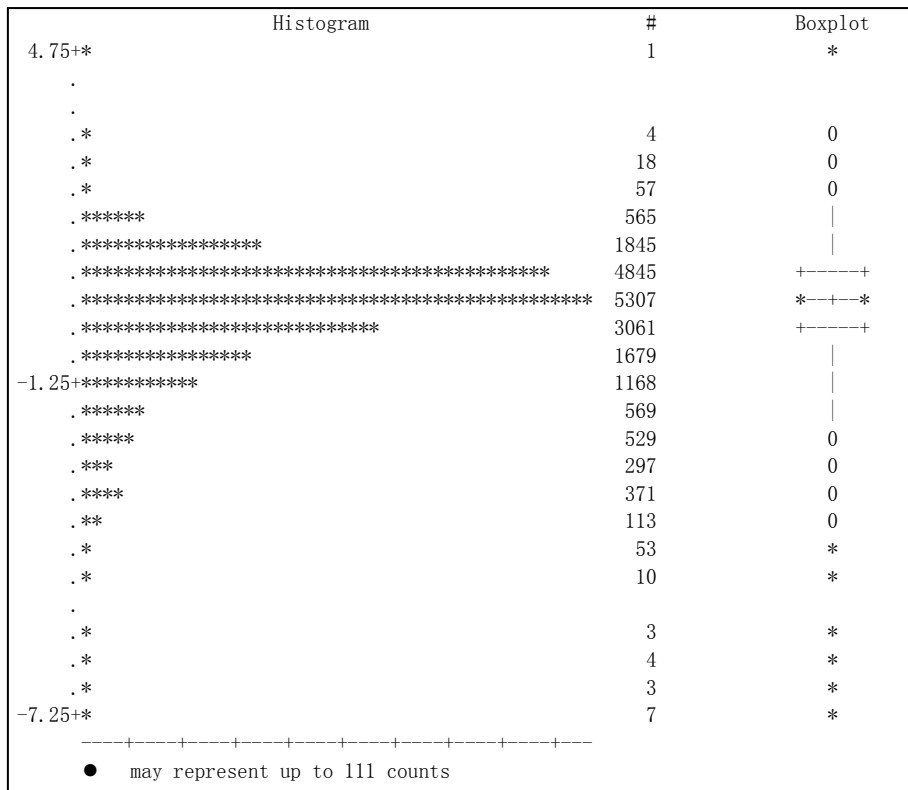
Figure 3-21 Leaf and stem plot and box plot of residuals for the model of simple/cantilevered steel bridges

3.6.2.3 *Continuous steel bridges*

The residual plot for the regression model of continuous steel bridges is shown in Figure 3-23. It can be seen from Figure 3-23 that the variance of the residuals is not constant and its magnitude is large. The stem and leaf plot and box plot for continuous steel bridges are shown in Figure 3-24. It can be seen that the distribution of the residuals is approximately normal. The Normal Probability Plot for the continuous steel bridges regression model is shown in Figure 3-25. It can be seen that the plot is close to reference line but that the distribution is skewed. Based on the evaluation of Figure 3-23, Figure 3-24, and Figure 3-25, it can be concluded that the residuals of the regression model for continuous steel bridges are not NIID.
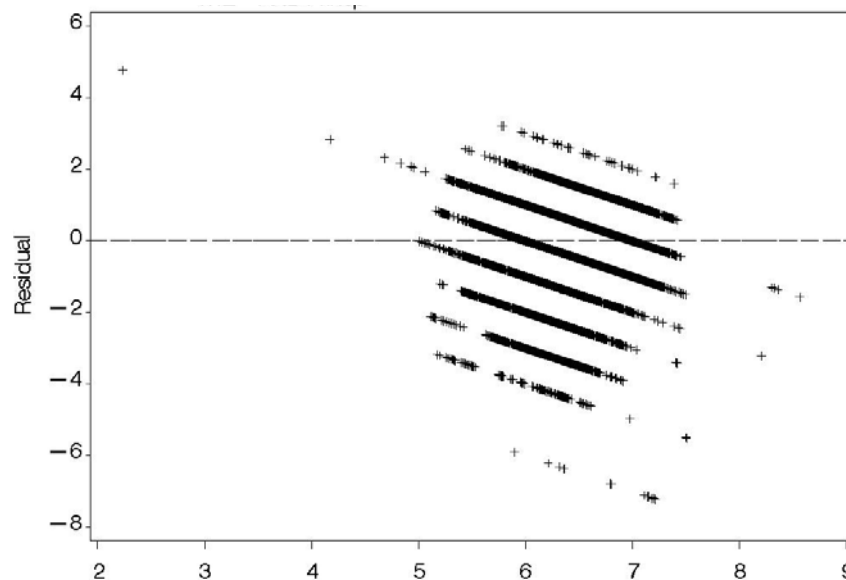
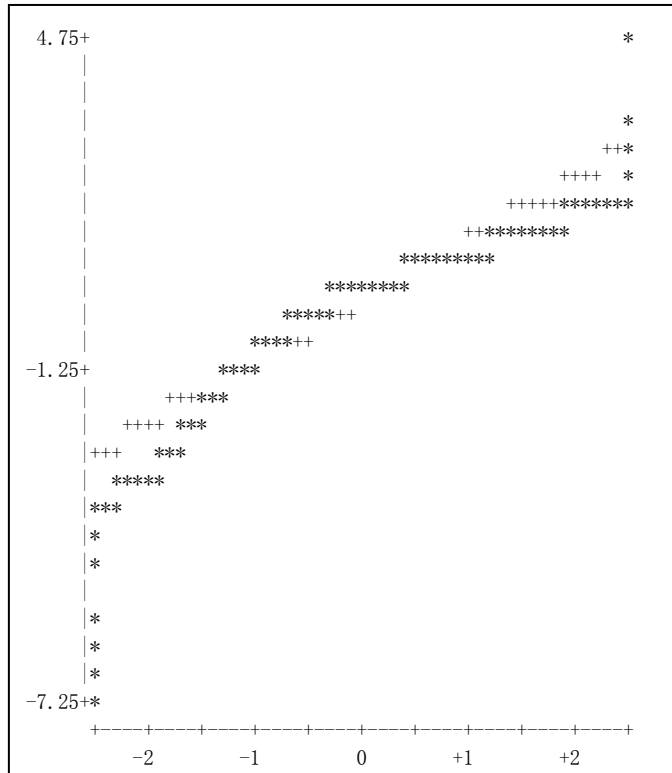**Figure 3-22 Normal probability plot for the model of simple/cantilevered steel bridges**
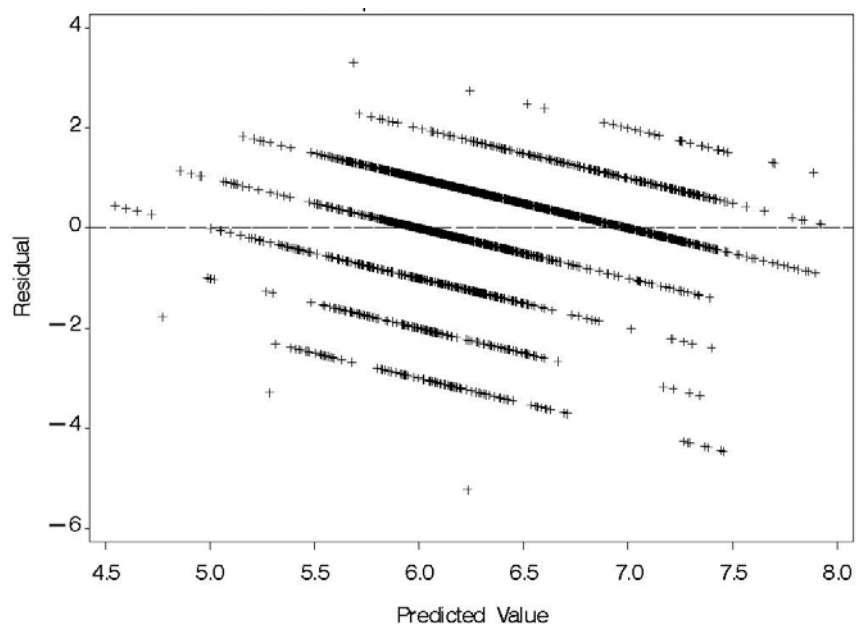

Figure 3-23 Residual plot of linear regression model for continuous steel bridges

```
              Histogram                           #              Boxplot
3.25+*                                            1                 0
   .*                                             1                 0
   .*                                            15                 0
   .******                                       76                 |
   .********************                        306                 |
   .*****************************************   639              +-----+
   .**********************************          561              *--+--*
   .***********************************************  705         +-----+
   .**********                                  148                 |
   .*************                               194                 |
   .*****                                        69                 0
   .******                                       84                 0
   .***                                          42                 0
   .****                                          50                0
   .*                                            10                 0
   .*                                             7                 *
   .
-5.25+*                                            1                 *
     ----+----+----+----+----+----+----+----+--
        ●    may represent up to 15 counts
```

Figure 3-24 Leaf and stem plot and box plot of residuals for continuous steel bridges

```
3.25+                                                    *
    |                                                  +*
    |                                            +++++ *
    |                                          +++++*******
    |                                       +********
    |                                     ********
    |                                 ******
    |                             *******
    |                          ***+++
    |                       ****
    |                   +++***
    |              +++++****
    |++    ***
    |******
    |*
    |*
    |
-5.25+*
     +----+----+----+----+----+----+----+----+----+----+
        -2        -1         0        +1        +2
```

Figure 3-25 Normal probability plot for continuous steel bridges

3.6.2.4 Prestressed concrete bridges

The residual plot for the regression model of prestressed concrete bridges is shown in Figure 3-26, where, it can be seen that the variance of the residuals has systematical trends. In addition, the magnitude of the residual is large and several outliers exist. The stem and leaf plot and box plot for prestressed concrete bridges are shown in Figure 3-27. It can be seen from Figure 3-27 the distribution of the residuals is skewed. The Normal Probability Plot for continuous steel bridges is shown in Figure 3-28, from which it is seen that the plot is close to reference line, however, the distribution is skewed. Based on the evaluation of Figure 3-26, Figure 3-27 and Figure 3-28, it can be concluded that the residuals of the regression model for prestressed concrete bridges are not NIID. Thus, the regression model for prestressed concrete bridges does not fit the observed data.
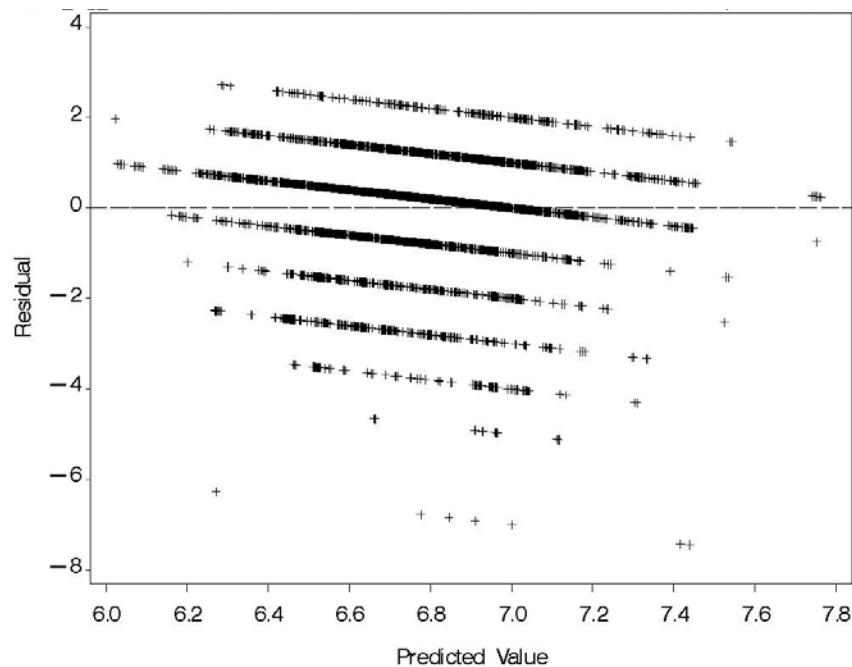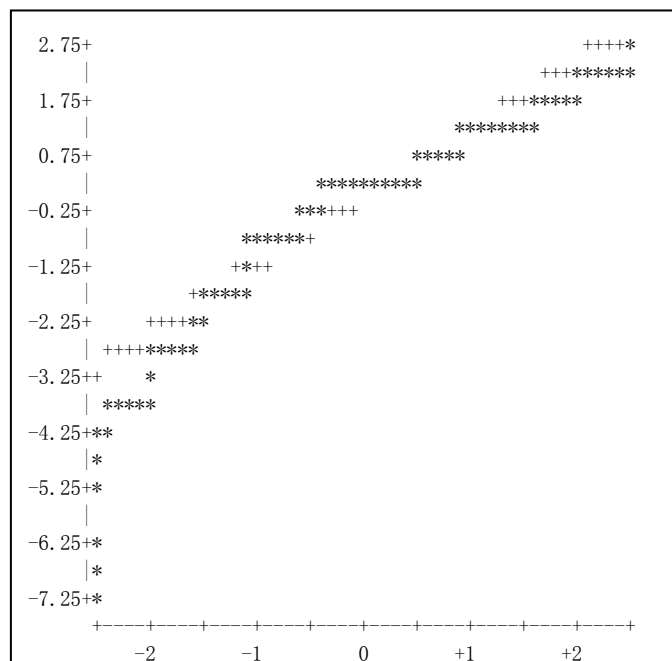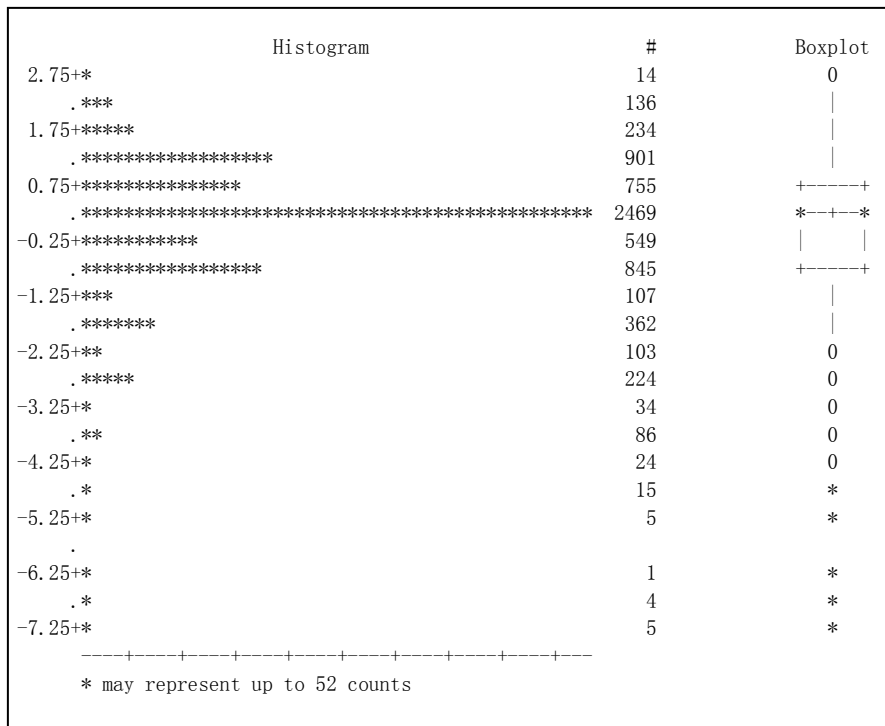
Figure 3-26 Residual plot for simple prestressed concrete bridges

```
                  Histogram                                #        Boxplot
 2.75+*                                                     14         0
     .***                                                  136         |
 1.75+*****                                                234         |
     .*****************                                    901         |
 0.75+***************                                      755       +-----+
     .*************************************************   2469       *--+--*
-0.25+***********                                          549       |     |
     .****************                                     845       +-----+
-1.25+***                                                  107         |
     .*******                                              362         |
-2.25+**                                                   103         0
     .*****                                                224         0
-3.25+*                                                     34         0
     .**                                                    86         0
-4.25+*                                                     24         0
     .*                                                     15         *
-5.25+*                                                      5         *
     .
-6.25+*                                                      1         *
     .*                                                      4         *
-7.25+*                                                      5         *
     ----+----+----+----+----+----+----+----+----+---
       * may represent up to 52 counts
```

Figure 3-27 Leaf and stem plot and box plot of residuals

```
 2.75+                                          ++++*
     |                                        +++******
 1.75+                                      +++*****
     |                                    ********
 0.75+                                 *****
     |                           **********
-0.25+                        ***+++
     |                      ******+
-1.25+                   +*++
     |                 +*****
-2.25+            ++++**
     |  ++++*****
-3.25++      *
     |  *****
-4.25+**
     |*
-5.25+*
     |
-6.25+*
     |*
-7.25+*
     +----+----+----+----+----+----+----+----+----+----+
       -2        -1         0        +1        +2
```

Figure 3-28 Normal probability plot

3.6.2.5 Discussion

Based on the results of residual analysis, linear regression models using the first order of explanatory variables can not reflect the relationship between explanatory variables and the abutment ratings for this research problem.

3.6.3 Linear regression analysis using first and second order of explanatory variables

Multivariate linear regression models considering quadratic and cross interaction terms were developed using bridge abutment rating as the response variable and bridge design and operation parameters as explanatory variables. In general, these types of models were not found to be adequate for predicting abutment damage.

3.6.3.1 Data used in the analysis

The inspection records of MDOT's simple/cantilevered steel highway bridges were analyzed. The response variable was taken as abutment rating. Eight quantitative variables and two qualitative variables were used as explanatory variables in the analysis (see Table 3-35).

Table 3-35 Explanatory variables definition

Parameter	Definition
matdiff (quantitative)	Annual temperature difference
Ageinsp (quantitative)	Age of bridges at the time of inspection
Approachtype[1] *(qualitative)*	Approach surface stiffness
ADTTinsp (quantitative)	Average daily truck traffic in the year of 1995
maxspan (quantitative)	Maximum span of the bridges
length: (quantitative)	Total length of the bridge (m)
deckwidth (quantitative)	Total deck width (m)
pin type[2] *(qualitative)*	Number of pins
Skew (quantitative)	Skew angle of the bridge (degree)

[1] The qualitative variable *approachtype* can take three values: 0, 1 and 2, to represent flexible approach surface, unknown, and rigid approach surface, respectively. It is recorded as two dummy variables: stif1 and stif2, with the value (stif1, stif2), where (0, 0) represents unknown , (1, 0) represents flexible approach surface type and (0, 1) represents rigid approach surface type.

[2] The qualitative variable *pintype* had two possible values, "0" represents without pin-and-hanger, and "1" represent with pin-and-hanger.

A box plot and histogram plot of abutment rating are shown in Figure 3-29 and Figure 3-30, respectively. It can be seen from these two figures that the abutment rating is not perfectly normally distributed (skewness exists). In order to avoid possible a multi-colinearity problem and the severe round off error caused by it, the seven quantitative variables were normalized before quadratic and cross interaction terms were added. The corresponding mean and standard deviation of the covariates are shown in Table 3-36.
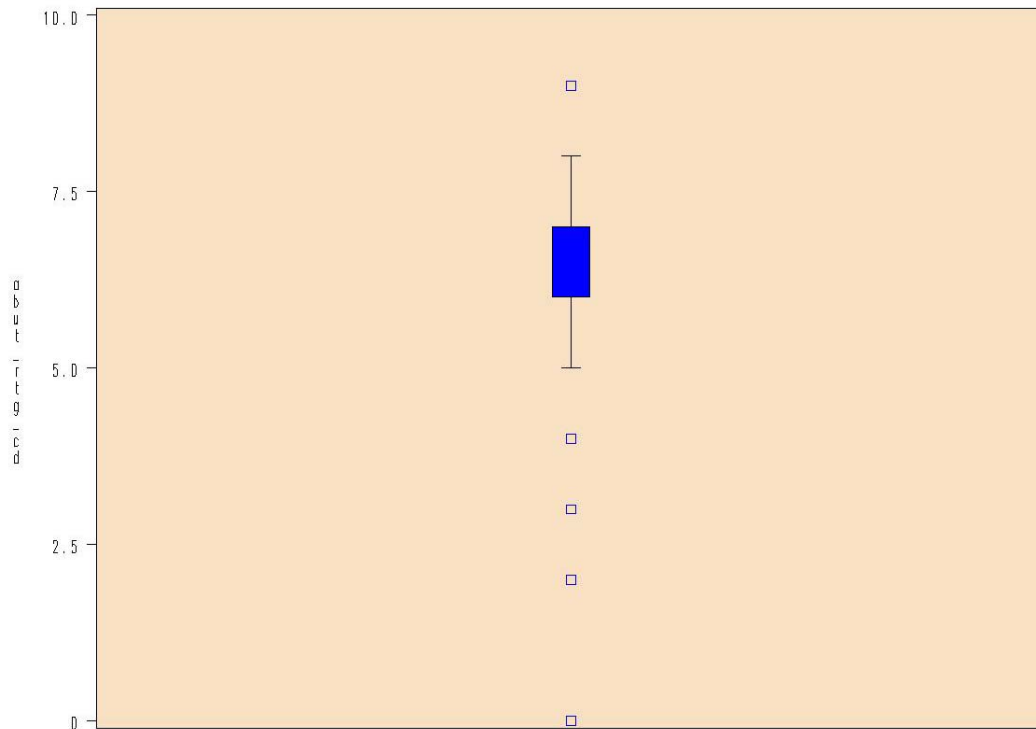
Figure 3-29 Box plot of abutment rating
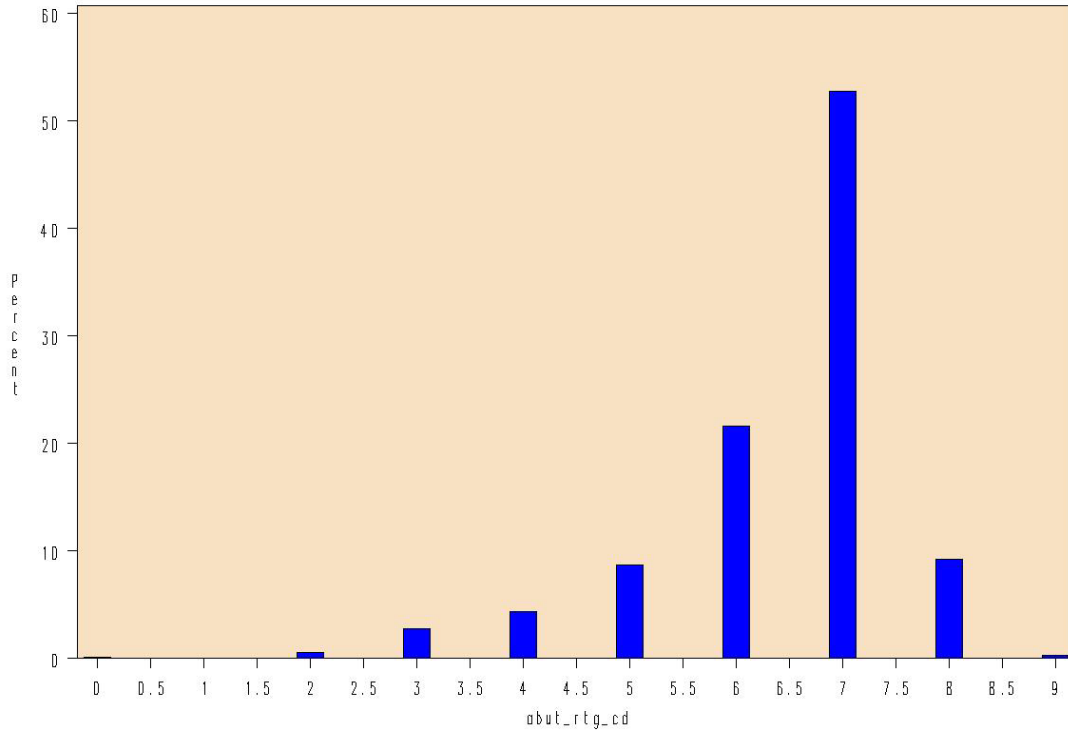
Figure 3-30 Histogram of abutment rating

Table 3-36 Mean and standard deviation of the quantitative variables

Parameter	Mean (μ)	standard deviation (σ)
length (m)	64.796	38.001
deckwidth (m)	15.394	6.957
skew (^{o})	19.265	18.078
ageinsp	36.46	12.127
Matdiff (^{o}F)	19.38	1.424
ADTTinsp	2762.1	3388.200
maxspan (m)	24.977	9.241

The covariates were recoded based on the following Equation: **(3-4)**:

$$x_i* = \frac{x_i - \overline{x_i}}{\sigma_i}$$

(3-4)

The qualitative variable "*approachtype*" was recorded to two dummy variables: *app1*, and *app2*, when *approachtype* = 0, *app1* = 0, *app2* = 0; when *approachtype* = 1, *app1* =1, *app2* =0;

when *approachtype* = 2, *app1* = 0, *app2* =1; the qualitative variable "*pintype*" can be viewed as a dummy variable itself, so no recoding was needed for it.

After the covariates were recoded, the quadratic and cross interaction term were added. No quadratic term for the dummy variables was added. No interaction term was added the between dummy variables "*app1*" and "*app2*", since they are derived from the same qualitative variables and thus the interaction between them will make no sense. After the recoding, the model included: 7 covariates, 3 dummy variables, 7 quadratic terms of the covariates, and 44 cross interaction terms for 61 explanatory variables in all. The response variable was the abutment rating "*abut_rtg_cd*".

3.6.3.2 *Selection of the optimal explanatory variables subset*

The statistical software SAS (SAS 2007) was applied to search for the optimal subset of explanatory variables. The criterion of Mallow's Cp was applied to select the optimal subset of explanatory variables.

All the possible combinations of 61 explanatory variables are evaluated by regression analysis module of SAS software "*SAS PROC REG*" (SAS 2007), the results are shown in Figure 3-31 and Table 3-37. The results in Table 3-37 are ordered by C_p value.
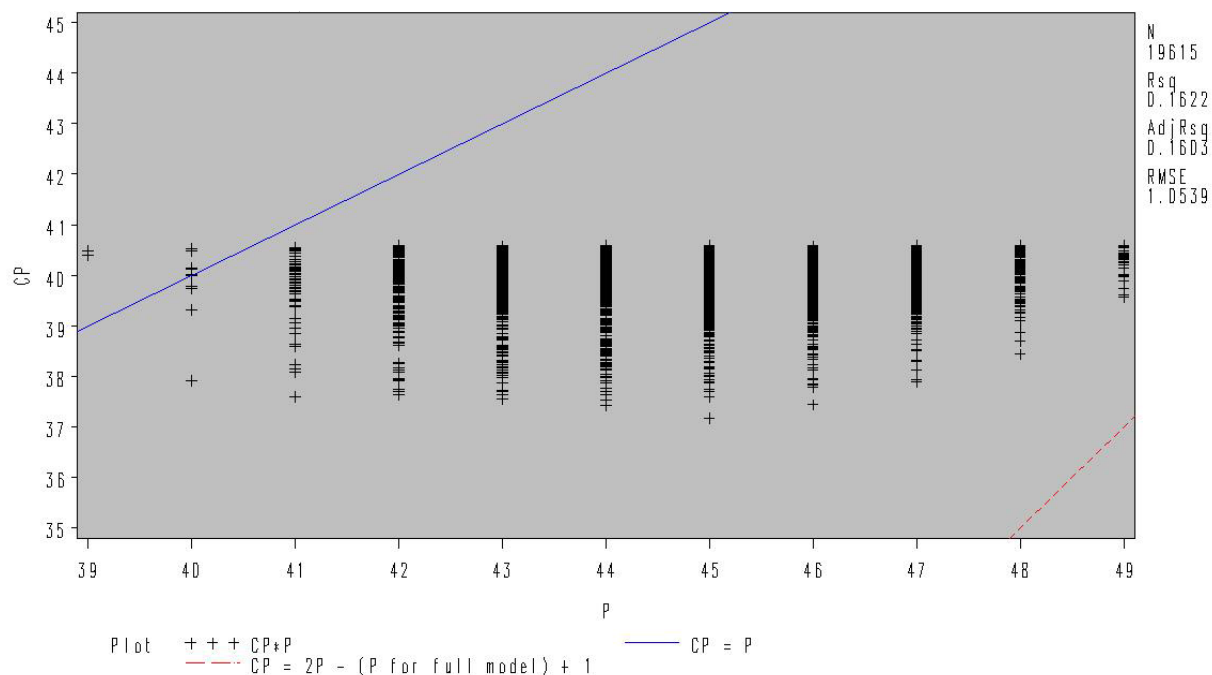
Figure 3-31 Mallow's C$_p$ against p

The top 4151 models in Table 3-37 were checked. The range of p was from 39 to 49; and as can be seen from Figure 3-31, most of the points fall under the $C_p = p$ line. Parsimonious models were preferred. The subset that contained 40 explanatory variables with the smallest C_p value (the sixth row in Table 3-37) was chosen.

Table 3-37 Results of Mallow's Cp Selection Method (Top 7 rows)

p	Cp	Variables in the model
44	37.18	length deckwidth ageinsp matdiff ADTTins maxspan pintype app1 app2 Len2 Dew2 Ske2 Age2 Adt2 Mas2 LenAge LenMat LenAdt LenMas LenAp1 DewSke DewAge DewMat DewAdt DewMas DewPin DewAp1 SkeMat SkeMas SkePin SkeAp1 SkeAp2 AgeMas AgeAp1 AgeAp2 MatAdt MatMas MatAp1 MatAp2 AdtMas MasPin MasAp1 PinAp1 PinAp2
43	37.43	length deckwidth ageinsp matdiff ADTTins maxspan pintype app1 app2 Len2 Dew2 Ske2 Age2 Adt2 Mas2 LenAge LenMat LenAdt LenMas LenAp1 DewSke DewAge DewMat DewAdt DewMas DewPin DewAp1 SkeMat SkeMas SkePin SkeAp1 SkeAp2 AgeMas AgeAp2 MatAdt MatMas MatAp1 MatAp2 AdtMas MasPin MasAp1 PinAp1 PinAp2
45	37.44	length deckwidth ageinsp matdiff ADTTins maxspan pintype app1 app2 Len2 Dew2 Ske2 Age2 Adt2 Mas2 LenAge LenMat LenAdt LenMas LenAp1 DewSke DewAge DewMat DewAdt DewMas DewPin DewAp1 SkeMat SkeMas SkePin SkeAp1 SkeAp2 AgeMas AgeAp1 AgeAp2 MatAdt MatMas MatAp1 MatAp2 AdtMas AdtAp1 MasPin MasAp1 PinAp1 PinAp2
43	37.52	length deckwidth ageinsp matdiff ADTTins maxspan pintype app1 app2 Len2 Dew2 Ske2 Age2 Adt2 LenAge LenMat LenAdt LenMas LenAp1 DewSke DewAge DewMat DewAdt DewMas DewPin DewAp1 SkeMat SkeMas SkePin SkeAp1 SkeAp2 AgeMas AgeAp1 AgeAp2 MatAdt MatMas MatAp1 MatAp2 AdtMas MasPin MasAp1 PinAp1 PinAp2
42	37.56	length deckwidth ageinsp matdiff ADTTins maxspan app1 app2 Len2 Dew2 Ske2 Age2 Adt2 Mas2 LenAge LenMat LenAdt LenMas LenAp1 DewSke DewAge DewMat DewAdt DewMas DewPin DewAp1 SkeMat SkeMas SkePin SkeAp1 SkeAp2 AgeMas AgeAp2 MatAdt MatMas MatAp1 MatAp2 AdtMas MasPin MasAp1 PinAp1 PinAp2
40	37.6	length deckwidth ageinsp matdiff ADTTins maxspan app1 app2 Len2 Dew2 Ske2 Age2 Adt2 LenAge LenMat LenAdt LenMas LenAp1 DewSke DewAge DewMat DewAdt DewMas DewPin DewAp1 SkeMat SkeMas SkePin SkeAp1 SkeAp2 AgeAp2 MatAdt MatMas MatAp1 MatAp2 AdtMas MasPin MasAp1 PinAp1 PinAp2
44	37.6	length deckwidth skew ageinsp matdiff ADTTins maxspan pintype app1 app2 Len2 Dew2 Ske2 Age2 Adt2 LenAge LenMat LenAdt LenMas LenAp1 DewSke DewAge DewMat DewAdt DewMas DewPin DewAp1 SkeMat SkeMas SkePin SkeAp1 SkeAp2 AgeMas AgeAp1 AgeAp2 MatAdt MatMas MatAp1 MatAp2 AdtMas MasPin MasAp1 PinAp1 PinAp2

3.6.3.3 Regression analysis and validation

In order to verify the model, residual plots against predicted values and explanatory variable "deck width" are shown in Figure 3-32 and Figure 3-33, respectively. Plots of residuals versus other predictors can be referred to Appendix A. The plot of residuals against predicted values is shown in Figure 3-32. It can be seen that there is a fan-shape pattern in the residual plot and that the variance of the residual is not constant. There are also some outliers in the plot.
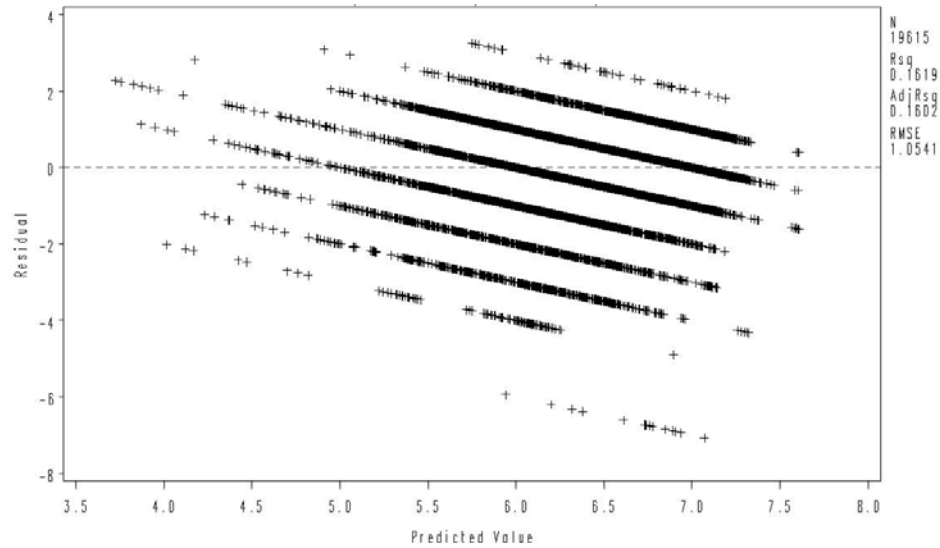
Figure 3-32 Plot of Residual against predicted values
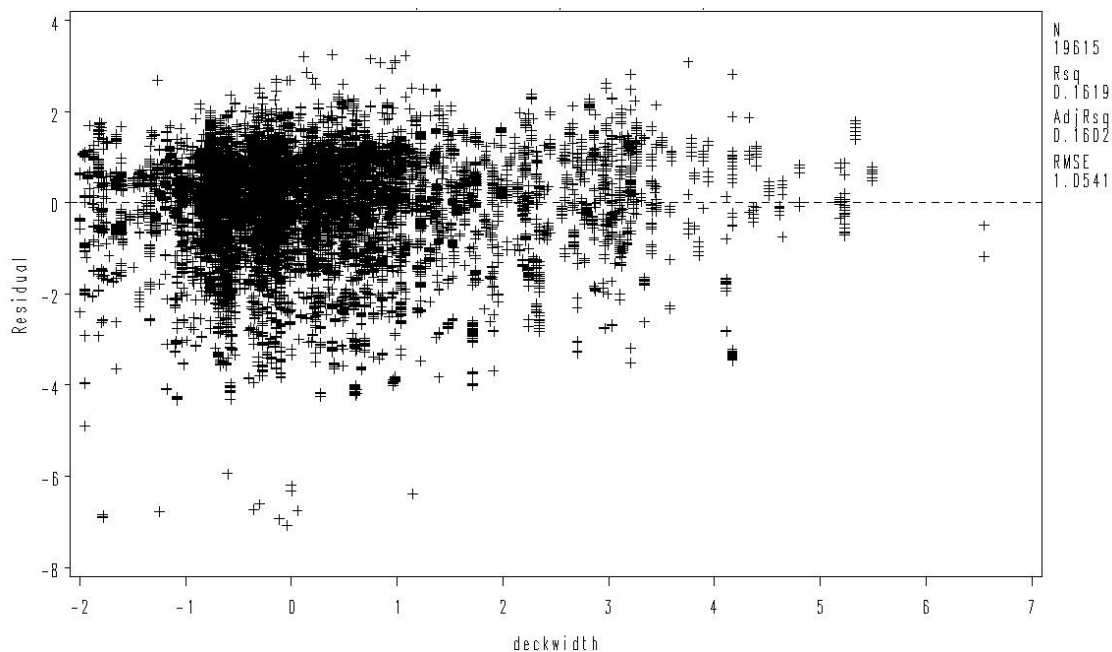
Figure 3-33 Plot of Residual against deckwidth

The plot of residual against deck width is shown in Figure 3-33. It can be seen that there is structural pattern in the residual plot. There are also some outliers in the plot. Nonetheless, the problem is not severe since most of the residuals fall within the range of ±2. The variance also seems to decrease with the increase of deck width. Since most bridge widths distributed within ±2 standard deviation around the mean, the decreased pattern is not serious.

Check of residual distribution is also an important procedure to validate the model. The stem-and-leaf plot and box plot are shown in Figure 3-34. It can be seen from the stem-and-leaf plot on the left that the distribution of residual is skewed. After viewing the box plot on the right, in addition to skew, there are also some outliers detected by the box plot. The normal probability plot of the residual is shown in Figure 3-35. The skew problem stands out again.

Based on the residual diagnosis above, it can be concluded that the NIID distribution of residuals can not be confirmed, thus, the regression model is not valid. Furthermore, none of the regression models developed in this research is adequate after model checking process. The regression analysis can not be proved to be a suitable method in identifying damage in bridge abutment.

```
            Histogram                                #        Boxplot
 3.25+*                                               8          0
    .*                                               18          0
    .*                                              102          0
    .****                                           438          |
    .***************                               1901          |
    .****************************                  3737        +-----+
    .**********************************************5762        *--+--*
-0.25+************************                      3103        +-----+
    .****************                              1844          |
    .********                                       968          |
    .*****                                          581          |
    .****                                           416          0
    .***                                            316          0
    .***                                            251          0
-3.75+*                                             104          0
    .*                                               50          *
    .*                                                1          *
    .
    .*                                                1          *
    .*                                                3          *
    .*                                               10          *
-7.25+*                                                1          *
    ----+----+----+----+----+----+----+----+----+---
    * may represent up to 121 counts
```
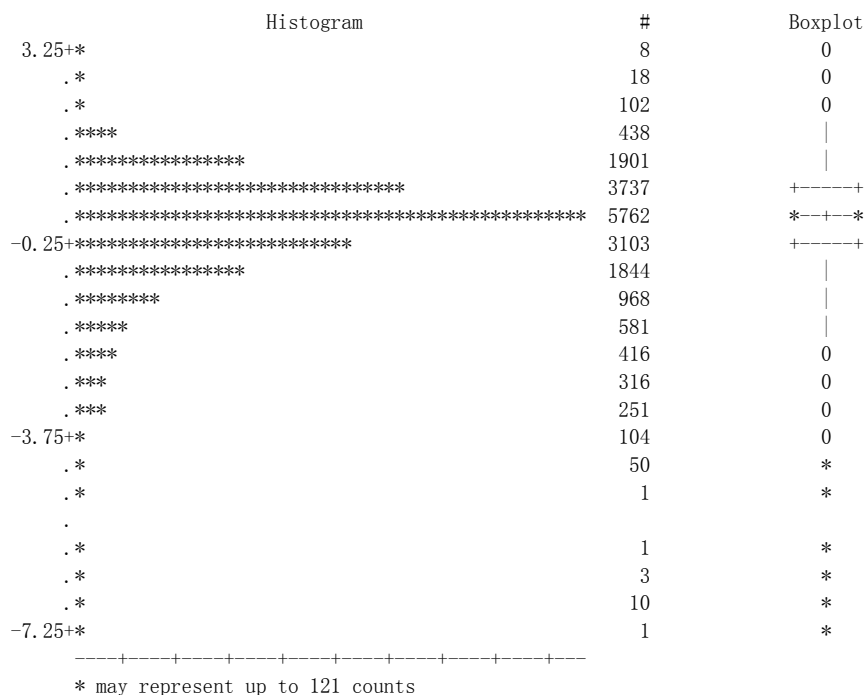
Figure 3-34 Stem and leaf plot and box plot of residuals

105

```
3.25+                                                    *
    |                                                   +*
    |                                              +++++ *
    |                                           ++++*******
    |                                       +*********
    |                                   *******
    |                              *********
-0.25+                         *****++
    |                       *****++
    |                     ****+
    |                  ++***
    |              +++++***
    |++     ***
    |  *****
-3.75+**
    |*
    |*
    |
    |*
    |*
    |*
-7.25+*
    +----+----+----+----+----+----+----+----+----+
      -2        -1        0        +1        +2
```
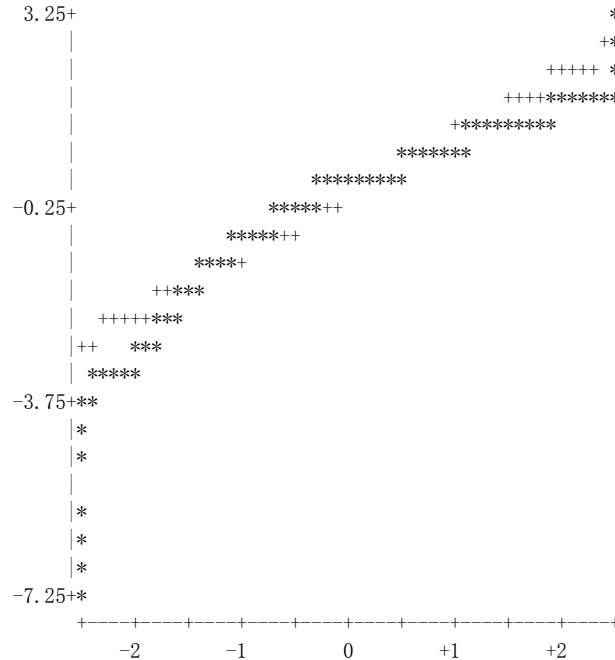
Figure 3-35 Normal Probability Plot of the residuals

3.7   Discussion

As expected, the frequency analyses revealed that older bridges have higher incidences of poor abutment performance. The higher number of bridges with poor abutment for stiff approaches (asphalt on concrete base or concrete) supports the assumption of pavement growth on abutment damage. Finally, poor performance of expansion joints was also clearly related to abutment performance. This could be indicative of abutment forces due to restrained temperature movements, poor bearing performance, and pavement growth problems.

Exploration of correlation coefficients between abutment rating and different parameters was carried out as part of Task III.2. The search for the key parameters by the different paths was represented by sorting the bridge population in the database in sub-divisions or sub-categories. Generally, pier rating was shown to have good correlation with abutment rating. Deck width, pin condition, age at inspection, built year, average daily total traffic, and average daily truck traffic are all shown to have some degree of correlation to abutment rating. The correlation coefficients differ according to the different data categorization and subdivision.

In the factorial analysis of simple/cantilevered steel bridges, two factors: pin type and approach surface type, were considered. The factorial effects were evaluated for the different levels of factors. Since the interaction term between them was significant, the difference between the effects of levels of one factor is considered within certain levels of the other factor. It was found that when the covariates were zero, the effect of pin type was not significant for flexible approaches, while for the other approach types, the effect was significant. The effects of different levels of approach type were always significant regardless of whether the bridge had a pin or not. Some of the factorial effects also changed with the variation of covariates.

Hypothesis tests concerning the association between design parameters and abutment condition for prestressed concrete bridges showed that there was an association between beam type and abutment condition. Proper linear regression models can not be developed only considering the first order of explanatory variables. The linear regression model using 40 covariates was a relatively good regression model for the current research problem. Covariates consist of the design parameters of the bridge and their quadratic and cross interaction terms. However, it is still not appropriate to reflect the complex problem of abutment distress. Evaluation of the residuals plots shows that most of them have fan-shaped patterns and outliers. The NIID assumption concerning the distribution of residuals can not be satisfied by the regression model and thus the model is not valid.

Another generalized linear regression model that can be developed is a multivariate logistic regression model. A multilayer perceptron using sigmoid activation function without hidden layer is equivalent to logistic regression (Bishop 1995, Dreiseitl and Ohno-Machado 2002, Hastie et al.2001). The multivariate logistic regression model can not be expected to have a better performance than the multilayer perceptron using sigmoid activation function with two hidden layers developed for this research. Thus, the logistic regression model will not be further considered.

4 Field Instrumentation (Task II)

4.1 Introduction

Field instrumentation in this research focused on the deployment of a strategic field monitoring scheme on four bridges with and without signs of substructure distress. The objectives of the field instrumentation were as follows:

- ➢ Evaluate damage patterns for different bridge super- and sub-structures;

- ➢ Record behavior of the abutment wall interact with super-structure and environment;

- ➢ Identify possible causes of typical damage.

The subtasks for field instrumentation were:

- ➢ Subtask II.1: Bridge Selection.

- ➢ Subtask II.2: Instrumentation Strategy and Implementation.

- ➢ Subtask II.3: Data Collection and Interpretation.

Field data were monitored at intervals of one month for one-year's time span.

4.2 Bridge Selection (Subtask II.1)

From 44 inspected bridges in this research (section 2.5), 4 bridges were selected for field instrumentation as shown in Figure 4-1. A review of the plans of the selected bridges showed that in all cases the bearing supports were connected to the abutment wall through bolts (refer to Appendix. B).In addition to the factors already considered in the selection of bridges for field inspection and the additional damage patterns and observations noticed during the field inspection, the accessibility of the bridge abutment and the overall bridge site was also taken into account. For each superstructure type, one bridge already showed abutment distress and one bridge with minor abutment distress but with the potential to develop further damage were selected for field instrumentation.

Table 4-1 Final instrumentation list

ID	Bridge key	Abutment Rating	Girder	Pavement	Year built	Width (ft)
A 2.1	25125031000S110	7 (6) [7]*	I or W	Asphalt over Concrete**	1954	67.9
A 1.7	82182291000S110	4 (3 & 4-5)[3 & 5]*	I or W	Concrete**	1972	63.6
C 2.4	25125132000S060	6 (7) [5 & 7]*	I	Concrete**	1971	121.7
C 2.1	63163174000S061	4 (4) [6 & 4]*	I	Asphalt over Concrete**	1964	59.7

*the value in the parenthesis is field inspection abutment rating by Dr. Burgueño, the value in "[ ]" is the field inspection abutment rating by a certified bridge inspection engineer (CTE Engineers, Lansing, MI)

**information updated according to field inspection.

4.3 Instrumentation Strategy and Implementation (Subtask II.2)

A field instrumentation strategy was developed and implemented to meet the objectives mentioned in section 4.1. Only one-half of one of the abutments for each bridge was provided with measuring points (see "shaded area" in Figure 4-1). As shown in Figure 4-1, traffic comes toward the instrumented part of the abutment wall. This abutment side was selected for monitoring as it might be able to capture any effects caused by truck braking. The location of the instrumented bridges and information on instrumented abutment is given in Table 4-2.
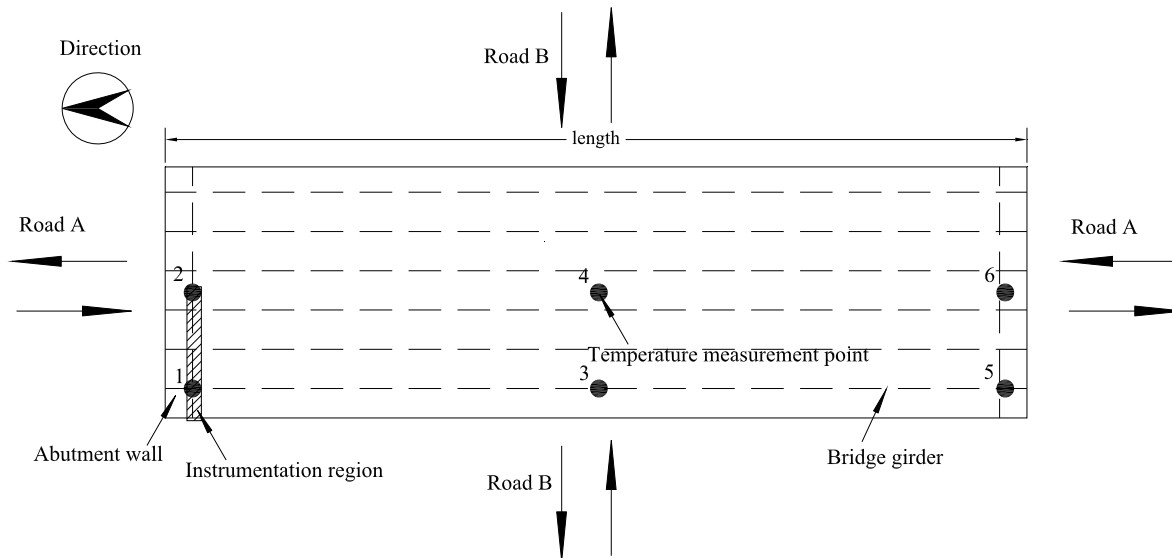
Figure 4-1 Location of bridge and instrumentation region

Table 4-2 Bridge location and information on instrumented abutment

ID	Road A	Road B	Direction	Width (ft)
A 1.7	I-94	I-275	West	63.6
A 2.1	Miller Rd	I-75	East	67.9
C 2.1	I-75	Rochester Rd	East	59.7
C 2.4	I-475	W Atherton Rd	South	121.7

4.3.1 Deployment of measuring points

The measuring points consisted of brass cylinders (Figure 4-2) embedded into the abutment wall. The brass cylinders have a threaded end where a screw-in seat can be attached (Figure 4-3). For girder ends, target discs were glued to the beam surface using an epoxy adhesive. The deployment of measuring points on bridge A 1.7 is shown in Figure 4-4. The deployment of measuring points on bridge A 2.1 is shown in Figure 4-5. The deployment of measuring points on bridge C 2.1 is shown in Figure 4-6. The deployment of measuring points on bridge C 2.4 is shown in Figure 4-7 and Figure 4-8.

110

Figure 4-2 Brass cylinders installed on the abutment wall

Figure 4-3 Measuring points with contact seats screwed on brass cylinders
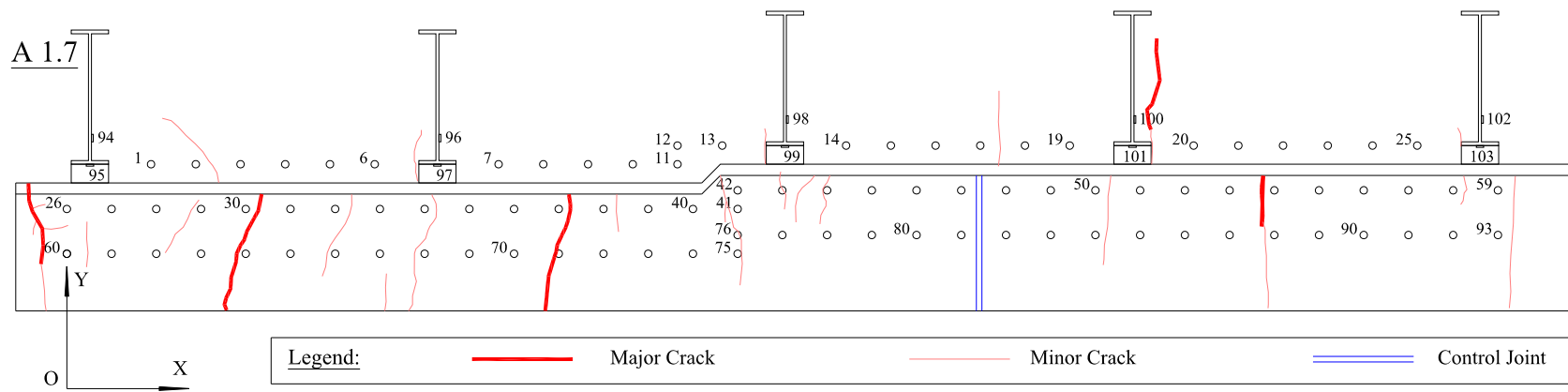
Figure 4-4 Deployment of measuring points on half of the abutment wall of A 1.7
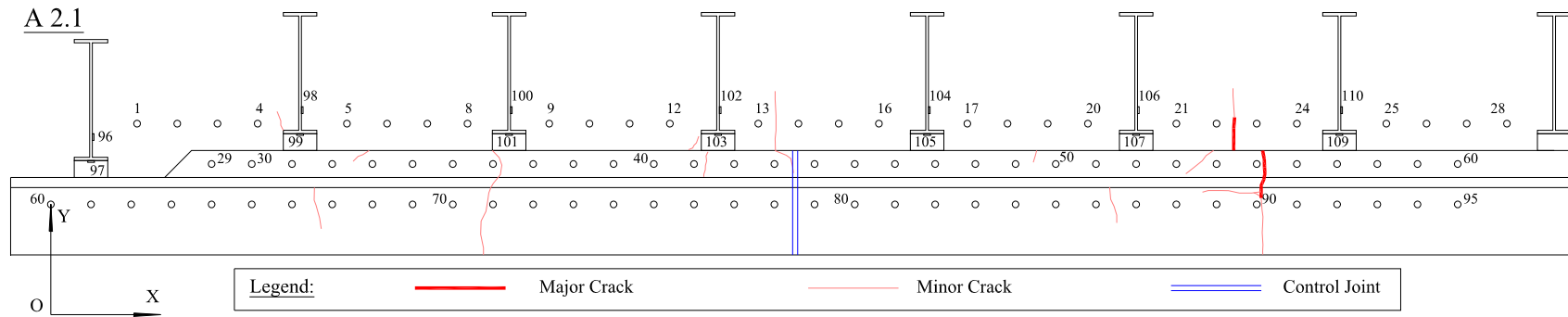
Figure 4-5 Deployment of measuring points on half of the abutment wall of A 2.1
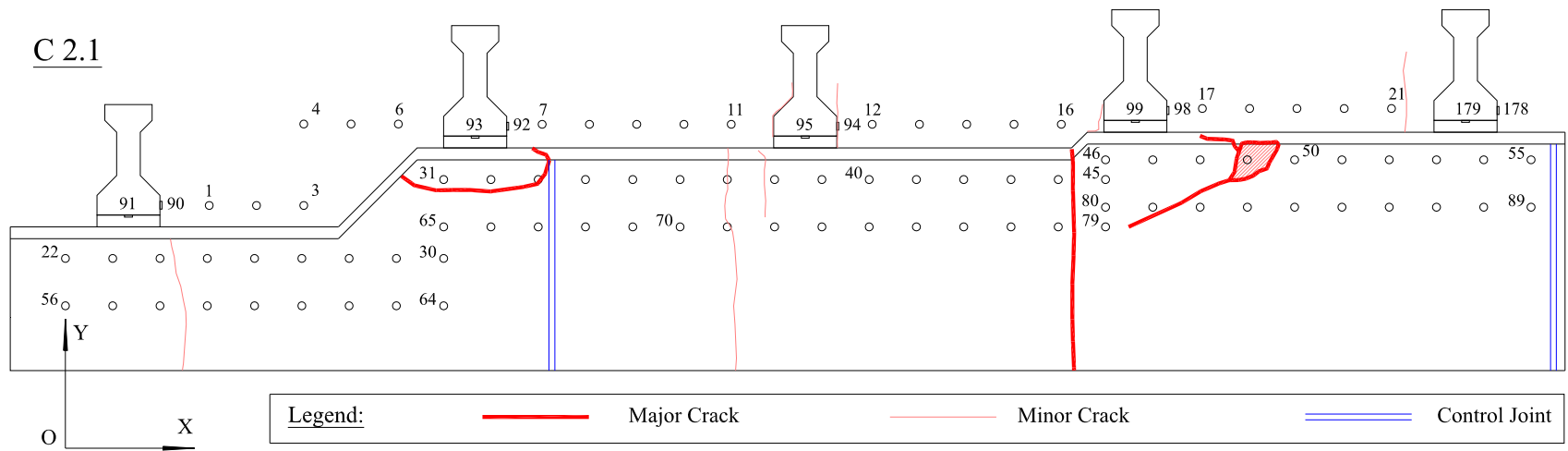
Figure 4-6 Deployment of measuring points on half of the abutment wall of C 2.1
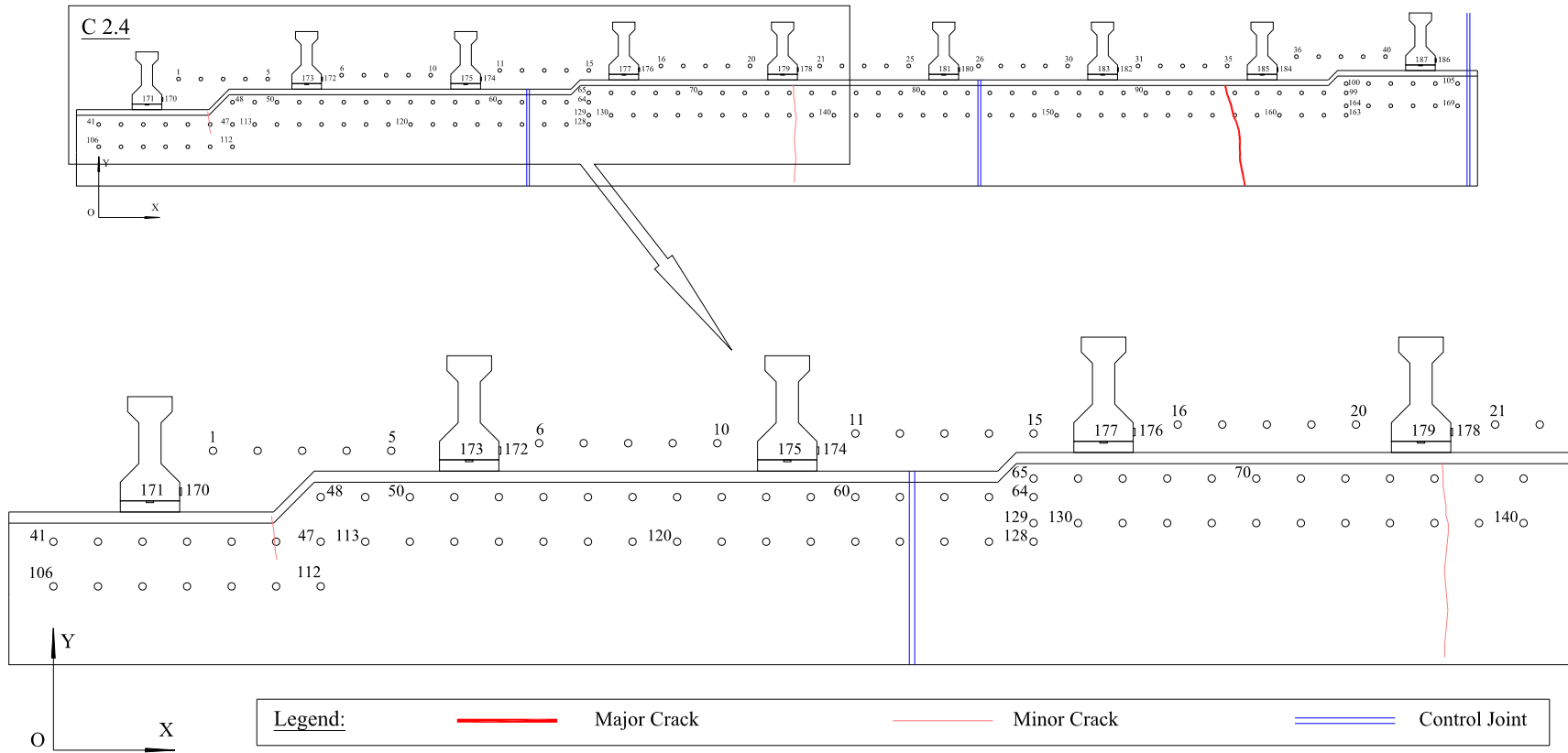
Figure 4-7 Deployment of measuring points on half of the abutment wall of C 2.4 (Magnification A)
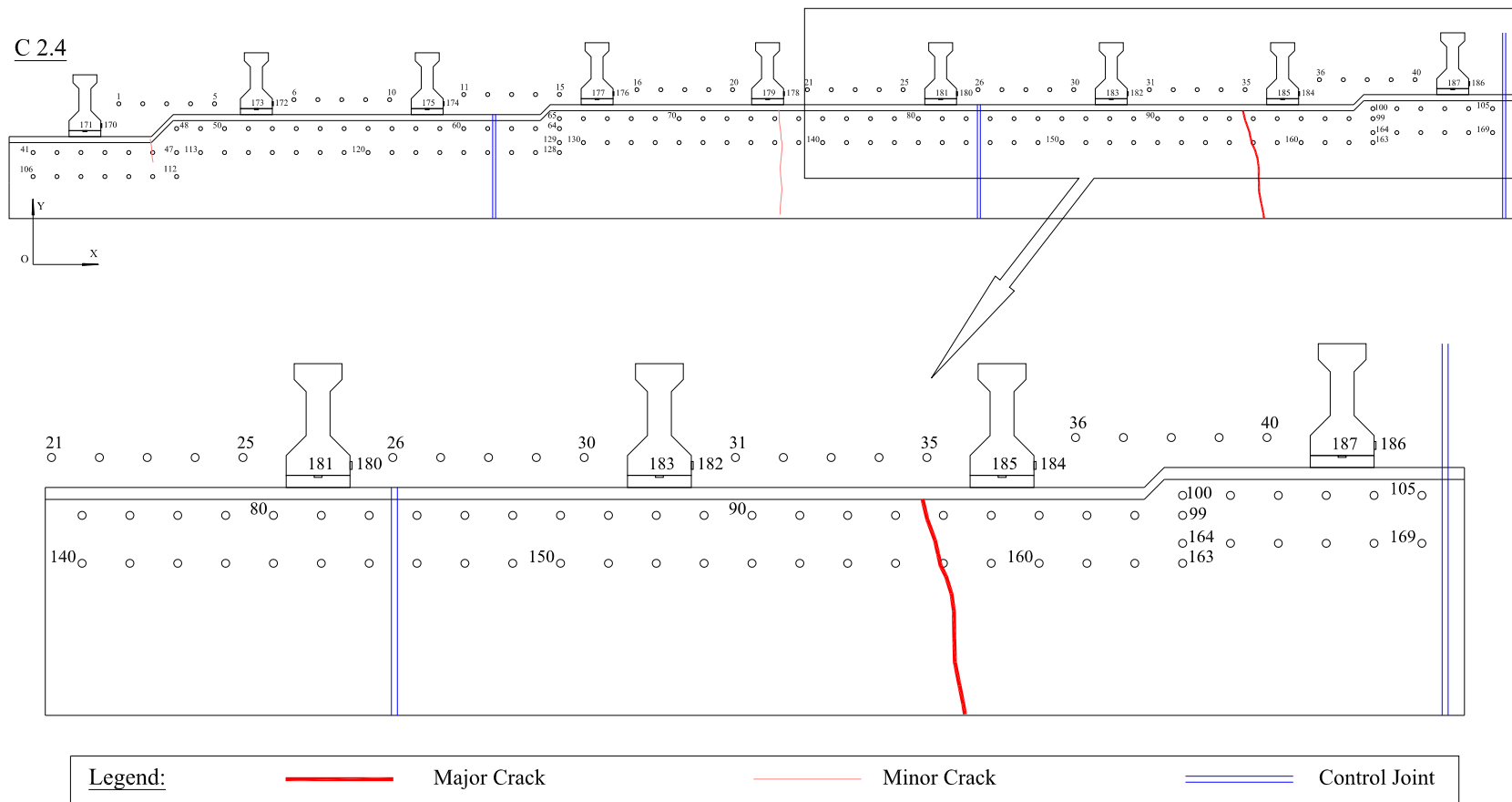
Figure 4-8 Deployment of measuring points on half of the abutment wall of C 2.4 (Magnification B)

4.3.2 Measured Variables

The variables from the mounted measuring points were:

➢ The deformation of the backwall and the abutment wall: the deformation of the backwall and the abutment wall were determined from the distance between the measuring points deployed on the backwall and the abutment wall (Figure 4-4, Figure 4-5, Figure 4-6, Figure 4-7, and Figure 4-8.)

The longitudinal displacement of the girder end: the location of measuring points to measure girder end displacement is shown in Figure 4-9.
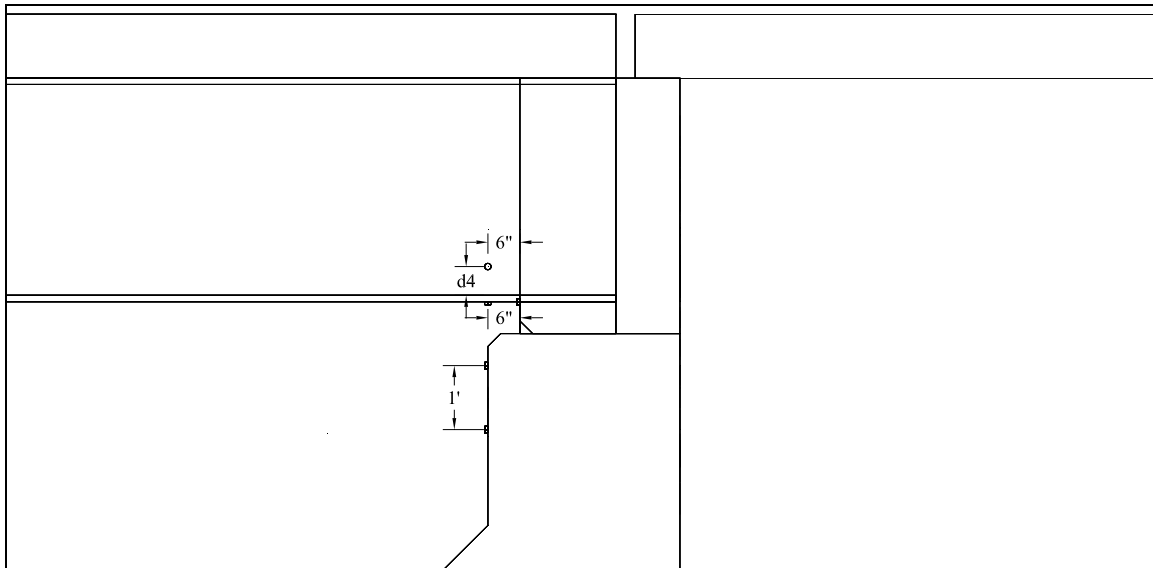
Figure 4-9 Measurement of girder end displacement

➢ Temperature of the bridge: temperatures of the bridge deck as well as the abutment wall were recorded at the start of the measurement process for each bridge. Temperatures at fifteen positions were measured using a Raynger ST non-contact thermometer. Six of them were distributed on the deck (Figure 4-1) and nine of them were located on the abutment wall (Figure 4-10).
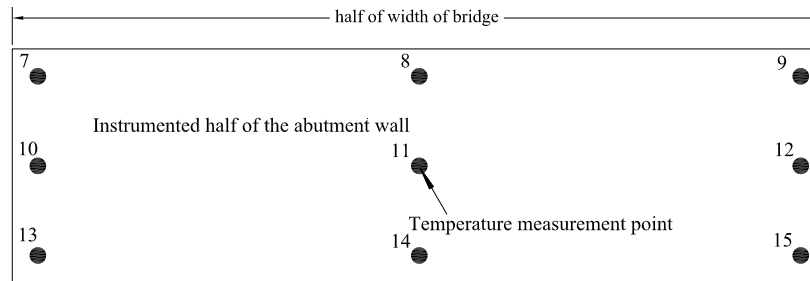
Figure 4-10 Temperature measuring points on bridge abutment (half of abutment wall)

4.3.3 Measurement schedule

The field monitoring data was collected over a period of one year at one-month intervals. Continuous monitoring, or more frequent measurements, was not required because the effects leading to abutment distress occur slowly over a long period. A major cause of abutment distress was believed to be thermal movements, which can be assessed by measuring extreme temperatures. Furthermore, the field monitoring plan was not intended to provide precise understanding of everyday bridge behavior but to reveal their long-term behavior under different circumstances. In the first eight months of, two sets of measurements were made in each round for the backwall and the abutment wall of each bridge. One set of measurements was taken on the brass cylinders directly (Figure 4-2). The other was done on the contact seats screwed on the brass cylinder (Figure 4-3). It was found that the data collected using the brass cylinder directly was more reliable, and thus, the measurements were taken only on the brass cylinders in the remaining five rounds.

4.4 Data Interpretation (Subtask II.3)

Data from the field measurements were plotted in three different perspectives to help identify the relations among horizontal strain (target variables), longitudinal and horizontal girder end movements (bridge behavior), and temperature at the bridge deck and bridge abutment wall (environmental variables). The calculated variations were determined by using values measured in December 2006 as reference or bias. Due to the limit of space, only representative figures were presented in this section, all figures (136 plots) can be found in Appendix C.

4.4.1 Distribution of Strains

The distributions of strains along the abutment wall and back wall together with girder end movement were plotted (Figure 4-11 and Figure 4-12). The legend "A1" represents the horizontal line six inches below the top of the abutment wall. Similarly, "A2" represents the horizontal line one and a half feet below the top of the abutment wall. "GM" means girder end movement; it is the average of values measured at the side of the girder and the bottom of the girder. Positive value means girder ends move away from the abutment wall, and vice versa. "MiC" signifies minor cracks in the abutment wall, "MaC" signifies major cracks, "CJ" means control joints. "Mic", "MaC" or "CJ" plotted on the upper level means they are at the level of "A1", lower level means they are at the level of "A2".

It can be observed that concrete in the vicinity of girder pull-out was subjected to tension and concrete in the vicinity of girder push-in was subjected to compression (Figure 4-11). Similar trends can be observed in the backwall (Figure 4-12). In general, cracks and control joints induced local peak horizontal strain in the abutment wall (Figure 4-11).
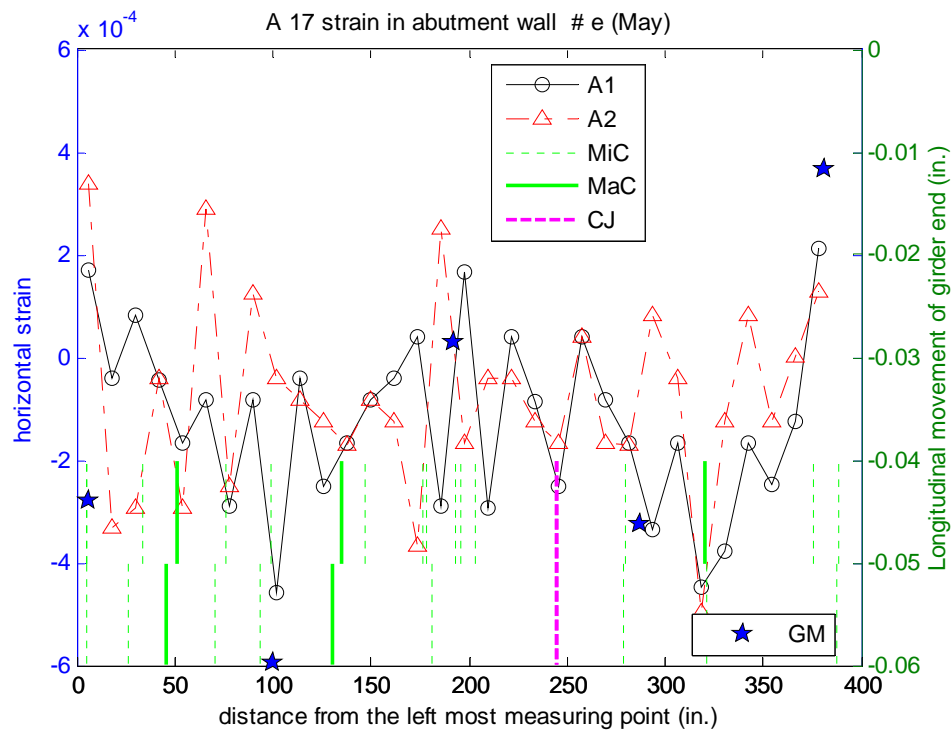
Figure 4-11 Distribution of horizontal strains, joints and cracks on abutment wall of bridge A 1.7
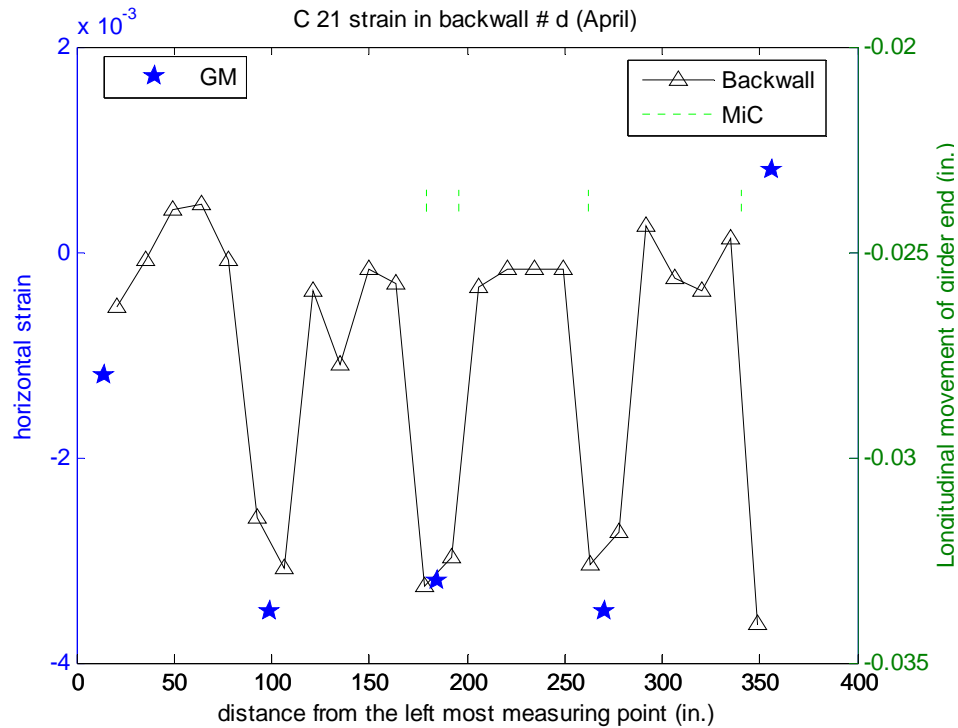
Figure 4-12 Distribution of horizontal strains and cracks on abutment wall of bridge C 2.1

4.4.2   Peak strain vs. time and temperature in region around girders

The second perspective in exploring field instrumentation data is to divide the instrumented abutment wall into regions around girders, as shown in Figure 4-13. The division of regions on abutment wall of bridge A 1.7 was taken as an example; the regions for the other three bridges were divided in the same manner. The maximum and minimum horizontal strains in each region were plotted together with changes of average temperatures in decks and abutment walls.
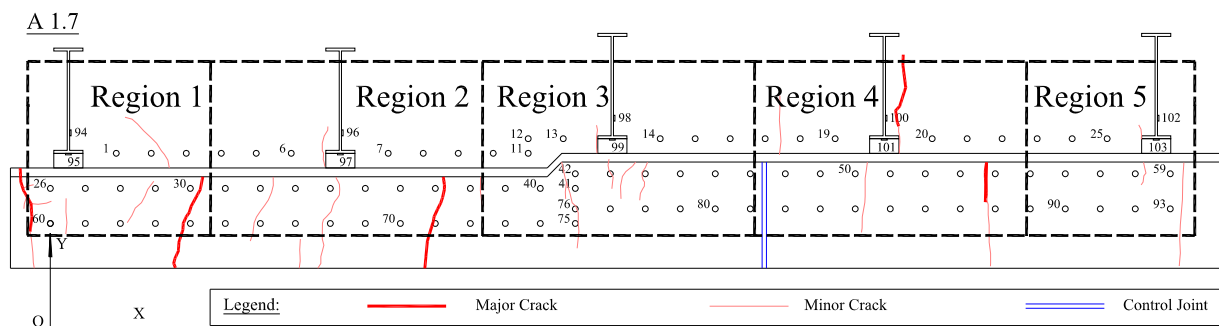
Figure 4-13 Division of measuring points on bridge A 1.7 by region
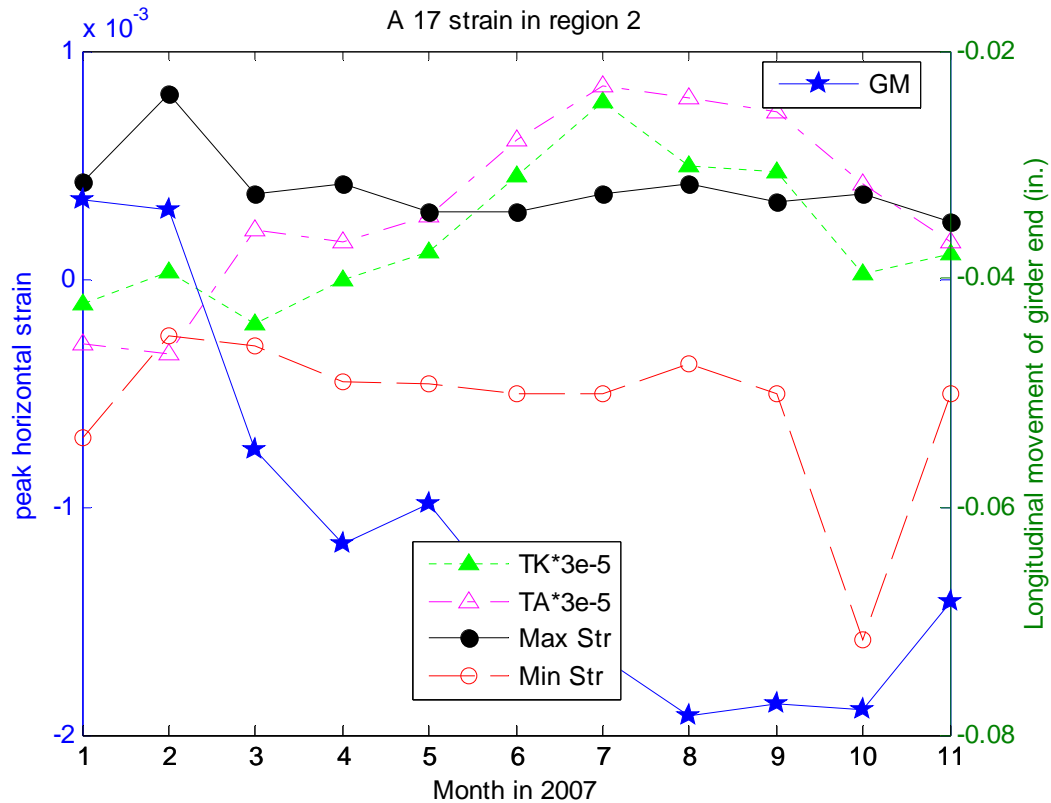
Figure 4-14 Peak strains in region 2 of bridge A 1.7

In Figure 4-14 and Figure 4-15, "TK" indicates the change of average temperature (Fahrenheit) in the deck of the bridge; "TA" means the change of average temperature (Fahrenheit) in the abutment wall of the bridge. "Max Str" represents maximum horizontal strain in the region; similarly, "Min Str" represents minimum horizontal strain in the region.

It can be seen from Figure 4-14 that the girder end movement varies reversely to the change of average deck temperature. The trend is reasonable since the expansion of deck tends to push girders toward the abutment wall and vice versa. The trend only exists for part of regions, so there must be some other reasons, such as pavement growth, contribute to the longitudinal movement of girder ends. It can be seen from Figure 4-15 that the maximum and minimum horizontal strain in the region change with the longitudinal movement of girder ends. Only part of bridges showed this matched pattern between peak strains and longitudinal movements of girder ends, some other bridges showed this matched pattern in a few months, and other cases in which variation of two variables doesn't match at all. Longitudinal movements of girder ends

120

can explain part of the strains in the abutment wall. No obvious relationship between temperature and horizontal strains in the abutment wall can be observed.
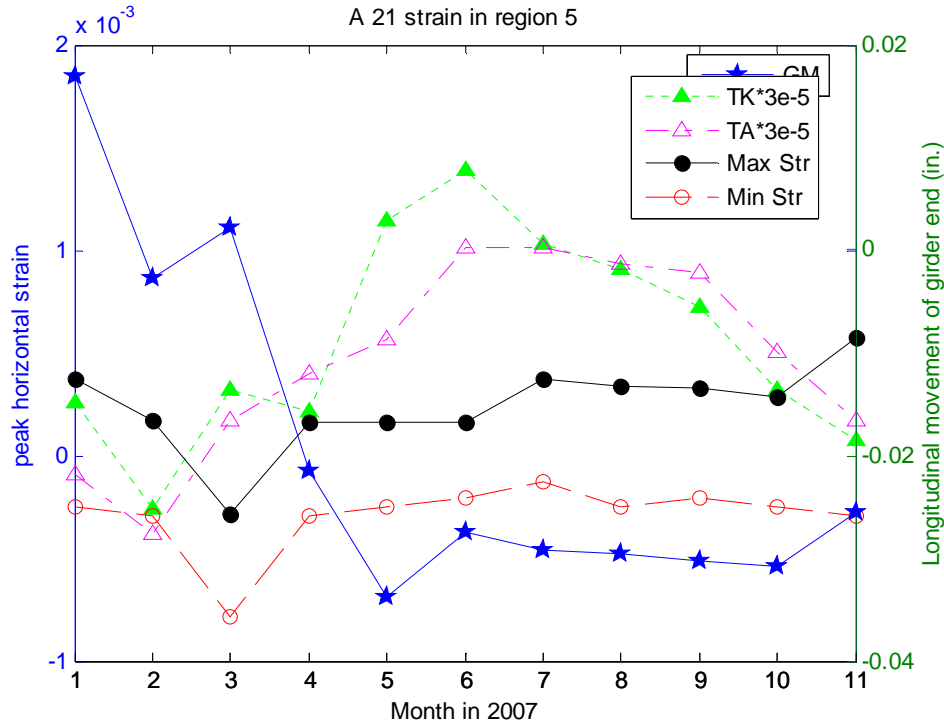
Figure 4-15 Peak strains in region 2 of bridge A 2.1

4.4.3   Peak strain vs. time and temperature in spacings between girders

The third perspective in exploring field instrumentation data is to divide the instrumented abutment wall into spacings between girders, as shown in Figure 4-16. The division of spacings on abutment wall of bridge A 1.7 was taken as an example; the spacings for the other three bridges were divided in the same manner. The maximum and minimum horizontal strains in each region were plotted together with changes of average temperatures in decks and abutment walls.
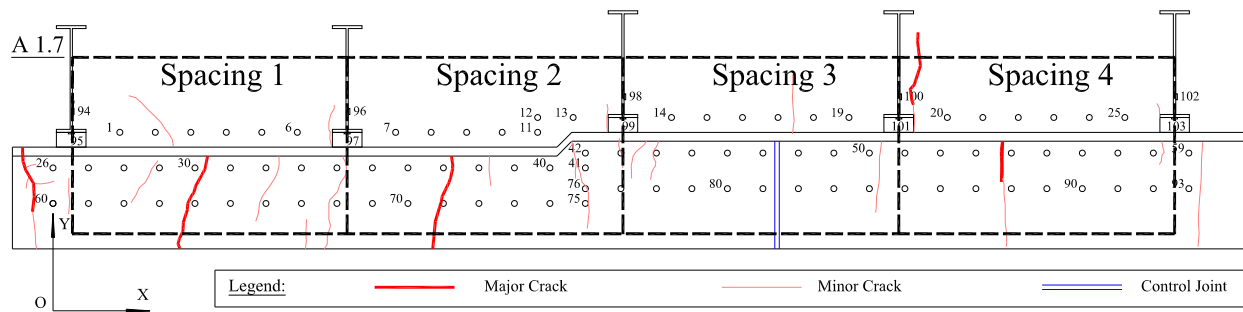
Figure 4-16 Division of measuring points on bridge A 1.7 by spacing

In some spacing of some bridges, the variation of peak horizontal strains approximately match the change of transverse distances between girder ends, as shown in Figure 4-17. "SC" in the figure represents change of transverse distance between girder ends. In some other cases, the match between variation trends was not so good. For a few bridges, transverse distances between girder ends varied with the change of average temperature in the bridge deck (Figure 4-18); however, contrary to the expectation, this trend was not true for the majority of cases. No direct association between average temperature variation and peak strain in spacing can be observed.
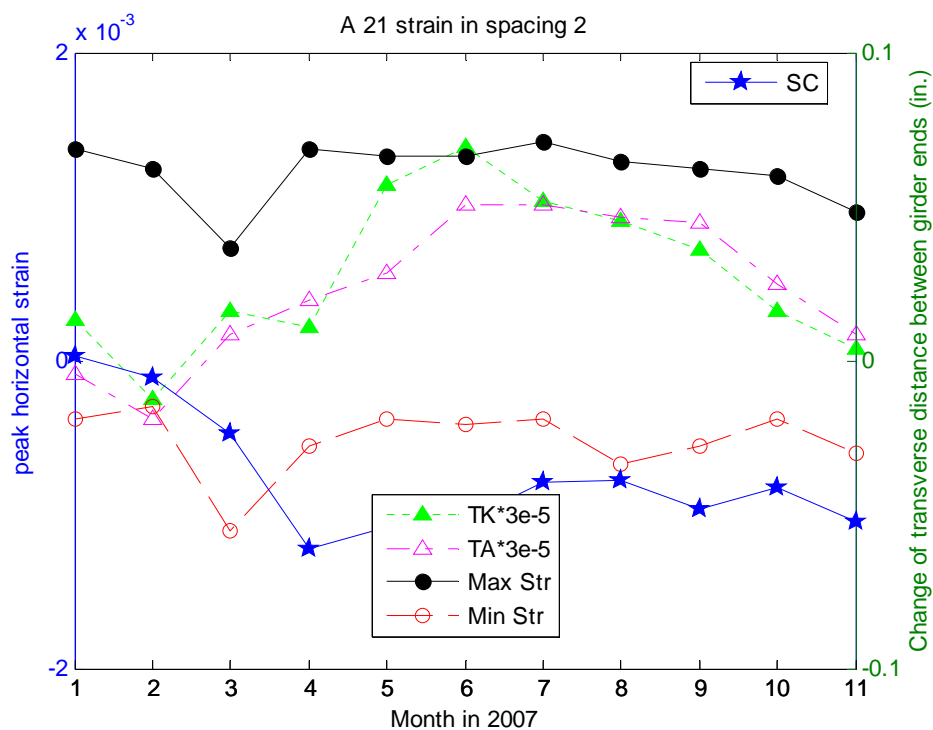
Figure 4-17 Peak strains in spacing 2 of bridge A 2.1
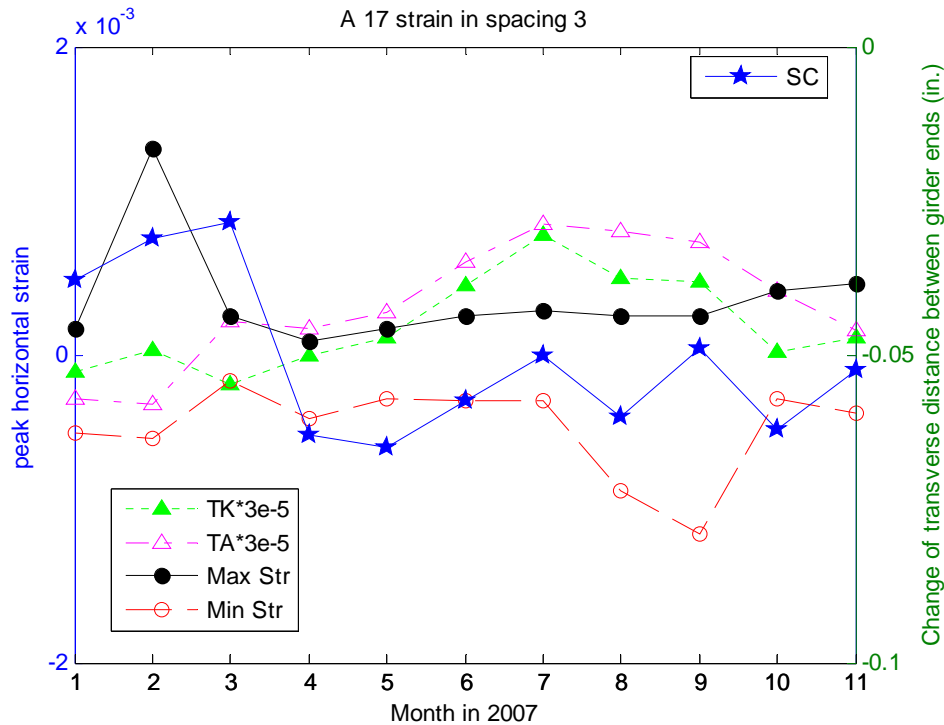
Figure 4-18 Peak strains in spacing 3 of bridge A 1.7

4.5 Discussion

Four MDOT highway bridges were instrumented during one year period. Two of them were simple/cantilevered steel bridges; two of them were prestressed concrete bridges. They were selected through statistical analyses of the information database and field inspection of 44 highway bridges, all of them had common feature of bridges that were susceptible to abutment damage. One steel bridge and one concrete bridge had poor abutments; the other two bridges had good abutments.

Variables measured for each bridge were: deformations of the abutment wall and backwall, longitudinal displacements of the girder end, and temperature of the bridge deck and the abutment wall.

The analyses of instrumentation results can be summarized as follows:

➢ On abutment wall and backwall, concrete in the vicinity of girder pull-out was subjected to tension and the concrete in the vicinity of girder push-in was subjected to compression.

- Cracks and control joints in the abutment wall and backwall induced local peak horizontal strain.

- For some regions around girders of some bridges, the girder end movement varies reversely to the change of average deck temperature. For the other cases, where this trend didn't exist, pavement pressure might play an important role in the girder movement.

- Maximum and minimum horizontal strains in the region around girders change with the longitudinal movement of girder ends for some cases.

- In some spaces of some bridges, the variation of peak horizontal strains approximately matched the change of transverse distances between girder ends.

- For a few bridges, transverse distances between girder ends varied (with a maximum of 0.1 in.) with the change of average temperature in the bridge deck (with a maximum of 60 ºF).

- No direct association between average temperature variation and peak strain in spacing (with a maximum of 2×10^{-3}) can be observed.

5 Finite Element Modeling and Parametric Studies (Subtask III.1)

5.1 Introduction

The finite element analyses (FEA, Task III.1) in this research were to serve three principal purposes: predicting effects of different assumed damage scenarios, parametric analyses investigating behavior of bridges of different design parameters, and creating additional data (virtual data) for the artificial neural network prediction models. Bridges of three structural types were simulated: simple/cantilevered steel bridges (SS), continuous steel bridges (CS), and prestressed concrete bridges with I girders (PC). Finite element program ABAQUS 6.6.1 (ABAQUS 2006) was used in the simulations. Numbers of models simulated for simple/cantilevered steel bridges, continuous steel bridges and prestressed concrete bridges were 450, 225 and 108, respectively. The material properties used in the finite element analysis (FEA) are summarized in Table 5-1.The element and mesh details used in the models are summarized in Table 5-2.

Table 5-1 Material properties

Material	Modulus of elasticity E (ksi)	Poisson's ratio	Coefficient of thermal expansion $(1/F)$
Concrete	3500	0.2	6.6 e-6
Prestressed concrete	4920	0.2	6.6 e-6
Steel	29000	0.3	6.6 e-6

5.2 Case Matrices and Analytical Models

Case matrices for FEA simulation were defined for three types of superstructures representative of MDOT highway bridges. The bridge models are to cover the most frequent range of the primary design parameters. The simulation cases were further refined in the range of the parameters within which the bridges were more susceptible to abutment distress.

Table 5-2 Element details used to simulate the structural members

Structural member	Material	Element type	Average element size (in)	Geometry (in)
Slab	Concrete	S4R: 4-node doubly curved thin or thick shell, with reduced integration, hourglass control, and finite membrane strains.	20	9 (thickness)
Girder top flange	Steel	S4R: 4-node doubly curved thin or thick shell, with reduced integration, hourglass control, and finite membrane strains.	5	0.75 (thickness)
Girder web	Steel	S4R: 4-node doubly curved thin or thick shell, with reduced integration, hourglass control, and finite membrane strains.	5	0.5 (thickness)
Girder bottom flange	Steel	S4R: 4-node doubly curved thin or thick shell, with reduced integration, hourglass control, and finite membrane strains.	5	0.875 (thickness)
Backwall	Concrete	S4R: 4-node doubly curved thin or thick shell, with reduced integration, hourglass control, and finite membrane strains.	5	24 (thickness)
Abutment wall	Concrete	C3D8: 8-node linear brick	5	30 (thickness)
Pier cap	Concrete	B31: 2-node linear beam in space	6	42 (width) 39 (height)
Link plate	steel	Springs: "point to point" spring element	height of web minus 8"	9 (width) 0.5 (thickness)
Prestressed concrete I girder	Prestressed concrete	C3D8: 8-node linear brick	5	Type III or Type IV

5.2.1   Simple/cantilevered Steel Bridge

For simple/cantilevered steel bridges, the simulation cases were the combination of the values in the last column of Table 5-3. Seventy five structural models were created. The damage scenarios were: pavement pressure, summer temperature increase and gradient, and winter temperature drop and gradient. The conditions of a pin-and-hanger assembly in good condition and the rusted (locked) pin-and-hanger assembly were simulated under each damage scenario. Thus, there were six simulations for each geometric bridge model and 450 simulations for this structural type. The analytical diagram for the simple/cantilevered steel bridge model is shown in Figure 5-1.

Table 5-3 FEA case matrix for simple/cantilevered steel bridges

Design parameters	Most frequent interval	Features indicate potential distress	Values taken in the simulation
number of spans	<=4	>=2 and <=4	[2]
Maximum span (ft)	>=40 and <=120	>=80 and <=140	[40, 80, 100, 120, 140]
deck width (ft)	>= 20 and <= 100	>=60 and <=80	[42.5, 58.5, 74.5]
skew (degree)	<= 60	<= 60	[0, 15, 30, 45, 60]
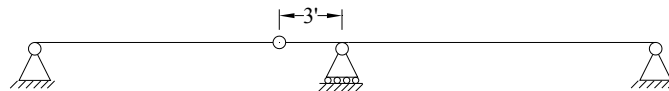
Figure 5-1 Diagram for simple/cantilevered steel bridges with 2 spans

5.2.2 Continuous Steel Bridge

For continuous steel bridges, the simulation cases were the combination of the values in the last column of Table 5-4. The pin-and-hanger assembly were modeled as "new" for pavement pressure and modeled as "rusted" (locked) for the temperature effects. Seventy five structural models and 225 simulations were done for this structural type. The analytical diagram for continuous steel bridges is shown in Figure 5-2.

Table 5-4 FEA case matrix continuous steel bridges

Design parameters	Most frequent interval	Features indicate potential distress	Values taken in the simulation
number of spans	<=4	>=4 and <=7	[4]
maximum span (ft)	>=40 and <=120	>=100 and <=180	[100, 120, 140, 160, 180]
deck width (ft)	>= 20 and <= 120	>=30 and <=60	[42.5, 50.5, 58.5]
Skew (degree)	<= 60	0	[0, 15, 30, 45, 60]
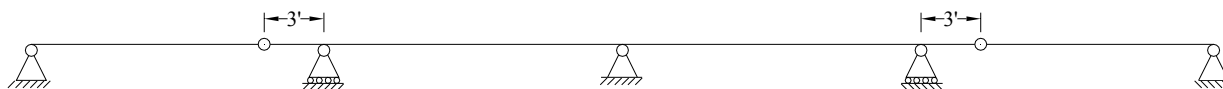
Figure 5-2 Diagram for continuous steel bridges with 4 spans

5.2.3 Prestressed Concrete Bridge

All of the prestressed concrete bridges with I-girders inspected in the summer of 2006 were simple supported. Thus, the number of spans in the case matrix was taken to be one (1), as shown in Table 5-5. The damage scenarios were: pavement pressure, summer temperature increase and gradient, and winter temperature drop and gradient. Thirty six structural models and 108 simulations were done for this structural type. The analytical diagram for prestressed concrete bridges with I girders is shown in Figure 5-3.

Table 5-5 FEA case matrix for prestressed concrete bridges

Design parameters	Most frequent interval	Features indicate potential distress	Values taken in the simulation
number of spans	<=4	>=2 and <=4	[1]
Maximum span (ft)	>=40 and <=120	>= 60 and <= 100	[60, 80, 100]
deck width (ft)	>= 20 and <= 100	>= 60 and <=70	[42.5, 58.5, 66.5]
skew (degree)	<= 60	>= 0 and <= 45	[0, 15, 30, 45]

Figure 5-3 Diagram of prestressed concrete bridge with I-girder

5.3 Simulation Strategies and Verification

5.3.1 Geometry and Mesh Details

5.3.1.1 Steel bridges

A two-span simple/cantilevered steel bridge was used as an example to describe models. The geometry of the bridge was the combination of the first values of each of the design variables in Table 5-3. The plan and side views of the bridge are shown in Figure 5-4 and Figure 5-5, respectively. The girder dimensions were determined by MDOT bridge design program for each bridge in the case matrices.
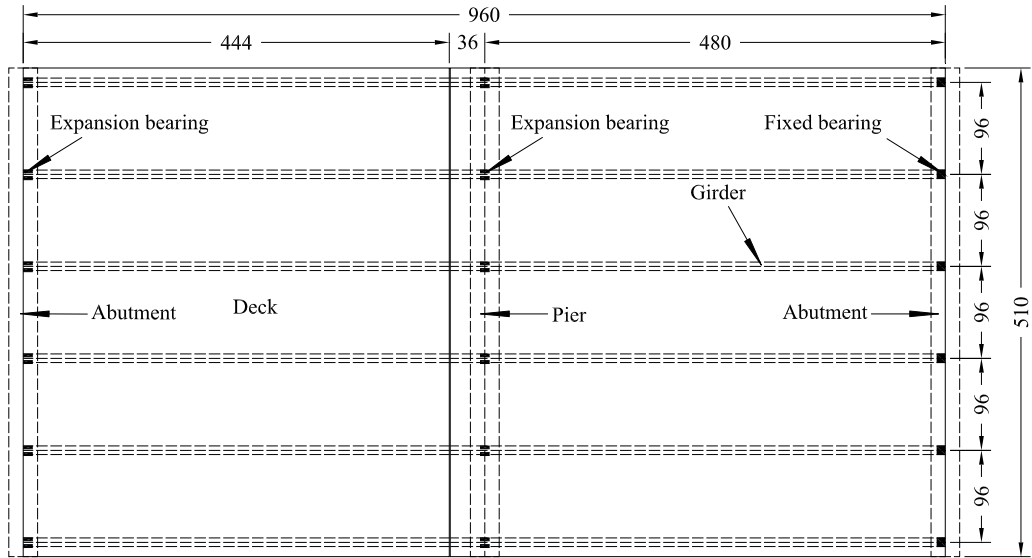
Figure 5-4 Bridge plan (unit: inch)
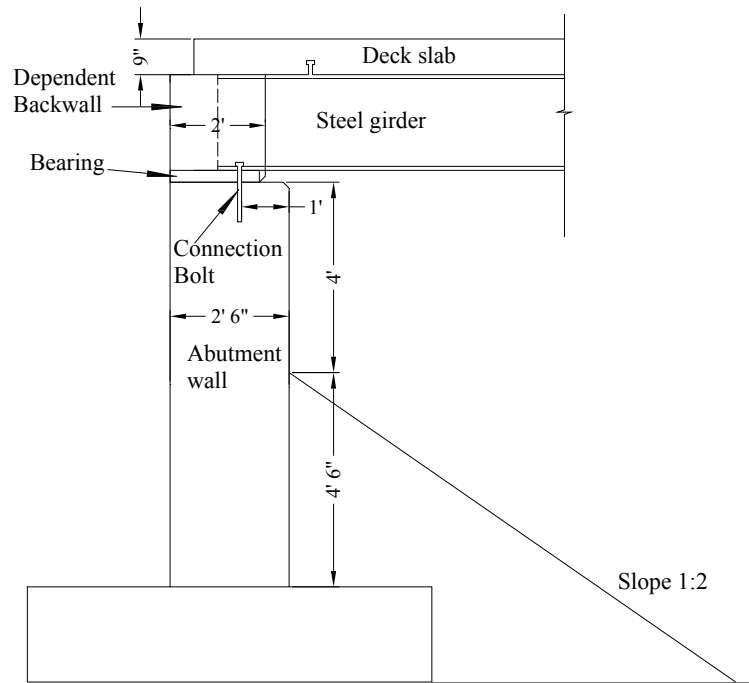
Figure 5-5 Bridge side view

Three-dimensional finite element (FE) models (Figure 5-6) were built using the general-purpose finite element program ABAQUS 6.6.1 (ABAQUS 2006) with an attempt to simulate the behavior of different bridges under possible damage-inducing demands. The concrete decks and the backwalls were modeled by shell elements and the cross frames were modeled by beam

elements (Figure 5-7). Girders were modeled according to the baseline design output of the MDOT bridge design program. For steel bridges, the flanges and webs were modeled by shell elements.
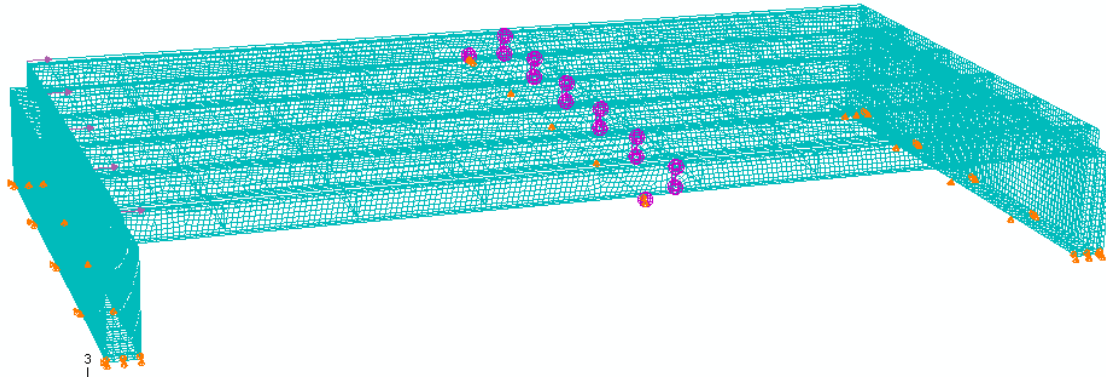
Figure 5-6 Bridge Model
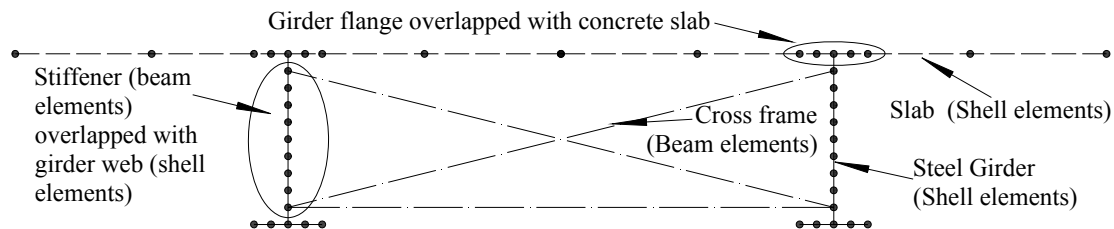
Figure 5-7 Modeling details of one span of bridge

The abutment walls were simulated by eight-node linear solid elements (Figure 5-8). Height of the abutment wall was taken to be 8'-6". Each girder was tied to the backwall by the web end and tied to the top of the abutment wall by single point (the center node of the bottom flange). The pin and hanger assembly was simulated by a "point to point" spring element (Figure 5-8 b and Figure 5-9). The spring element used here only had stiffness in the direction of two linked points, so the two girders connected by it could freely move or rotate in other directions. The stiffness of the spring element was taken to be the product of the elastic modulus of the steel and the sum of cross-section areas of two link plates.

(a) Back wall and abutment wall   (b) Pin and hanger assembly
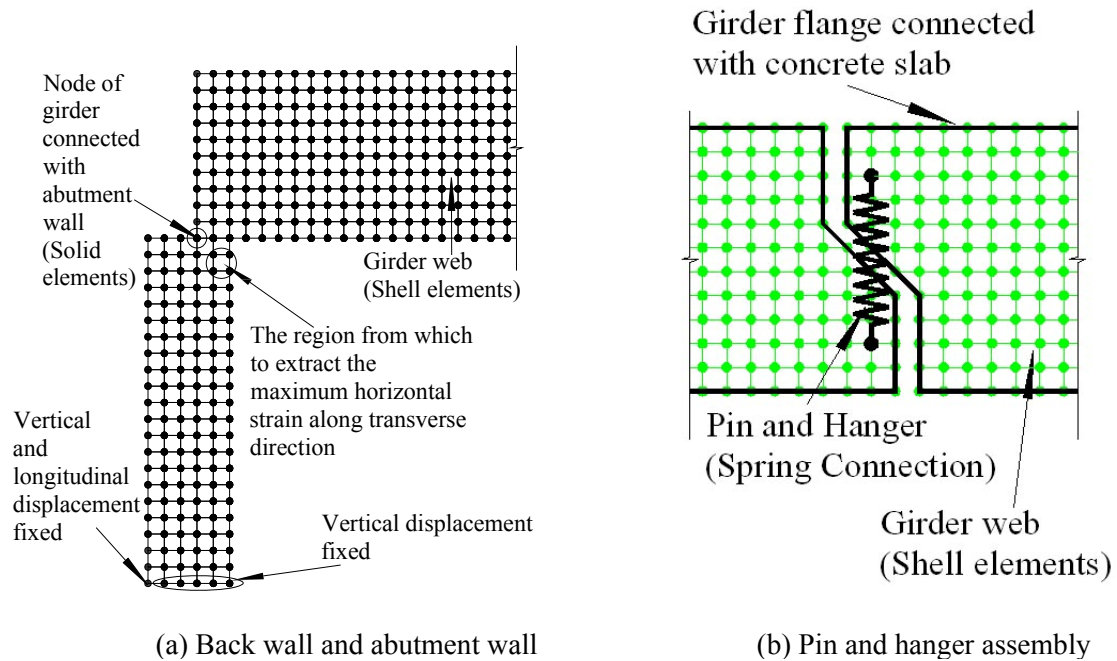
Figure 5-8 Modeling details
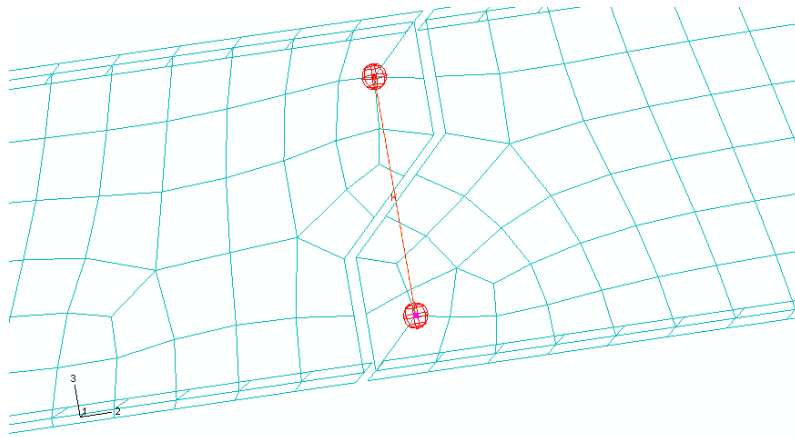
Figure 5-9 Pin and hanger detail in model built in ABAQUS

The cross section of two vertical plates in the cross frame was taken to be 3.51"×0.4" to simulate the stiffeners. Other members of the cross frame was taken to be L 4×4×5/16.

5.3.1.2 *Prestressed Concrete bridges*

For prestressed concrete bridges in the case matrix (Table 5-5), dimensions of prestressed concrete girders were determined by MDOT bridge design program. Referring to MDOT Bridge Design Guides (MDOT 2001), for bridges with span length of 60 ft, Type III prestressed concrete I beam was used; for bridges with span lengths of 80 ft and 100 ft, Type IV prestressed concrete I beam was used. The concrete compression strength for the prestressed concrete bridges was assumed to be 7 ksi. Refer to Table 3.5.1-1 of ASSHTO (2007), the unit weight of concrete was taken as 0.147 kcf. According to Equation (5.4.2.4-1) of ASSHTO (2007), the modulus of elasticity for the prestressed concrete I girder was estimated with Equation (5-1). Eight node linear solid elements were used to model the prestressed concrete I girder. The mesh of a prestressed concrete I girder is shown in Figure 5-10. A prestressed concrete bridge model is shown in Figure 5-11.

$$E_c = 33,000 K_1 w_c^{1.5} \sqrt{f_c^{'}} = 4920 \text{ ksi} \tag{5-1}$$
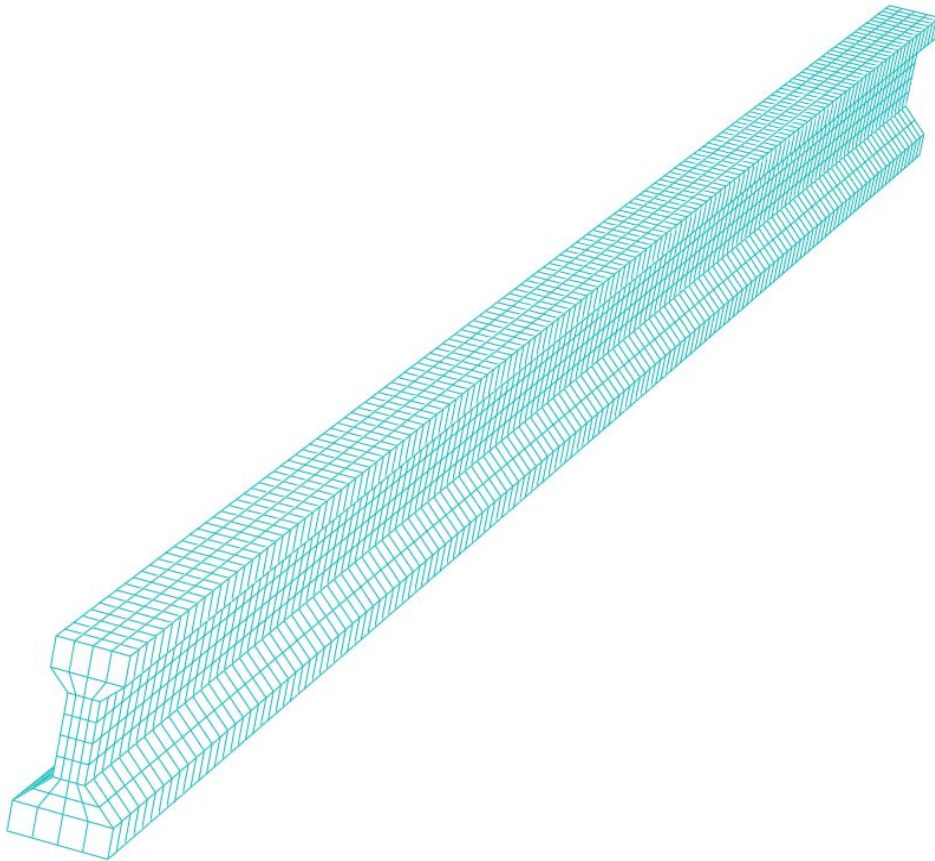
Figure 5-10 Mesh of prestressed concrete I girder
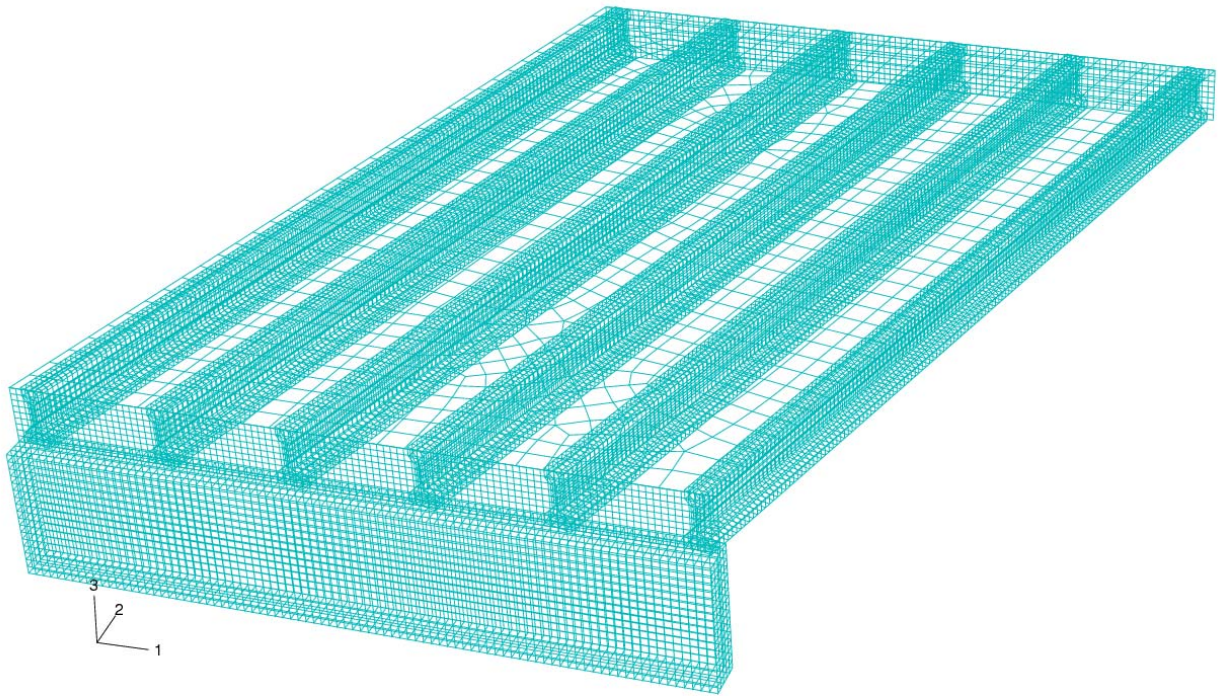
Figure 5-11 Prestressed concrete bridge model

5.3.2 Boundary Conditions

The vertical displacements at the bottom of abutment walls and pier cap were set to be zero. The horizontal boundary condition at the bottom surface of the abutment wall is shown in Figure 5-12. The boundary condition at the pier cap is shown in Figure 5-13.

Bottom surface of the abutment wall $u = 0$

v (longitudinal direction)

$v = 0$

u (transverse direction)
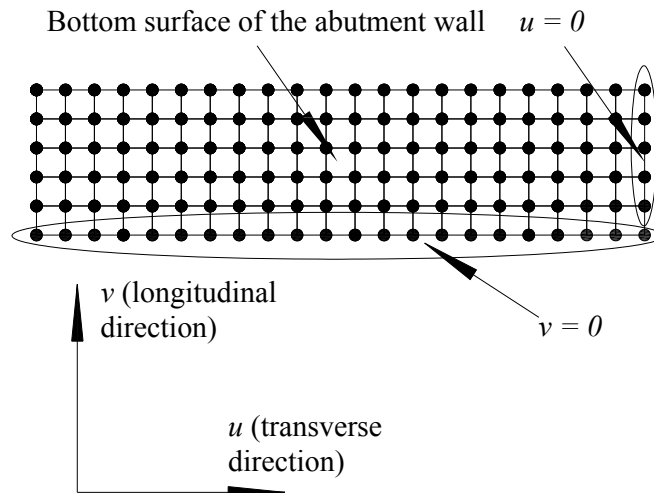
Figure 5-12 Boundary condition at the bottom surface of the abutment wall
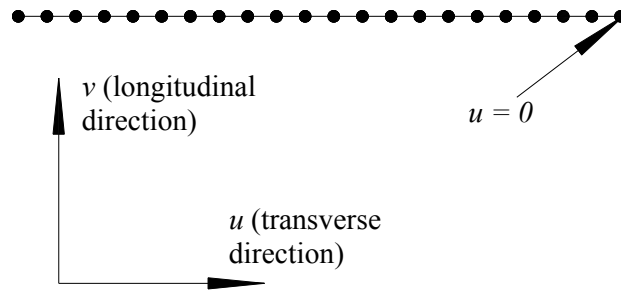
Figure 5-13 Boundary condition at the pier cap

5.3.3 Significance of Cross Frames/Diaphragms

A two-span simple/cantilevered steel bridge with different cross frame arrangements was analyzed to investigate the significance of cross frames for the current analyses. The span length of the bridge was 100 ft and the skew angle was 60 degrees. Three structural models with different cross frame spacings were analyzed. The cross frames deployments were: 25 ft cross frame spacing (normal case), 50 ft cross frame spacing and no cross frames. The largest values of maximum principal stress in the front top part of the abutment wall are summarized in Table 5-6.

Table 5-6 The maximum principal stress (ksi) in the front top part of the abutment wall

Cross frame deployment	Pavement pressure (unlocked pin)	Summer (locked pin)	Pavement error ratio	Summer error ratio
Normal (25 ft)	35.4	13.2		
Large spacing (50ft)	35.1	13.1	1.0%	0.5%
No cross frame	34.8	13.0	1.7%	1.4%

It can be determined from Table 5-6 that the errors induced by different cross frame deployments are trivial. Two major functions of cross frames/diaphragms can be summarized as: prevention of buckling and redistribution of the unevenly distributed loads among the girders (AASHTO 2007). The bridge models simulated in this research were linear elastic models, thus, there was neither local buckling nor lateral torsional buckling problems. The loads induced by pavement pressure and temperature field were distributed in a relatively even pattern. Thus, the cross frames in the finite element models of this research have trivial influence to the results and

can not be categorized as primary members. Therefore, the cross frames/diaphragms were neglected in the FE models of continuous steel bridges and prestressed concrete bridges.

5.3.4 Variation of Girder Cross Section and Simplification

For most bridges, the girder cross section varies in the longitudinal direction. These varied cross sections were simplified as a constant cross section for ease of model generation. In order to evaluate the simplification strategies, different simplification approaches were applied to a two-span simple/cantilevered steel bridges with the span length of 100 ft. Models with three types of sections were analyzed: varied cross sections, the constant cross section taken the geometry of the smaller section, and the constant cross section taken the geometry of the larger section. Each of three damage scenarios was applied to the models. The results were summarized in Table 5-7. It can be seen that the simplification had trivial influence on the maximum stress caused by the pavement pressure. For the temperature variation, the simplification had some influences; however, if the girder cross section was simplified to be the smaller cross section, the error ratio was acceptable. So the girder cross sections were assumed to be constant throughout the length of the bridges in the simulations, the dimensions of the smaller cross sections of the girders were used. Beam sections used for FEA models of simple/cantilevered steel bridges and continuous steel bridges are listed in Table 5-8 and Table 5-9; respectively.

Table 5-7 Maximum stress in top part of abutment wall (ksi)

	Pavement Pressure	Summer	Winter	Pavement error ratio	Summer error ratio	Winter error ratio
Small Girder	5.0733	2.108	243.50%	0.00%	8.23%	8.15%
Large Section	5.1048	2.631	302.60%	0.62%	14.54%	14.15%
True Section	5.0733	2.297	2.651			

Table 5-8 Beam sections used for FEA models of simple/cantilevered steel bridges

Span length (ft)	Top flange (in)		Web (in)		Bottom flange (in)	
	Thickness	Width	Thickness	Depth	Thickness	Width
40	0.77	9.02	0.47	24.1	0.77	9.02
80	0.75	10	0.5	42	0.75	12
100	0.75	12	0.5	48	0.875	14
120	0.75	17	0.563	54	0.875	18
140	1	22	0.5	60	1	22

Table 5-9 Beam section used for FEA models of continuous steel bridges

Span length (ft)	Top flange (in)		Web (in)		Bottom flange (in)	
	Thickness	Width	Thickness	Depth	Thickness	Width
100	0.75	15"	7/16	48	0.875	15"
120	0.875	20"	7/16	48	0.875	15"
140	1.125	25"	1/2	60	1.125"	25"
160	1.125	26"	9/16	66	1.125"	26"
180	1.125	22"	9/16	78	1.125"	22"

5.4 Damage scenarios

After evaluating possible damage scenarios and feasibility of simulating them through FEA, three scenarios were simulated: pavement growth, temperature field in summer, and temperature field in winter.

5.4.1 Pavement Growth

While pavement growth is a physical phenomenon that seems to be well accepted, a quantifiable measure of the pressure generated by pavement growth is an elusive issue. Richards (1979) conducted field testing to determine the stresses in concrete pavements and instrumented six sites (three of them adjacent to a bridge). A stress level of 1 ksi was observed. Burke (1998, 2004) estimated the pavement pressure to be greater than 1 ksi. Shober (1997) estimated the

pavement pressure to be 1 to 2 ksi. Richards and Burke did their studies in Ohio, while Shober performed his evaluation in Wisconsin. Since both states neighbor Michigan and have similar climatic condition, it was reasonable to assume that the pavements of Michigan may behave in a similar manner. Thus, their results provide a valuable reference in defining a magnitude for the pressure due to pavement growth. Thus, based on the noted research studies, the pavement growth pressure was set at 1 ksi for these simulations.

5.4.2   Temperature Field

Two potential damage scenarios simulated in the FEA were summer temperature field and winter temperature field. The temperature variation specified in AASHTO (2007) was piecewise linear temperature curvature. It was complicated to be applied in the FE models especially consider the large number of models needs to be simulated. Three simplification approaches were evaluated in order to find an appropriate approximation, as refer to Appendix D. A linear temperature gradient through the deck was found to be an reasonable simplification to the piecewise linear temperature curvature.

5.4.2.1   *Temperature Variation*

Temperature ranges in bridges were given in the AASHTO LRFD Bridge Design Specifications (2007). Data from this source were reproduced in Table 5-10. Here, the temperature range was taken to be -30 to 120 ºF for steel bridges and 0 to 80 ºF for concrete bridges.

Table 5-10 Temperature Ranges (Part of Table 3.12.2.1-1 of AASHTO Specification)

CLIMATE	STEEL OR ALUMINUM (º F)	CONCRETE (º F)
Cold	-30 to 120	0 to 80

The temperature gradient was defined in Figure 3.12.3-2 of the AASHTO LRFD Bridge Design Specifications (2007), and is reproduced in Figure 5-14. In Michigan, T_1, T_2 and T_3 can be taken to be 41º F, 11 º F, and 0 º F, respectively for concrete pavement surfaces. The value of "A" is taken to be 12".
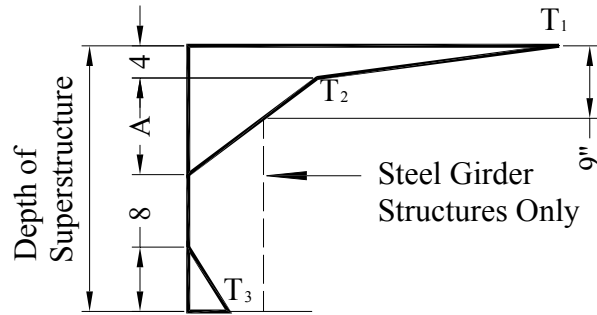
Figure 5-14 Positive vertical temperature gradient in concrete and steel structures (units: inches, Figure 3.12.3-2 of AASHTO Specification)

5.4.2.2 Simplification approach

The temperature distribution in the deck was simplified as linear and the temperature field in other parts of the bridge was simplified as constant. Thus, the temperature gradient for steel bridges in Figure 5-14 was transformed to the simplified gradient shown in Figure 5-15 by equating the areas under the temperature curves of both figures. The calculation is as follows:

$$\left[\frac{1}{2}\times30\times4\right]+\left[\frac{1}{2}\times(11-6.4)\times5\right]+[(11-6.4)\times4]=\frac{1}{2}\times9\times(T_4-6.4)$$

$$T_4 = 26.4\ ^\circ F$$

The temperature gradient in winter was obtained by multiplying the summer gradient by – 0.3, which is $T_4^{'} = -0.3 \times T_4 = -7.9\ ^\circ F$. Temperatures at the other parts of the structure are calculated as:

$$\frac{T_6}{11} = \frac{A-5}{A}$$

$$T_6 = T_5 = 6.4\ ^\circ F$$

For winter time, the temperature in the other parts of the bridge was taken as:

$$T_6^{'} = T_5^{'} = -0.3 \times T_6 = -1.9\ ^\circ F$$
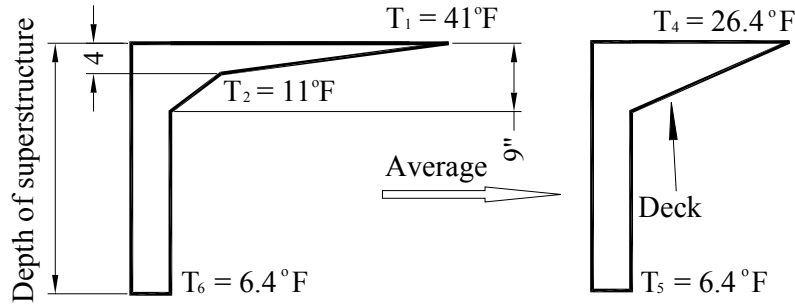
Figure 5-15 Simplification of temperature gradient for steel bridges

Similarly, the temperature gradient for concrete bridges in Figure 5-14 was transformed to the simplified gradient shown in Figure 5-16. The calculation is as follows:

$$\left[\frac{1}{2}\times30\times4\right]+[4\times11]+\left[\frac{1}{2}\times5\times\left(11\times\frac{5}{12}\right)\right]+\left[5\times11\times\frac{7}{12}\right]=\left[\frac{1}{2}\times9\times(T_4-0.6)\right]+[0.6\times9]$$

$$T_4 = 32.2 \text{ °F}$$

The temperature gradient in winter was the temperature in summer multiplied by –0.3, which was $T_4' = -0.3\times T_4 = -9.7$ °F. The depth of the concrete superstructure is taken to be the average depths of Type I, II, III and IV prestressed I beams plus the deck thickness:

$$d = \frac{1}{4}(28+36+45+54) = 40.75 \quad (in.)$$

Temperatures at other parts of the structure are calculated as:

$$\frac{1}{2}\times7\times\left(11\times\frac{7}{12}\right)=d\times T_5$$

$$T_5 = 0.6 \text{ °F}$$

The temperature gradient in winter is the temperature in summer multiplied by –0.3, which is:

$$T_5' = -0.3\times T_5 = -0.2 \text{ °F}.$$
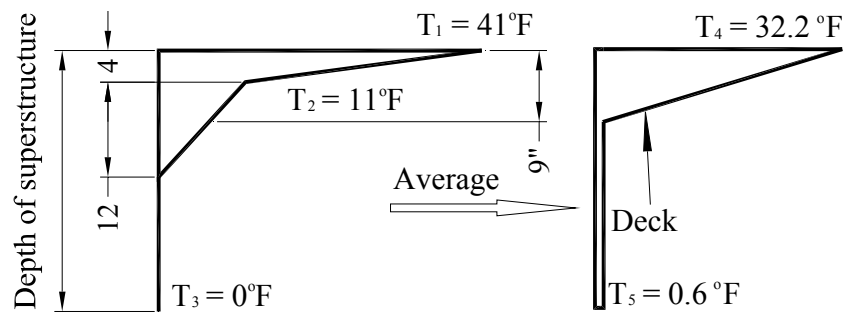
Figure 5-16 Simplification of temperature gradient for concrete bridges

The temperature values for the simulations are summarized in Table 5-11.

Table 5-11 Temperature values for linear temperature gradient in the deck

Structures (Members)		Construction (Fahrenheit degree)	Winter (Fahrenheit degree)	Summer (Fahrenheit degree)
Steel Bridge	Top of the deck	60.0	-37.9	146.4
	Other members	60.0	-31.9	126.4
Concrete Bridge	Top of the deck	60.0	-9.7	112.2
	Other members	60.0	-0.2	80.6

5.5   Result Variables

Values of two variables were extracted from each simulation: largest value of maximum principal stress along the top of the abutment wall and maximum horizontal strain from the elements in the front top corner of the abutment wall (Figure 5-17).

Contour images of the principal tensile stresses on the abutment wall are shown in Figure 5-18. The location of the extracted maximum principal stress is the point where the girder connected to the abutment wall (Figure 5-17). At this location, the model results are meshing sensitive. In order to avoid this mesh sensitivity, the maximum horizontal strain from the elements in the front top corner of the abutment wall was also extracted (Figure 5-17).
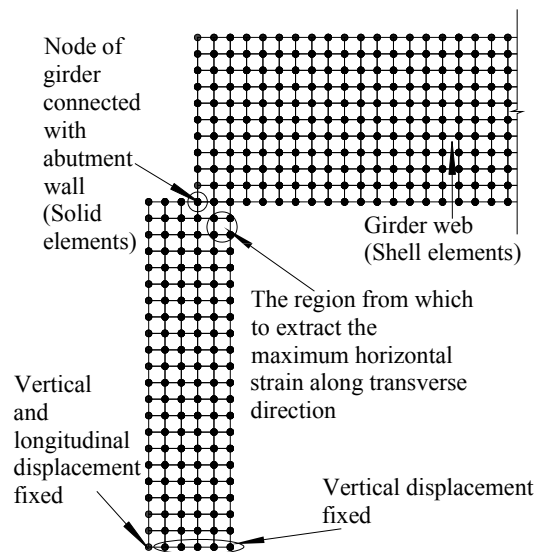
Figure 5-17 The region to extract the largest value of maximum principal strain
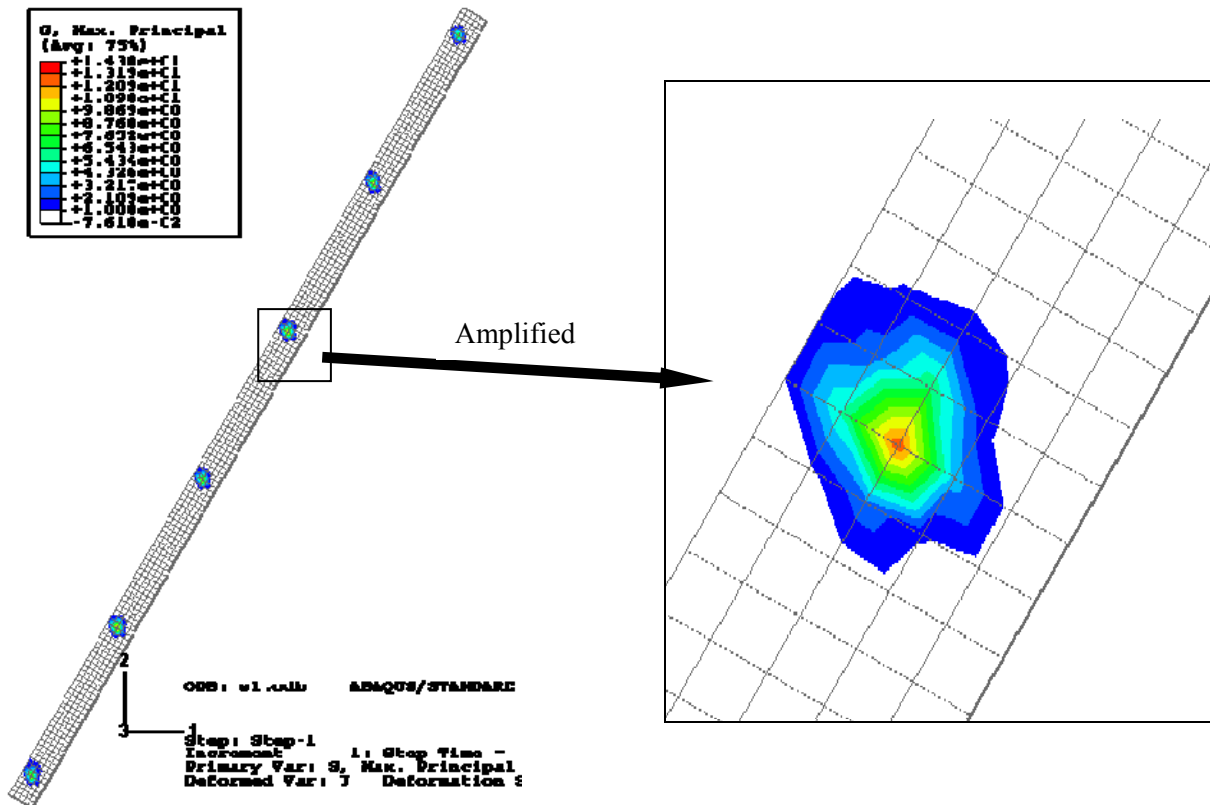
(a) Top view of the abutment wall   (b) Amplified view

Figure 5-18 Principal tensile stresses in the abutment wall

5.6   Results Interpretation and Parametric Analysis

The results of FE simulations were plotted using skew angle as abscissa and result variables as ordinate. A complete reference of all these plots can be referred to Appendix E. Most of the maximum principal stresses exceeded the tensile strength of the concrete by a large margin because the analysis was linear elastic and the stresses could increase well beyond tensile strength of the material. Extreme assumptions in the modeling process also contribute to the large stress values. For example, the pin and hanger assembly could still allow some movement even though they were rusted, and the abutment wall could have slightly displacement and rotation, etc. Thus, interpretation focused the variation trends of the result variables to the change of design parameters and damage scenarios.

5.6.1   Simple/cantilevered steel bridge

1. For bridges subjected to the pavement pressure, as shown in Figure 5-19 and Figure 5-20, the maximum stress increased significantly with the increase of the skew angle. The maximum horizontal strain didn't change a lot when the skew angle is between 0 to 30 degree and increase significantly when skew angle is larger than 30 degree (Figure 5-21, Figure 5-22). The lock of pin and hanger assembly alleviated the maximum stress and strain. The span length and width of the bridge didn't have a significant effect on the maximum stress and strain.
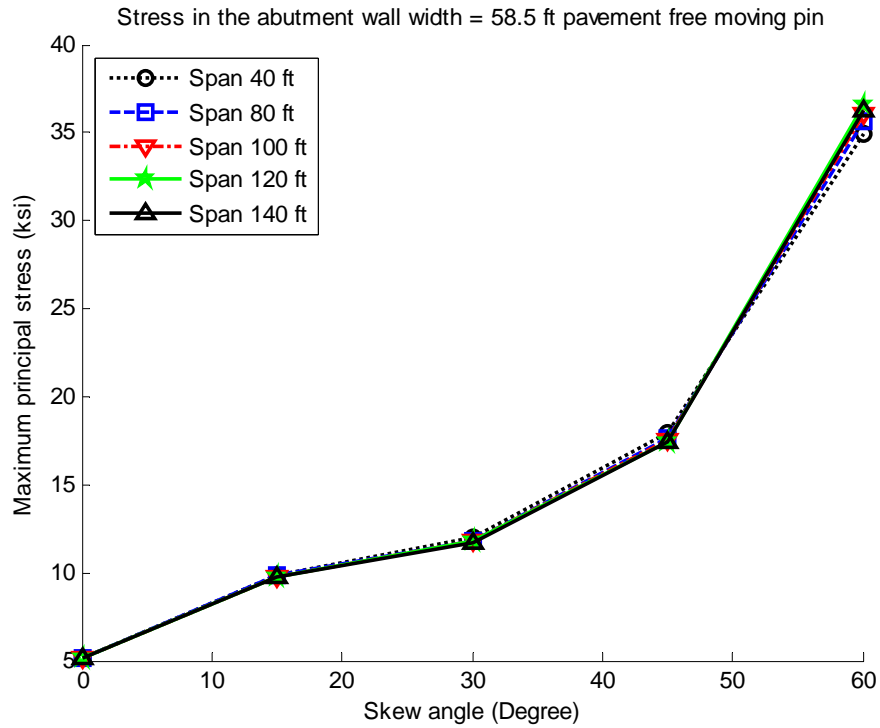
Figure 5-19 Maximum stress of bridges under pavement pressure (free moving pin and hanger)
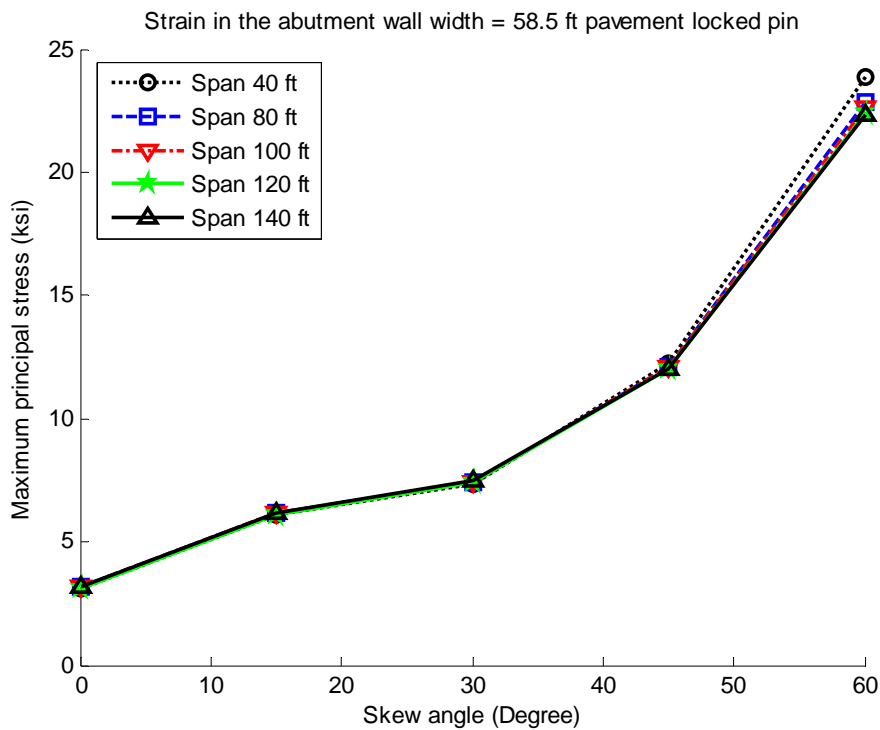
Figure 5-20 Maximum stress for bridges under pavement pressure (pin and hanger locked)
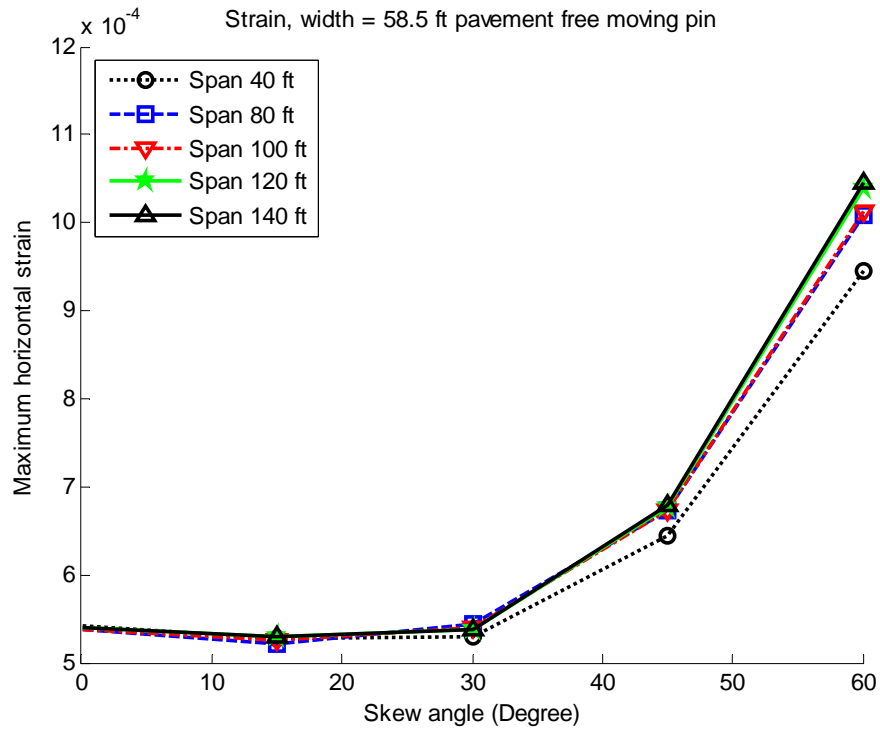
Figure 5-21 Maximum horizontal strain for bridges under pavement pressure (free moving pin and hanger)
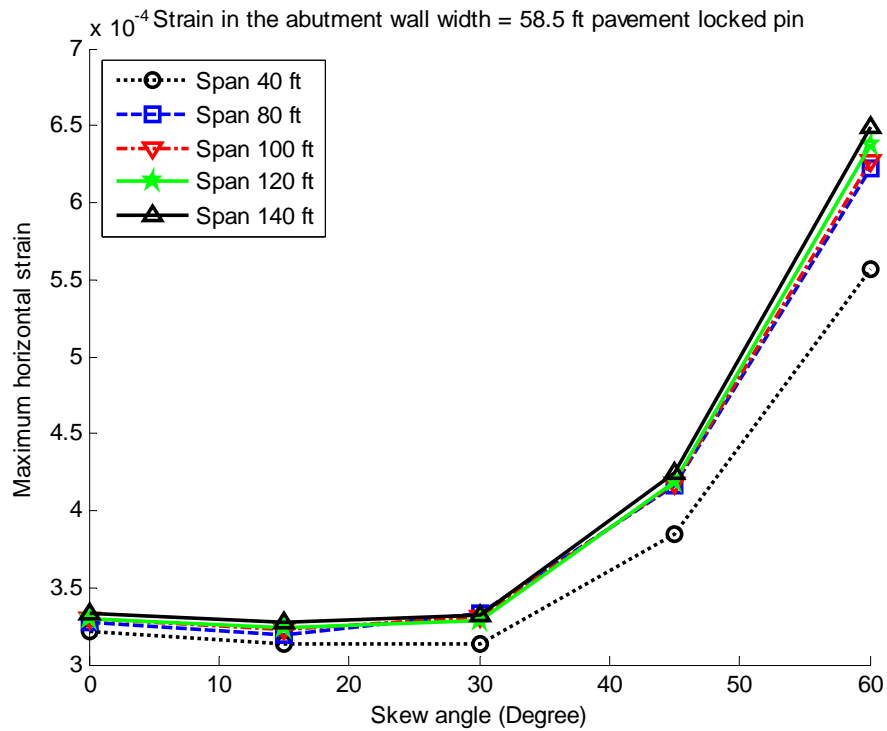
Figure 5-22 Maximum horizontal strain for bridges under pavement pressure (pin and hanger locked)

2. For bridges in summer time, The lock of pin and hanger assembly had a significant effect on the maximum stresses, as shown in Figure 5-23 and Figure 5-24; maximum stresses in the abutment walls of bridges with locked pin and hanger were much larger than those in the abutment walls of bridges with free moving pin and hanger. When pin and hanger were locked, both the skew angle and the span length had a significant influence on the maximum stress, longer bridges and bridges with larger skew angles were subjected to larger maximum stresses. The maximum horizontal strain follows similar trends: increased with the increase of the skew angle and the span length; it also increased with the increase of bridge width slightly; furthermore, the lock of pin and hanger only increase the maximum horizontal strain by a moderate amount.
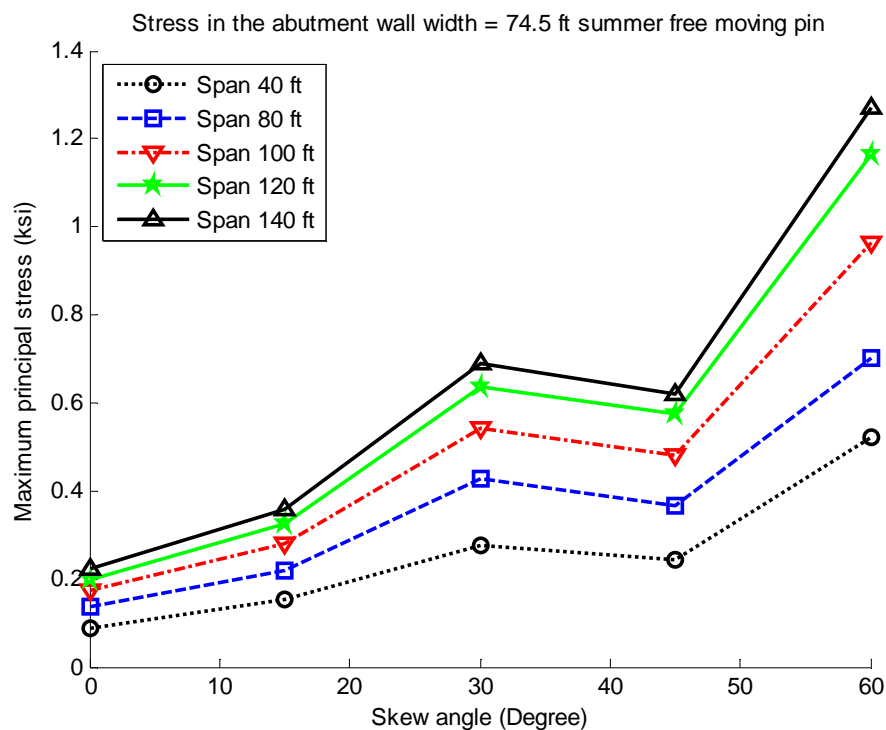
Figure 5-23 Maximum stress of bridges in summer time (free moving pin and hanger)
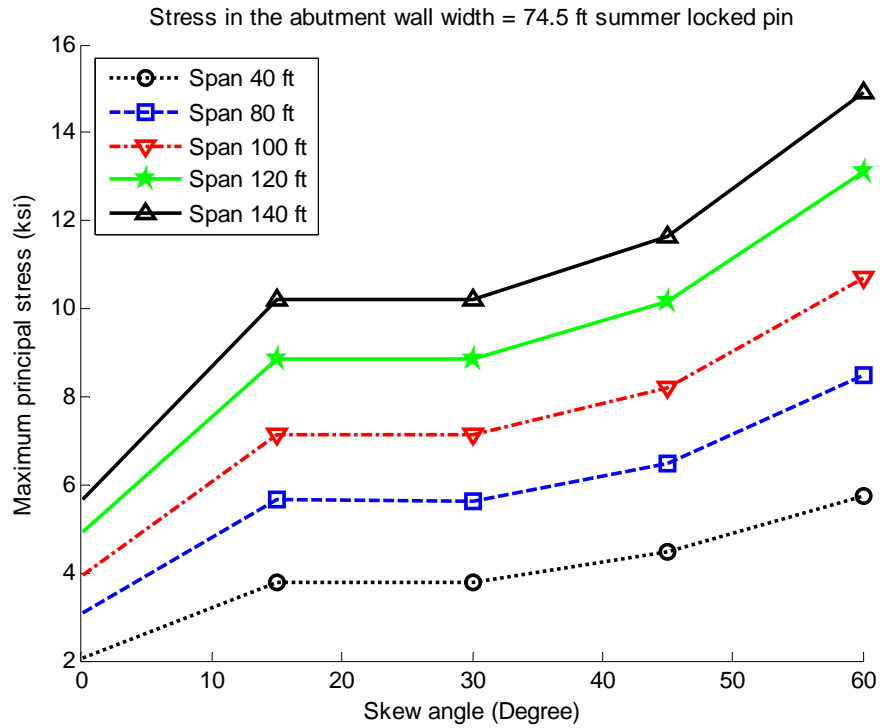
Figure 5-24 Maximum stress of bridges in summer time (pin and hanger locked)
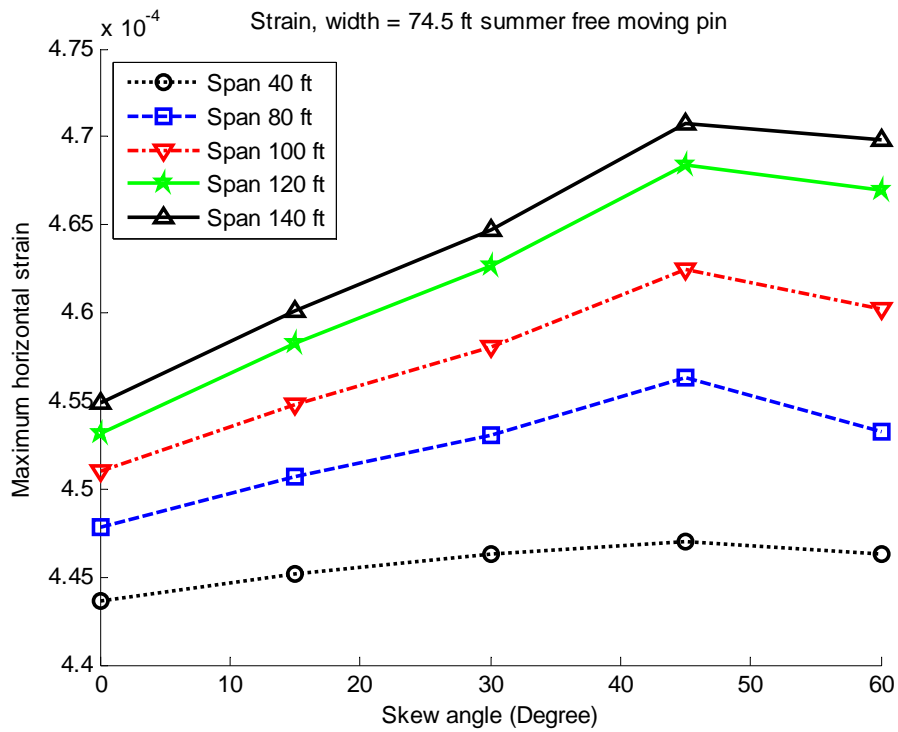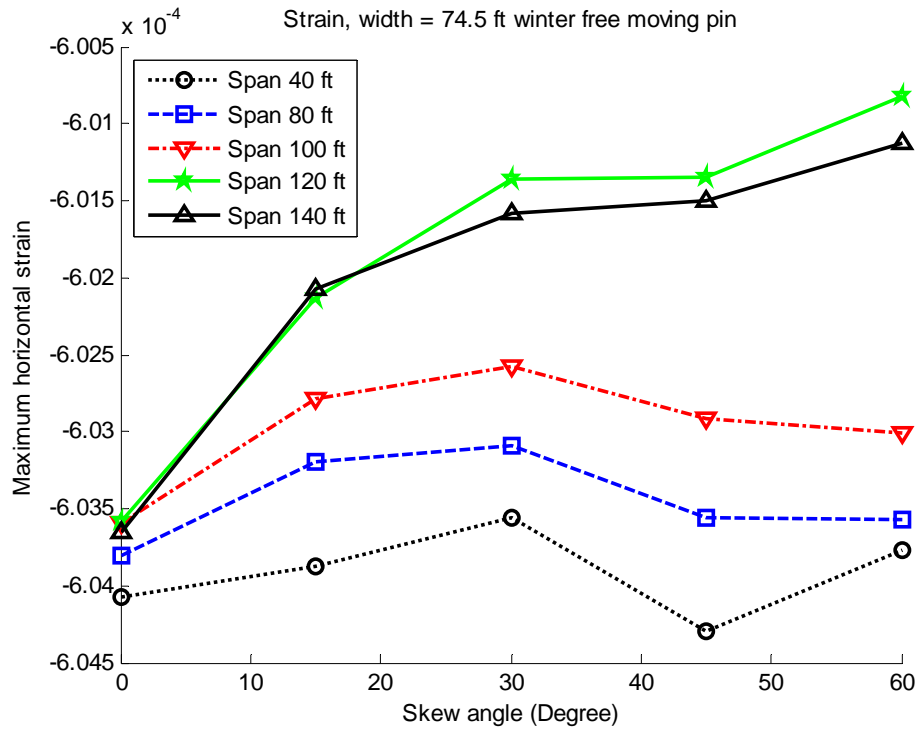

Figure 5-25 Maximum horizontal strain of bridges in summer time (free moving pin and hanger)
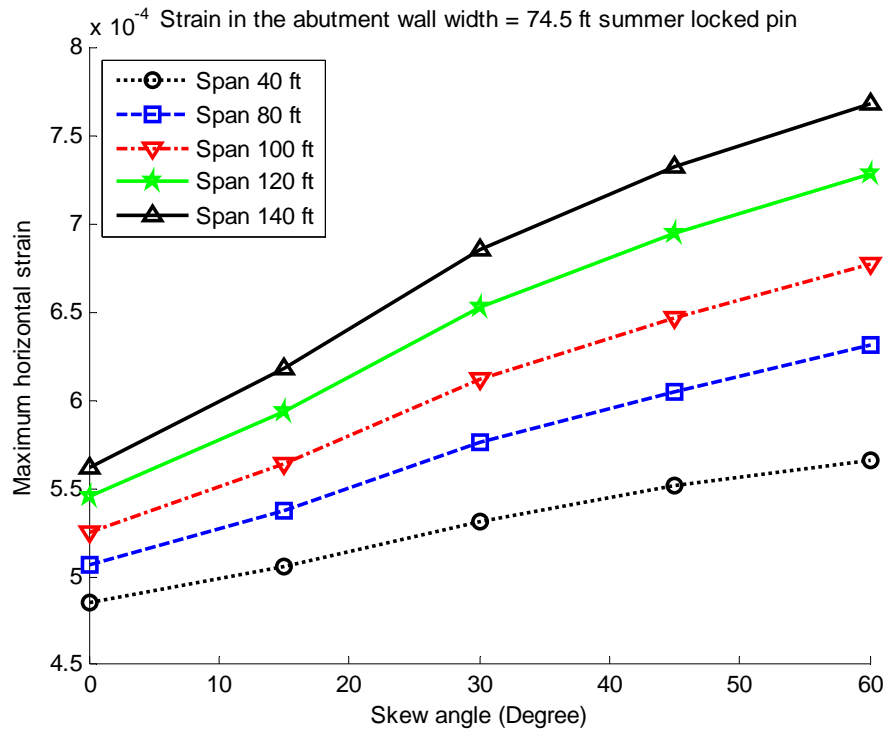
Figure 5-26 Maximum horizontal strain of bridges in summer time (locked pin and hanger)

3. For bridges in winter time, the variation trends of maximum stresses were similar to those in summer time; the maximum horizontal strains were negative. As shown in Figure 5-27 and Figure 5-28, when pin and hangers were fine, the influence of design parameters to maximum horizontal strain was trivial, when pin and hangers were locked, bridges with longer span tended to have less horizontal compressive strain in the abutment wall.

Figure 5-27 Maximum horizontal strain of bridges in winter time (free moving pin and hanger)
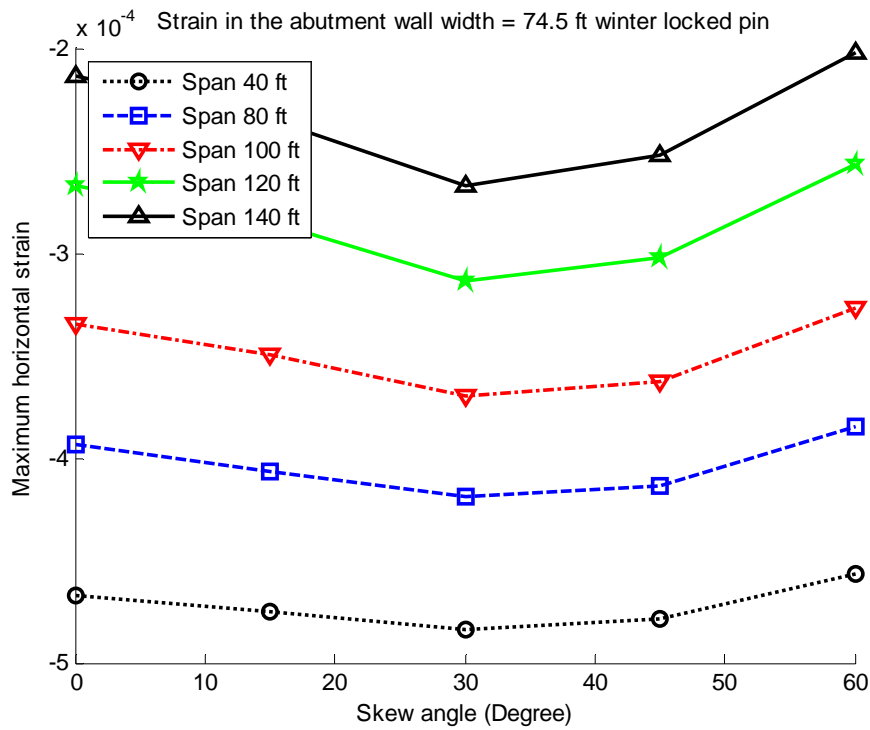
Figure 5-28 Maximum horizontal strain of bridges in winter time (locked pin and hanger)

4. Comparing the effects of three damage scenarios, the maximum stresses that were generated by the pavement pressure were larger than those of the winter time temperature field, which were larger than those in the summer time temperature field. As mentioned at the beginning of section 5.6, the absolute value of result variables deviate from reality by a large margin, the conclusion about the relative magnitude of response intrigued by in different damage scenarios can only serve as a reference.

5.6.2   Continuous steel bridges

1. For bridges with free moving pin and hanger assembly subjected to the pavement pressure, stress and strain increased significantly with the increase of the skew angle, they also increased slightly with the increase of decd width. The effect of span length on maximum strain or stress was trivial (Figure 5-29 and Figure 5-30).
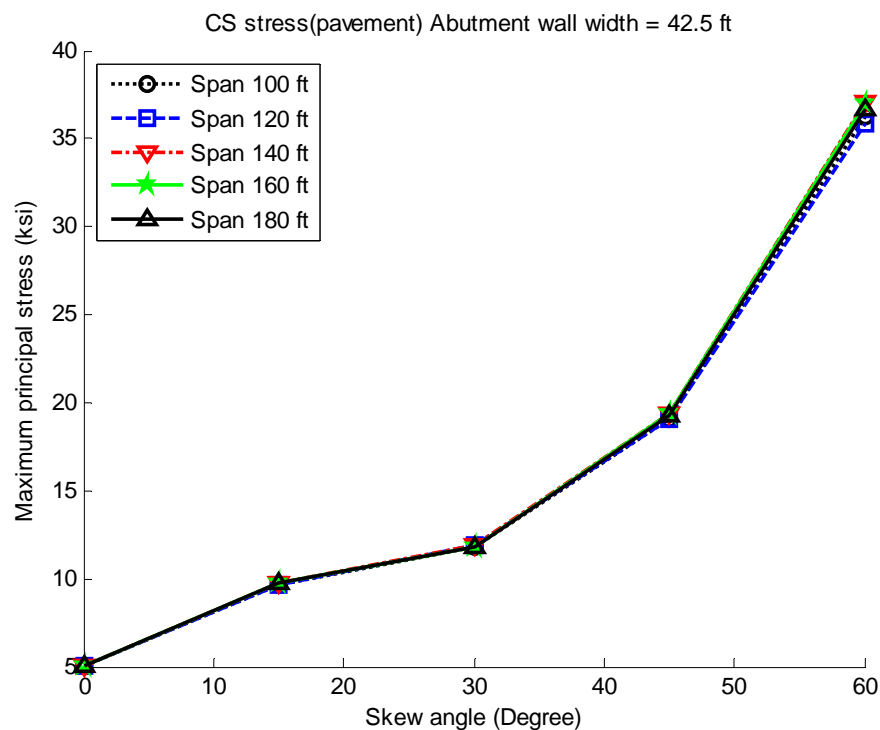

Figure 5-29 Maximum stress of bridges under pavement pressure (free moving pin and hanger)
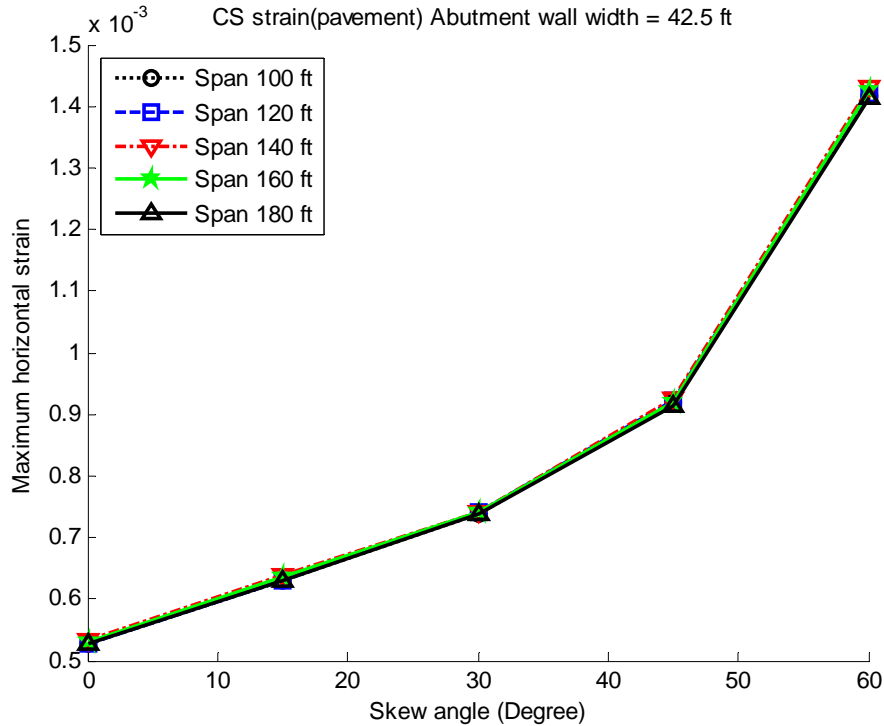
Figure 5-30 Maximum horizontal strain of bridges under pavement pressure (free moving pin and hanger)

2. For bridges in summer time with locked pin and hanger, it can be seen from Figure 5-31 and Figure 5-32 that maximum stress and strain increased with the increase of skew angle. The width of bridge had trivial influence on the stress and strain in the abutment wall. Generally, the stress and strain increased with the increase of the span length. It was noted that the stress and strain of bridge with span length 160 ft was larger than 180 ft, it was because the flange of the 160 ft span bridge was thicker than the 180 ft span bridge, the web depth of former was less than later according to the output of MDOT bridge design program.

3. For bridges in winter time with locked pin and hanger, variation trends for maximum principal stress was similar to those in summer time. The magnitude of the horizontal strain was much smaller (Figure 5-33).
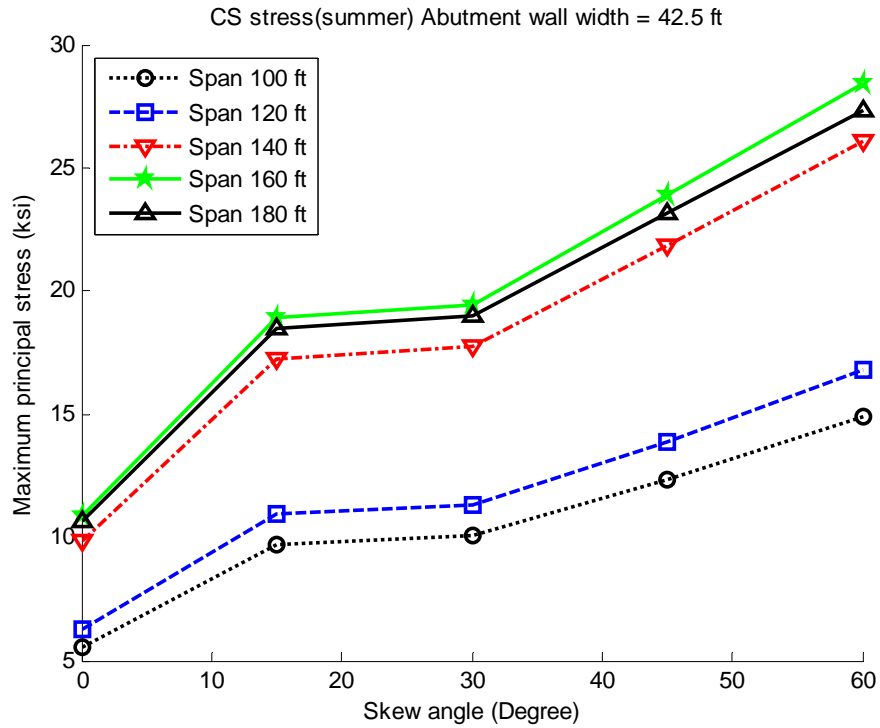
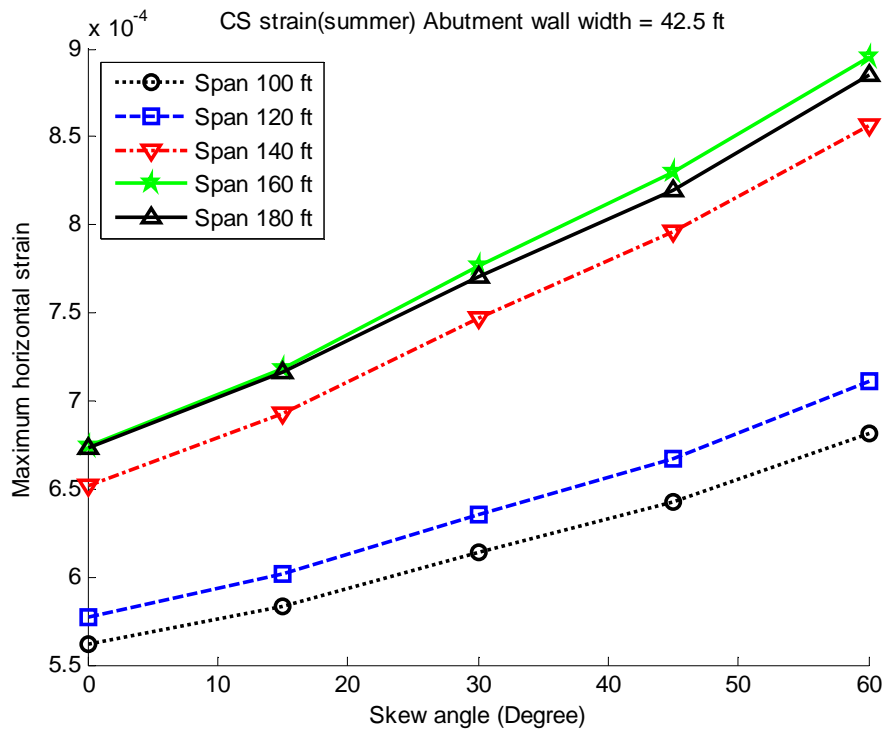**Figure 5-31 Maximum stress of bridges in summer time (pin and hanger locked)**

Figure 5-32 Maximum horizontal strain of bridges in summer time (pin and hanger locked)
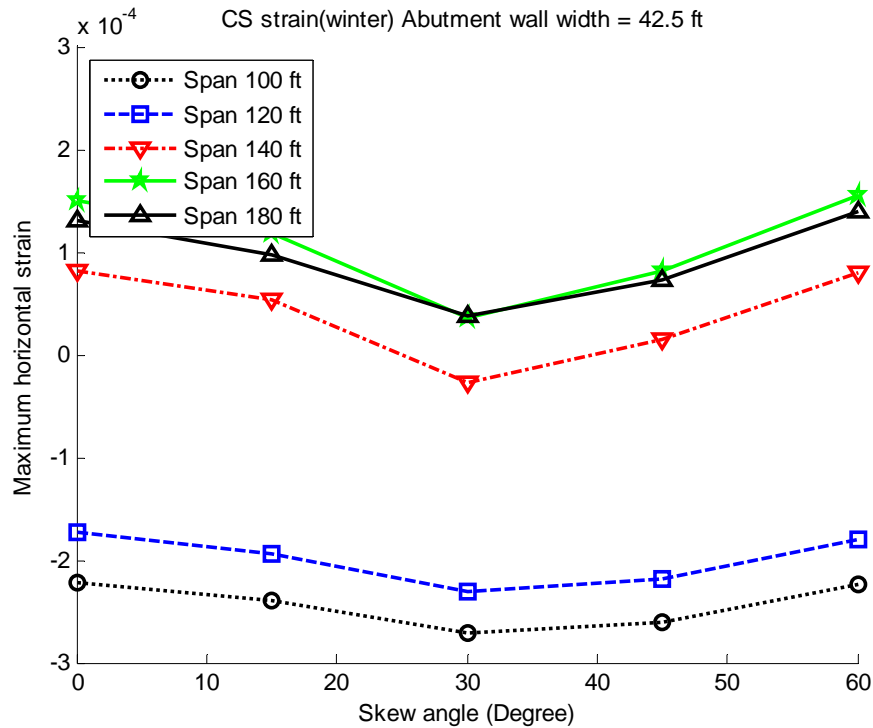
Figure 5-33 Maximum horizontal strain of bridges in winter time (pin and hanger locked)

4. Comparing the effects of three damage scenarios, the maximum stresses that were generated by the pavement pressure were larger than those generated by summer and winter temperature effects; the differences were smaller than those for simple/cantilevered steel bridges. As mentioned before, these comparisons of magnitudes of response variables can only serve as a reference.

5.6.3 Prestressed concrete bridges

1. For bridges under pavement pressure, maximum stress increase with the increase of skew angle, when skew angle was less than 30 degree, the effect of skew on maximum horizontal strain was trivial; when the skew angle was larger than 30 degree, maximum horizontal strain increased significantly with the increase of skew angle (Figure 5-34 and Figure 5-35). The effects of span length and bridge width to the stress and strain in the bridge abutment walls were trivial.
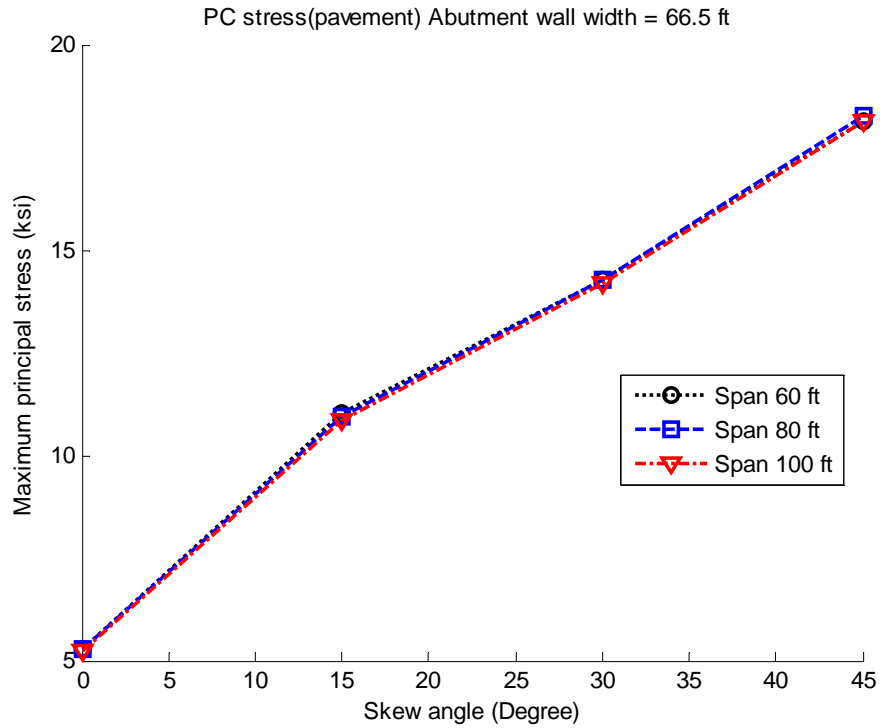
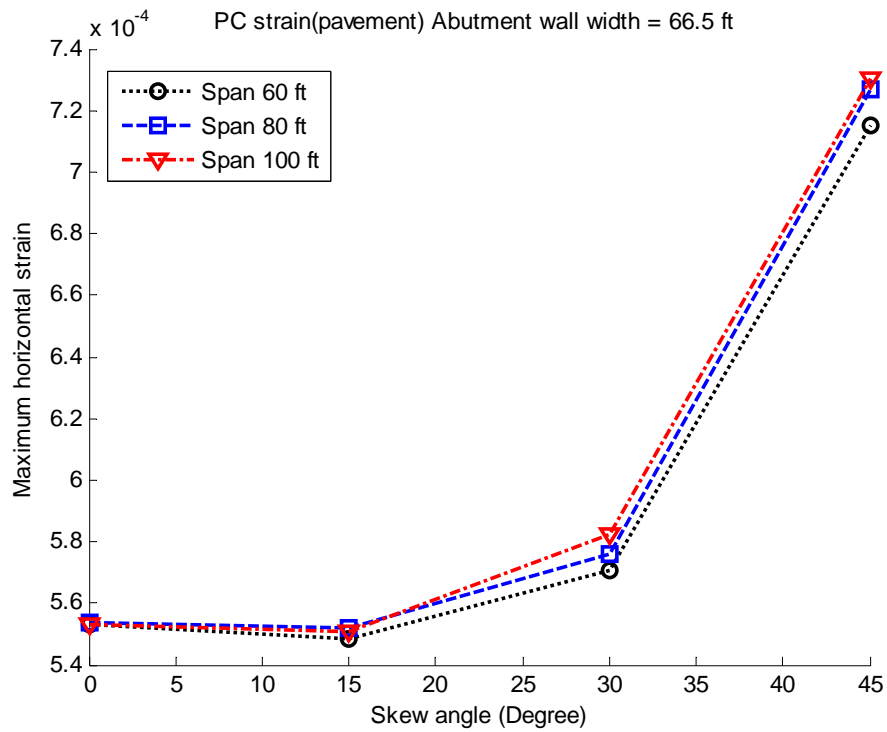**Figure 5-34 Maximum stress of bridges under pavement pressure**

Figure 5-35 Maximum horizontal strain of bridges under pavement pressure

2. It can be seen from Figure 5-36 and Figure 5-37, for bridges in summer time, maximum principal stress and maximum horizontal strain increased with the increase of skew angle when the skew angle was less than 30 degree. Generally, stress and strain would increase slightly with the increase of span length; the effect of bridge width was trivial.

3. Generally, the variation trends of stress for bridges in winter were similar to bridges in summer. It can be seen from Figure 5-38 that the region of abutment below the top was in compression in winter. The compressive strains varie little with the variation of design parameters.

4. Since the bearing condition on one side of the bridge was pin connected and on the other side was allowing girder to move horizontally. The stress and strain induced by pavement growth were much larger than those induced by temperature effect.
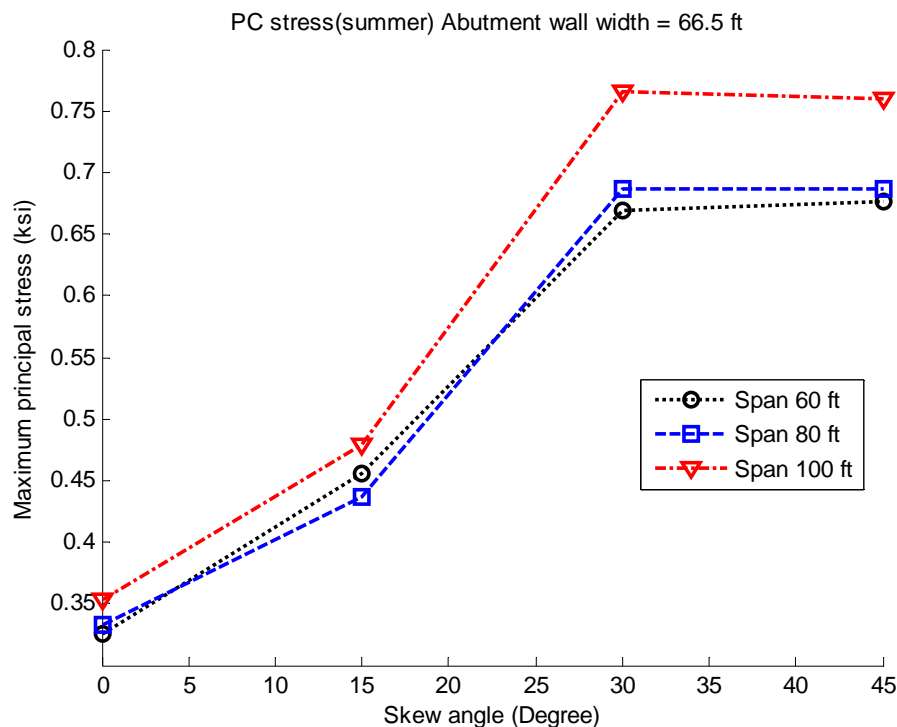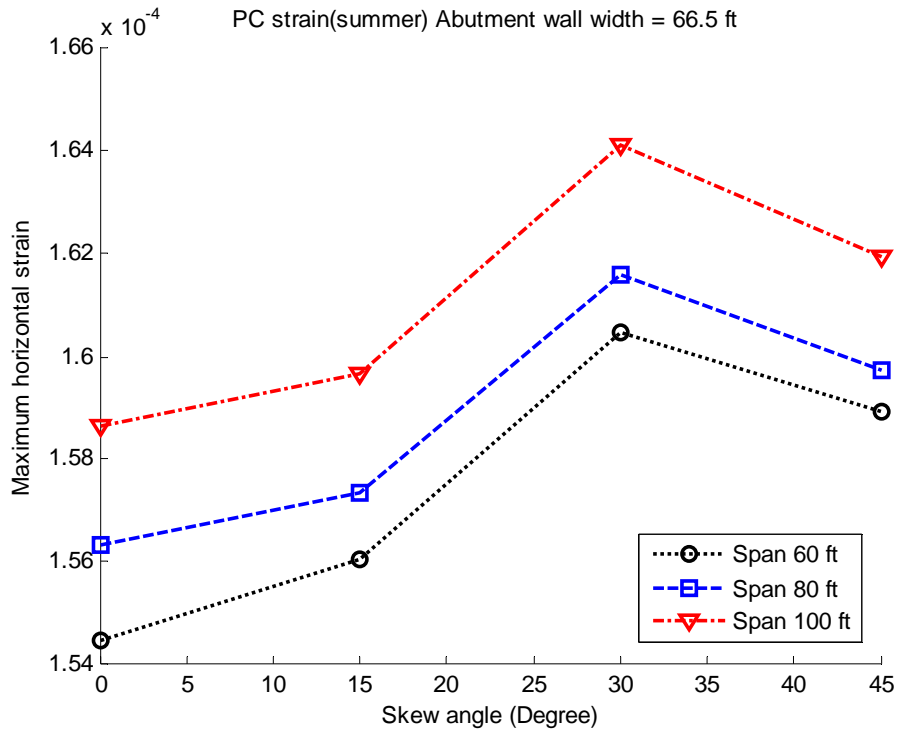

Figure 5-36 Maximum stress of bridges in summer

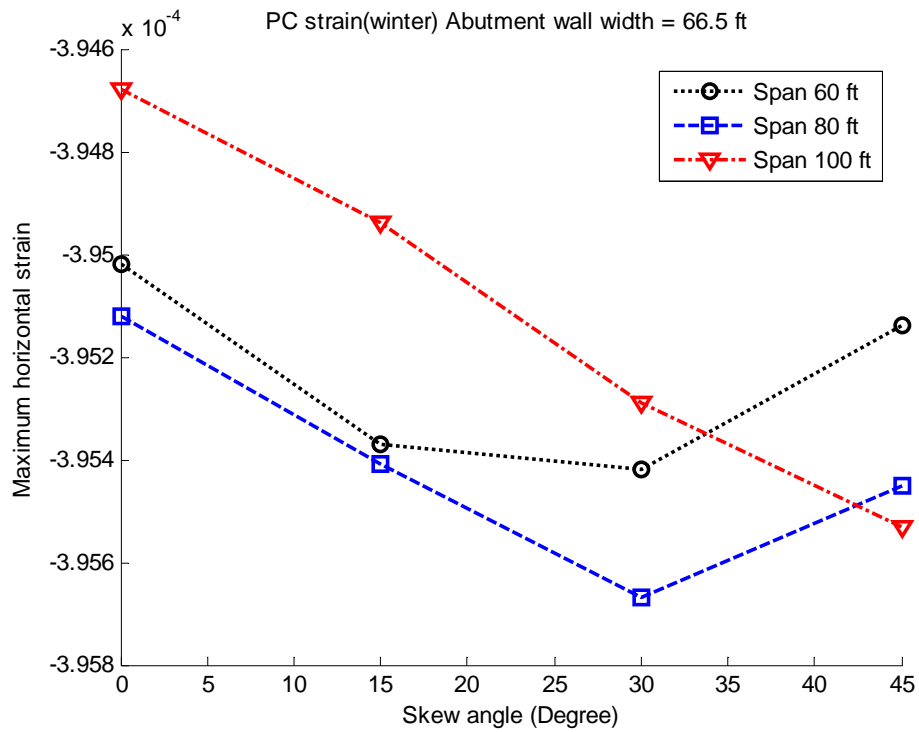**Figure 5-37 Maximum horizontal strain of bridges in summer**

Figure 5-38 Maximum horizontal strain of bridges in winter

5.7 Discussion

The behavior of highway bridges with three different structural types were simulated using commercial FEA program ABAQUS: simple/cantilevered steel bridges (SS), continuous steel bridges (CS), and prestressed concrete bridges with I girders (PC). Each of the structural types was simulated using three damage scenarios: pavement growth, summer temperature field, and winter temperature field. Four hundred and fifty simple/cantilevered steel bridges, 225 continuous steel bridges and 108 prestressed concrete bridges were simulated. The conclusions derived through FE simulations can be summarized as follows:

➢ Stress and strain in bridge abutments increased with the increase of skew angle. This pattern could be more dramatic when the skew angle is larger than 30 degrees.

➢ For bridges under pavement pressure, the effect of span length on the stress and strain in the abutment wall was trivial. In summer or winter temperature field, the effect of span length was moderate.

➢ Generally, the effect of bridge width on the stress and strain in the abutment wall was trivial.

6　Artificial Neural Network Simulation (Subtask III.3)

6.1　Introduction

Artificial neural networks (ANNs) are essentially models for computation and knowledge representation inspired by the understanding and abstraction of the biological structure of neurons and the operation of the human brain (Kartam et al. 1997). A neural network is a highly interconnected network of many simple linear or nonlinear processors, or operations in parallel fashion (Figure 6-1). Each processing unit receives multiple inputs through weighted connections from neurons in the previous layer to which it is connected, performs appropriate computation (adding inputs, computing a new activation level, or comparing input to a threshold value), and transmits output to other processing units or as a network output using an assigned transfer function. Thus, a neural network performs operations by propagating changes in activation, or stimulation, through weighted connections between the processors, and it stores what has been "learned" as strengths of the connections between the processors. The system adjusts the weights of internal connections to minimize errors between the network output and target output. This learning occurs even when the input data contains errors or is incomplete, which is one of the problems that must be addressed for structural distress in bridge substructures. The propagation of the activation and thus the "computation" performed by the network depends on the layout and the strengths of the connections between the processors. A neural network thus has the ability to synthesize through training an associative memory that may generate appropriate output when presented with an unfamiliar set of inputs.
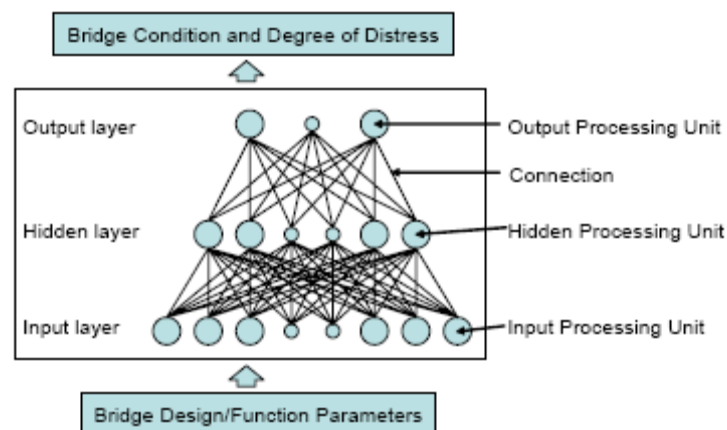

Figure 6-1 Schematic of a neural network

The non-linear nature of ANNs makes them suitable for performing functional approximation, classification, and pattern recognition. Neural networks thus have many qualities that make them particularly attractive in pattern-recognition applications that are not easily achieved by other means. Some of the important qualities of neural networks are (Graybill and Iyer 1994):

➢ They "learn" by example and can be conditioned to respond correctly to a stimulus.

➢ They can automatically perform knowledge abstraction and statistical analyses on data that is presented to them and this information becomes encoded into the network internal structure.

➢ They can generally respond correctly even in the presence of noise or uncertainty in the in-formation network making them suitable for use in poor signal/data environments.

➢ They can satisfactorily predict the outcome of complex problems or those with high degree of nonlinear behavior.

ANNs are then highly useful to problems where patterns of information represented in one form need to be mapped into patterns of information in another form. Applications of ANNs to civil engineering is increasingly common including: classification/interpretation tasks (inverse mapping from observations to known causes), diagnosis (inverse mapping from observed effect to cause), modeling (mapping from cause to effect), and control (inverse mapping from observed state to control applied forcing functions).

Commonly used ANNs are multilayer perceptron (MLP), radial basis function network (RBF), support vector machine (SVM), self-organizing map (SOM) etc. This research first developed prediction models using using MLP, RBF, SVM, and supervised SOM (SSOM), respectively, then, evaluated the accuracy of different ANNs for the bridge abutment distress problem. MLP and SVM were found to be good prediction models for the problem. In the later part of the research, ensemble of neural networks and fuzzy-neural networks were developed to overcome the unbalance, subjectivity of the manual inspection database. The prediction models can predict the abutment rating of highway bridges given the explanatory variables. A stand-

alone executable program "Bridge Abutment Damage Diagnosis" was developed based on the prediction model using ensemble of neural networks.

6.2   Artificial Neural Network Models

6.2.1   Multilayer perceptron network model

A multilayer perceptrons model is a network composed of several layers of neurons. Each neuron is a computation unit, which, given an input value, calculates an output value through an activation function. The multilayer perceptrons model is then composed of neurons assumed to be organized in layers, each consisting of one or more neurons. The input vector enters ANN through an input layer, which is followed by one or several hidden layers. The computation result is given out through output layer. The output of the previous layer contributes to the input of the next layer after being modified by synaptic weights. A back propagation algorithm minimizes the sum of the squares of the error computed at the output layer, and, thus, seeks global optimization of the network (Haykin, 1999). In each iteration, the synaptic weights are updated through the back propagation algorithm. The relationship between input variables and output variables is stored in the synaptic weights after training such that a trained network can predict the output values from novel inputs. A typical structure of an MLP ANN is shown in Figure 6-2. If designed for the prediction of the damage in bridge abutments, the input layer with p neurons would input p bridge design and service parameters and the output layer would have k neurons to represent k condition levels of the bridge abutment. Two hidden layers are shown in the model schematic of Figure 6-2.

Several factors are important for a good generalization of the MLP:

➢ Architecture of the network;

➢ Selection of input variables and preprocessing of input data;

➢ Network parameters, such as, the activation function, the learning rate, etc. (Haykin, 1999);

➢ Danger of overfitting;

Over fitting should be avoided because the paramount goal of a prediction model is to make predictions for novel data instead of training data. The Matlab$^{®}$ toolbox was be used to develop the MLP ANN models.
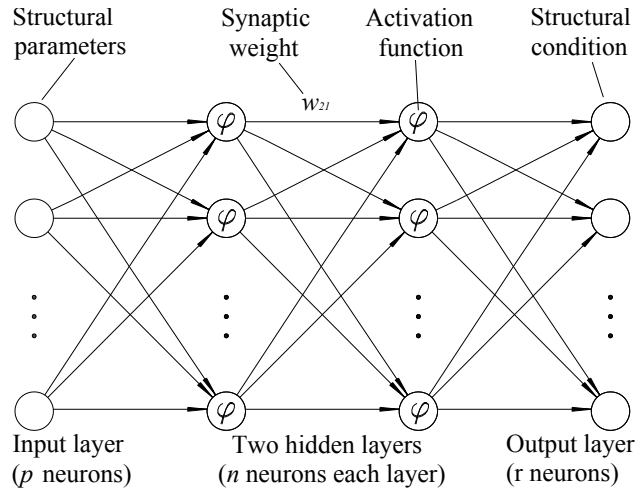

Figure 6-2 Diagram of MLP

6.2.2 Radial basis function network model

The radial basis function network is based on the idea of curve fitting, searching for a hyper surface in a multidimensional space that best fits the training data. The hyper surface is composed by the combination of a set of basis functions. The parameters of the basis functions and their combination weights can be derived from the training process. The Gaussian function was used in the paper as the basis function. The two most important parameters in RBF networks are the number of basis functions (n_b) and the width of basis functions (σ). The diagram of RBF in two dimensional space is shown in Figure 6-3. The value the output variable can be calculated from the hyper surface given novel input values. Generalized RBF network was coded in this research.
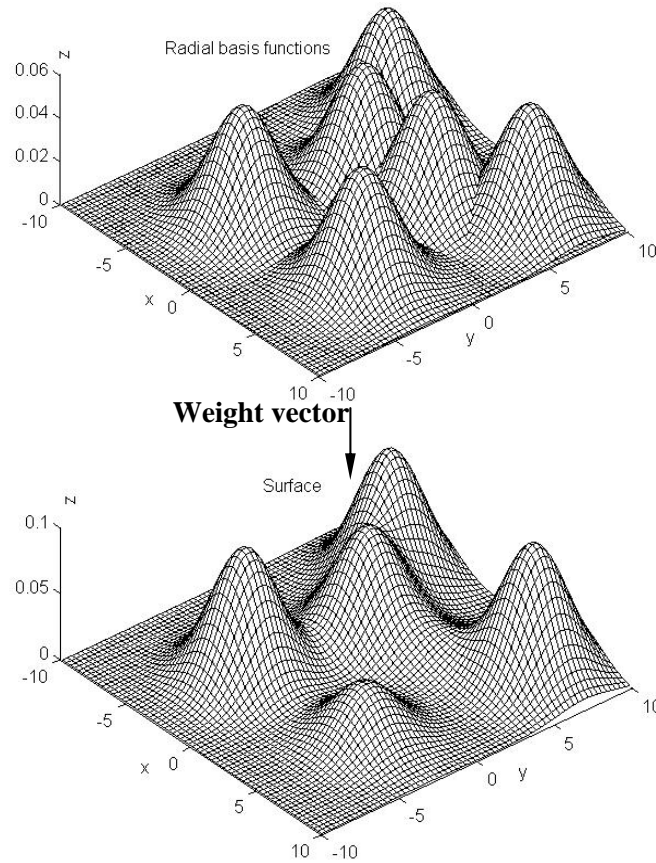
Weight vector

Figure 6-3 Diagram of RBF

6.2.3 Support vector machine

Support Vector Machine (SVM) models have become an important technique in soft computing. The approach is related to statistical learning theory (Vapnik, 1999). The concept is that a series of separation boundaries might be able to separate two separable classes of data in a hyper space. The idea of SVM is to search for the decision boundary that maximizes the marginal distance between the boundary and the closest points in each data class (Figure 6-4). Sub-optimal decision boundaries (dashed lines in Figure 6-4) also separate circles from squares (ie. two data classes) for the training data. However, compared to the max-margin (optimal) decision boundary, sub-optimal boundaries provide a better chance for the test patterns to fall on the other side of the boundary and thus be misclassified. Nonetheless, sub-optimal decision boundaries can not be expected to have a good generalization performance.
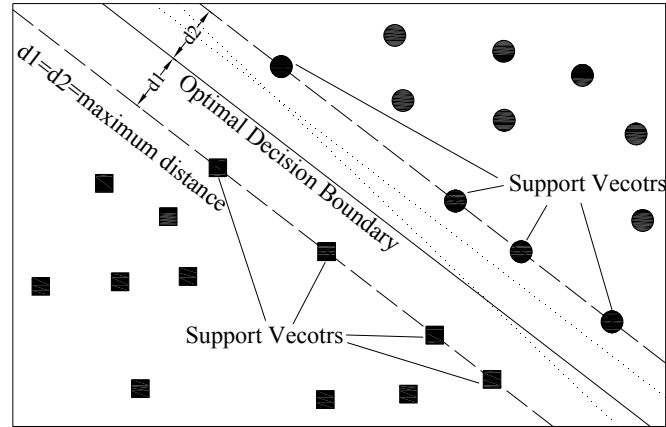
Figure 6-4 Optimal decision boundary decided by SVM

Most of the real world problems will not be linearly separable; however, the non linearly separable vectors x_i might be linearly separable after being transformed to vectors $\varphi(x_i)$ in a higher dimensional space. The notation "$\varphi(\cdot)$" represents the nonlinear transformation from input space to a higher dimensional feature space. This transformation is achieved by the application of a "Kernel Trick", that is, the use of a kernel function (inner product of some functions of input vectors) to avoid carrying out transformation $\varphi(\cdot)$ for each vector explicitly. A freely distributed SVM toolbox (Gunn 1997) with a radial basis function as kernel function will be used for a single SVM classifier. A single SVM classifier will be designed for this research for the classification between two levels of structural conditions. The one against one method (Hsu & Lin, 2002) will be used to enable a series of single SVM classifiers to work together to solve the multi-class classification problem, such as the prediction of structural condition rating. Two important parameters for the SVM model to be used in this research are width of the radial basis function d, and trade off parameter c between the error and the separation margin.

6.2.4   Supervised self organizing map

The development of Self Organizing Map (SOM) was motivated by the structure and function of the human brain; neurons of different regions are responsible for different tasks: vision, hearing, etc. By the same logic, different neurons in the SOM catch features of data in different classes. Neurons in the map usually laid on a one or two dimensional lattice, and trained

by winner takes all rule, that is, for each training pattern, only one neuron win (Haykin, 1999; Kohonen, 1990). SOM is organized in a way that captures and store the feature of the training pattern in weights after training. The important parameters for SOM are number of rows and columns in the original lattice (n_r, n_c).

A self-organizing map is a kind of unsupervised learning network by nature. By providing proper supervised training it can also be transformed into a supervised learning network. Several steps are needed to achieve this: 1) Create and train an ordinary SOM. The topology of the map and its weight vectors will represent the features of the training data. Each neuron in the map will win certain number of training vectors in a way that the weight vector of this neuron represents their common features; 2) Count the number of training vectors each neuron has won. The class of training vectors that is most populous among all won by the neuron is assigned to the neuron. 3) In testing, there will be a single winning neuron for each test vector and the class of the winning neuron will be assigned to it as the predicted value. Codes were programmed to convert SOM to supervised SOM (SSOM) in this research.

6.3   Evaluation of ANN Models for Abutment Distress Problem

The explanatory variables used in training the networks were decided through statistical analyses in section 3. The proper setting of ANN parameters is one of the key issues to build a good prediction model. Some rules of thumb have been developed for each ANN Models; and no rigorous theoretical procedure was available until this paper was finished. Parameters of ANNs were determined by the combination of rules of thumb and trial and error. It was impossible to test every possible parameter combinations since multiple parameters existed for each ANN with infinite possible values for each parameter. The approach in the paper was as follows: for parameters x and y, first select k values that spread over their ranges respectively, and build ANN models with each of k^2 combinations between [x_1, x_2 ...x_k] and [y_1 y_2...y_k]. Parameters of the model with minimum testing error, (x_i, y_j) would be the center of next trial. Then in the similar procedure, select k values that spread over [x_{i-1}, x_{i+1}] and [y_{j-1}, y_{j+1}], respectively, and find the refinement of the optimal combination. This search process can be further refined until

satisfactory testing error is reached. The method is susceptible to local minimum, while it was still a practical way to solve the problem when no rigorously theoretical method is available.

The MLP ANN with 2 hidden layers, 130 neurons in each hidden layer and a learning rate $\eta=0.05$ had the best performance. In order to avoid over training and thus improve the prediction power of the network, the number of epochs (n_e) during training shall not be too large, and the mean square error (*mse*) to stop the training process shall not be too low. For the best model, *ne= 10,000,* and *mse = 0.05.*

Predictions of the trained MLP ANN are listed in the confusion matrix shown in Table 6-1 together with the manual inspection (i.e., true) values. A confusion matrix (Kohavi & Provost, 1998) contains information about actual and predicted classifications and can be used as a measure of the model performance (Silva et al., 2004). In this section, the columns represent the predicted values and rows represent the manual inspection (or true) value. The numbers in the cells with row and column numbers between 0 and 9 represent the numbers of observations that fall into those categories. Accordingly, the diagonal elements (darker gray cells) represent the number of correct predictions, where being far away from the diagonal implies the prediction is far away from the actual response. The row labeled correct ratio (CR) gives the ratio of the number of correct predictions to the number of all instances for that given level of response (given in the "True Sum" row). Subjectivity in the rating of structural members is well recognized and a margin of error of ±1 has been found to be representative (Phares et al., 2001). Thus, an acceptable prediction band width could be defined within the confusion matrix by considering a prediction acceptable if it is within ±1 of the true response value. The expanded band width in the confusion matrix is shown by a lighter gray shade along the main diagonal in Table 6-1. Considering all records that fall within the acceptable bandwidth, an acceptable ratio (AR) could be used as another criterion to evaluate the performance of the network. Additionally, a distress identification ratio (DIR) was defined as the number of inspection cases whose inspection (or true) value is less than 4 and was predicted to be less than 4. The DIR can be calculated as the sum of the top left 5×5 square sub-matrix of Table 6-1 divided by the sum of the first half of the row "True Sum".

Table 6-1 Confusion matrix of abutment rating prediction using MLP

Predicted \ True	0	1	2	3	4	5	6	7	8	9	Sum
0	3	0	0	0	0	0	0	2	2	0	7
1	0	0	0	0	0	0	0	0	0	0	0
2	0	0	5	0	1	5	8	2	2	0	23
3	0	0	2	23	22	17	61	112	32	0	269
4	0	0	0	6	71	20	127	185	36	0	445
5	1	0	0	2	22	162	557	632	78	0	1454
6	0	0	2	0	1	20	516	442	35	0	1016
7	0	0	0	9	29	78	1251	5226	807	2	7402
8	1	0	0	0	1	1	37	273	272	1	586
9	0	0	0	0	1	0	7	14	3	2	27
True Sum	5	0	9	40	148	303	2564	6888	1267	5	11229
Correct ratio (%)	60.0	N/A	55.6	57.5	48.0	53.5	20.1	75.9	21.5	40.0	55.9
Acceptable ratio (%)	60.0	N/A	77.8	72.5	77.7	66.7	90.6	86.3	85.4	60.0	86.4

The RBF with parameters $n_b = 3$ and $\sigma = 290$ had the optimal performance. The SVM with parameters $d = 4$ and $c = 50$ had the best performance. The confusion matrix for SVM predictions is shown in Table 6-2. The SSOM with parameters $n_r = 16$ and $n_c = 19$ had the optimal performance. The performances of the best prediction models (MLP, RBF SVM and SSOM) were compared in Figure 6-5. MLP and SVM showed better performance among the four, RBF was not good because of poor DIR value; even though it had the highest AR value.

Table 6-2 Confusion matrix of abutment rating prediction using SVM

| Predicted \ True	0	1	2	3	4	5	6	7	8	9	Sum
0	1	0	0	0	0	0	1	16	0	0	18
1	0	0	0	0	0	0	0	0	0	0	0
2	0	0	29	0	0	1	2	12	0	0	44
3	0	0	8	112	13	15	41	114	6	0	309
4	0	0	0	24	143	64	134	350	14	0	729
5	0	0	0	6	27	508	554	988	46	1	2130
6	0	0	0	16	5	111	1598	1781	81	0	3592
7	0	0	0	14	25	82	618	4374	170	0	5283
8	1	0	2	6	5	29	283	1637	671	1	2635
9	0	0	0	0	0	0	12	23	4	5	44
True Sum	2	0	39	178	218	810	3243	9295	992	7	14784
Correct ratio (%)	50.0	N/A	74.4	62.9	65.6	62.7	49.3	47.1	67.6	71.4	50.3
Acceptable ratio (%)	50.0	N/A	94.9	76.4	83.9	84.3	85.4	83.8	85.2	85.7	84.2
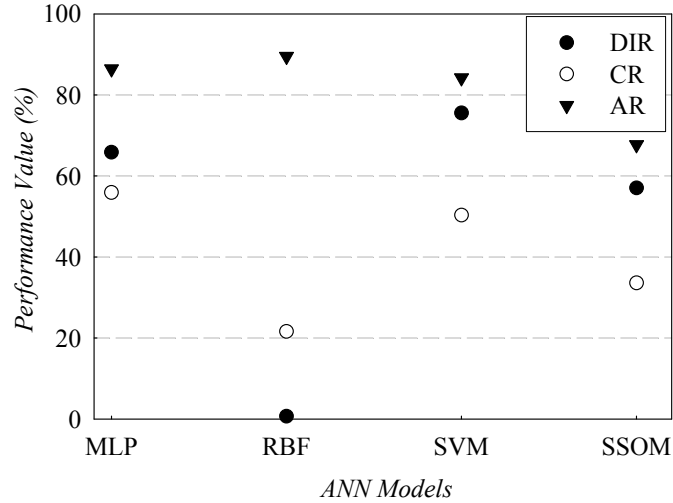
Figure 6-5 Performance of ANN models

The MLP and the SVM models were applied to retrieve and predict the conditions of the abutment walls of a simple/cantilever steel bridge (bridge A 1.5) in State of Michigan. The deterioration curves for this bridge are shown in Figure 6-6. The abutment rating predicted by the ANN models are shown by the stepwise solid line; the stepwise shape is decided by the nature of the integer 0 to 9 rating scale. Data points corresponding to the manual ratings currently available in the database for this bridge are also shown as dotted-connected triangles. Confidence bands for the deterioration curves are also shown in the figure as dashed curves. The width of the stepwise confidence band is twice of each standard deviation of the predicted value. The center of the band is biased from the predicted value to account for the asymmetrical deviation of the model; the amount of bias is decided by the ratio of those manual ratings above the predicted value to those below. Therefore, both the width and bias of the confidence band change with the predicted value. Since the abutment condition degraded gradually, the stepwise confidence bands were smoothed to curves through the Lowess method using a first-degree polynomial. Since ANN models are non-parametric model, the confidence levels for the confidence bands were hard to derive through statistical methods; however, the confidence level can be obtained through testing as shown in Table 6-3.
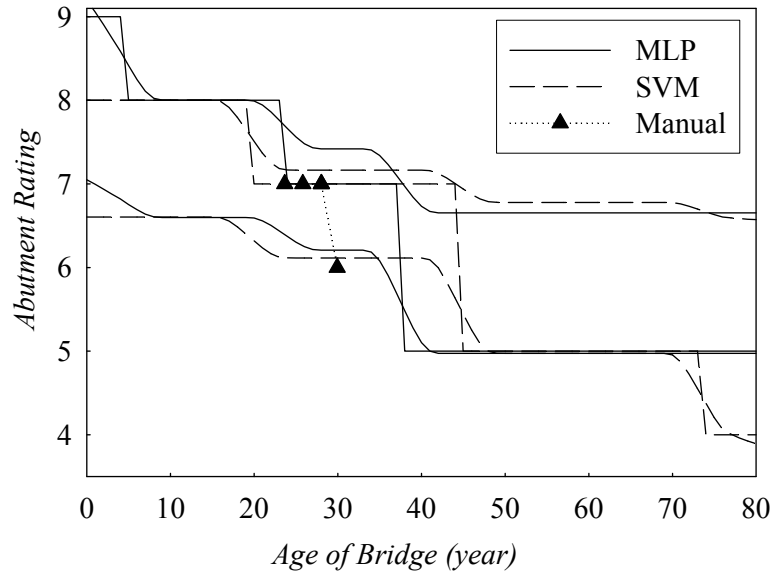
Figure 6-6 Abutment Deterioration Curve for Bridge A 1.5

Table 6-3 Confidence level of the confidence bands of the MLP and the SVM

Predicted value	0	2	3	4	5	6	7	8	9
MLP(%)	100	47.8	23.0	49.0	49.4	94.3	70.6	93.0	70.4
SVM(%)	5.6	72.7	58.6	46.8	49.9	94.1	82.8	87.6	20.5

It should also be noted that not all the deterioration curves have the same shape as seen in Figure 6-6. The development of different degradation curves had shown that for some bridges abutment deterioration was predicted to occur earlier than others and/or degrade at different rates. There are also some deterioration curves looks weird. Further discussion about this issue can be referred to section 6.7.

6.4 Ensemble of Neural Networks

6.4.1 Introduction

In section 6.3, ANN models had been developed with reasonable abutment damage prediction accuracy. These models can hardly be further improved considering the difficulties with the database, such as the unbalanced distribution of inspection records and the subjectivity

of the manual inspection process (FHWA 2001). Data unbalance arises since the cases of severe damage are relatively rare in comparison with the large number of structures in relatively good condition. Regarding subjectivity, studies have shown that in the national bridge inventory (NBI) system (integer rating scale of 0 to 9), ratings at the same structure assigned by 49 bridge inspectors from 25 state departments has a 68% possibility to be in a ±1 interval around the mean and 95% when the interval expands to ±2 (Phares et al. 2001). Even if all the bridges with the same design parameters were inspected by the same engineer, the ratings might still be different because construction quality, traffic and environmental conditions can not be identical. In addition to unbalance and subjectivity, relationships between variables in maintenance databases are highly nonlinear and the values of some variables in some observations are missing or subject to human error.

An *ensemble* of networks was thus explored to overcome the obstacles in the database and establish damage prediction models with improved accuracy. The concept of combining estimators to achieve better performance has been applied in a variety of fields for some time (Sharkey 1999). Hansen and Salamon (1990) proved theoretically and experimentally that an ensemble of neural networks can improve prediction accuracy. They also proposed several ways of voting for the ensemble and concluded that the ensemble of neural networks performed better than individual neural networks. Hansen et al. (1992) applied neural network ensembles in the recognition of handwritten digits and demonstrated that an ensemble of networks outperformed the best individual network in the ensemble by 20 ~ 25%. Zhou et al. (2002) applied neural network ensembles in lung cancer cell identification. Images of specimens were used as input and cancer diagnoses were used as output. By using the 'bagging' approach in data organization and two stages with full voting in the first stage, network ensembles were shown to have better performance than individual networks. Yun et al. (2003) and Lee et al. (2004) applied an ensemble of neural networks for structural health monitoring. Modal parameters were used as input for the network and element level damage indices were used as output. The ensemble of networks was found to significantly improve the identification of damage. In predicting market clearing prices, Guo and Luh (2004) proposed an ensemble of networks using a weighted voting scheme which outperformed both individual neural network and an ensemble of networks using ensemble-averaging voting.

The ensembles of neural networks listed above had good performance in their areas of application; however, none of them was developed based on a highly unbalanced database. For this research, a novel training data organization strategy was devised through bagging within categories to overcome the unbalance in training data. Modified majority voting, subjectivity voting, and evaluation voting schemes are proposed to address the subjectivity in training data. The ensemble of networks using the novel data organization strategy and voting schemes was developed and shown to predict bridge abutment damage in the State of Michigan with an accuracy of 81% to 86%, which is 13% ~ 18% higher than the best individual neural network in the ensemble.

6.4.2 Ensemble of Neural Networks

An ensemble of neural networks is a set of individually trained neural networks, from which predictions for novel inputs are obtained through the combination of individual predictions by certain voting schemes (Opitz and Richard 1999). The diagram of an ensemble of networks is shown in Figure 6-7. In this research, neural networks in the ensembles were multilayer perceptrons with a back propagation algorithm (section 6.2).

The performance of network ensembles is expected to be better when the errors of the individual networks in the ensemble are more independent (Hansen et al. 1992, Sharkey 1999). Kolen and Pollack (1990) demonstrated that back propagation is sensitive to initial conditions. The effects of variation in initial conditions to the generalization of the network are not likely to be as significant as the variation of training datasets (Sharkey 1999). In this research, both the training datasets and the initial weights are different for different neural networks in an ensemble.
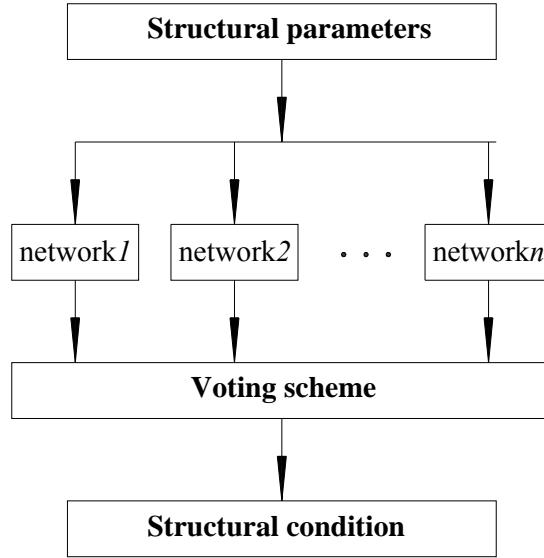
Figure 6-7 Diagram of ensemble of MLPs

6.4.2.1 *Data Organization*

The principal motive for devising a novel data organization scheme is to overcome the unbalanced distribution of structural inspection records in the database, which is a challenging issue for an individual network. Two major approaches to organizing datasets are *bagging* (Breiman 1996; Duda et al. 2001; Sharkey 1999) and *boosting* (Duda et al. 2001; Schapire 1990). Bagging is a procedure to produce multiple training sub-sets by drawing samples randomly from the original training set with replacement. Boosting is a procedure to produce multiple training sub-sets in a manner that the subsequent selection is focused on the samples that are not recognized well by the classifiers training on the previous training sub-sets. Compared with boosting, bagging has been proven more resilient to noise (Opitz and Maclin 1999; Quinlan 1996), which is also a major difficulty in using a structural inventory system database. Bagging is effective in making a full use of small datasets; and Breiman (1994 1996) proved that bagging can improve the accuracy of unstable prediction models, such as neural networks.

In this research, the concept of bagging was applied after modification—bagging within each structural condition to alleviate the difficulty of rare damage records. Each network in the ensemble was trained by a different dataset. Each data set contained the same number of records (n_1) for each structural condition and these n_1 records were randomly selected from each category with replacement. As a result, the training set for each individual network was balanced

and different from each other and the errors of these networks had some degree of independence. The procedure of bagging within categories is schematically shown in Figure 6-8.
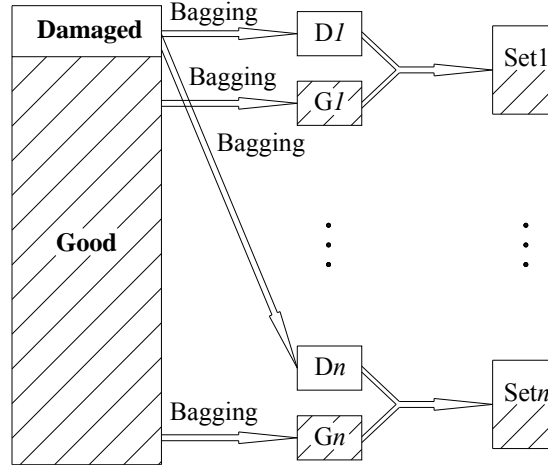

Figure 6-8 Data organization scheme

6.4.2.2 Voting Scheme

Voting scheme refers to the way to combine the individual answers of the neural networks to reach a final prediction by the ensemble. The voting schemes applied in this research were:

(a) Plurality Voting: The final prediction of the ensemble is the one that receives more "votes" from individual networks than the other possible predictions.

(b) Modified Majority Voting: In a majority voting scheme, the final prediction of the ensemble is the one that receives more than half of the votes from individual networks. In this research, a *modified* majority voting scheme was applied. If no structural condition obtains more than half of the votes, the prediction will be the worst structural condition that receives more than a quarter of the votes. If no structural condition obtains more than a quarter of the votes, the prediction will be the worst structural condition that receives more than the average number of votes.

(c)Weight Voting: Weights are assigned to neural networks in the ensemble based on the mean square error in their training phase. As such, a larger training mean square error results in a lower weight for that neural network. The votes are multiplied by the corresponding weights before added to the collection boxes.

(d) Subjectivity Voting: This voting scheme takes into account the subjectivity of the manual inspection ratings. When an individual network "decides" that the structural rating is x, the voting scheme recognizes that there is a possibility that the actual rating is $x+1$ or $x-1$, and with a smaller possibility for $x+2$ or $x-2$. As shown in Figure 6-9, in a 0-9 rating scale, when a network in the ensemble predicts "7", the count for "7" will be increased by 0.7. Counts for "5", "6", "8", and "9" will be increased by 0.02, 0.08, 0.16, 0.04, respectively, based on the subjective bias trend (FHWA 2001).

(e) Evaluation Voting: Instead of combining the predictions of some individual neural networks, the evaluation voting scheme takes into account the values of all output neurons of the networks in the ensemble. For output neurons that represent the same structural condition in different neural networks, their values were summed to obtain a probability value for that structural condition. The structural condition that has the highest probability value will be the prediction of the ensemble.
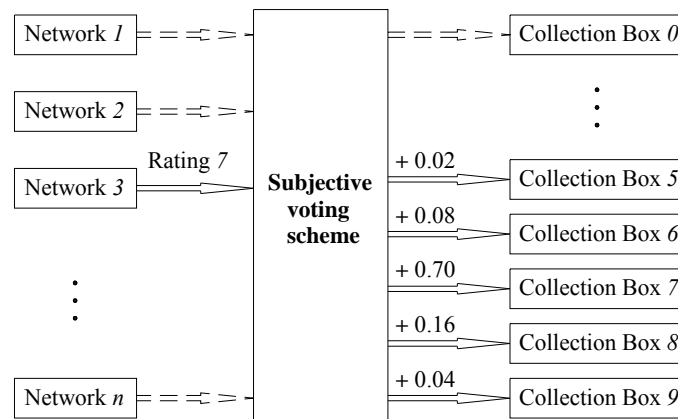

Figure 6-9 Example of subjectivity voting scheme

6.4.2.3 *Performance Indicator*

In addition to DIR, a false alarm ratio (FAR) was used as an indicator to evaluate the performance of prediction models. FAR is defined as the ratio of 'good structures' identified as damaged to all 'good structures'. Because failure to identify a damaged structure will have a more serious impact than identifying a good structure as damaged, the philosophy in developing a structural damage prediction model should be to increase the DIR as much as possible without

raising the FAR too much. In this study, the criterion to evaluate the prediction models was the difference between the DIR and half of the FAR.

6.4.3 Application

6.4.3.1 Ensemble of Networks

The structure of each individual neural network can be referred to Figure 6-2, the parameter values were: *p=13, n=50,* and *r=8.* One third of the records in each abutment rating category were selected and combined as test data; the remaining records were used as training data. Only 59 records showed an abutment rating of "9" in the training data. Thus, all of them were used in the composition of training sets for every individual neural network. For records with other abutment rating values, 200 were selected from each rating category through a bagging procedure to be combined to form one individual training dataset. In the training of individual networks, the mean square error and the maximum number of epochs to stop were set at 0.15 and 10000, respectively. A neural network was excluded from the ensemble when its mean square error from the training phase was greater than 0.25.

6.4.3.2 Evaluation of Voting Schemes

The weight w_i for the *i*th network in the weight voting scheme was calculated as:

$$w_i = \sqrt{2.5 - 10 \times mse_i} \qquad \text{(6-1)}$$

where, mse_i is the mean square error of the *i*th network in the training phase. It was mentioned in the report of Federal Highway Administration (2001) that there is a tendency to assign a rating lower than it should be for structural members with good condition, similarly, the tendency to assign a rating higher than it should be for structural members with poor condition also exists. The collection algorithm for the subjective voting scheme considering these subjective tendencies is shown in Table 6-4. The values in the individual cells of the table mean that when the network predicts the rating in the row title the collection box in the column title will be increased by that value. The DIR and FAR were calculated with Equations (4-2) and (4-3), respectively:

$$DIR = \frac{n_{id}}{n_d} \times 100\% \qquad \text{(6-2)}$$

$$FAR = \frac{n_{fd}}{n_g} \times 100\% \qquad \textbf{(6-3)}$$

where, n_d is the number of records in which the *abutment rating* from the manual inspection was "3" or "4;" among the n_d records, n_{id} is the number of records in which the predicted rating was also "3" or "4;" n_g is the number of records in which the *abutment rating* from the manual inspection was greater than "5;" among n_g records, n_{fd} is the number of records in which the predicted rating was "3" or "4."

Table 6-4 Collection algorithm for subjective voting

Prediction	Collection box						
	3	4	5	6	7	8	9
3	0.9	0.08	0.02				
4	0.15	0.8	0.04	0.01			
5	0.04	0.16	0.7	0.08	0.02		
6		0.04	0.16	0.6	0.16	0.04	
7			0.02	0.08	0.7	0.16	0.04
8				0.01	0.04	0.8	0.15
9					0.02	0.08	0.9

The DIR and FAR values versus the number of neural networks in the ensembles for different voting schemes are plotted in Figure 6-10 and Figure 6-11, respectively. From these figures, it can be seen that the performance of the ensemble of neural networks improves with the increase of numbers of networks in each ensemble up to a size of 50 to 60. No significant improvement is observed after the number of networks in the ensemble exceeds 60.
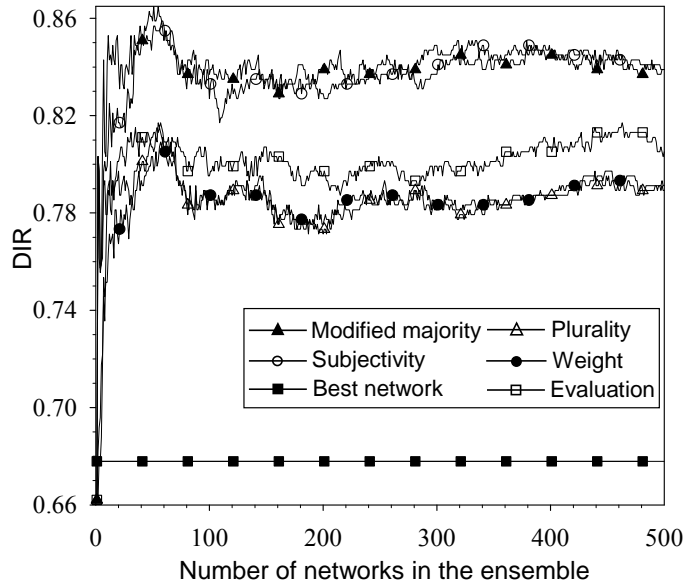
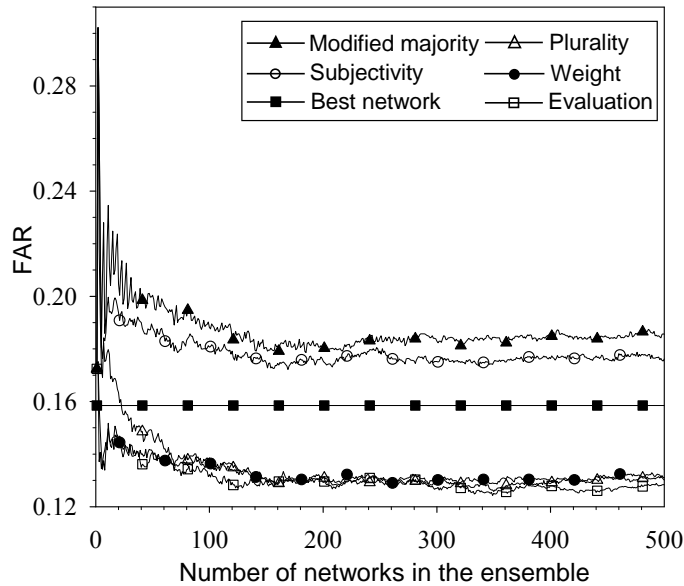**Figure 6-10 DIR versus number of networks in committee machine**

Figure 6-11 FAR versus number of networks in committee machine

The performance of the best ensemble of neural networks using different voting schemes is shown in Table 6-5. It can be seen from Table 6-5 that the modified majority voting scheme reached the highest DIR, followed by the subjectivity voting scheme. The evaluation voting scheme had the lowest FAR and decent DIR, outperforming both weight and plurality voting scheme for both indicators.

Table 6-5 Evaluation of different voting schemes

Voting scheme	Number of networks	DIR	FIR	Indicator
majority	51	86.48%	19.89%	0.7654
Subjectivity	58	85.88%	18.78%	0.7650
Evaluation	463	81.71%	12.77%	0.7532
Plurality	56	81.51%	14.54%	0.7424
Weight	59	81.11%	13.90%	0.7416

6.4.3.3 Bridge Abutment Deterioration Curves

To illustrate the use of the ANN ensemble in developing life-degradation curves, an ensemble of 51 networks using a modified majority voting scheme was applied to predict the abutment condition of an existing continuous steel bridge. The abutment deterioration curve of the bridge is shown in Figure 6-12. A confidence band was evaluated through the confusion matrix (Kohavi & Provost, 1998) of the prediction model, which is shown in Table 6-6. The confidence level was 91.33% in the case abutment damage exists. The confidence level was 74.54% for 75 years life of the bridge.

In the development of Figure 6-12, the age span for the manual inspection rating is relatively short because manual inspections according to the NBI system started in Michigan in the early 1990s. This is another difficulty in the exploitation of structural inventory system database as it is very difficult to extrapolate structural member degradation trends from such a short span of manual inspection. Furthermore, a major part of the highway bridges in Michigan was built in 1960s and 1970s. Thus, most of these age spans were concentrated within 30 years, with very few inspections records for very "young" or very "old" bridges. Thus, the ensemble of neural networks anneals the information from different structures to predict the conditions of each structure in the future and retrieve the historical path of the development of structural damage in bridge abutment.

It should also be noted that not all the deterioration curves have the same shape as seen in Figure 6-12. The development of different degradation curves had shown that for some bridges abutment deterioration was predicted to occur earlier than others and/or degrade at different rates. There are also some deterioration curves looks weird. Further discussion about this issue can be referred to section 6.7.
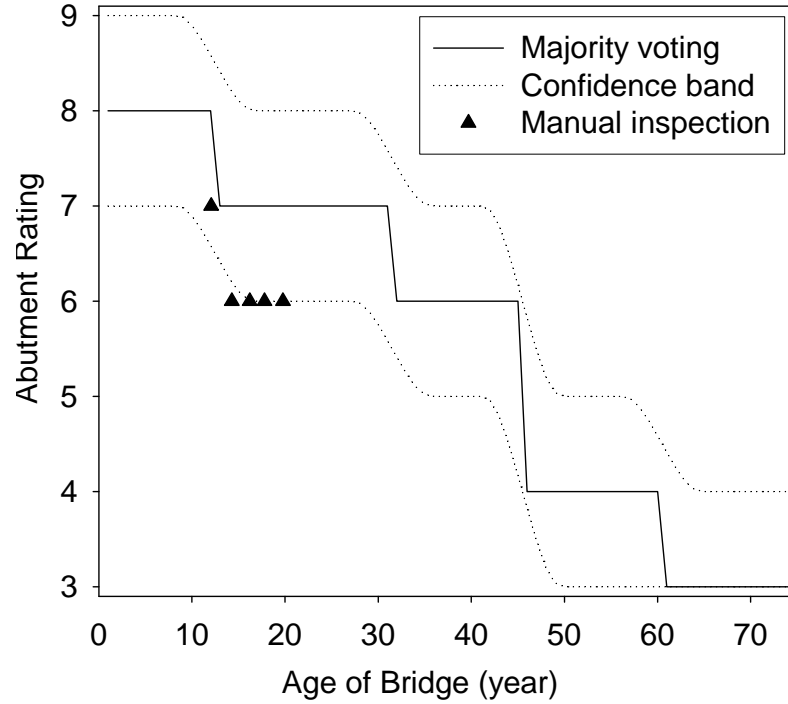
Figure 6-12 Abutment deterioration curve of a continuous steel bridge

Table 6-6 Confusion matrix of ensemble of neural networks using majority voting

Prediction	Manual inspection						
	3	4	5	6	7	8	9
3	141	54	94	159	295	14	3
4	24	216	127	226	325	35	2
5	8	26	243	279	430	34	3
6	7	11	60	470	556	55	2
7	1	4	26	130	1064	106	4
8	0	4	23	85	619	377	7
9	2	5	1	3	21	12	9

6.4.4 Analysis of Synaptic Weights

The synaptic weights between input layer and first hidden layer of MLPs in the ensemble of networks (refer to first layer of synaptic weights in Figure 6-2) were investigated in order to get some hints about the relative importance of input parameters to the abutment rating. There is no theoretical foundation for such an association between the values of synaptic weights and the

significance of input variables. The absolute values of mean synaptic weights were used as a reference for relative significance of input parameters for two reasons: first, the relationship between the explanatory variables and abutment conditions are highly complicated and no crystal clear relationship or one to one association can be derived for them. Secondly, the input variables were normalized before pass to the network in this research, some noisy factors such as scale were ruled out. The statistics of synaptic weights for all 51 networks in the ensemble were listed in Table 6-7.

Table 6-7 Statistics of synaptic weights between input layer and first hidden layer

Explanatory variables	Mean	Standard deviation	Importance rank
Bitumen Approach	0.05930	2.449	1
ADTT	0.04444	1.295	2
Concrete Approach	-0.04214	2.477	3
Mixed Approach	-0.03862	1.794	4
Temperature	0.03622	1.547	5
Prestressed concrete bridge with spread box girder	0.03099	1.791	6
Continuous steel structure	-0.03047	2.107	7
Simple/cantilever steel structure	-0.02706	2.126	8
Skew angle	0.02438	1.495	9
Deck width	0.01382	1.413	10
Prestressed concrete bridge with I girder	0.00745	2.115	11
Age	-0.00655	1.508	12
Length	-0.00652	1.463	13

It can be seen from Table 6-7 that three indicator variables for approach surface ranked 1st, 2nd, 4th respectively, indicate that the approach surface type is significant for the condition of bridge abutment. It is interesting to notice that the synaptic weights for bitumen approach was positive value, those for mixed or concrete approach pavement were negative value. The weight for concrete pavement was the least among the three, indicates that concrete approach pavement

might contribute to the low rating of bridge abutment. This conforms with the assumption that pavement pressure might lead to damage in bridge abutment wall. The inference here will be further referred in section 7.

6.5   Fuzzy Neural Network Model

An artificial neural network can map complicated input-output relationship and fuzzy sets can account for the subjectivity in manual inspection using vague decision boundaries. By combining them, a fuzzy-neural network was developed to predict structural condition using design and operation parameters. In the training phase, integer structural ratings were transformed to membership values of fuzzy sets; in the testing phase, predicted membership values were back transformed to integer structural ratings through another neural network. Samples that can be used in training the back transform neural network were limited and duplications and noise vectors were utilized to improve the generalization capacity.

A fuzzy set (FS) is a collection of members whose relationship with the set is defined by a membership function. The key feature of a fuzzy set is its continuous and gradual boundary, contrary to the rigorous and crisp boundary of an ordinary set. This feature is close to the thinking and decision making process of a human being (Zadeh 1965) and enables FS to address uncertainties in the database (Yao 1980). ANN and FS can be combined to develop a fuzzy-neural network (FNN) model (Jain & Martin 1999, Pal and Mitra 1999) to map a nonlinear relationship using a dataset with uncertainty and subjectivity.

Pal and Mitra (1992) applied an FNN in speech recognition and concluded that generally, the fuzzy-neural model performed better than conventional neural networks. Juang et al. (1999) applied an FNN to solve uncertainty in the input and output parameters in geotechnical problem and showed that FNN was superior to conventional neural networks. FNN was also applied in medical data (Mitra and Hayashi 2000). An FNN was used to predict wind-induced pressures on a large gymnasium roof and was found to outperform the conventional neural networks (Fu et al. 2007). Taha and Lucero (2005) used fuzzy sets with a wavelet-neural network in structural health monitoring using dynamic response variables and identified damage accurately.

6.5.1 Fuzzy Sets

Fuzzy sets are often defined by linguistic variables (Zadeh 1975, 1994). The value of membership function of a linguistic variable signifies the degree to which the output belongs to that linguistic variable. The value of membership function is in the range of [0, 1], where 1 means the highest degree of membership and 0 means lowest degree. Thus, a membership function enables FS to account for the imprecision or subjectivity exists in real world problems.

FS is a suitable tool for damage assessment of structures considering the subjectivity of manual inspections and the large variance in structural ratings. Transforming discrete integer ratings to continuous membership values of linguistic variables, such as *"damged", "poor", "moderate", "good", and "excellent"*, can reflect the thinking process of structure inspectors better than discrete integer ratings. It is more reasonable to use these linguistic variables as the output variable of an ANN.

Gaussian function was used as the membership function of the FS as shown in Figure 6-13. The activation function used in the ANN was sigmoid function, it was most effective when the input values is distributed in the range [-1, 1]. Values of membership functions were transformed to range [-1, 1] by multiplying by 2 and subtracting 1, as shown in Figure 6-14.
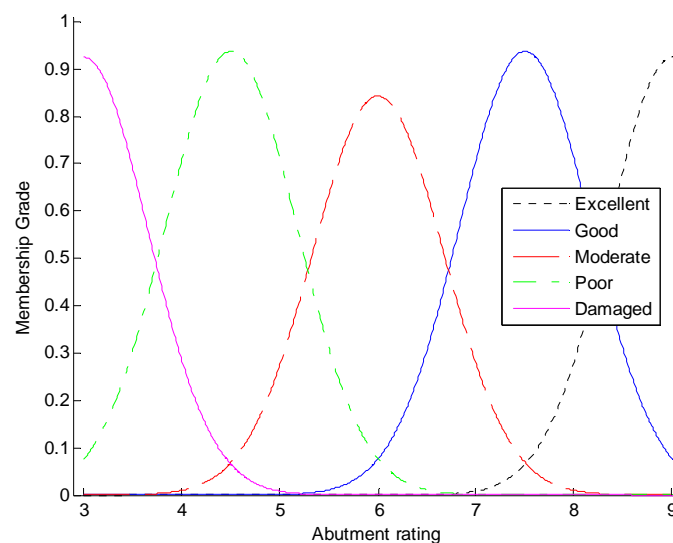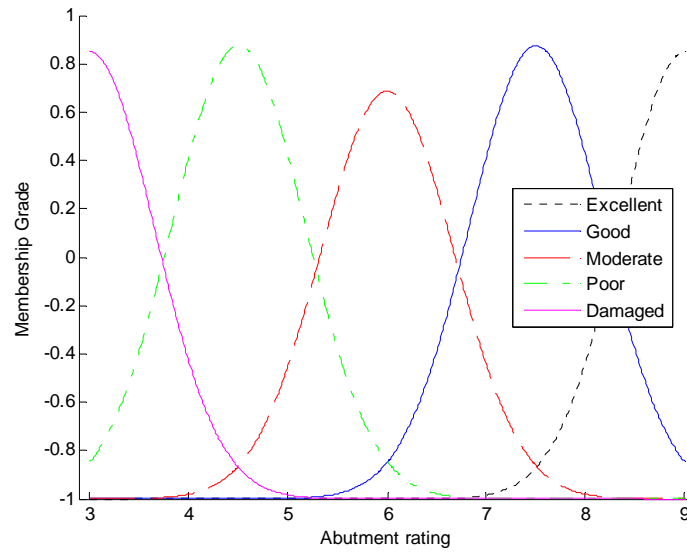

Figure 6-13 Membership function of fuzzy sets

Figure 6-14 Membership function of fuzzy sets after modification for ANN

6.5.2 Fuzzy-Neural Network

An FNN can be developed by incorporating a fuzzy output processing module into a conventional neural network, as shown in Figure 6-15. The ANN in an FNN will use the membership values of linguistic variables as outputs.
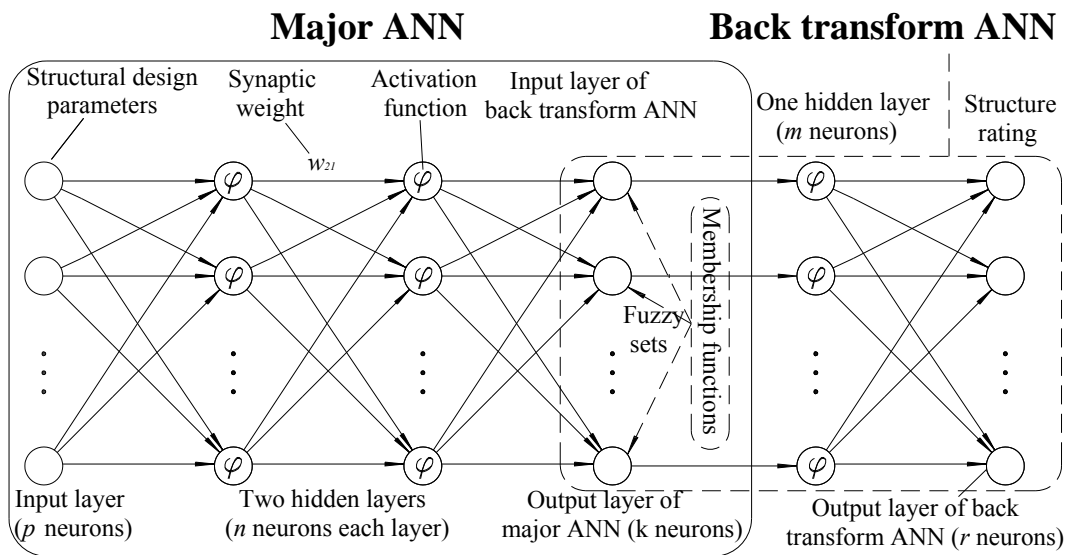

Figure 6-15 Schematic of an FNN model

A fuzzy output transform module includes two transformation processes. One process is to transform "vague" structural rating into "linguistic" variables to serve as output variables in the training of MLP ANN. The other process is to transform the "linguistic" output of the MLP ANN back to the form of structural ratings that directly indicate conditions of structures in prediction phase. Another MLP ANN model needs to be developed for this back transformation.

The structure of the ANN can refer to Figure 6-15, the parameter values were: *p=13, n=145,* and *k=5.* One third of the records in each abutment rating category were picked out and combined as test data; the remaining records were used as training data. If the number of remaining records in any category was larger than 1500, those extra records were excluded from the training data to ensure some extent of balance. In the training of the neural network, the mean square error and the maximum number of epochs to stop were set at 0.05 and 30000, respectively.

6.5.3   Back transforming scheme

Sparseness of training points was a major difficulty in the development of a neural network to transform membership values of linguistic variables back to structural ratings. For instance, 7 integral structural ratings were transformed to five linguistic variables in the training of the neural network, only 7 known points (7 integral ratings) were available in the 5 dimensional spaces (5 linguistic variables) in the training of the back transform ANN. Neural network can not be properly trained using such sparse training data. By duplicating each training point and adding a random noise vector to each of the duplications, the 7 known points would be expanded to 7 spheres of points, and, thus, cover the space better and improve the generalization of the back transforming ANN. The magnitude of the random noise to reach the optimal generalization depended on the distance of the training points, structure of neural networks, etc. The ratings that showed structural damage were duplicated more than the other ratings to improve the chance of identifying structural damage after processed by fuzzy transform module.

The structure of back transformation MLP ANN had 1 hidden layer, refer to Figure 6-15, k=5, m=100, and r=7. In the training of back transformation module, 9400 vectors were included in the training dataset, for abutment rating 3 and 4, there were 4200 vectors for each of them, for

ratings 5-9, there were 200 vectors for each of them. The components in the random vector were random values in the range of [-0.1, 0.1]. The mean square error and the maximum number of epochs to stop training were set at 0.02 and 1000, respectively.

6.5.4 Results

The DIR and FAR of the fuzzy neural network were 82.31% and 14.61%, respectively. Comparing with the DIR and FAR of a conventional MLP ANN, which are 65.84% and 2.65%, respectively (section 6.3), FNN model gain a 16.47 % improvement of DIR at the cost of 11.96 % increase of FAR. The confusion matrix of the fuzzy neural network is shown in Table 6-8. It can be seen from Table 6-8 that the FNN model can identify damage in bridge abutments well. It should also be pointed out that the model can not give a prediction of the rating "5". This might be caused by the noise vectors adding in the training of the back transformation model. It can also be noticed that most of the test patterns with manual inspection rating "5" were predicted as "4" or "6". The deviation was acceptable considering the large variance of manual inspection.

Table 6-8 Confusion matrix of FNN

Prediction	Manual inspection						
	3	4	5	6	7	8	9
3	110	34	46	60	150	11	0
4	52	218	235	191	319	45	2
5	0	0	0	0	0	0	0
6	18	50	213	877	1134	170	8
7	2	13	77	216	1604	319	11
8	0	2	3	6	100	81	7
9	1	3	0	2	3	7	2

6.5.5 Bridge Abutment Deterioration Curve

The FNN model was applied to predict the abutment condition of one prestressed concrete bridge in the State of Michigan. Its abutment deterioration curve is shown in Figure 6-16. A confidence band was evaluated through the confusion matrix of the prediction model (Table 6-8). The confidence level was 82.3% in case abutment damage exists and 81.4% for 75 years life of the bridge. It should also be noted that not all the deterioration curves are in the exactly same shape as Figure 6-16. Some bridge abutments deteriorated at an earlier time than others, some of them degraded faster than others, some of them show peculiar trends due to the improper prediction of the model or the inherent difficulties in the structural inventory database. Further discussion about this issue can be referred to section 6.7.
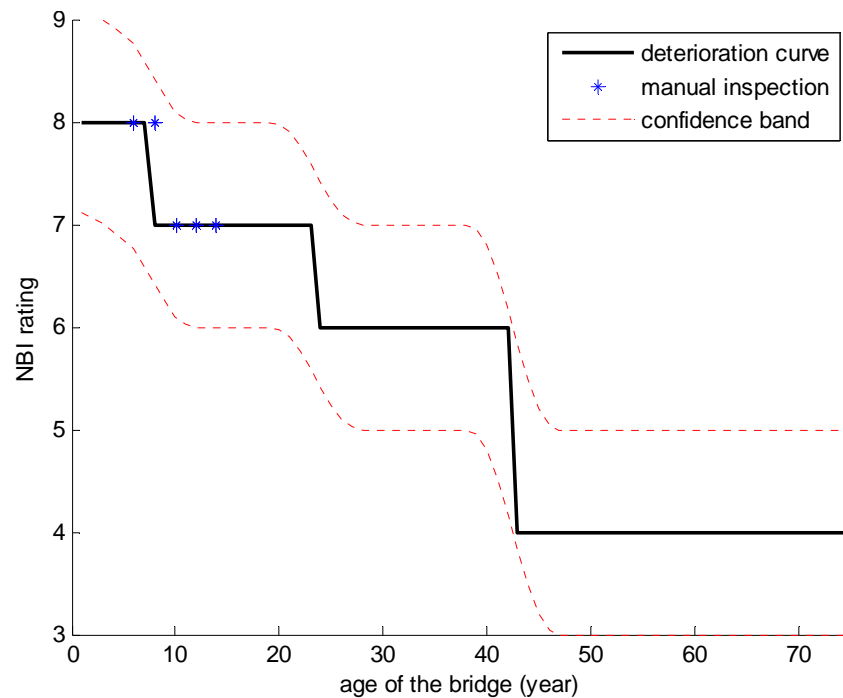
Figure 6-16 Abutment deterioration curve of a prestressed concrete bridge

6.6 Software Development: Bridge Abutment Damage Diagnosis (SbNet)

The computer program, named Bridge Abutment Damage Diagnosis (SbNET), was developed for MDOT engineers to predict the condition of bridge abutment wall given design parameters. SbNET is a stand-along executable compiled from Matlab codes and pre-trained ensemble of networks described in section 6.4. After the analysis and evaluation of stepwise deterioration curves derived using ANN models, it was found that most of them can be approximated by logistic curves. Thus, SbNET provides has the option of providing deterioration curves according to the discrete solution from the ANN ensembled (termed "exact" in the program) or fitted to logistic curves using function (6-4) using Matlab's curve fitting toolbox. SbNET can make predictions either using design parameters for bridges in design or by MDOT Bridge ID for existing bridges. The output of SbNET including: bridge deterioration curve, predictions saving in txt files, the bridge abutment rating given the age of the bridge. Deterioration curves for the bridge abutment wall of a continuous steel bridge are shown in Figure 6-17. The SbNET User's Manual can be referred to Appendix F.

$$f(x) = a \cdot \frac{1 + m \cdot \exp\left(\dfrac{b-x}{t}\right)}{1 + n \cdot \exp\left(\dfrac{b-x}{t}\right)} \tag{6-4}$$
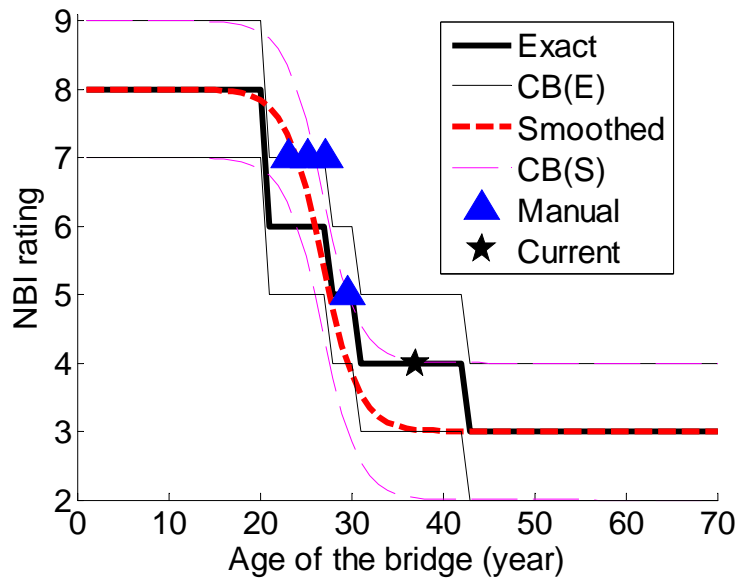

Figure 6-17 Deterioration curve of bridge 82182104000S070

6.7 Discussion

Four major types of neural network models were developed to predict the abutment condition based on manual inspection database. MLP and SVM showed reasonable accuracy. In order to overcome the unbalance and subjectivity of manual inspection database, ensemble of neural networks and fuzzy-neural networks were applied.

An ensemble of neural networks with novel voting schemes was applied to improve the identification of damage in bridge abutment. The unbalance of structure inspection databases was overcome by organizing the training data using bagging within each structural condition. Several new voting schemes were devised; with modified majority voting, subjective voting, and evaluation voting schemes showing good performance. The damage identification ratio of an ensemble of networks reached 81% to 86%, which exceeded the best individual networks in the ensemble by 13% to 18%. The ensemble of networks obtained optimal or close to optimal performance when 50 to 60 neural networks were included in the ensemble. An ensemble of neural network was the optimal prediction model derived through this research for the prediction of highway bridge abutment condition.

Previous research (Freund and Schapire 1996; Quinlan 1996; Opitz and Maclin 1999) has shown that most of the improvement in performance is achieved with the first few (10 to 25) additional classifiers (i.e., neural networks). For the structural damage prediction problem, a similar trend exists except that considerably more networks are needed to achieve most of the improvement. The reason for this difference is the characteristics of the presented problem of abutment damage prediction and the corresponding bridge inventory database. In order to obtain a balanced training dataset, a small part of the records showing good structural condition were selected in each round of bagging. Consequently, more networks are needed to "learn" most of the knowledge from the records with good structural conditions.

A fuzzy neural network was developed to identify damage in bridge abutment. A fuzzy transform module was designed to alleviate the negative effect of subjectivity in manual inspections by using linguistic variables and membership functions instead of integer structural ratings. Gaussian function was used as the membership function of the fuzzy sets. In the training of back transform network of the fuzzy transform module, the sparseness of the training dataset was alleviated by duplicating the training data and adding noise to the duplications. The accuracy

in identifying structural damage is improved by focusing on damage patterns in the training of back transform network. An FNN model was used in predicting structural damage in abutment walls of highway bridges in State of Michigan. The DIR of the FNN model reached 82.31%, which exceeded the conventional network by 16.47 %.

It was proposed to combine the manual inspection data (evidential data), finite element simulation data (virtual data) and field instrumentation data (dynamic data) in the training of the neural network, efforts had been made in this work; however, the improvement of the network can not be improved by this approach for the following reasons:

➢ A large gap existed between the explanatory and response variables of the evidential database and virtual database. The virtual database only simulated the behavior of bridge using in the perspective of mechanics, most of the explanatory variables for were bridge design parameters. On the other hand, evidential database recorded the life of bridge in all aspects, mechanics, environmental, human behavior, etc., its explanatory variables included not only design parameters, but also operation and environmental factors. The response variables of virtual database were stresses and strains in the structure; the response variables of evidential database were subjective manual inspection ratings.

➢ The dynamic database is too sparse: only four bridges were instrumented, the information of dynamic database will be drowned in the sea of evidential database.

➢ In dynamic database, the variable derived from field data was horizontal strain in the abutment wall, which was also different from those of evidential database.

Considering the prediction model using the ensemble of networks had good performance, no further trials in the combining of databases were made.

The computer program SbNET was developed to help MDOT engineers in maintenance of existing bridges and designing new bridges. It was based on a well-trained ensemble of neural networks and was able to predict bridge abutment condition given design parameters or MDOT Bridge ID. SbNET can be a promising diagnostic tool as maintenance and repairs can be more efficiently managed with reliable prediction of future structural conditions and its deterioration

trend. The software can also be used as a predictive tool for new designs and to evaluate and compare the life-time performance of abutment damage for different bridge design options.

Due to the inherent difficulties in the manual inspection database, not all the deterioration curves show a clear and reasonable trend as shown in Figure 6-17, even though the optimal tool for the problem had been developed to its best performance. Examples of deterioration curves that are not as good are shown in Figure 6-18. For bridge 67167017000S050 the deterioration curve has a long flat range before major distress is predicted. It can also be seen that the deterioration curve matches the manual inspection records well. It may be inferred that this bridge was well design and maintained, and that no major environmental or operational factors will cause its abutment walls to deteriorate seriously before 40 years of service. The deterioration curve for Bridge 23123151000S020 has a "bump" in the middle. It can be seen from the figure that the deterioration curve matches the manual inspection records well before the bump occurs. Probably, the bump occurs because the ensemble of neural networks did not generalize that pattern well. The deterioration curve looks reasonable if the bump point is removed. For Bridge 82182191000S020, the deterioration curve predicted by the ANN network is very strange, predicting that the condition of the bridge abutment walls will deteriorate dramatically after 20 years of their service and that then, after remaining in a poor condition for 23 years, the abutment walls of the bridge will be restored into fair condition. Two sources might contribute to the obviously unfeasible shape of the predicted deterioration curve. One source is that the ENN does not generalize the patterns well enough and thus make a wrong prediction. Another reason is that highway bridges are often repaired and the abutment walls are restored to good condition after damage is observed. The prediction model also incorporated the records of restored abutment walls into the prediction model. Thus, the ENN may have learned some of these patterns.
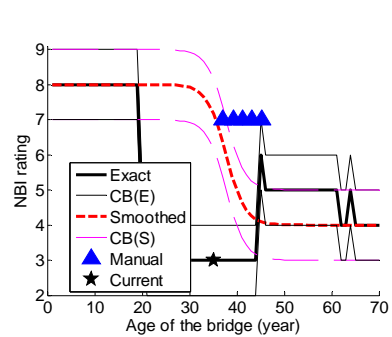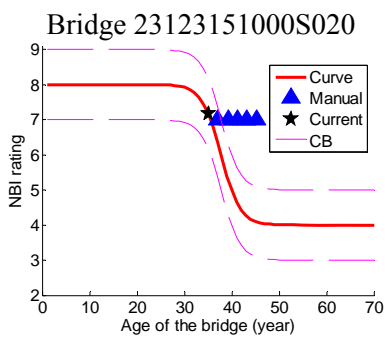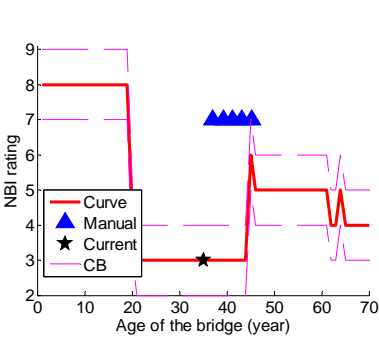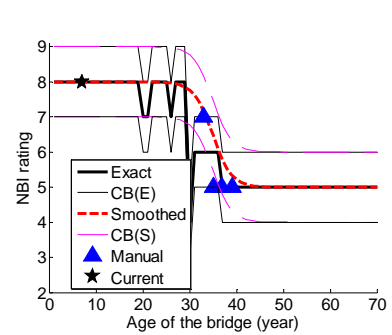
Integer (Exact) Predictions
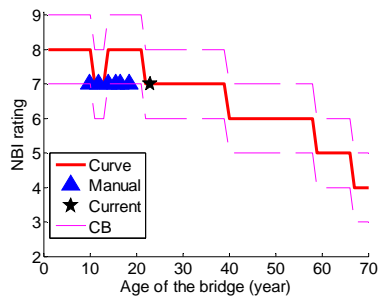
Logistic Fitted Curve
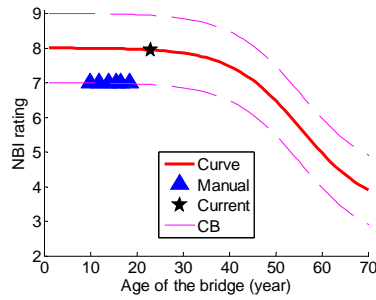
Integer and Logistic Curves

Bridge 67167017000S050
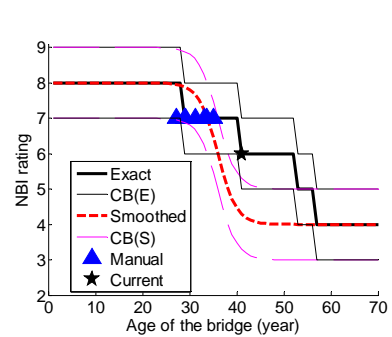

Bridge 12112033000S040

Bridge 23123151000S020
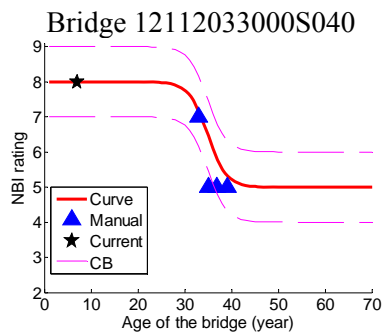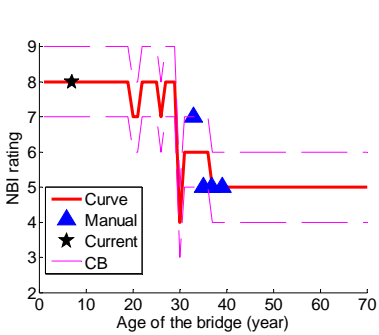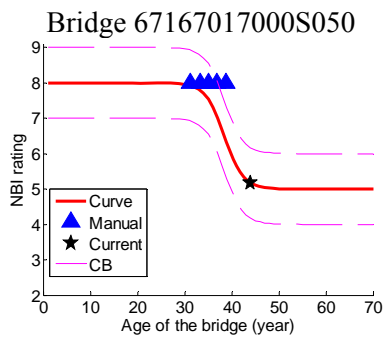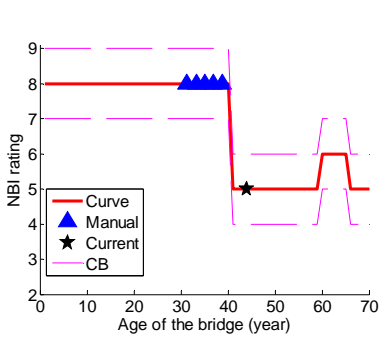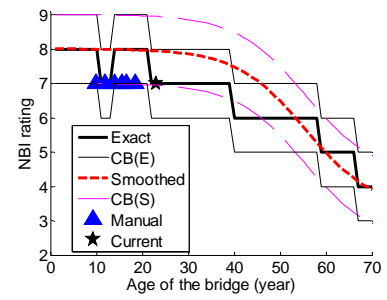
Bridge 82182191000S020

Figure 6-18 Deterioration curves

7 Potential Causes of Abutment Damage and Distress Relieving Strategies

7.1 Introduction

One of primary goals of this research was to identify the potential causes of abutment damage in highway bridges. All five major research efforts described in sections 2, 3, 4, 5, and 6 contributed to this goal. Three major causes of bridge abutment damage are listed here according to their significance: Pavement pressure, transverse temperature effect, and longitudinal temperature effect. The evidenced for the identification and methods to alleviate the abutment damage are presented in the following sections.

7.2 Pavement Pressure

7.2.1 Description

The mechanism of pavement pressure generation was explained in detail by Burke (1998, 2004). The pavement pressure passed to the abutment wall through bridge superstructure and induced damage as shown in Figure 7-1.

7.2.2 Evidence

7.2.2.1 *Evidence A: comparison of different bridges*

The conditions of two abutment walls for one bridge (Bridgekey 82182194000S150) were found to be different from each other significantly during the field inspection in summer 2006. The west abutment was rated as "7" (Figure 7-2), its approach ended by a "T" intersection nearby (Figure 7-3), little pavement pressure can be accumulated. The east abutment was rated as "3 or 4" (Figure 7-4), its approach extended to a road (Figure 7-5), very large pavement pressure can thus be generated along the pavement of the road.

7.2.2.2 Evidence B: investigation of different structural members of the same bridge

Bridge 82182291000S110 had distress in the abutment wall (Figure 7-6), the approach pavement of the bridge was concrete (Figure 7-7); a large pavement pressure could be accumulated in them. The pin and hanger assembly is fine (Figure 7-8), thus, only small forces can be transferred to the abutment wall through longitudinal temperature effects of the bridge super structure.
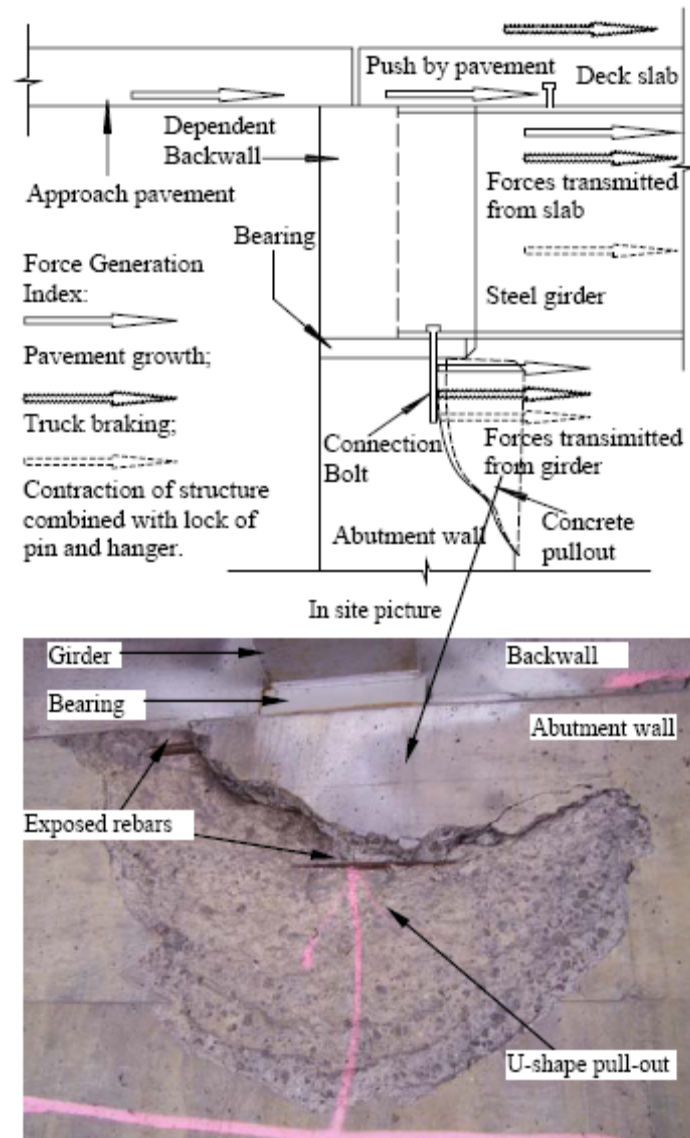
Figure 7-1 Concrete pullout caused by pavement pressure

Figure 7-2 West abutment of bridge B 1.2

Figure 7-3 West approach pavement of bridge 82182194000S150

Figure 7-4 East abutment of bridge 82182194000S150

Figure 7-5 East approach pavement of bridge 82182194000S150

Figure 7-6 Abutment distress in bridge A 1.7

Figure 7-7 Approach pavement of bridge A 1.7

Figure 7-8 Pin and hanger assembly of bridge A 1.7

7.2.2.3 Analysis of synaptic weights of artificial neural networks

Referring to section 6.4.4, the absolute value of synaptic weights of three indicator variables for approach surface ranked 1st, 2nd, and 4th, respectively, in Table 6-7, indicated that the approach surface type was significant for the condition of bridge abutment.

7.2.2.4 Analyses of field instrumentation

The analyses of field instrumentation results indicate that the horizontal strain in the bridge abutment wall related to the longitudinal movements of girders; however, temperature effects can only explain these movements for part of the bridges. Pavement pressure had a high chance to induce the longitudinal movement of girders together with temperature effects.

7.2.3 Alleviation strategies

7.2.3.1 Flexible approach pavement

Flexible approach pavement such as bitumen can reduce the pavement pressure significantly. Statistical analyses also showed that bridges with bitumen approach slab surface have less abutment distress than bridges with other pavement surface.

7.2.3.2 Pressure Relief Joints

Pressure relief joints (Burke, M. P., Jr. 1998, Smith et al. 1987) is a transverse joint designed to relieve the stress in the pavement, and, thus, the pressure accumulated and passed to the abutment wall can be alleviated by introducing relief joints the pavement close to the bridge.

7.2.3.3 Improve sealing of expansion joints

The contamination of expansion joints is a major reason for the generation of pavement pressure (Burke 2004). Prevention of the contamination of joints by improving the sealing can be helpful in alleviating the pressure in pavement and thus protecting the bridge abutments.

7.3 Transverse Temperature Effect

7.3.1 Description

Transverse expansion of the super structure would induce vertical cracks in the abutment wall, as shown in Figure 7-9.
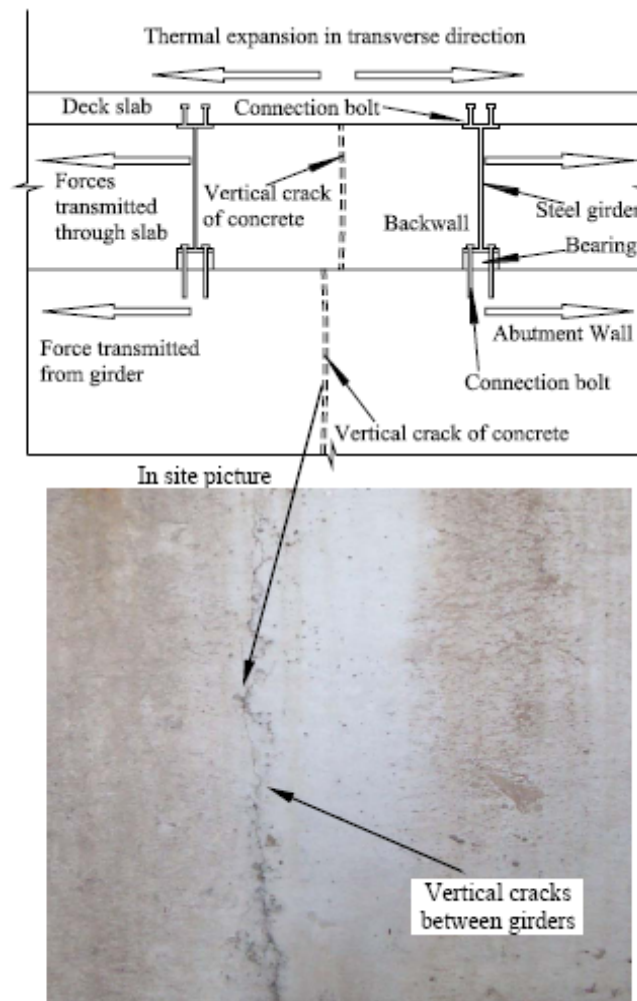

Figure 7-9 Bridge abutment damage with their possible causes

7.3.2 Evidence

7.3.2.1 In-site observation

Some of vertical cracks in the abutment wall were in the horizontal position between girders (Figure 7-10).
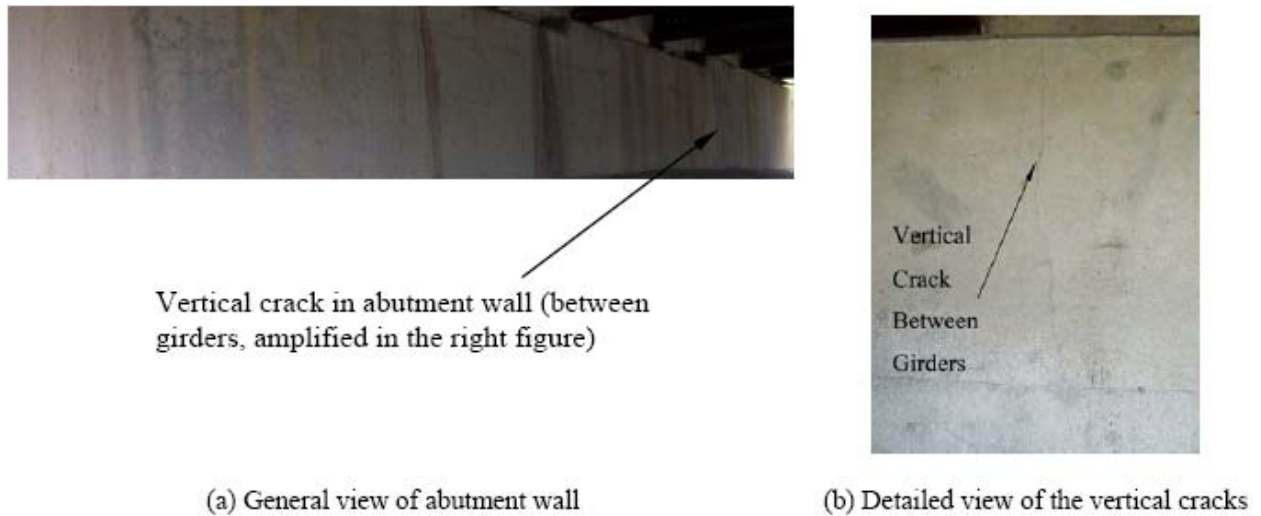
Figure 7-10 Overview and Close-up of Abutment Distress for Bridge A 1.4

7.3.2.2 Field instrumentation

It was found through the analyses of field instrumentation results that, in some spacing of some bridges, the variation of peak horizontal strains approximately match the change of girder spacings. For a few bridges, the girder spacing varied with the change of average temperature in the bridge deck.

7.3.2.3 Analyses of synaptic weights of artificial neural networks

Referred to section 6.4.4, the explanatory variable "temperature" ranked 5th in Table 6-7, indicated that temperature was significant for the condition of bridge abutment.

7.3.3 Alleviation strategy

7.3.3.1 Expansion bearings

Elastomeric expansion bearings can be helpful to reduce the transverse force passed through super-structure to the abutment wall.

7.3.3.2 Contraction joints

It was noticed during the process of field measurement that the vertical cracks occurred in the part of abutment wall where no contraction joint existed for long span. Provide contraction joints in the abutment wall would be helpful in reducing vertical cracks. It was suggested to place thin joints at frequent intervals rather than use thick joints at large intervals.

7.3.3.3 Small skew angle

It was found through finite element simulations that in most cases, stresses and strains in bridge abutment walls increased with the increase of skew angle. The increase was faster when the skew angle exceeds 30º. It was suggested to keep the skew small in the design of highway bridges to alleviate the damage in the abutment wall induced by temperature as well as pavement growth.

7.4 Longitudinal Temperature Effect

7.4.1 Description

As shown in Figure 7-1, when the pin and hanger assembly of steel bridges were rusted and could not accommodate the longitudinal movement of the girder, longitudinal force would be generated at the bearings at then transmitted to the abutment wall.

7.4.2 Evidence

7.4.2.1 Finite element analysis

FEA Simulation showed that stresses to some magnitude can be generated in the abutment wall during temperature variation when the pin and hanger assembly were locked.

7.4.2.2 Field instrumentation

The evidences derived from the field instrumentation that support the assumption were as follows:

> On abutment wall and backwall, concrete in the vicinity of girder pull-out was subjected to tension and the concrete in the vicinity of girder push-in was subjected to compression.

> For some regions around girders of some bridges, the girder end movement varied reversely to the change of average deck temperature.

> Maximum and minimum horizontal strains in the region around girders changed with the longitudinal movement of girder ends for some cases.

7.4.2.3 Analyses of synaptic weights of artificial neural networks

Referred to section 6.4.4, the explanatory variable "temperature" ranked 5th in Table 6-7, indicated that temperature was significant for the condition of bridge abutment.

7.4.3 Alleviation strategies

7.4.3.1 Expansion bearings

Elastomeric expansion bearings can be helpful to reduce the longitudinal force passed through superstructure to the abutment wall.

7.4.3.2 Avoid pin and hanger assembly or keep them in good condition if used

Avoid using pin and hanger assembly in the design of bridges to reduce possible secondary stresses during the operation phase. Removing pin and hanger from bridges can also help to reduce the rust in other structural members. If pin and hangers are applied in the bridge, keep them in good condition so that it can accommodate certain longitudinal movement of the girder, and thus, reduce the stress induced in the abutment wall.

7.5 Discussion

Potential causes of abutment damage in highway bridges in State of Michigan were derived and proofed through the creation of information database, statistical analyses, field inspection and instrumentation, finite element analysis, and artificial neural network simulation. They were

listed in the order of relative significance as: pavement pressure, transverse temperature effect, and longitudinal temperature effect.

The strategies proposed to alleviate abutment damage included:

> Use flexible approach pavement;

> Add pressure relief joints for existing bridges with rigid approach pavement;

> Improve the sealing of expansion joints in approach pavement;

> Use expansion bearings at the abutment wall;

> Use small skew angle for new bridges;

> Avoid using of pin and hanger assembly or keep them in good condition if used.

8 Summary and Conclusions

In order to indentify the causes of bridge abutment damage, suggest alleviation strategies, and develop prediction tools; a series of analyses, simulations and investigations were performed in this research. Information database was initiated at the beginning stage of the study and was further supplemented and completed with the progress of the research. The conclusions of this research were based on statistical analyses, field instrumentation, finite element simulation and parametric study, artificial neural network simulation, and engineering analyses and judgment.

At the completion of this study, major conclusions can be summarized as:

➢ Potential causes of bridge abutment damage and their relative importance;

➢ Strategies to alleviate structural distress in bridge abutments;

➢ Diagnostic models and compiled prediction software developed based on the application of artificial neural networks.

8.1 Summary of Research Findings

An information database to the problem of bridge abutment distress was created by literature review, exploration of the MDOT's NBI field inspection database, field visits to typical bridges, and by State DOT surveys. A major part of the information database consists of bridge inspection records that documented design and operation parameters as well as abutment inspection ratings of MDOT highway bridges.

Using the created information database, statistical analyses were carried out to determine the significance of explanatory variables for bridge abutment damage as well as to provide information for other analyses and simulations in the research. It was found that adequate regression models cannot be developed because of the difficulties in the complicated database. The complexity consists of data unbalance, subjectivity, errors, and missing values. Eight explanatory variables were found to be significant for abutment damage, and thus, were used in developing neural network prediction models and finite element simulations. Furthermore,

approach pavement type was confirmed to be an important factor for abutment condition through frequency analyses, correlation analyses, factorial analyses, and hypothesis tests.

Four MDOT highway bridges were instrumented during a one year period. Two of them were simple/cantilevered steel bridges and two were prestressed concrete bridges. They were selected through statistical analyses of the information database and from the field inspection of 44 pre-selected highway bridges, all of which had common features that were susceptible to abutment damage. Of the four instrumented bridges, one steel and one concrete bridge had poor abutment and the remaining two bridges had a good abutment. The variables measured for each bridge were: deformations along the backwall and abutment wall, longitudinal displacements of the girder end, and temperature of the bridge deck and the abutment wall. Field monitoring data showed that the deformations along the abutment wall closely related to the longitudinal and transverse girder movement. Temperature variation in the deck and abutment wall can partly explain the girder movements, with the possibility that a major part of the remaining girder movement was induced by pavement pressure.

Seven hundred and eighty three finite element simulations were conducted with the effort to investigate the behavior of highway bridges under different damage scenarios. It was found that bridges with larger skew angles are subjected to larger stresses and strains on the abutment wall. This phenomenon is more obvious when the skew angle is larger than 30º. The length of the bridge had moderate to trivial effect on the response of the abutment wall depending on the different damage scenarios. Deck width was found to have a minimal influence on the stress and strain in the abutment wall.

Four major types of neural network models were developed to predict the abutment condition based on the manual inspection database. Multilayer perceptron and support vector machine neural network models showed reasonable accuracy. In order to overcome the unbalance and subjectivity of the manual inspection database, an ensemble of neural networks and fuzzy-neural networks were applied. An ensemble of neural networks with novel voting schemes was found to be optimal and robust for the problem in this research because the unbalance of structure inspection databases was overcome by organizing the training data using bagging within each structural condition. The damage identification ratio of an ensemble of networks reached 81% to 86%, which exceeded the best individual networks in the ensemble by 13% to 18%.

A program for Bridge Abutment Damage Diagnosis (SbNet) was developed to help MDOT engineers in the maintenance of existing bridges and design of new bridges. The software is based on a well-trained ensemble of neural networks and can predict bridge abutment condition given design parameters or MDOT Bridge ID. The output of SbNET includes the bridge deterioration curve as well as structural condition predictions for bridge abutment rating given the age of the bridge. The software can also be used as a predictive tool for new designs and to evaluate and compare the life-time performance of abutment walls for different bridge design options.

Potential causes of abutment damages in highway bridges in State of Michigan were identified based on the supporting evidence from the creation of the information database, statistical analyses, field inspections, instrumentation, finite element analyses, and artificial neural network simulations. Based on this research, the causes of abutment distress listed according to their relative significance are thought to be:

➢ Pavement pressure,

➢ Transverse temperature effect, and

➢ Longitudinal temperature effect.

Under the influence of the damage causes, bridges with following design features were more susceptible to abutment damage:

➢ Concrete approach pavement,

➢ Poorly designed seals for expansion joints on approach pavement,

➢ Fixed bearings on the abutment wall,

➢ No control joints in the abutment wall or control joints distributed at large intervals,

➢ Large skew angle, and

➢ Large total length.

Under the influence of the damage causes, bridges with following operation features were more susceptible to abutment damage:

➢ Rusted bearings,

➢ Rusted pin and hangers for cantilevered steel bridges,

➢ Close of expansion joints on approach pavements, and

➢ Large average daily truck traffic (ADTT).

8.2   Recommendations

Based on the analyses, simulations and investigations throughout the research and the identified damage causes, following alleviation strategies can be suggested:

> Use flexible approach pavement;

> Add pressure relief joints in approach pavement for existing bridges with rigid approach pavement;

> Improve the sealing of expansion joints on approach pavement;

> Use expansion bearings at the abutment wall;

> Distribute control joints in the bridge abutment wall at frequent intervals;

> Use small skew angle for new bridges;

> Avoid using of pin and hanger assembly or keep them in good condition if used.

The developed diagnostic software SbNET, which can make predictions either using design parameters for bridges during design or by MDOT Bridge ID for existing bridges, can be used as a tool to assist the management of the primary and/or avoidance of future abutment distress.

In conclusion, the project has lead to a thorough understanding of the causes behind structural distress in bridge abutments, a rational ranking of the primary causes, and the development of diagnosis and predictive models to assist the management and/or avoidance of future distress.

APPENDIX A Residual Plots of Linear Regression Models

Please refer to the separate Appendix volume accompanying this report.

APPENDIX B Design Plan and Bearing Details of Instrumented Bridges

Please refer to the separate Appendix volume accompanying this report.

APPENDIX C Analyses of Field Instrumentation Data

Please refer to the separate Appendix volume accompanying this report.

APPENDIX D Temperature Fields in FE Simulation

Please refer to the separate Appendix volume accompanying this report.

APPENDIX E Finite Element Simulation Results

Please refer to the separate Appendix volume accompanying this report.

APPENDIX F Bridge Abutment Damage Diagnosis (SbNET) 1.2 User's Manual

Please refer to the separate Appendix volume accompanying this report.

REFERENCES

AASHTO (2007), AASHTO LRFD Bridge Design Specifications;

ABAQUS Inc (2006), ABAQUS/Analysis User's Manual-version 6.6.1;

Askeland, D. R., Ksslinger, F., Wolf, R. V., "Investigation of Bridge Pin Failure." Report to Missouri Highway and Transportation Commission. Nov. 15, 1987.

Ayyub, B. M. and McCuen, R. H. (1997), Probability, Statistics & Reliability for Engineers. CRC Press, Boca Raton, New York;

Bellnoit, J., Yen, B. T., and Fisher, J. W., "Stresses in Hanger Plates of Suspended Bridge Girders." *Transportation Research Record 950*, Second Bridge Engineering Conference Vol. 2, 1990.

Breiman, L. (1994), "Heuristics of instability in model selection," *Annals of Statistics,* 24(6).

Breiman, L. (1996), "Bagging Predictors," *Machine Learning,* 24, 123-140.

Briaud, J.-L., Maher, S.F., and James, R.W., "Bump at the End of the Bridge," *Civil Engi-neering*, May 1997; 67, 5, pp. 68-69.

Burke, M. P. (1998), Pavement pressure generation: neglected aspect of jointed pavement behavior, *Transportation Research Record*, n 1627, p 22-28;

Burke, M. P. Jr. (2004), Reducing Bridge Damage Caused by Pavement Forces, *Concrete International*, January/February 53-57/83-89.

Duda, R. O., Hart, P. E. and Stork, D. G. (2001), *Pattern Classification*, 2nd edn, John Wiley & Sons, New York, 475-476.

Elewa, M.A., "Effect of Secondary Structural Components on the Serviceability of Steel Girder Bridges," Ph.D. Dissertation, Department of Civil and Environmental Engineering, Michigan State University, East Lansing, MI, May 2004.

Elewa, M.A., and Burgueño, R., "Effect of Unintended Fixity of Bearings on the Service-ability of Steel Bridges," submitted for presentation and publication to the 2005 Annual Meeting of TRB, Washington, D.C., July 31, 2004.

El-khoury, A., Washer, G., and Weigel, T. A., "Finite Element Modeling of a Pin Connec-tion." Structural Material Technology: An NDT Conference, Feb. 1996, San Diego, CA

Federal Highway Administration (FHWA 2001), Reliability of Visual Inspection for Highway Bridges, Volume 1: Final Report.

Freund, R. J. and Wilson, W. J. (1997), Statistical Methods, Revised Edition, Academic Press, pp 30-34;

Freund, Y. and Schapire, R. (1996), "Experiments with a new boosting algorithm," *Processings of the Thirteenth International Conference on Machine Learning,* 148-156.

Fu, J.Y., Liang, S.G. and Li, Q.S. (2007), Prediction of wind-induced pressures on a large gymnasium roof using artificial neural networks. Computers and Structures, 85: 179-192.

Graybill, F. A., and Iyer, H.K., "Regression Analysis – Concepts and Applications," Dux-bury Press, Belmont, CA, 1994, pp. 701.

Gunn, S. R. (1997), Support Vector Machines for Classification and Regression. Technical Report, Image Speech and Intelligent Systems Research Group, University of Southampton;

Guo, J. J. and Luh, P. B. (2004), "Improveing Market Clearing Price Prediction by Using a Committee Machine of Neural Networks," *IEEE Transactions on Power Systems,* 19 (4), 1867-1876.

Haldar, A. and Mahadevan, S. (2000), "Probability, Reliability and Statistical Methods in Engineering Design"; John Wiley & Sons, Inc, New York/ Chichester /Brisbane/ Weinheim / Singapore /Toronto.

Hansen, L. K., Liisberg, C. and Salamon, P. (1992), "Ensemble Method for Handwritten Digit Recognition," *Proceedings of the IEEE-SP Workshop on Neural Networks for Signal Processing,* 333-342.

Hachem, Y., Zografos, K. and Soltani, M.(1991), "Bridge inspection strategies," *Journal of Performance of Constructed Facilities,* 5 (1), 37-56.

Hansen, L. K., Liisberg, C. and Salamon, P. (1992), "Ensemble Method for Handwritten Digit Recognition," *Proceedings of the IEEE-SP Workshop on Neural Networks for Signal Processing,* 333-342.

Hansen, L. K. and Salamon, P. (1990), "Neural Network Ensembles," *IEEE Transactions on PatternAnalysis and Machine Intelligence,* **12**(10), 993-1001.

Hartle, R. A., Amrhein, W. J., Wilson, K. E. and Baughman, D. R. (1991), *Bridge inspector's training manual 90,* Federal Highway Administration, U. S. Department of Transportation, Washington, D.C.;

Haykin, S. (1999), *Neural Networks: A comprehensive foundation*, 2nd edn, Prentice Hall, Upper Saddle River, New Jersey.

Hsu, C.-W. & Lin, C.-J. (2002), A comparison of methods for multi-class support vector machines, *IEEE Transactions on Neural Networks*, **13** (2), 415–425.

Jain, L. C. and Martin N. M. (1999), Fusion of neural networks, fuzzy sets, and genetic algorithms: industrial applications. CRC Press, 1999.

Juang C. H., Ni, S. H. and Lu, P. C., (1999) Training Artificial Neural Networks with the Aid of Fuzzy Sets. Computer-Aided Civil and Infrastructure Engineering, **14**: 407-415.

Kartam, N., Flood, I., and Garret, J.H., (Editors) (1997). "Artificial Neural Networks for Civil En-gineers: Fundamentals and Applications," American Society of Civil Engineers, New York, NY, pp. 216.

Kohavi, R. & Provost, F. (1998), Glossary of Terms, *Machine Learning*, **30**, 271-274.

Kohonen, T. (1990), The self-organizing map, Proceedings of the Institute of Electrical and Electronics Engineers, **78**, 1464-1480.

Kolen, J. F. and Pollack, J. B. (1990), "Back Propagation is Sensitive to Initial Conditions", *Technical Report TR 90-JK-BPSIC.*

Kuliki, J.M., Murphy, R.E., Mertz, D.R. and Fisher, J.W., "Fatigue Cracking on I-79 Bridges in West Virginia." Proceedings of the 3rd annual International Bridge Conference, Pittsburgh, 1986, pp. 93-102.

Kutner, M. H., Nachtsheim C. J., Neter J. & Li, W. (2005), *Applied Linear Statistical Models*, 5th edn, McGraw-Hill/Irwin, New York;

Lee, J., Yi, J. D., Kim, J. D., and Yun, C. B.. (2004), "Health Monitoring Method Using Committee of NeuralNetworks," *Advances in Nondestructive Evaluation,* 1983-1988.

Long, J.H., Olson, S.M., Stark, T.D., and Samara, E.A., (1998), "Differential Movement at Embankment-Bridge Structure Interface in Illinois," *Transportation Research Record 1633*, Paper No. 98-1575, pp. 53-60.

MDOT (2001), Bridge Design Guides. Lansing, MI.

Montgomery, D. C., Peck, E. A. & Vining, G. (2006), Introduction to Linear Regression Analysis, 4th edn, John Wiley & Sons;

Mitra, S., and Hayashi, Y. (2000), Neuro-fuzzy rule generation: survey in soft computing framework. IEEE Transactions on Neural Networks, **11**(3): 748-768.

Myers, J., Nanni, A., Stone, D., Vellore, S.G., and Earney, T.P., "Precast I-Girder Crack-ing: Causes and Design Details," Technical Report No. RDT 01-008/RI 97-021, University of Missouri-Colombia/University of Missouri-Rolla, June 2001, pp. 175.

Myers R. H., Montgomery D. C. and Vining, G. G. (2002), Generalized Linear Models With Applications in Engineering and the Science, John Wiley & Sons.

Opitz, D. and Maclin, R. (1999), "Popular Ensemble Methods: An Empirical Study," *Journal of Artificial Intelligence Research,* 11, 169-198.

Pal, S. K. and Mitra, S. (1992), Multilayer Perceptron, Fuzzy Sets, and Classification. IEEE Transactions on Neural Networks, **3**(5): 683-697.

Pal, S. K. and Mitra, S. (1999), Neuro-fuzzy pattern recognition methods in soft computing. New York: John Wiley & Sons.

Phares B. M., Rolander, D. D., Graybeal, B. A. & Washer, G. A. (2001) "Reliability of Visual Bridge Inspection," Public Roads, March/April, 22-29;

Quinlan, J. R. (1996), "Bagging, boosting, and c4.5," Proceedings of the Thirteenth National Conference on Artificial Intelligence, 725-730.

Roeder, C.W., "Proposed Method for Thermal Bridge Movements," *Journal of Bridge En-gineering*, Vol. 8, No. 1, January/February 2003, pp. 12-19.

Roeder, C.W., J.F. Stanton, and T. Feller. Low temperature behavior and acceptance crite-ria for elastomeric bridge bearings. NCHRP Rep. NO. 325, Transportation Research Board, Washington, D.C. 1989.

SAS Institute Inc (2004) SAS 9.1 Documentation.

Schapire, R. (1990), "The Strength of weak learnability," *Machine Learning,* 5(2), 197-227.

Sharkey, A. J. C., editor (1999), Combining Artificial Neural Nets: Ensemble and Modular Multi-Net Systems, Springer, London.

Shober, S. F. (1997), Great Unsealing: A Perspective on PCC Joint Sealing, *Transportation Research Record 1597,* p 22-30;

Silva, A., Cortez, P., Santos, M.F., Gomes, L., & Neves, J. (2004), Multiple organ failure diagnosis using adverse events and neural networks, *Proceedings of the 6th International Conference on Enterprise Information Systems*, 401-408.

Smith, K. D., Snyder, M. B., Darter, M. I., Reiter, M. J. and Hall, K. T. (1987) Pressure Relief and Other Joint Rehabilitation Techniques. FHWA, U. S. Department of Transportation, 1987.

SPSS Inc. (2004), SPSS® 13.0 Base User's Guide;

Sybase Inc. (2004), Getting Started InforMaker;

Richards, A. M. (1979), Measurement Of Stress In Concrete Pavements, *Transportation Research Record*, n 713, p 9-15;

Taha, M.M. and Lucero, J. (2005), Damage identification for structural health monitoring using fuzzy pattern recognition. Engineering Structure; **27**:1774-83.

Tindal, T.T., and Yoo, C.H., "Thermal Effects on Skewed Steel Highway Bridges and Bearing Orientation," *Journal of Bridge Engineering*, Vol. 8, No. 2, March/April 2003, pp. 57-65.

Vapnik, V. N. (1999), *The Nature of Statistical Learning Theory*, 2nd edn, Springer.

Weisberg, S. (2005), Applied Linear Regression, 3rd edition, John Wiley & Sons;

Yao J. T. P. (1980), Damage Assessment of Existing Structures. Journal of the Engineering Mechanics Division, August: 785-799.

Yun, C. B., Lee, J. W.; Kim., J. D. and Min, K. W. (2003) "Damage Estimation Method Using Committee of Neural Networks*" Proceedings of SPIE - The International Society for Optical Engineering,* **5047**, 263-274.

Zadeh, L. A. (1965), Fuzzy Sets. Information and Control, **8:**338-353.

Zadeh, L. A. (1975), Linguistic Variable and Its Application to Approximate Reasoning. Information Sciences, **8** (4) 199-249.

Zadeh, L. A. (1975), Linguistic Variable and Its Application to Approximate Reasoning. Information Sciences, **8** (4) 301-357.

Zadeh, L. A. (1975), Linguistic Variable and Its Application to Approximate Reasoning. Information Sciences, **9** (1) 43-80.

Zadeh, L. A. (1994), Fuzzy Logic, Neural Networks, and Soft Computing. Fuzzy Systems, 77-84.

Zhou, Z., Jiang, Y., Yang, Y. and Chen, S. (2002), "Lung Cancer Cell Identification Based onArtificial Neural Network Ensembles," *Artificial Intelligence in Medicine*, **24**, 25-36.